Application of vertical profiled mortar connections in precast concrete shear walls

Rens Van

Source picture on front page: Website Samonco, Montage prefab beton; (viewed on 3-4-2019)

URL: http://samonco.be/

Application of vertical profiled mortar connections in precast concrete shear walls

A graduation thesis by:

Rens Y. Van

Graduation Committee

Dr. ir. drs. C.R. Braam Chairman

Ir. D.C. van Keulen Daily supervisor

Dr. ir. P.C.J. Hoogenboom

Dr. Ir. K.C. Terwel

Prof. dr. ir. D.A. Hordijk

Faculty of Civil Engineering and Geosciences

TU Delft

April 2019

TU Delft

INGENIEURSSTUDIO DCK

Preface

This report contains the master's thesis which concludes my study in Civil Engineering at the University of Technology in Delft. It is part of the requirements for a Master of Science degree in Civil Engineering, of which I completed the specific tracks Building and Structural engineering. The content of this research combines the objectives of these two tracks, where Structural Engineering is more researched based, whereas Building Engineering focusses on the connection with building practice.

I am proud of the research that is done and how I dealt with the difficulties faced on my way to this point. This couldn't be achieved without the assistance and supervision of my committee members. Therefore I would like to thank C.R. Braam, P.C.J. Hoogenboom, K.C. Terwel, D.A. Hordijk and in particular my daily supervisor D.C. van Keulen for sharing his ideas and opinion, providing parts of the literature and further information and giving me a chance to do this research in association with his company Ingenieursstudio DCK.

Therefore I also thank my colleagues at the office of DCK for their hospitality and a great time the last year. Also thanks to Dijeannio Hobson for the inspiring conversations at the office about the research topic.

Moreover I would like to thank Silvia Lemmens for her mental support, giving her opinion with or without being asked and her help by reading sections of the report. Furthermore I am glad with the help of Ruben Frijns and Niels Hofstee by reading parts of the report as well. Since designing a lay-out is not my strength, I am also very thankful to Merel Dubbeldam for her graphical review and assistance with the design of the presentation slides.

I would like to thank family and friends that also gave their feedback and asked me about the progress of the research and thus kept high time pressure. At last, thanks to H.R. Schipper, without whom I wouldn't have found this interesting research topic.

Rens Van

Delft, April 2019

Abstract

Building in precast concrete has multiple benefits over building with in situ concrete. The most important ones are a reduced construction time on site, a smaller minimally required construction site, better control of the concrete quality in the factory and, if applied well, a high repetition factor for building equipment. Despite all these advantages, tall stability structures are often still designed as a monolithic structure. The large amount of connections between all the separate elements reduces the overall stiffness of the stability structure. Since the dimensions of the stability structure of a tall building are often determined by the required building stiffness, a monolithic structure is preferred in most cases.

Multiple types of connections can be applied in the joints between precast concrete wall elements. One of these for the vertical joints is the profiled mortar connection, which was developed and tested by D.C. van Keulen (Van Keulen, 2018). The profiled joint of this connection is filled with thixotropic mortar, whereby the use of formwork is unnecessary. Furthermore the reinforcement in this type of connection is concentrated in the horizontal joints between two superimposed wall elements, whereby the connections are constructed more easily and faster. So application of these connections will lead to an efficiently constructible shear wall.

The aim of this research is to find a practical approach to model the vertical profiled mortar connection in a finite element model of a shear wall structure. For this purpose the linear shear stiffness of the connection and the structural effects, by which it is determined, were analysed first. The two investigated effects that determine the magnitude of the shear stiffness are the characteristics of the mortar joint and the lateral stiffness. The former comprises the properties of the mortar and the profile of the joint. The latter is the resistance to dilatation of the joint that is provided by the in plane stiffness of the surrounding precast concrete wall elements and the axial stiffness of the transverse reinforcement in the horizontal joints. Dilatation of the joint would be caused by the horizontal component of the diagonal compressive forces that develop in the mortar joint due to shear locking.

The magnitude of this lateral stiffness is determined by design parameters following from the architectural and structural design. The size and location of openings in the shear wall, the stiffness of the applied precast concrete and the stiffness of the transverse reinforcement are the four design parameters of which their influence on the lateral and shear stiffness was analysed in a parameter study. Based on this analysis, the size and location of the window openings are designated as the two most relevant of these four design parameters.

Furthermore, the influence of two characteristics of the mortar joint was also analysed in the parameter study. These properties are: the axial stiffness and angle of the compression diagonals in the joint. It appears that they have a larger influence on the shear stiffness of the connection than the design parameters related to the lateral stiffness have. So the characteristics of the joint are considered to be more important for the shear stiffness of the connection than the lateral stiffness and its related design parameters.

Keeping the goal of the research in mind, with the information of previous analyses a method was developed that tries to calculate the shear stiffness that can be assigned to linear interface elements that model the vertical connections.

The developed calculation method makes use of values for the joint properties, which are determined by a calibration to the test results, and it uses an approximated value of the lateral stiffness. For this approximation, the concrete wall elements are schematised as Timoshenko beams. These are subjected to a perpendicular distributed load in order to define their stiffness, which is used as measure for the in plane stiffness of the concrete wall elements. Combined with the axial stiffness of the transverse reinforcement, it defines the approximated lateral stiffness.

Based on the performed parameter study's results, an analytical relation was found that calculates the linear shear stiffness of the vertical profiled mortar connection from the combination of the lateral stiffness and the axial stiffness and angle of the compression diagonals in the joint. This relation is subsequently used to calculate the shear stiffness based on the lateral stiffness defined by the Timoshenko beam approximation. This shear stiffness is assigned to vertical interface elements that model the vertical connection between two adjacent precast shear wall elements.

Application of the calculation method leads to a significant error of the shear stiffness. This error is caused by the inaccuracy of the approximated lateral stiffness, whereby the largest error is found for the cases where the influence of the lateral stiffness is the largest. In the extreme case the real shear stiffness was 27% smaller than the value that was calculated.

Nevertheless, this calculation error leads to only a small difference in top deflection of a shear wall with averagely sized window openings. In the extreme case for this shear wall, the difference in top deflection is 1.8% between the upper and lower limit of the calculation method's band width. This error is so small that the calculation method can be applied to determine the shear stiffness that is the input for the interface elements. However, the difference in top deflection caused by the band width of the calculation is too large to be able to compare the performance of the vertical profiled mortar connections with that of other types of connections in a precast concrete shear wall.

Since the error of the calculation is caused by the inaccuracy of the lateral stiffness and this error leads to relatively small variations of the shear wall's top deflection, it is finally suggested to include the contribution of the lateral stiffness in a different way. In that case the shear stiffness of the interface elements is simply calculated by a single formula that only considers the two joint properties that have been analysed: the axial stiffness and angle of the compression diagonals in the joint. A reduction factor can be applied to take into account the effect of the lateral stiffness, but if this isn't done, the error of the top deflection is at most 3.2% for the shear wall analysed in this research. Nevertheless it is advised to include the correction factor to reduce the error of the modelling approach. The advantage of this method is that the lateral stiffness, of which the magnitude appeared to be hard to determine, is included by a simple factor instead of a complex Timoshenko approximation. Moreover further in depth research into the lateral stiffness is less necessary for application of this approach. For these reasons, it is seen as a very practical and easy approach to model the vertical profiled mortar connections.

Table of contents

1 Introduction

The choice between precast or in situ concrete is always based on multiple aspects such as costs of materials and labour, design and construction time, technical requirements, experience of the contractor, the conditions on the building site, quality of the materials and the possibilities for transportation.

The essential difference between building in precast or in situ concrete is that the former results in a construction process in which completed building components are assembled on site, whereas the latter results in a process where the building components are produced on site. Building in precast concrete can have benefits over building with in situ concrete. The most important ones are a reduced construction time on site, a smaller minimally required construction site, better control of the concrete quality in the factory and if applied well, a high repetition factor for building equipment.

Despite all these advantages, tall stability structures are often still designed as a monolithic structure. The large amount of connections between all the separate elements reduces the overall stiffness of the stability structure. Since the dimensions of the stability structure of a tall building are often determined by the required building stiffness, a monolithic structure is preferred in most cases.

Research has been done on the stiffness of precast stability structures with respect to monolithic concrete structures (van Keulen, 2010; van Keulen & Vamberský, 2012). Several parameters of the element layout used in precast concrete shear walls determine the global stiffness. The most influencing parameter is the configuration of the elements. Two options are possible: a masonry or a stacked configuration (Figure 1.1). Currently the masonry type is common practice. It is relatively stiff and a big advantage is the possibility to keep the vertical joints structurally open, which reduces the amount of work and costs. The main advantage of a stacked configuration is its regularity. This reduces the total amount of precast elements, the amount of different precast elements, the vertical transport on site and it increases the repetition factor of the moulds in the precast concrete factory. In this configuration however, the vertical joints must be able to transfer shear forces, whereas for the masonry configuration the joint overlapping elements transfer shear by dowel action. When shear force transfer over the vertical joints is guaranteed, the “columns” of wall elements work together as a coherent structure, enabling the stacked configuration to be as stiff as the masonry type (van Keulen & Vamberský, 2012). The mechanism is illustrated in Figure 1.2.

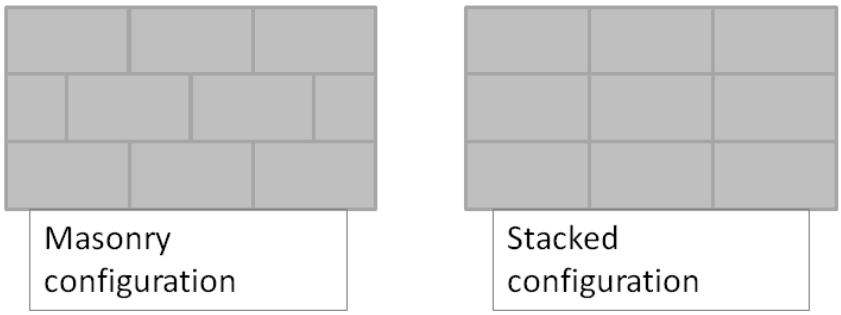

Figure 1.1 Element configurations

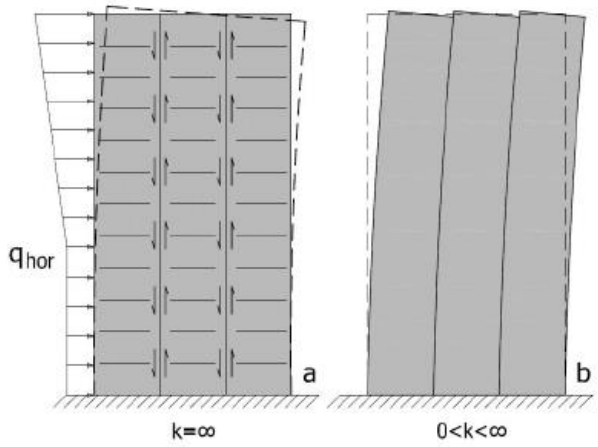

Figure 1.2 Vertical shear stresses in the joints of a precast shear wall (Van Keulen, 2018)

1.1 Vertical shear connections developed and tested by Van Keulen

One of the current solutions for the vertical joints in a shear wall is to apply a "cast-in-place loop connection". This connection is illustrated in Figure 2.4. In this case the joints are filled on site with cast-in-place reinforced concrete. However, this method contradicts the benefits of precast concrete with respect to construction speed, since it requires significantly more labour on site.

For the PhD-research of ir. D.C. van Keulen several profiled mortar connections that could be used for the vertical interfaces between precast wall elements, were developed and tested (van Keulen, 2015). These connections are shown in Figure 4.1. A principle sketch of these connections is provided in Figure 1.3. The connections have two important properties, leading to three major advantages: the joint is filled by thixotropic mortar and the required transverse reinforcement is not distributed over the entire length of the joint, but concentrated in the horizontal joints at floor level (see Figure 1.3). Due to the use of thixotropic mortar, application of formwork is unnecessary. By avoiding the use of distributed reinforcement, there aren't any steel bars piercing the moulds that are used for manufacturing of the wall elements. Therefore simpler moulds can be used, resulting in an easier fabrication process. Furthermore, elements without protruding steel are easier to handle during transport and construction. Lastly, the construction speed is increased by preventing the use of formwork and the application of reinforcement in the joint itself. These three benefits, an easier production process, easier handling and transportation of the elements and a reduced construction time on the building site, completely agree with the intended benefits of constructing in precast concrete.

So application of the new profiled mortar connections in combination with a stacked configuration can lead to a very efficient design for a prefabricated concrete stability structure, which competes with a monolithic structure.

Figure 1.3 shows a principle sketch of one of the connections that Van Keulen developed. The main variables determining the shear stiffness and capacity of the developed connections are the properties of the joint (e.g. type of mortar, geometry of the profile and present surface roughening), present normal stress in the joint and the lateral stiffness of the adjacent elements. The last is the in-plane stiffness of the adjacent wall elements, giving resistance to any dilatation of the joint. This dilatation is caused by the horizontal components of the diagonal compression forces that transfer vertical shear forces over the joint. These forces are indicated by the diagonal arrows in Figure 1.3. The three main variables were varied among the different tests that were performed by Van Keulen. Therefore, the test results indicate the relation between these variables and the properties of the connection.

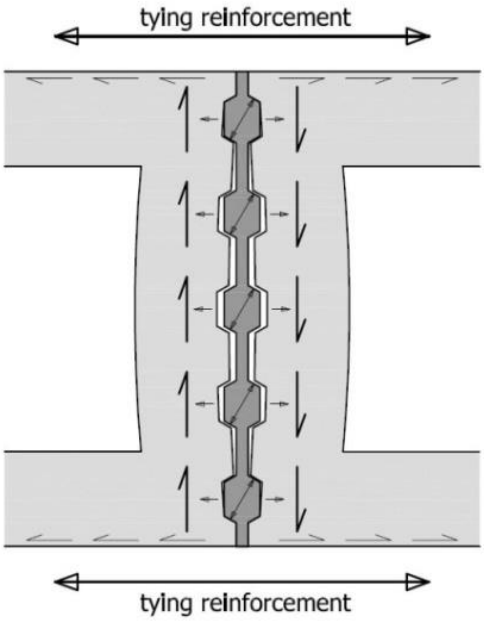

Figure 1.3 Principle of the connection applied in a wall (side view) (Van Keulen, 2018)

1.2 Problem statement

So, the use of vertical profiled mortar connections in combination with a stacked element configuration can lead to an efficient precast concrete design that structurally competes with the walls having a masonry configuration. However, the current information on the behaviour of the developed connections is limited and mainly consists of Van Keulen's test results. Before these connections can be applied in structural design, more research into their behaviour is needed.

The translation of the results into an approach to model the connections in a precast concrete shear wall, requires more research into the effect of the main variables that were named in previous section. This research focusses on this translation from test results to modelling approach by analysing the influence of the main variables on the connection's properties and by developing a way to model the connections in finite element models of precast concrete shear walls. The problem statement of the research can therefore be formulated as:

"How can the vertical profiled mortar connection be modelled in practical situations?"

As the problem statement indicates, the focus of this research is on the application of the connections in structural design situations and choices on scope, modelling and research aspects are made accordingly. In chapter 5 an overview will be given of all research aspects that play a role in modelling the connection. After that, the scope of the research will be determined in more detail.

1.3 Outline of the report

This report starts with an overview of the knowledge obtained from literature. Chapter 2 discusses literature on connections in precast concrete structures and vertical profiled shear connections in particular. Chapter 3 elaborates on the structural behaviour of a shear wall and chapter 4 concludes the literature study with an overview of Van Keulen's test results.

Using the information obtained from the literature study, an overview is made of all the aspects that should be investigated in order to describe the behaviour of the vertical profiled shear connection completely. This overview is provided in chapter 5. Subsequently, the scope of this research is set by selecting some of the relevant aspects to elaborate on. This scope definition is described in paragraph 5.2. Paragraph 5.3 continues with an overview of the specific research questions that are within the scope of this research and that are investigated in the remaining of the report.

Chapter 6 forms the beginning of the model study. This chapter describes the transition from Van Keulen's test setup to a finite element model that is suitable for research. The developed finite element model is used to analyse the test setup in the finite element package DIANA 10.2. This analysis is described in chapter 7. Subsequently, the test setup model is expanded to one of a complete shear wall. This model is used for a parameter study that has been performed to analyse the influence of different parameters on the connection's properties. This parameter study is discussed in chapter 8.

Based on the parameter study some conclusions could be drawn about the way different parameters influence the behaviour of the connection, but several questions remain unanswered. The further research that tries to gain more insight into these questions is described in chapter 9. Chapter 10 includes the analytical formulas that have been derived in order to describe the behaviour of the modelled connection. Using these formulas, the setup of the practical modelling approach, that the problem statement aims at, is developed and described in paragraph 10.4. The practical modelling approach is then evaluated on a shear wall model in chapter 11, which concludes with a final proposal for a practical modelling approach in paragraph 11.5 and a calculation example in paragraph 11.6.

Chapter 12 summarizes the conclusions of this research and the recommendations for further research.

Appendix A provides a list of all used symbols, where the reader can retrieve the meaning of symbols used in the diagrams and formulas presented in coming chapters.

2 Literature study: Connections in precast concrete

In precast concrete structures, the connections between the elements determine the cooperation between the precast concrete elements. This thesis will focus on vertical connections between wall panels, but several other connections are present in a precast structure. Figure 2.1 shows the type of connections that are usually present in a precast concrete structure (Lagendijk & Hordijk, 2016):

1. Floor to floor
2. Floor to beam
3. Beam to column
4. Column to column or foundation
5. Floor to wall
6. Floor to wall shear connection
7. Vertical wall connection
8. Horizontal wall connection

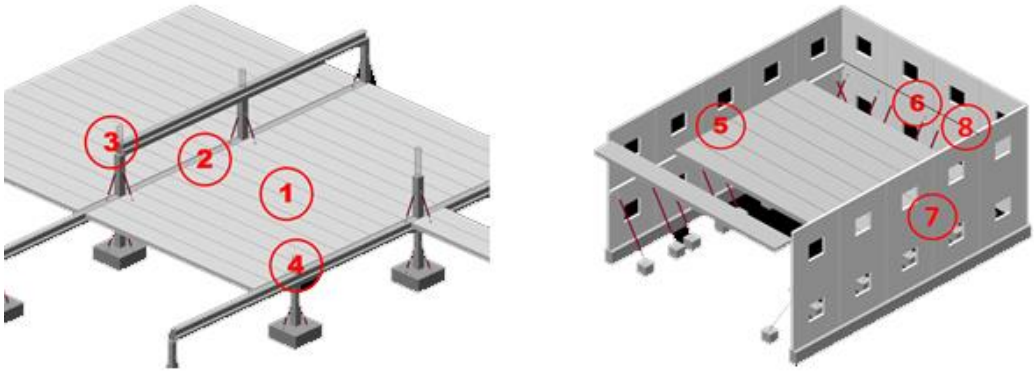

Figure 2.1 Location of connections in precast concrete structures (Lagendijk & Hordijk, 2016)

Besides connection 7, also connections 5, 6, and 8 interact with the precast wall panels. These three connections will therefore influence the behaviour of the vertical connection. Figure 2.1 and Figure 2.3 for example show options for the floor to wall connection. Whether the floor is supported by a corbel or integrated in the wall determines the location of the transversal tie reinforcement with respect to the wall panels. This reinforcement is used as tying reinforcement by the vertical profiled mortar connection, that is investigated in this thesis. This is indicated in Figure 1.3. The horizontal connections between two stacked wall panels are often executed as smooth mortar joints with or without starter bars.

The vertical joints between two adjacent wall panels are in most cases structurally open when the shear wall is designed according to the masonry element configuration of Figure 1.1. If a vertical shear connection is applied, as is required for a stacked element configuration, several options are possible. So called wet joints can be used, of which the cast-in-place loop connection in Figure 2.4 is an example. This connection can be executed with a straight or a profiled joint. For the type that is shown in Figure 2.4, a big disadvantage is the need of formwork when the joint is filled with mortar or concrete. If the wall panels are executed with a recess on the side

where the loop reinforcement protrudes from the panel, formwork is unnecessary, as Figure 2.5 shows.

Welded connections are an example of a dry connection. In this case a steel plate is casted into the wall elements. Reinforcement bars that are attached to this plate are connected to the main reinforcement net of the wall element in order to facilitate force transfer from the plate to the wall panel. This steel plate is then welded to the plate that is casted in the wall element that is to be connected. An impression of this type of connection is given in Figure 2.6, with a view on the inside of the wall and a view from the outside of the wall.

This chapter starts with a short explanation of the principles of connection design. The second paragraph discusses the mechanisms whereby forces are transferred in connections and the way these mechanisms interact. The third paragraph provides a more detailed description of what is known from literature about the behaviour of profiled shear connections. This knowledge is most applicable to the profiled mortar connections that are analysed in this thesis. The chapter ends with a short summery of conclusions based on the performed literature study.

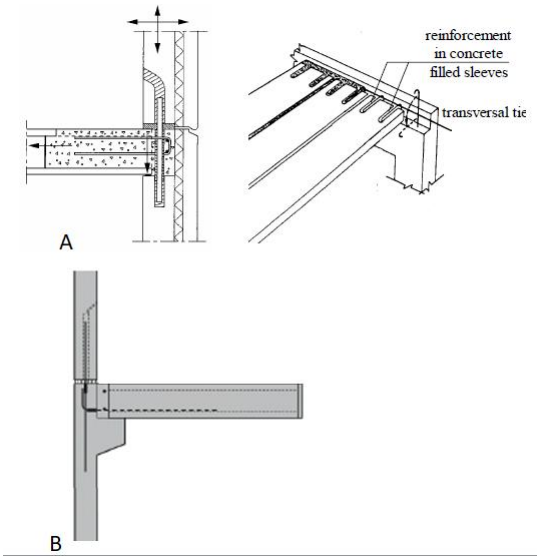

Figure 2.2 floor-wall connections a. floor integrated in the wall (FIB, 2008, p. 95 & 257) b. floor supported by corbel (TU Delft, 2016, p. 10.10)

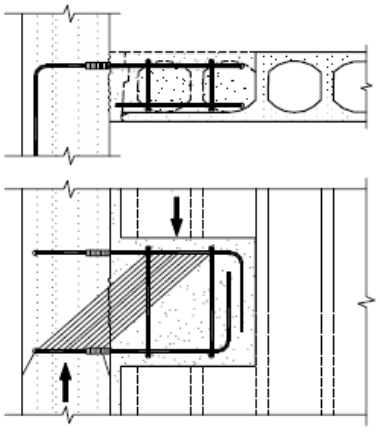

Figure 2.3 floor-wall shear connection (FIB, 2008, p. 21)

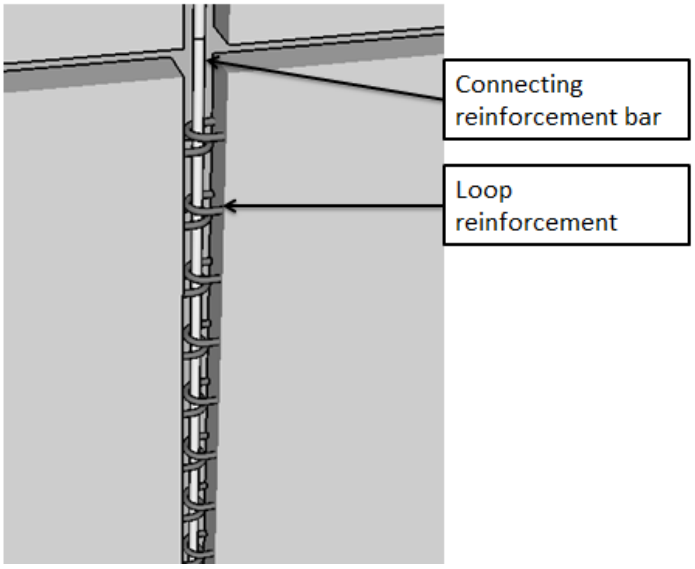

Figure 2.4 Sketch of the cast in place loop connection

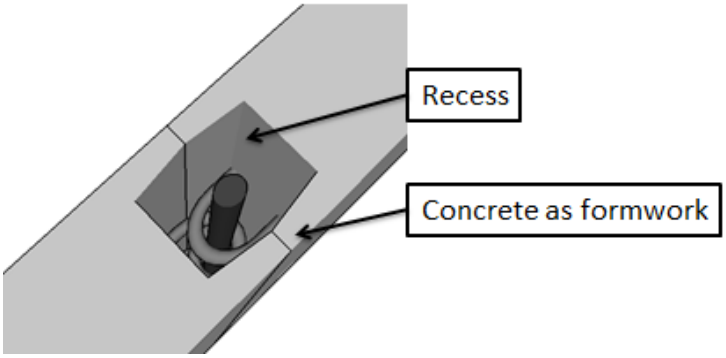

Figure 2.5 The cast in place loop connection with recesses

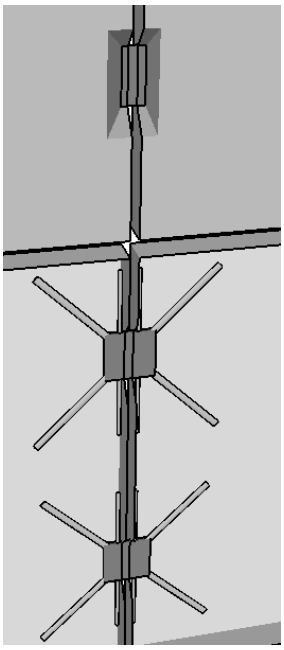

Figure 2.6 Sketch of the welded plate connection

2.1 General guidelines for connections

The main difference between a structure of in situ and precast concrete for a structural engineer is the presence of connections between all elements. The purpose of the connections is to create a coherent structure. In designing connections many aspects must be considered. For example the structural behaviour, the type of structure and the construction methods must be taken into account. This paragraph describes these general aspects of connection design.

Two books written by the International Federation of Structural Concrete give an overview of the design guidelines for connections in precast concrete (FIB, 2014; FIB, 2008).

The purpose of a connection is to "*transfer forces between the precast concrete elements in order to obtain a structural interaction when the system is loaded. The connection should secure the intended structural behaviour of the superstructure and the precast subsystems*" (FIB, 2008, p. 31). Two terms are often confused: joint and connection. A joint is solely the interface between elements, whereas the connection is the combination of all the elements that play a role in the transfer of forces from one element to the other. A connection even includes the parts of the adjacent concrete elements where the internal forces are disturbed due the force transfer, the so called disturbed regions or connection zones. When one connection is a chain of structural elements, it even contains multiple joints (FIB, 2008, pp. 2-3,31).

2.1.1 Aspects concerning structural behaviour

Several aspects in connection design related to structural behaviour must be taken into account (FIB, 2014, pp. 97-102; FIB, 2008, pp. 31-34).

- Capacity to transfer forces due to regular loads
- Capacity to transfer forces due to accidental loads
- Movements and deformations of connected structural members as a result of time-dependent or temperature effects, but also regular loads
- Ductility
- Durability

It is obvious that a connection must be able to resist loads caused by gravity and wind or earthquake loads. In case of accidents like collision or explosions the connections must be able to facilitate an alternative load path if necessary. Therefore some additional capacity is required. Design of connections to transfer forces is not just about the connecting components. Also the connection zone in the adjacent concrete element must be designed for the large local forces. Strut and tie models provide a tool to design the reinforcement required for spreading the local forces over the elements.

Imposed deformations as a result of creep, temperature differences, shrinkage or swelling must be considered as well. There are basically two options to deal with this: restraining all imposed deformations and design for the resulting extra loads or enable all movements of the structure to prevent extra loads. Proper design of joints can make these movements possible. For example dilatation joints could be used. A connection can also get damaged by regular deformations as the Figure 2.7 indicates.

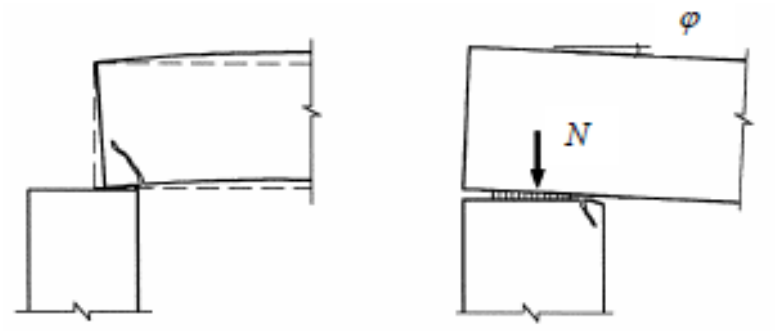

Figure 2.7 Damage of a beam column connection caused by beam deformation (FIB, 2008, p. 41)

An important safety requirement is to prevent brittle failure of a structure. This leads for example to a minimal reinforcement ratio of concrete beams. However, a ductile beam spanning between two brittle moment resisting connections with an ultimate capacity lower than the failure load of the beam will still fail in a brittle way. Therefore the connections must be designed with enough ductility. Two terms are often confused: ductility and deformability. The deformability of a structural element just indicates the deformation at failure. It doesn't provide any information about the capacity of the structural element at failure. When an element is ductile, it is able to deform a lot while keeping (a large portion) of its ultimate strength (FIB, 2014, p. 100). In order to make a connection ductile, a balanced design can be applied. The aim of this design is to let the connection deform maximally while keeping its strength. In order to do so, all the brittle elements of the connection must have an ultimate strength larger than the ultimate strength of the most ductile element (FIB, 2008, pp. 49-50).

Another structural requirement is the minimal durability of the connections. Besides that corrosion of elements must be avoided, the maintenance of the connections must be considered. Quite often the connections are unreachable in the finalised structure, wherefore their life-time must be longer than that of the other parts of the building structure (FIB, 2014, p. 101).

2.1.2 Aspects concerning construction processes

When designing the connections, the construction aspects must be taken into account as well. The minimal requirement is to use constructible connections. Some aspects to consider in order to obtain constructible connections are (FIB, 2014, pp. 97-102; FIB, 2008, pp. 55-70):

- Dimensional tolerances
- Simple Connections
- Governing strength and stability requirements during construction
- Congestion of concrete
- Accessibility of the connections

Dimensional tolerances are required due to inaccuracies in construction. The dimensions of precast concrete elements for example are never exactly as intended, due to variations in the manufacturing process. Furthermore the placement of the elements on site can never be completely accurate. The connections must allow for small dimensional variations in the structure compared to the drawings.

Simplicity of the connections will reduce the risk of incorrect production. Furthermore it will also reduce the building costs. A simple connection is preferably with the least amount of different components.

When a lot of components are cast in the adjacent concrete elements, congestion of the concrete during pouring might occur. This should be avoided. Furthermore the whole connection must be reachable for construction workers during the erection phase. A classic example of an incorrect design is a bolted connection in a tubular section, where the bolt inside the tube is unreachable.

While designing connections, the acting loads during the construction phase must be considered as well. The governing load situation that the connection must be designed for can take place in this phase or special stability requirements during this phase where the total structure is incomplete are governing for design.

The way the connections have to be installed is preferably in line with the intended speed of precast construction. Furthermore the connections are preferably designed well for transport and storage of elements. Some aspects to consider in relation to these topics are given in literature (FIB, 2014, pp. 140-141; FIB, 2008, pp. 56-60):

- Weather sensitivity
- Fast hoisting operations
- Use of standardized connections with standard element sizes
- Repetition of connections
- Damage during transport and storage

Having a less weather sensitive construction process enlarges the period suitable for operations. This increases the construction speed.

A critical activity on site is the hoisting of concrete elements to their final positions. Purely vertical hoisting results in the fastest erection. However, when the connections do not allow this and require horizontal placement or placement under an angle, the construction process is slowed down and gets more difficult. For example when horizontal loop reinforcement is applied in the connections between wall panels, vertical placement isn't possible without adjustments. Figure 2.8 shows the procedure in this case: the loops are bent upwards to allow vertical placement and afterwards they are bent to their original position again. For this reason Sorensen, Huang, Olesen and Fischer designed a connection with vertical loop reinforcement (Sorensen, Hoang, Olesen, & Fischer, 2017).

Although the vertical loop reinforcement is a better alternative, it still has another drawback. The loop reinforcement protrudes from the concrete elements. This is more difficult and expensive to produce, since the cast in reinforcement penetrates the formwork during pouring. Furthermore protruding elements might lead to less efficient transportation or difficulties during storage. The risk of damage to the connections or elements during these activities is also larger.

Using standardized connections with a high repetition factor makes the process cheaper and easier to perform. When each connection is exactly the same, the manufacturers and construction workers will know exactly what to do, which reduces the risk of mistakes. Standard items are mostly readily available which reduces costs and the risk of delay.

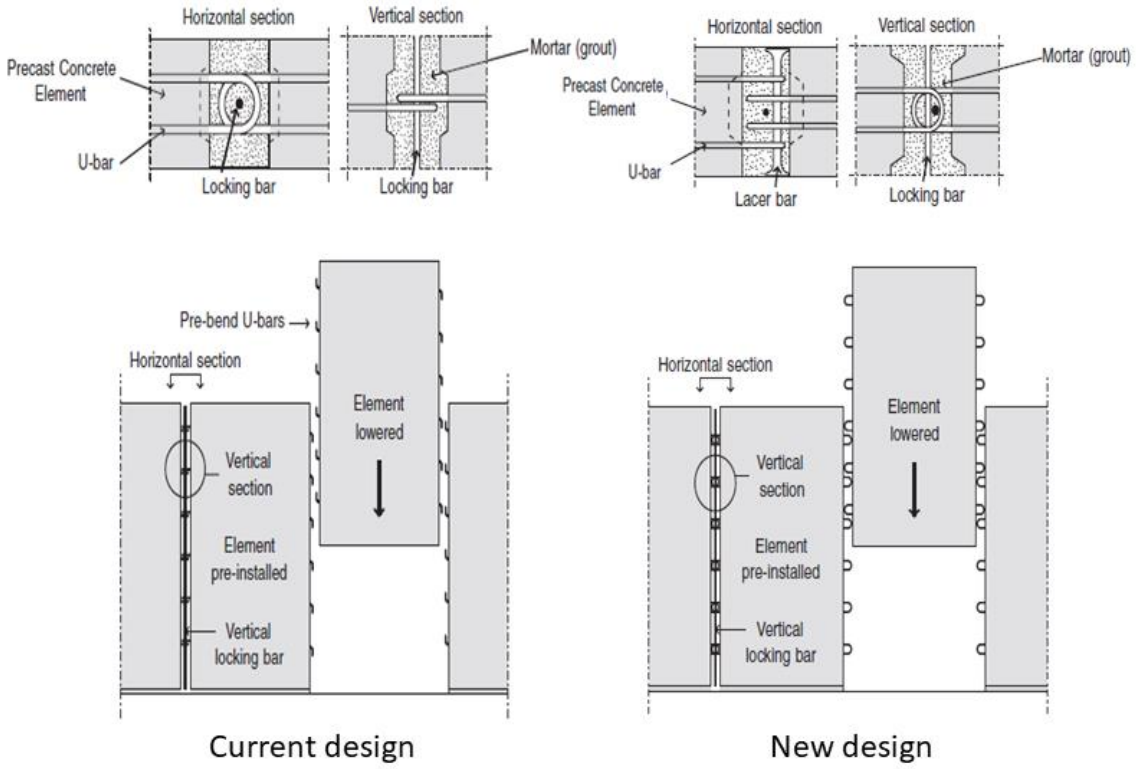

Figure 2.8 Vertical hoisting of two different vertical shear connections (Sorensen, Hoang, Olesen, & Fischer, 2017)

2.2 Force transfer in connections

This paragraph discusses the principles of load transfer in connections. Several mechanisms contribute to the transfer of compressive, tensile and shear forces. Understanding of these mechanisms is crucial for working on connections in precast concrete engineering.

2.2.1 Transfer of compressive forces

Compressive forces in a structure are mainly a result of dead loads and live loads on the structure. Two examples of connections transferring compressive forces are connections between column ends and supports of beams and floor slabs.

Compression joints are usually executed with bearings between the ends of the connected elements. This can be a hard bearing, like a steel plate, a mortar bearing or a soft bearing, like a rubber pad. A bearing is considered to be hard if its modulus of elasticity is at least 70 percent of the elasticity of the adjacent elements (Bachmann & Steinle, 2011, p. 175).

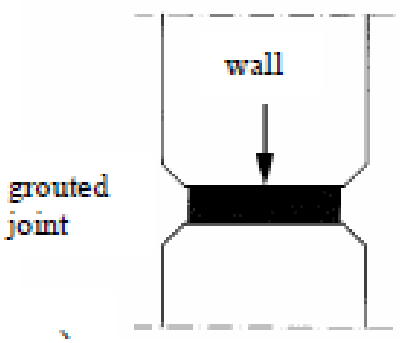

Figure 2.9 Bearing between two vertical concrete elements (FIB, 2008, p. 93)

The bearings between the elements are required because a direct contact faces some problems. If elements are directly connected, the irregularity of the contact surfaces can cause stress concentration, eccentric application of forces and torsional effects (FIB, 2014, p. 111). The bearings equalize the contact surface and mitigate these effects. Only under certain circumstances with small movements and forces a direct contact surface is allowed (FIB, 2014, p. 111). Although other literature indicates that some regulations do always require a bearing layer (Bachmann & Steinle, 2011, p. 175).

Steel bearings are often required when large compressive forces are transferred. Elastomeric bearings are often used in connections between horizontal and vertical elements. Floor slabs are often supported by bearing strips, when the horizontal force transfer is arranged in a different manner (FIB, 2008, p. 98). Mortar joints are often used in vertical elements with moderate compressive forces. The horizontal joints between precast wall elements are filled with mortar in most cases.

Compression joints are often combined with other actions as well. For example a connection in a clamped column must also transfer bending moments. This will lead to extra demands on the detailing of the joints. Furthermore, the expected deformations in the joint lead to requirements on the dimensioning. As Figure 2.7 indicates for example, the bearings supporting a floor must have a sufficient height and offset from the corbel end to prevent damage (FIB, 2008, p. 41).

Before the mechanisms, playing a role in compressive connections, are considered, the failure of concrete under compression is looked at. Two tests are available to determine the compressive strength: a cube and a cylinder compression test. The cylinder test gives 20 percent lower values for the strength, since it can be seen as a purely uniaxial test. In a cube test, the stress state is two dimensional. The cube wants to expand in the direction perpendicular to the load, but this expansion is prevented by the test setup. Frictional forces between the cube and the steel plates above and below induce a lateral compressive stress in the cube, which increases the capacity (Fennis & Walraven, 2013, p. 23). When the lateral deformations are not constrained, the ultimate compressive strength isn't reached and the cube fails in a shear or tensile failure, whereby cracks parallel to the loading direction occur (FIB, 2008, p. 103). Figure 2.10 shows the behaviour of a tested cube. Understanding this effect is important while looking at compression connections. The lateral stresses play an important role in this case.

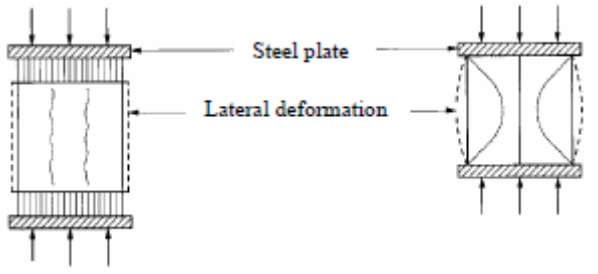

Figure 2.10 Behaviour of concrete in a cube compressive test. a. without lateral restraints b. with lateral restraints (FIB, 2008, p. 103)

Two mechanisms induce lateral tensile stresses in the adjacent concrete elements (FIB, 2014; FIB, 2008; Bachmann & Steinle, 2011):

- Different lateral expansion of the connection layers
- Divergence and convergence of stress

Consider a connection between two concrete column ends with a layer of a different material in between (Figure 2.11). Poisson's ratio is different for both materials and so is their lateral strain as a consequence of the axial load. The difference in lateral strain leads to a difference in desired lateral expansion between each of the layers. However, if friction forces in the interface between the layers restrain lateral movements of the material layers, shear stresses will develop in the interfaces. These shear stresses will result in lateral tensile or compressive forces in the concrete elements and the bearing layer.

Whether lateral tension or compression occurs in a material depends on the ratio of the Poisson's ratio over the Young's modulus for both materials. When this ratio is lower for the concrete elements than for the bearing material, as is the case for a steel bearing, the concrete would expand more in lateral direction. The frictional restraint causes lateral compressive stresses in the concrete, having a positive effect on its bearing capacity. In the steel bearing tensile stresses will occur (Figure 2.11a) (FIB, 2008, pp. 100-102). Exactly the opposite is the case for elastomeric bearings, having a larger ν/E ratio. In that case the prevented deformation will induce lateral tensile stresses in the concrete elements and compressive stresses in the bearing (Figure 2.11b). These tensile stresses will generally be larger than the splitting tensile strength, wherefore lateral reinforcement is required in the concrete elements (FIB, 2008, p. 103).

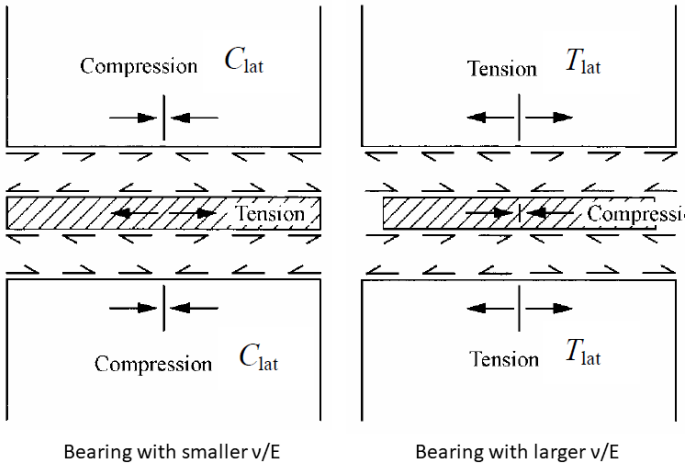

Figure 2.11 Lateral stresses due to expansion effect. A. bearing with smaller ν/E. B. bearing with larger ν/E ((FIB, 2008, p. 102) original from BLF (1995) and Basler and Witta (1966))

Especially for elastomeric bearings transferring a high compressive force or dealing with large movements, the use of reinforced bearings can be an option. In that case steel sheets are applied in the rubber bearing. These sheets take up the lateral tensile forces instead of the concrete (Bachmann & Steinle, 2011, pp. 187-188).

The ν/E ratio of mortar is also smaller than that of concrete, resulting in compressive stresses in the mortar and tensile stresses in the concrete. While the compressive stresses are of major importance, since those provide the large axial compressive strength of the mortar, the tensile stresses in the concrete are normally smaller than other effects in this case (FIB, 2008, p. 102).

The second effect causing lateral tensile stresses has to do with the flow of forces in the connection (FIB, 2008, pp. 108-109). At a certain distance from the connection the stress in the column is uniformly distributed. If the bearing area is smaller than the cross-sectional area of the column, the uniform stress must converge to the bearing area. After passing the joint, the

stress diverges again. Converging and diverging of stresses results in lateral stresses as well, since the stress trajectories change direction. Figure 2.12 illustrates this effect in a strut and tie model. The transversal tensile stresses must be taken up by splitting reinforcement.

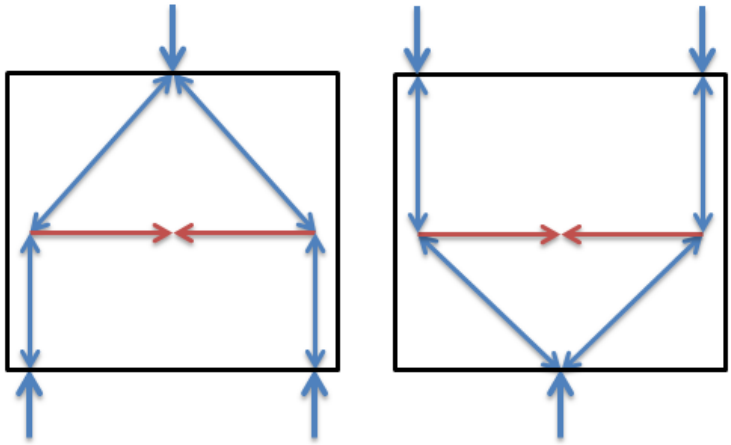

Figure 2.12 Strut and tie models for divergence and convergence

Although the connection is likely to fail in a different manner, the check on sufficient bearing capacity must always be made. In order to check the compressive stress compared to the capacity, one must consider the effective loading area, which is dependent on the type of bearing pad used (FIB, 2008, p. 107).

The compressive connection will in almost all cases fail due to secondary tensile stresses. Therefore the focus is on designing the required lateral reinforcement. The force taken by this reinforcement is the summation of the splitting force and the force due to restricted lateral expansion, possibly enlarged by a present horizontal force (FIB, 2008, p. 111).

2.2.2 Transfer of tensile forces

For the transfer of tensile forces, other types of connections are necessary. As commonly known, the tensile strength of concrete is limited. A tensile force could be transferred between elements by adhesion of the concrete elements and the grout or concrete in the connection. However, it should always be assumed that the joint section is cracked (FIB, 2008, p. 135). This holds because the possible adhesion between grout and the precast element is to a large extend dependent on insecure executional aspects, such as surface roughness and cleanliness of the element surfaces (FIB, 2014, p. 107). Furthermore restrained movements, shrinkage for example, can cause cracks, whereby the bond is gone.

So when designing a tensile connection, steel elements must be used to transfer the force from one element to another. These elements must be linked to the main reinforcement of the precast concrete elements. The tensile connections can be realised by using bolts, welds, protruding overlapping loop reinforcement or continuous bars over the joint (FIB, 2008, p. 135). Bolted connections can be made with cast in threaded sockets, which prevents the use of projecting steel from the elements. However, smart solutions are required to design a bolted connection with sufficient dimensional tolerances. Welds can be used to connect protruding reinforcement bars or steel plates cast in the element's faces (FIB, 2008, p. 138). Furthermore welds are sometimes used to connect anchor plates to the steel bars transferring the tensile forces. The way these welds are executed on anchor plates affects the characteristic behaviour of the connection (Bachmann & Steinle, 2011, p. 192).

An example of a connection with a continuous bar is the connection between two hollow core slabs that is illustrated in Figure 2.13.

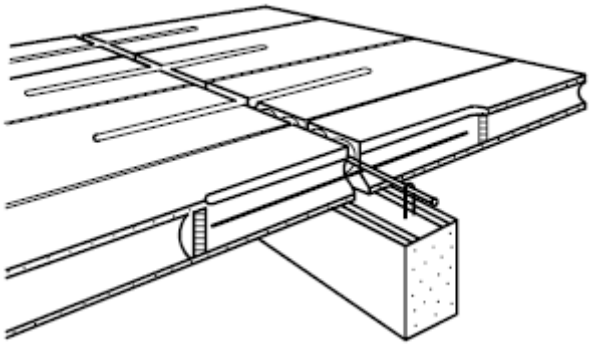

Figure 2.13 Connection between hollow core slabs (FIB, 2008, p. 135)

In this case horizontal grooves, in which the reinforcement bars are placed during construction, are made at the end of both floor slabs. The grooves are later filled with grout. This is called indirect anchorage, the opposite of direct anchorage, whereby the bars are casted in during production (FIB, 2008, p. 136). When direct anchorage is applied, the bars projecting from both elements are usually connected by overlap in joint between the two concrete elements that is filled on site (FIB, 2014, p. 104). The overlap must be sufficiently long to transfer the tensile forces by bond between the steel bars or a weld can be applied.

Different failure mechanisms determine the capacity of tensile connections (FIB, 2008, p. 139).

- Splitting failure of the concrete
- Pull out failure
- Extensional failure of the bar
- Failure of the welds (If applied)

The reinforcement bars are anchored in the concrete elements either by bond or by the use of an anchor plate, bend or hook. In order to rely on bond of the ribbed reinforcement, the anchorage length must be sufficient. If there isn't enough space to accommodate the required length, one of the anchors can be applied. In this way pull out of the reinforcement bar is prevented. The anchorage of the bars induces splitting tensile stresses in the concrete element. These stresses must be resisted by applying enough concrete cover or transverse splitting reinforcement. The two failure modes are illustrated in Figure 2.14.

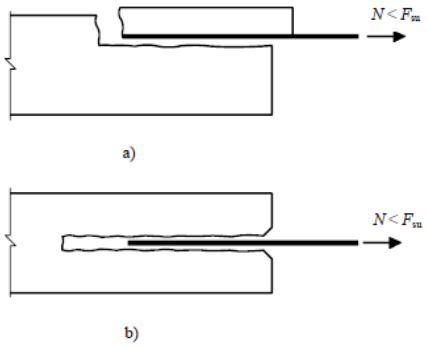

Figure 2.14 a. splitting failure b. pull out failure (FIB, 2008, p. 139)

In relation to splitting forces the use of end anchors is unfavourable since they introduce relatively large local forces into the concrete, whereas anchorage by bond distributes the forces over a certain transmission length. Two types of pull-out failure are specific for the application of anchors: Concrete cone pull-out and anchor slippage. The anchors must be placed sufficiently deep in the concrete element to prevent concrete cone pull out and the size of the anchor must be large enough to prevent anchor slippage (FIB, 2008, pp. 139-141).

The transfer of tensile forces by bond between the reinforcement bar and the concrete takes place over a certain "transmission length", which isn't necessarily equal to the full anchorage length. The transferred tensile force is spread over the transmission length resulting in smaller splitting forces in the concrete element (FIB, 2008, pp. 141-143).

The bond stresses are not equally distributed over the complete transmission length. The highest stresses occur at the end of the bar where the load is introduced (the active end), the lowest occur at the embedded end of the bar (the passive end). Since the bond stresses aren't uniform, the slip of the bar relative to the concrete isn't either. When a relatively small force is transferred, the bond stresses and slip at the passive end will be equal to zero, while this is definitely not true for the active end of the bar (Figure 2.15a). The difference in shear slip in both ends results in an elongation of the bar. The passive end of the bar doesn't move, since the slip at this place is equal to zero (FIB, 2008, pp. 141-143).

For a bar transferring a larger force, the anchorage and transmission length become equal, whereby the bond stresses and slip at the passive end aren't equal to zero but still smaller than at the active end (Figure 2.15b). The bar partly moves as a rigid body and partly elongates. For even larger forces the distribution of the bond stress reaches the capacity at each location along the bar and therefore becomes more uniform. For this reason, the full bond capacity over the full anchorage length is taken into account in ULS design.

Due to locally high bond stresses near the active end, the concrete starts cracking at this location. This reduces the bond stresses and might even eliminate force transfer along the first part of the bar (FIB, 2008, pp. 141-143). These reduced stresses are indicated by dashed lines in Figure 2.15.

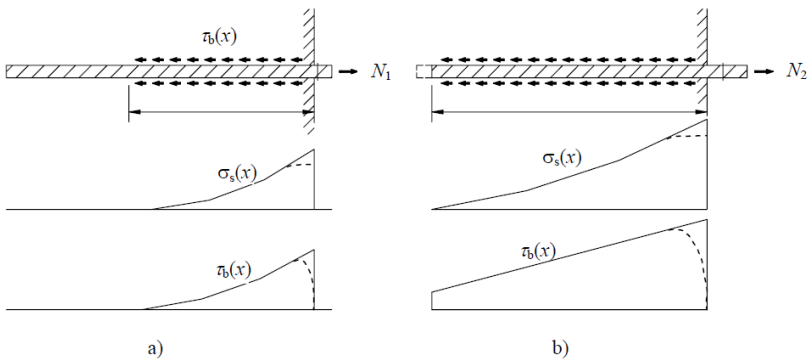

Figure 2.15 Anchorage of a tension bar. a. For a small tensile force. b. For a large tensile force. (FIB, 2008, p. 141)

As commonly known a structure must be able to redistribute forces when at a certain location the capacity is reached and it must show significant deformation before failure in order to warn people. For this reason ductility design is applied which demands connections to behave in a ductile manner. As discussed, the properties of end anchors and bond between the

reinforcement and the concrete element determine the capacity for concrete splitting and pull-out failure, two brittle failure modes. A properly designed tensile connection fails by extensional failure of the reinforcement. In this way the full ductility of the steel is used before failure occurs. The capacity governed by the two brittle failure modes must therefore be larger than the tensile capacity of the reinforcement. This sets strict requirements for the dimensions of end anchors and anchorage lengths.

Another type of tensile connection is the loop connection (See Figure 2.4, Figure 2.8 and Figure 2.38). The precast elements have protruding reinforcement loops which are connected in a joint that is casted in situ. This type of connection is also able to transfer shear forces and bending moments. It is often applied in continuous slabs (FIB, 2008, p. 191) and profiled shear joints.

Figure 2.16 illustrates the force transfer in the loop connection. The tensile forces in the reinforcement introduce a radial compressive stress in the concrete between the overlapping loops. This compressive stress is transferred by a compression diagonal to the adjacent reinforcement loop protruding from the connected concrete element. Concrete splitting tensile stresses occur in plane of the loops by the radial distribution of the compressive stress and also in plane of the diagonal concrete strut due to the inclination of the compressive stress. The loop reinforcement itself deals with the tensile stresses in plane. In order to take up the tensile stresses in plane of the strut, transverse reinforcement bars are required (FIB, 2008, pp. 191-192). In order to prevent concrete crushing of the diagonal strut, specific requirements are set for the dimensions of the connection (FIB, 2008, pp. 192-193). Application of the transverse reinforcement and the correct dimensions ensures the structural integrity and ductility of the connection, which fails by rupture of the steel. Maybe the transverse reinforcement can also contribute to the force transfer by dowel action (See section 2.2.3.3), but this isn't explicitly mentioned in studied literature.

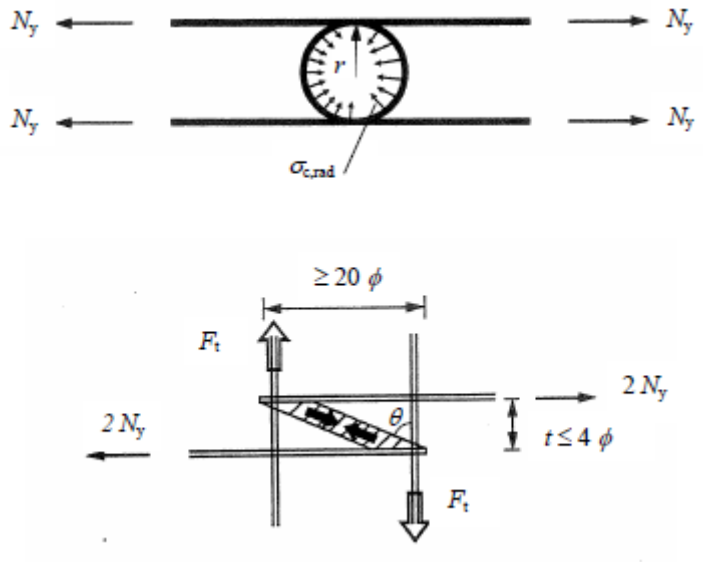

Figure 2.16 force transfer in a loop connection (FIB, 2008, p. 192)

Another way of transferring tensile forces is by using a dowel connection (Figure 2.19). Dowels are steel bars, connecting two or more elements, that are placed perpendicular to the direction of loading. In this way the dowels transfer the tensile forces by shearing. In the paragraph 2.2.3 dowel action is discussed in detail since it is mainly used to transfer shear forces.

2.2.3 Transfer of shear forces

In a structure shear forces are transferred between floor slabs and wall panels, two adjacent floor slabs and different wall panels of a stability wall. Different mechanisms can be used to transfer the shear forces from one element to another. These mechanisms are described in plenty of literature (Bachmann & Steinle, 2011; FIB, 2014; FIB, 2008; van Keulen, 2015; ten Hagen, 2012):

- Adhesion
- Friction due to external compression
- Friction due to clamping forces induced by transverse reinforcement
- Dowel Action
- Shear locking or mechanical interlocking

This paragraph describes the mechanisms for shear transfer and their possible interaction. Understanding of these mechanisms is essential for the investigation into shear connections. It must be noticed that shear can also be transferred by mechanical devices in the elements connected by welds. This type of connection does not specifically rely on any of the five mechanisms and is therefore not discussed any further.

2.2.3.1 Adhesion

Bond between the precast element and the joint grout or concrete is caused by adhesive forces between the two materials. Shear transfer by adhesion behaves very stiff, like a monolithic structure. However, as already mentioned, adhesion is very easily affected by executive circumstances and restrained deformations of the structure. In many cases the interface must be assumed as cracked, whereby force transfer by adhesion isn't possible.

2.2.3.2 Shear friction

In structural engineering friction in a contact surface is often used to transfer shear forces. In a raft foundation for instance, the resultant horizontal force on the structure is transferred to the soil by friction between the concrete slab and the soil. This concept is for example regularly applied in the foundation of hydraulic structures. The capacity of this transfer mechanism in that case can be determined by the following formula: $F = \mu * N$. Here μ is the friction coefficient of the specific contact surface and N the force acting normal to the contact surface. This formula indicates the importance of a constant normal pressure in the joint for the friction mechanism to take place.

Figure 2.17 shows schematically the transfer of shear forces by friction between concrete elements and joint grout or concrete. The normal force N_c can originate from different effects. In a horizontal joint of a load bearing wall, a normal gravity force will always be present. In other connections the joint can be prestressed, which is a rather complicated and expensive option, or transverse reinforcement can be applied. This reinforcement is initially unloaded, but will be stretched as a result of dilatation of the joint. The horizontal shear load will cause a certain slip of the cracked interface. The crack will open as a result of the roughness of the contact surface, as illustrated in Figure 2.17c. The dilatation of the joint imposes an elongation of the steel reinforcement. The tensile force in the reinforcement is compensated by a compressive force in the concrete, facilitating friction to take place.

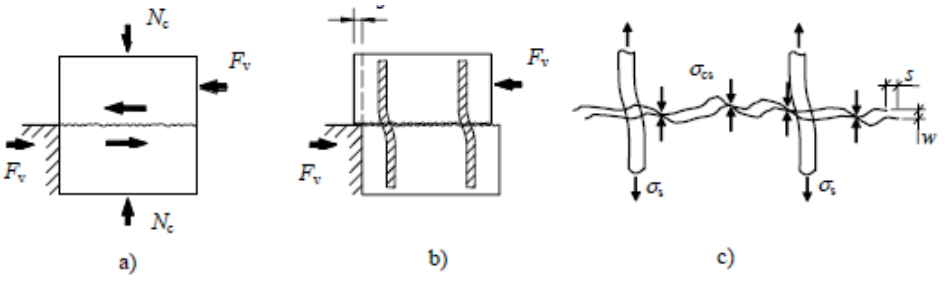

Figure 2.17 Shear friction a. compression by external load b & c. compression by lateral reinforcement (FIB, 2008, p. 199)

The process is clearly governed by two characteristics: The normal force and the roughness of the surface. Both determine the relations between shear slip and dilatation and shear resistance. The importance of the surface roughness leads to the desire of classifying interfaces according to their roughness. Different methods are developed for this purpose, among which the classification of the Eurocode (FIB, 2008, pp. 222-224).

The relation between the slip and dilatation width is presented in Figure 2.18a. First the dilatation increases with increasing slip, but at a certain point the effect of the surface's largest unevenness is fully included whereby the separation of the surfaces remains constant. The maximum dilatation is larger for a rougher surface. As the figure indicates as well, a large normal stress reduces the maximum dilatation. The normal stress crushes the irregularities in the joint surface, reducing the maximum dilatation. The most prominent irregularities will crush the first, whereby a more uniform roughness develops over the joint, improving the uniformity of the shear stress distribution over the joint (FIB, 2008, pp. 124-129). Just like the relation between the slip and dilatation, the relation between slip and shear resistance is also asymptotic, as shown in Figure 2.18b in the upper diagram.

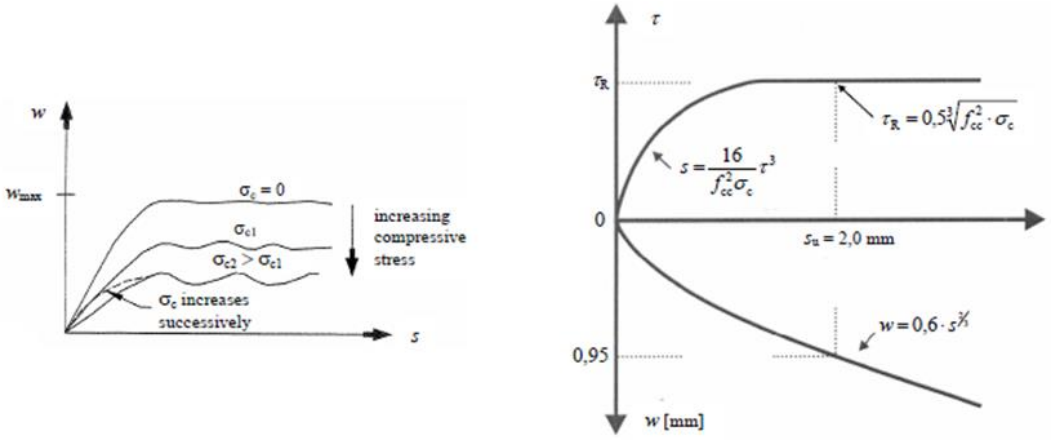

Figure 2.18 a. slip-dilatation relation b. shear-slip relation (FIB, 2008, pp. 225,229)

According to the basic formula for shear friction: $F = \mu * N$, the capacity can be increased by either improving the surface roughness or creating a larger normal stress. The latter can be obtained by applying a larger amount of transverse reinforcement bars, all elongated by the dilatation of the joint (FIB, 2014, p. 107). However, the capacity won't rise to infinity. The upper limit is determined by the compressive strength of the concrete (FIB, 2008, p. 199). This upper limit is described by the study of Nielsen in 1984 (FIB, 2008, pp. 235-236). The combination of the vertical compressive stress and the horizontal shear stress leads to an inclined compressive

force in the concrete relative to the face of the joint. Theory of plasticity is applied to evaluate the force equilibrium of the shear force, tensile force in the steel and concrete compressive force at the moment when the steel yields and the concrete crushes. This evaluation determines the amount of reinforcement leading to the maximum capacity. This depends on the angle between the compressive forces and the joint, which is determined by the friction coefficient.

The transverse reinforcement must be anchored in the concrete elements. Just as for tensile connections, this can be done by bond or end anchors. The major difference between the two is the magnitude of the tensile force that develops. In a bar with end anchors without bond, the elongation of the bar is spread over its full length, whereas in a bonded bar the elongation is localized near the joint interface. The relation for the stress in the bar is given by:

$$\sigma_{bar} = E * \frac{w_{joint}}{L}$$

The elongation of the bars in both cases is equal to the dilatation of the joint. However, since the stress is inversely proportional to the length over which the elongation occurs, the force in the bar anchored by bond is much larger. This results in a larger compressive stress over the joint and so a larger shear capacity. The maximum capacity is normally reached when the steel yields and the compressive stress in the concrete is equal to: $\sigma_{concrete} = \rho * f_y$ (FIB, 2008, pp. 230-233). For reinforcement anchored by bond and a relatively rough interface surface, the friction mechanism will show the stiffest behaviour. This combination will lead to a large increase in normal compressive stress for relatively small shear slip (FIB, 2008, p. 234).

Besides the factors discussed previously, the angle between the steel bars and the friction interface also influences the capacity of the joint. If the bars are not perpendicular to the interface, the component of the force in the bar along the interface directly contributes to the shear capacity and the perpendicular component contributes to the shear capacity by introducing a perpendicular compressive stress over the joint (FIB, 2008, p. 234).

2.2.3.3 Dowel action

Another way to transfer shear forces is by dowel action of steel bars. The bars are placed perpendicular to the direction of the force and therefore loaded by pure shear. Figure 2.19 illustrates the loading conditions of the dowel.

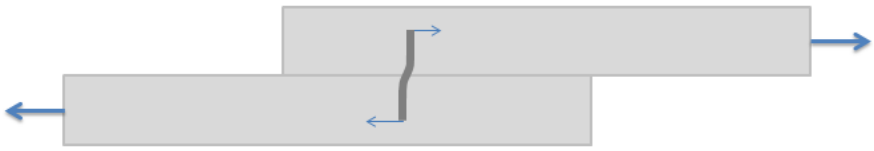

Figure 2.19 Schematic representation of dowel action

The mechanism can fail in three different manners (FIB, 2008, p. 203):

- Steel shear failure
- Concrete splitting failure
- Steel flexural failure with local concrete crushing

Occurrence of the first failure mode is prevented by applying a bar with a sufficiently large cross section. The second failure mode can occur as a result of the concentrated dowel force and is prevented by a large concrete cover or the use of splitting reinforcement designed by a strut and tie model. So in practical situations the third failure mode, which is the most ductile one, will govern the capacity.

When evaluating the dowel capacity, the analogy with a beam on an elastic foundation is applied. As Figure 2.20 shows, the bearing stress in the concrete is not uniformly distributed over the length of the dowel, according to this analogy (FIB, 2014, p. 106; FIB, 2008, p. 203).

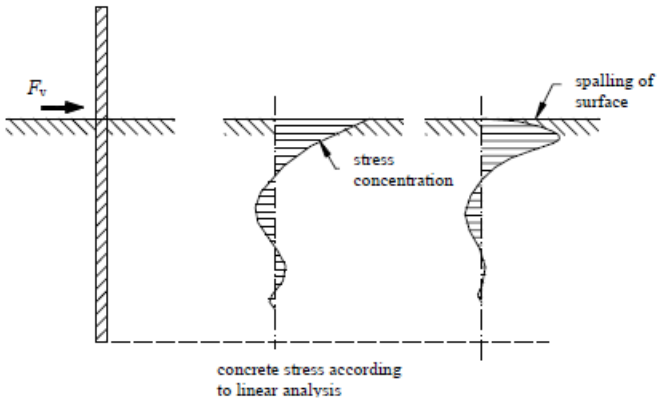

Figure 2.20 Dowel action model, similar to beam with elastic foundation (FIB, 2008, p. 203)

Large concrete bearing stresses occur near the joint surface leading to a maximum bending moment in the dowel at a small distance below the joint. In the plastic model created by Hojlund-Rasmussen in 1963, the equilibrium of the dowel is analysed when both the concrete and the steel are in the plastic state (FIB, 2008, pp. 205-207). This means a plastic hinge has developed at the location of maximum bending in the bar and the concrete bearing stress over the distance between the joint surface and this hinge is equal to the crushing capacity of the concrete in a tri-axial state (This is the part with the highest concrete bearing stresses according to Figure 2.20). The shear force in the steel bar at the location of the plastic hinge is equal to zero. So the load must be equal to the bearing reaction over the distance between the joint surface and the hinge. From this condition the distance between the hinge and the joint is determined. Thereafter the equilibrium of the induced bending moment and the plastic bending capacity of the dowel provide the definition of the maximum shear force that can be transferred by the dowel. The method is applied for dowels in different configurations, resulting in a specific capacity for each case.

Although a dowel connection can have a large strength, its stiffness is relatively small, since large slippage is required to utilize the full capacity of the connection (FIB, 2008, p. 205).

2.2.3.4 Combination of shear friction and dowel action

The book by FIB describes the combination of the two discussed effects (FIB, 2008, pp. 220-222). It can be understood by now, that the transverse reinforcement of a connection based on shear friction will also transfer part of the shear force by dowel action. The ratio between the two effects is not quantified, but analysed qualitatively and depends mainly on two parameters:

- The anchorage of the transverse reinforcement
- The roughness of the joint interface

The way the bars are anchored determines to a great extend their axial stress as a result of joint dilatation. When a bar isn't anchored at all, the only mechanism contributing to the shear capacity is dowel action. On the opposite, when the bar is anchored by bond the tensile stress especially near the joint becomes too large to have any capacity of the bar left for dowel action.

A joint with a rough surface will lead to a larger contribution of shear friction, whereas a perfectly smooth surface doesn't rely on friction at all. The mechanism of shear friction with a rough surface will generally result in a smaller slip than required for full use of dowel action. So in a joint with a very rough interface, the dowel action cannot really develop and will therefore hardly contribute.

Especially for bars with end anchors a combination of the two mechanisms transfers the shear force between the elements. The total capacity is the summation of the two contributions. In this case a reduced steel strength must be taken into account for the dowel action capacity, since part of the tensile strength is already used by the elongation due to the shear friction. The following formula can be applied for a combined action, with the first term the capacity for dowel action and the second term the capacity for shear friction (FIB, 2008, p. 221):

$$F_{shear,R} = \alpha_0 \phi^2 * \sqrt{f_{cc,max} * (f_{yd} - \sigma_s)} + \mu * \sigma_s * A_s$$

In general the dowel effect of the reinforcement is relatively small compared to the contribution to shear friction (Bachmann & Steinle, 2011, p. 204). The unity check for dowels loaded by a combination of pull-out resistance and dowel action is given by (FIB, 2008, p. 237):

$$\left(\frac{\sigma_s}{f_y}\right)^{0,2} + \left(\frac{F_{v,dowel}}{F_{vRd,dowel}}\right)^{0,2} \leq 1{,}0$$

2.2.3.5 Shear locking

Another important shear transfer mechanism is shear lock, occurring in a profiled joint. The profiles are created in the precast concrete factory by the shape of the moulds. The indented surfaces of the profile enable shear transfer between precast concrete elements by a compressive force. The major advantage of the mechanism is the large strength it develops with a minimal shear slip, the reason for its name. Figure 2.21 shows the force transfer in the profiled interface. When the force cannot be perpendicular to the contact surface, some shear friction will develop in the interface as well. The combination of both mechanisms will in that case transfer the shear force. This is discussed in more detail in the next paragraph.

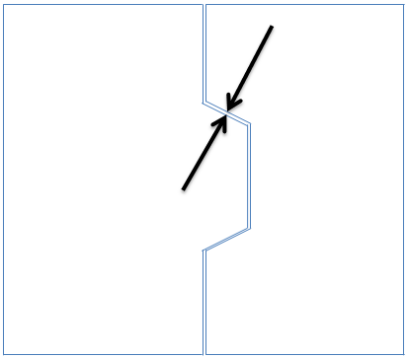

Figure 2.21 Mechanical interlocking

2.3 Profiled shear connections

This paragraph zooms in on profiled/keyed shear connections, which are illustrated in Figure 2.28. This kind of connection is often applied for vertical joints between wall panels, organised in a stacked configuration. The connection consists of a joint filled with mortar or concrete between two profiled faces of precast concrete elements and transverse reinforcement resisting dilatation of the joint. This reinforcement can either be concentrated or distributed over the connection. The whole connection may use all five shear transfer mechanisms of previous paragraph to transfer shear forces from one element to the other.

The mortar connections developed by Van Keulen, of which the behaviour is further analysed in this study, are profiled shear connections as well. Characteristic for these connections are the filling with mortar instead of concrete and the use of concentrated instead of distributed reinforcement. So understanding of the profiled shear connection's behaviour is essential for the research performed in this thesis. This paragraph describes the knowledge obtained from previous research. Chapter 4 will discuss the conclusions of Van Keulen's study.

Most available literature only deals with aligned profiled joints, like the joint shown in Figure 2.28, at which the profiled surfaces of both elements are mirrored in a vertical axis through the joint. Van Keulen also developed new profiles, which will be dealt with in this research project as well (van Keulen, 2015). These profiles are only discussed in Chapter 4, whereas all information in this paragraph is based on the aligned profile.

The paragraph starts with describing the structural mechanism of a single shear key. Thereafter some characteristics of a complete keyed shear connection are discussed. These are the influence of transverse reinforcement and lateral stiffness, the strength and stiffness properties of a keyed shear joint and the effect of shrinkage. The paragraph concludes with an overview of results from previous parameter studies.

2.3.1 Force transfer in a single shear key

In each of the shear keys a diagonal compressive strut will develop, as illustrated in Figure 2.22. This shear locking contributes most to the shear transfer. While the vertical component of the compressive force in this strut transfers the vertical shear force V between the elements, the horizontal component pushes the two elements aside. In order to let the mechanism function, the horizontal motion of the elements must be prevented by a resistant transverse force H. This can be done by applying reinforcement in the joint, tying the elements together (FIB, 2014, pp. 124-126). The advantage of shear lock is the possibility to transfer the shear force mainly by compression in the diagonal strut, resulting in a relatively small shear slip and therefore a relatively stiff behaviour.

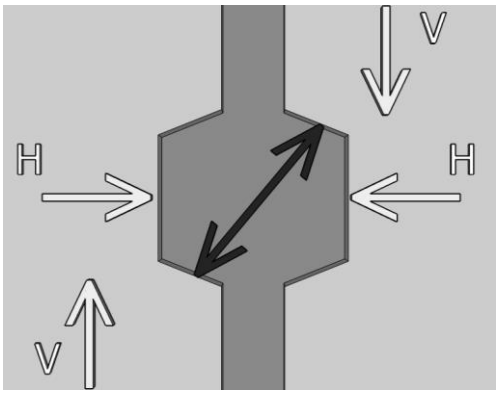

Figure 2.22 Shear lock principle in one shear key

In order to explain the process in a shear key in more detail, the angles beta and gamma are defined as indicated in Figure 2.23.

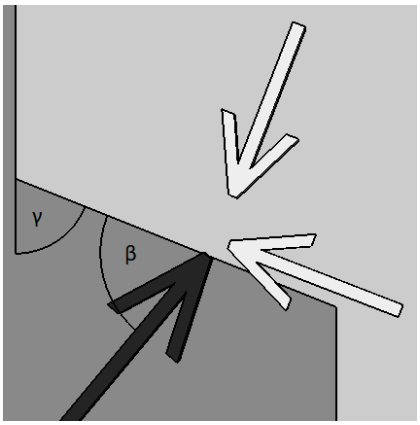

Figure 2.23 Resulting forces on the joint-element interface for a diagonal force acting under an angle

Research by Cholewicki describes the force transfer on the interface in more detail. He states that the vertical shear force V is transferred partly by shearlocking via the diagonal force and partly by shear friction via a frictional force developed in the interface. The frictional force is transferred as a shear force in the joint material to the interface at the other side, where it is again transferred to the adjacent element by friction in the interface surface (Cholewicki, 1971). The force transfer for beta equal to 90 degrees is illustrated in Figure 2.24.

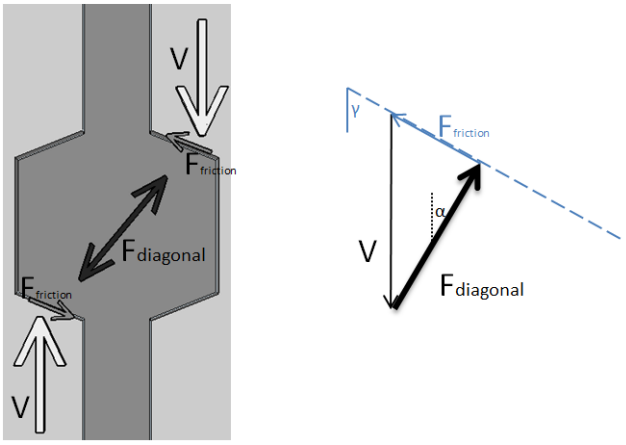

Figure 2.24 Force equilibrium in a shear key with sufficient friction in the interface

The equilibrium of forces deviates from that of Figure 2.24 in three cases:

- The frictional capacity of the interface is too small
- The angle beta is smaller than 90 degrees
- The angle beta is larger than 90 degrees

The research by Cholewicki states that if angle gamma (Figure 2.23) becomes smaller than 56 degrees, the friction developed in the contact surface is no longer sufficient to take up the required part of the vertical shear force. In that case transverse horizontal reinforcement must be applied to provide equilibrium. The component of this horizontal force H dissolved along the friction surface compensates for the insufficient frictional force. The component of the force perpendicular to the interface is taken up by the diagonal compressive force (Cholewicki, 1971). This is illustrated in Figure 2.25, where H_s is the component of the horizontal force parallel to the friction plane and H_n the component normal to the plane. As can be seen in the force diagram, the force in the diagonal is H_n larger than it would be if the frictional force was sufficiently large. This would be if the friction capacity is at least equal to $F_{friction}$ plus H_s.

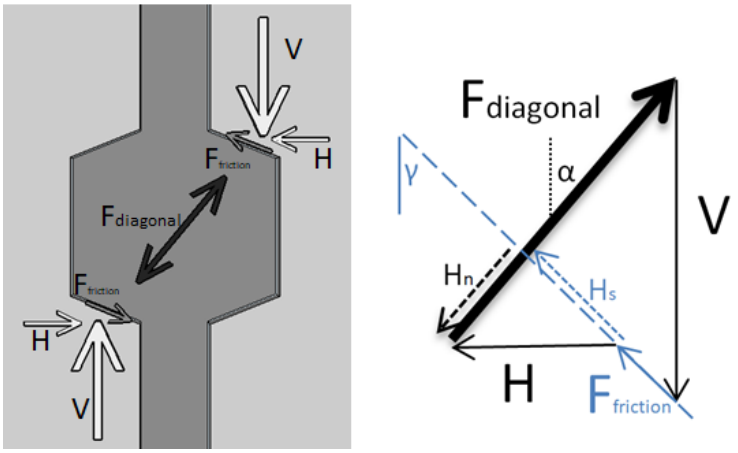

Figure 2.25 Force equilibrium in a shear key with insufficient friction in the interface

So far Cholewicki described a situation with a perpendicular diagonal, but if the diagonal force is not exactly perpendicular to the plane of the interface, the equilibrium of forces changes. When the diagonal force is steeper, a smaller friction force develops in the interface, since the diagonal force is more in line the vertical load. When the diagonal force is more horizontal, a larger frictional force is required, but the frictional capacity is limited. Therefore more reinforcement is in most cases required to take up the large horizontal component of the diagonal force in this situation. The equilibrium of both situations is illustrated in Figure 2.26.

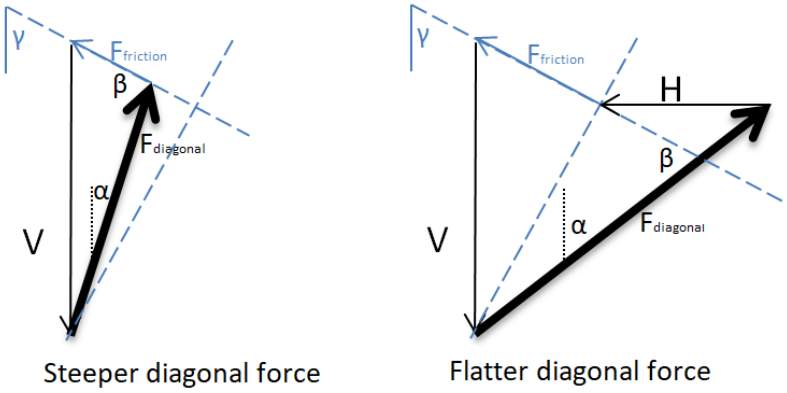

Figure 2.26 Equilibrium situation for non-perpendicular diagonal forces

The maximum capacity of a shear key is reached when it fails by one of the failure mechanisms (FIB, 2008, p. 248), which are illustrated in Figure 2.27. In failure by mechanism A, a crack parallel to the compression diagonal develops due to lateral tensile stresses. Failure mechanism B illustrates the failure by crushing and shearing of the compressive strut. In mechanism C a shear crack develops across the shear key and in D the joint slips over the indented surface (van Keulen, 2015, p. 13; FIB, 2014, p. 125). After failure of the shear key, friction in the crack still transfers a shear force between the elements.

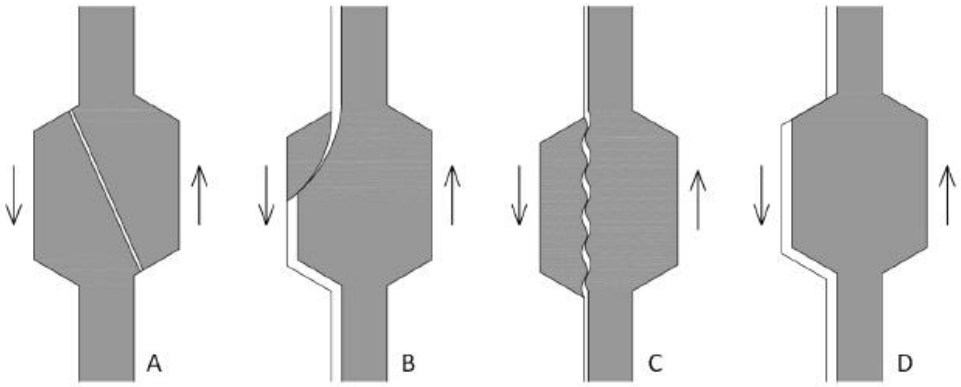

Figure 2.27 Failure mechanisms of a shear key (van Keulen, 2015, p. 14)

2.3.2 The effect of reinforcement and lateral stiffness in profiled shear connections

The layout of a profiled shear connection is illustrated in Figure 2.28. The joint between the wall panels contains several shear keys, where diagonal struts can develop. The compression diagonals in the joint exert a horizontal force on the adjacent concrete elements. The integrity of the connection is provided by transverse reinforcement keeping the elements and the connecting joint material together. This reinforcement can be distributed over the full height of the joint or concentrated at the upper and lower horizontal joints as illustrated in Figure 2.28. This section describes the differences between the two options.

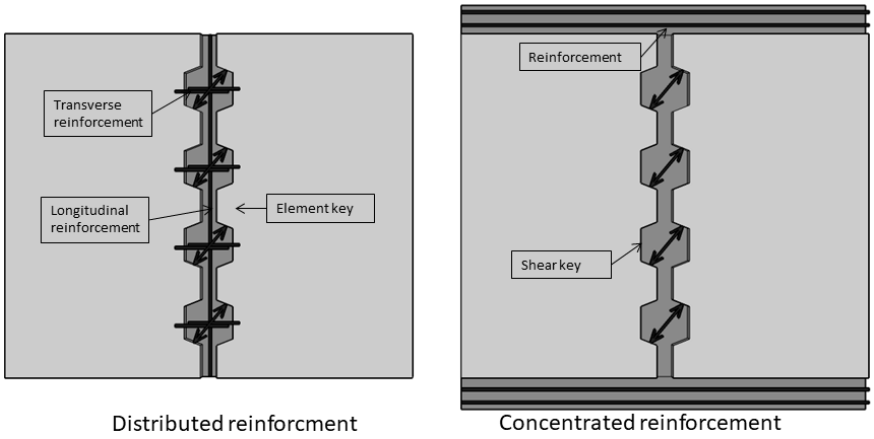

Figure 2.28 Profiled shear joint reinforced in two ways a. distributed reinforcement b. concentrated reinforcement

In case distributed reinforcement is applied, usually horizontal reinforcement loops with a transverse bar are used (FIB, 2014, p. 125). The connection with this type of reinforcement is illustrated in Figure 2.28a and in more detail in Figure 2.38. The way this reinforcement transfers the tensile force is described in section 2.2.2. Although the distributed reinforcement is beneficial for the transfer of forces, the use of this type of reinforcement is rather inconvenient with respect to fabrication and construction, as discussed in paragraph 2.1. An alternative with vertical loops (Figure 2.8) is developed by Sørensen et al. resulting in more manoeuvrability, while keeping the complications in fabrication (Sorensen, Hoang, Olesen, & Fischer, 2017).

With reinforcement concentrated in the horizontal joints at floor level, the in plane bending stiffness of the precast elements must be sufficient to keep contact between the elements and the joint material (van Keulen, 2015). The principle is illustrated in Figure 2.29. If openings in the wall elements are present, the in plane stiffness is relatively low, which affects the behaviour of the joint. In this case the "columns" between the openings and the joint can be seen as beams simply supported by the tension ties. The lateral stiffness of the connection is therefore partly determined by the bending stiffness of these columns. Applying concentrated reinforcement is discommended for joints between perpendicular walls, for which the required stiffness cannot be provided (Bachmann & Steinle, 2011, p. 71). At one side of the joint the stiffness must be provided by the out of plane bending stiffness of the wall panel, which is generally rather low. The effect is illustrated in Figure 2.30.

The shear stiffness of the connections with concentrated reinforcement depends among others on the lateral stiffness provided by the adjacent elements. The exact relation between the lateral stiffness and the shear stiffness is yet unknown, but based on the results of Van Keulen a lower lateral stiffness is expected to lead to a lower shear stiffness (van Keulen, 2015). Van Keulen also concludes, based on his test results, that the shear capacity of a profiled joint is increased by increasing the lateral stiffness (van Keulen, 2015, p. 47).

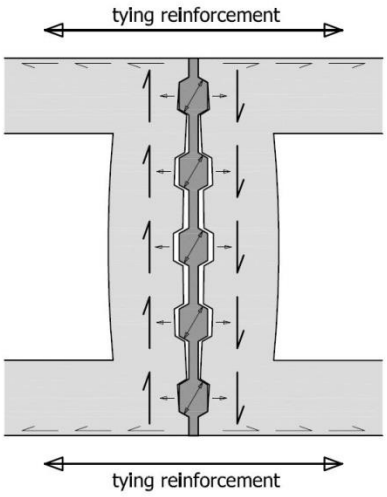

Figure 2.29 Principle of unreinforced mortar joint with concentrated tension ties (van Keulen, 2015)

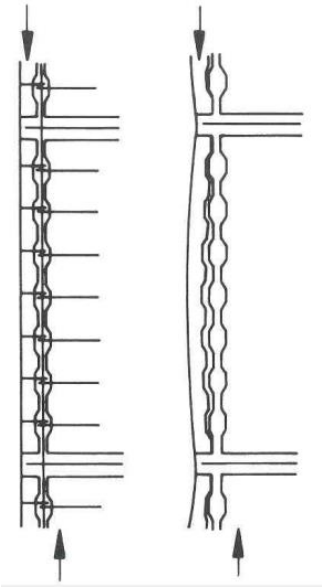

Figure 2.30 Recommended reinforcement for perpendicular walls (Bachmann & Steinle, 2011, p. 71)

The amount of required transverse reinforcement can for instance be determined by the formula proposed by H. Schwing ((Bachmann & Steinle, 2011, pp. 206-207) as published by H. Schwing 1980). According to this method the amount of required reinforcement depends on the shear key geometry, the material properties of concrete and steel and the present perpendicular compressive stress. For concentrated reinforcement Schwing proposes an extra increase of the amount of steel by a factor of 1/0.85.

Schwing distinguishes connections with concentrated or distributed reinforcement by this factor, which indicates their capacity is not the same. The difference in capacity is important to know. Previous studies mainly focused on the difference in obtained capacity, when considering concentrated reinforcement, but the difference in shear stiffness is also of importance. Distributed reinforcement is more common and therefore investigated more thoroughly in past research.

In the SBI97 report on keyed shear joints (Hansen, et al., 1976) two tests are compared, one with concentrated and one with distributed reinforcement. Here it was concluded that the efficiency of the concentrated reinforcement is just ten to twenty percent smaller than for the connection with the best reinforcement distribution along the joint, but this difference is of the same order as the scatter of the test results (Hansen, et al., 1976). Tests performed by Cholewicki indicate that the effect of the location of reinforcement on the capacity of the joint is not significant (Cholewicki, 1971). It seems reasonable to expect a reduction in capacity when the reinforcement is applied externally.

Applying concentrated reinforcement also influences the shear stress distribution over the joint. As discussed, distributed reinforcement provides a relatively large uniform lateral stiffness along the joint. Therefore all the shear keys will have the same stiffness and capacity. For a joint with concentrated reinforcement the lateral stiffness is largely dependent on the adjacent precast elements. Especially when these elements contain openings, the lateral stiffness deviates over the height of the joint. It will be the largest close to the reinforcement at the upper and lower boundary and the smallest at the location next to an opening in the adjacent wall elements. This will lead to a less uniform force distribution over the shear keys, for which the largest shear forces will be transferred by the upper and lower shear key.

The force transfer within a shear key is also different when distributed reinforcement is applied. First of all the reinforcement crossing each shear key doesn't only contribute indirectly by providing horizontal equilibrium, it will also directly transfer shear forces by dowel action (Cholewicki, 1971). However, the mechanism of dowel action is less stiff than shear lock, whereby its effect is neglected by Cholewicki. Secondly, the reinforcement will provide an extra shear key (Hansen, et al., 1976). Hansen et al. are not explaining this statement any further, but Van Keulen mentions a changed force transfer as a result of pushing of the diagonals against the reinforcement (Van Keulen, Vertical mortar connections for shear transfer between precast concrete large panel elements, 2018). Combining the two statements it can be concluded that the reinforcement loops that are crossing the shear key enable two compression diagonals to develop, while just one diagonal is present in an unreinforced key. This will enlarge the shear capacity.

2.3.3 Strength and stiffness behaviour of a profiled shear joint

The profiled shear connection transfers shear forces mainly by shear lock in the created shear keys. However, the other transfer mechanisms discussed in the previous paragraph play a role as well. The stiffness relation between shear slip and shear stress for the joint has been described by many (FIB, 2008; Hansen, et al., 1976; Olesen, 1975; van Keulen, 2015; Sorensen, Hoang, Olesen, & Fischer, 2017; Abdul-Wahab, 1986; Cholewicki, 1971)

As is stated in the book by FIB on structural connections, the shear transfer in a profiled joint appears as a combination of adhesion, friction, dowel action and shear lock. However, adhesion will only contribute when the shear slip is rather small, since a larger shear slip causes the interface to crack. Mobilised by the shear slip, the other three mechanisms start transferring the shear force. In this stage the resistance of the joint can be determined by summation of the effects. The contribution of each effect depends on its stiffness. Dowel action for example takes place for relatively large displacements, whereby its contribution will be rather small (FIB, 2008, pp. 246-248).

Many tests have been performed on profiled shear connections. All papers describing these tests and their results also provide empirical formulas for the shear capacity and often the cracking load as well. All these formulas are created to agree with the specific test results and are therefore only applicable in specific cases. Currently the Eurocode provides a formula for the shear capacity of a concrete to concrete joint. Although this formula is originally used for interfaces between concrete elements casted on different times, it is also applied for profiled mortar joints. Together with this formula a couple of dimensional requirements are set for the profiling and transverse reinforcement, which are indicated in Figure 2.31.

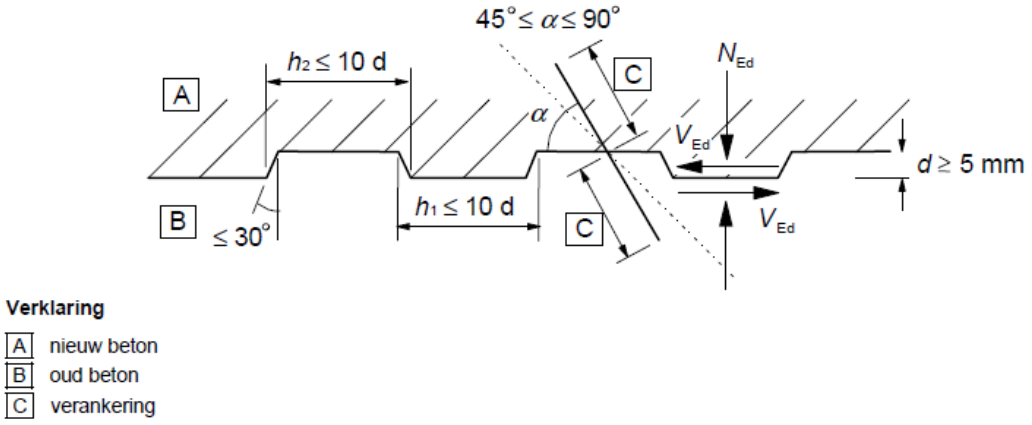

Figure 2.31 Profiled joint dimensions (NEN, 2011)

The formula is given as (NEN, 2011):

$$v_{Rdi} = c * f_{ctd} + \mu * \sigma_n + \rho f_{yd} (\mu \sin \alpha + \cos \alpha) \leq 0{,}5\, \nu f_{cd}$$

The first term is the contribution of cohesion, the second term the contribution of friction as a result of transverse compressive stress. The third term is partly the contribution to the shear capacity of friction due to transverse compressive stress induced by the reinforcement and partly the direct contribution of axial forces in the inclined reinforcement. The advantage of having a profiled surface is taken into account by applying a larger value for c and μ, equal to 0.5 and 0.9 respectively. So the shear lock effect is not included by a separate term. The effect of dowel action of the reinforcement is neglected completely.

In the SBI 97 report on keyed shear joints (Hansen, et al., 1976) a summary is given of several tests performed on profiled shear connections in the years before 1976. The results of these tests show a large correspondence in the shear stress-slip behaviour of the joints, despite the different test conditions. Figure 2.32 shows the observed relation in a schematic way.

Initially the shear stresses are completely transferred by adhesion in the interfaces of the precast elements and the joint mortar or concrete. The connection acts very stiff in this stage, since it basically behaves monolithic. However, this transfer mechanism's capacity is rather low, because adhesion failure occurs for relatively small values of the shear stress by cracking of the interface between the elements and the joint material. Force transfer is mainly taken over by developed compressive struts in the shear keys, whereby the stiffness of the joint is somewhat reduced compared to the first stage. The transfer of forces by diagonal struts is schematically

illustrated in Figure 2.22. When the joint material eventually starts cracking at the cracking load, a noticeable gradual reduction in stiffness takes place. The shear slip increases faster than the shear resistance until the point where the ultimate capacity is reached. At this point the compression diagonals fail as a result of one of the failure modes shown in Figure 2.27. The occurring type of failure depends among others on the geometry of the shear key. The post critical behaviour depends largely on the type of failure that has occurred. Some results show a large ductility, while others do not (Hansen, et al., 1976). The residual strength of the joint is provided by the possible amount of shear friction acting in the crack surface. This can only take place with sufficient lateral stiffness to keep the friction surface under compression.

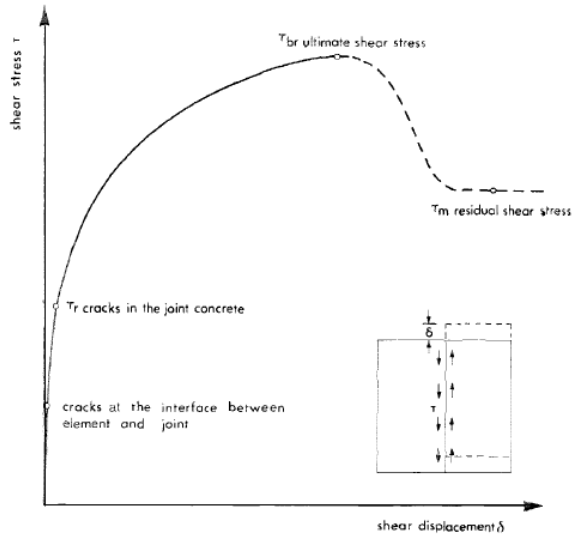

Figure 2.32 Global Stress-Slip relation for profiled shear connections (Hansen, et al., 1976)

When the keyed shear joint is compared to a joint with a smooth surface, the difference is clearly visible. Figure 2.33 shows the relatively large initial stiffness and capacity for a joint with shear keys. The residual strength based on friction is equal to that of the smooth joint, since the force transfer is similar (FIB, 2008, p. 249). The increased capacity of a keyed surface compared to a smooth surface can be 40 percent larger according to the test on drypack grout joints described by Rizkalla et al. (Rizkalla, Foerster, & Scott Heuvel, 1989). However, tests on other unreinforced grouted shear key joints state the increase of capacity is around 60 percent and even the residual strength increases by 25 percent (Rizkalla, Serrette, Scott Heuvel, & Attiogbe, 1989).

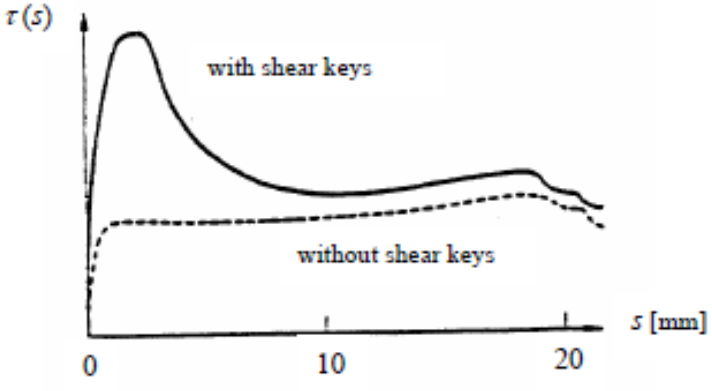

Figure 2.33 Comparison between joint with and without shear keys ((FIB, 2008, p. 249) originally from SBI (1979))

Several sources describe a phenomenon that only occurs in aligned profiled shear joints (Abdul-Wahab, 1986; Cholewicki, 1971; FIB, 2008). For this type of joint compression diagonals aren't just formed in each shear key, as in Figure 2.28, but also between two successive keys, as in Figure 2.34. These larger diagonals are steeper, whereby their reaction to vertical shear is stiffer. Therefore the force transfer is mainly provided by these diagonals. After certain crack development in the joint, the diagonals within one key are cancelled out. The large diagonals take over the full force transfer. The effect of this property of aligned profiles on the shear slip relation is for example clearly observed in the tests by Van Keulen, which are discussed in section 4.1.2 (van Keulen, 2015).

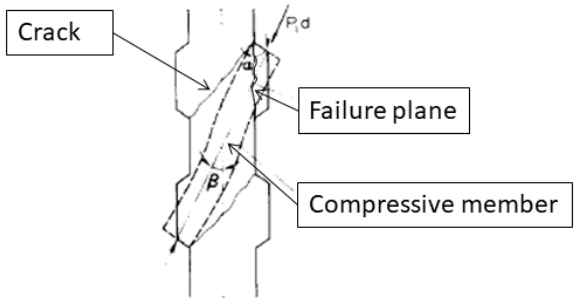

Figure 2.34 Compression diagonal over two shear keys in aligned profile (Cholewicki, 1971)

2.3.4 The effect of shrinkage of the joint material

The shear slip behaviour of the joints as discussed in the previous section assumes an initial adhesive force in the interface between precast element and joint material. This bond will enable a monolithic response of the joint for loads smaller than the interface capacity. When the interface is loaded beyond its capacity, an interface crack is formed resulting in transfer by friction in the interface. The behaviour is schematically shown in Figure 2.35.

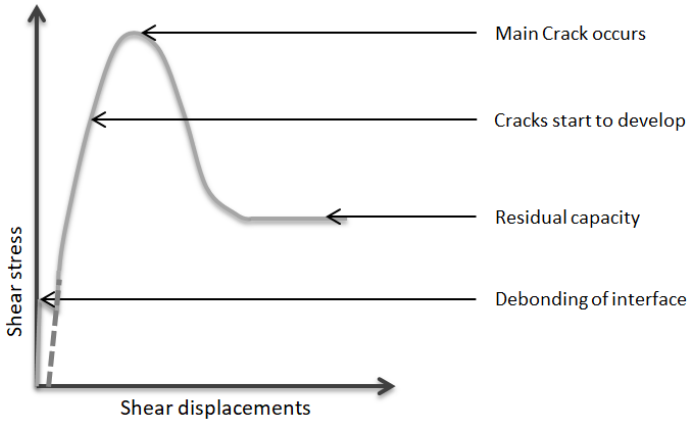

Figure 2.35 Schematic representation of joint behaviour

However, this behaviour is obtained in test situations where shrinkage of the joint material is compensated for or hasn't occurred yet. In practice the joint material will shrink after it is applied at the construction site. This causes an initial crack along the interface between the precast concrete elements and the joint material. This crack will obstruct the adhesive forces that do develop in a test (Hansen, et al., 1976). Consequently the theoretical shear-slip relation of Figure 2.35 won't be valid for a practical application. The practical shear-slip relation isn't known from literature, but can be estimated. Since the crack will create a gap between the joint material and the precast elements, the joint will firstly deform until a contact surface is restored,

thereafter force transfer takes place by friction and shear lock. The first peak in Figure 2.35 isn't observed, since the initial stiffness is considerably lowered by lack of adhesion and debonding doesn't take place. The hypothetical shear slip relation with shrinkage is shown by the dashed line in Figure 2.35.

This shrinkage behaviour holds for shear connections where old types of mortar are applied. Nowadays special types of mortar are developed that hardly shrink. It should be investigated if a joint with such a modern mortar can transfer shear forces by adhesion. If so, the stiff behaviour of this shear transfer mechanism may be taken into account, which is very beneficial for the design of stability wall structures.

It should be noted that the precast elements will shrink as well. However, since the elements are casted earlier, the major part of the shrinkage has already taken place by the time of installation.

Some studies did consider the effect of shrinkage cracks on the characteristic properties of the profiled joint. One of these tests was performed by Hansen and Olesen on joints with concentrated reinforcement, as described in the SBI97 report on keyed shear joints (Hansen, et al., 1976). Based on these tests some conclusions were made:

- The influence of shrinkage on the cracking and ultimate load was minimal
- The stiffness seems to be reduced by shrinkage, there is spoken of "some correlation"

The tests were performed on relatively small specimens. The effect of shrinkage might be more significant for larger elements. Furthermore other tests performed by Hansen also indicate that the capacity of the joint is not affected by initial shrinkage cracks (Hansen H. , 1967).

The question arises what the effect over the complete shear wall would be. The behaviour in a complete wall is described in the SBI97 report and in an article by one of co-authors of this report, S.Ø. Olesen (Hansen, et al., 1976; Olesen, 1975). Figure 2.36 shows an aligned reinforced mortar joint where a shrinkage crack, creating a gap, is present at the right joint-element interface. Due to this gap any shear force is in first instance transferred by dowel action of the concentrated reinforcement in the horizontal joint, as seen in Figure 2.36a. However, the shear capacity of the dowels is limited whereby cracks develop in the horizontal joint when the loading shear force reached a certain value. This cracking process induces larger displacements of the wall panels, leading to a closure of the shrinkage crack. Consequently the vertical joint takes over the shear force transfer by friction and shear lock, as seen in Figure 2.36b.

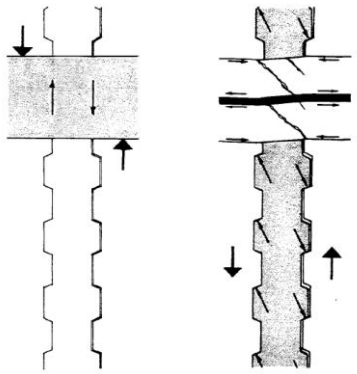

Figure 2.36 Shear transfer in a joint subject to shrinkage (Olesen, 1975)

When the load is increased, eventually cracks will develop in the joint material and for a certain value of the load the vertical joint fails as well. Since the shear stresses aren't uniformly distributed over the shear wall, the redistribution of forces from the horizontal to the vertical joint develops gradually over the wall while the load increases. For this reason a vertical joint in the lower part of the wall might already reach its capacity, while at another place the shear force is still transferred by dowel action. That is why the ductility of the vertical joints is of large importance for the way the complete wall fails. If the joints fail in a brittle manner, this might lead to a chain reaction, resulting in brittle failure of the wall. If the joints do have a certain ductility, the shear stresses redistribute over the wall, whereby the total load can still be increased until many other joints have reached their capacity as well (Olesen, 1975).

A more detailed study into the aspects that play a role in the shrinkage behaviour of the profiled mortar connections is necessary. Some aspects can have such a significant influence on the behaviour that the process explained above isn't applicable anymore. Examples of these aspects are the application of mortar with an expansion component and the lateral expansion of the adjacent wall elements due to the vertical load acting on them. However, in first instance this study will consider a situation where the interface is cracked as a result of shrinkage.

2.3.5 Parameters influencing the behaviour

Factors as geometry, concrete strength, joint material strength and reinforcement influence the behaviour of the shear connection. This section describes these relations according to the information found in literature.

2.3.5.1 Angle of the shear key surface

The angle of the shear key surface partly determines the strength and ductility of the keyed shear connection, as was investigated by Eriksson et al. for unreinforced keyed shear connections. The influence of a varying angle is indicated by the results of the study presented in Figure 2.37.

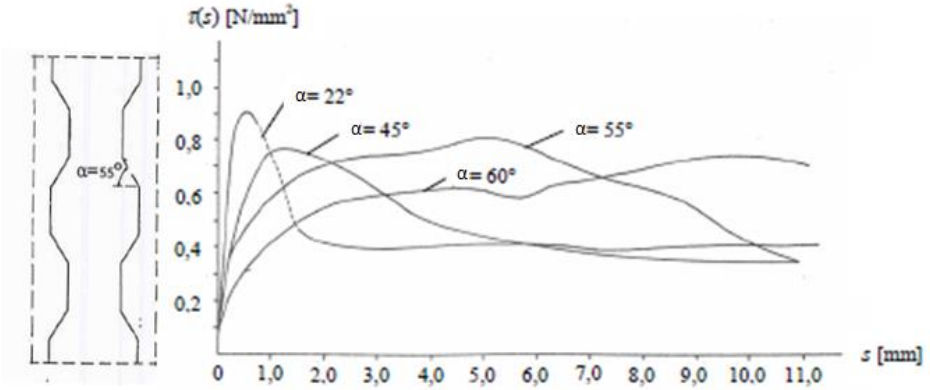

Figure 2.37 Effect of shear key angle ((FIB, 2008) original from (Eriksson, Karrholm, & Petersson, 1978))

As the results show, a smaller angle results in a larger capacity of the shear key. However, the ductility of this joint is drastically lower than for the other angles. This is a very unfavourable property since it increases the chance of progressive failure in the wall where this joint is applied. A sufficient ductility is achieved for angles larger than 45 degrees, wherefore the initial capacity and stiffness are lower and the residual strength is larger (Eriksson, Karrholm, & Petersson, 1978). The differences in stress slip relation are significant, indicating a remarkable

difference in behaviour for the keys with different angles. The results show a different cracking behaviour of the joints. A joint with a large angle cracks at the interface of joint concrete and precast elements, indicating slipping failure. For a joint with small angled keys, cracks occur in the joint concrete, showing similarities with key shear off.

2.3.5.2 Depth and height of the keys

Various papers discuss the dependency of the failure mode on the depth-height ratio of the shear keys (Hansen, et al., 1976; Sorensen, Hoang, Olesen, & Fischer, 2017; Olesen, 1975). The height and depth of a key are indicated in Figure 2.38. Although all of them base their conclusions on tests with distributed transverse reinforcement and concrete as filling material, the information is still useful since the conclusion might be applicable to unreinforced keyed joints as well. It is stated that a shear key with a large depth relative to the height fails by complete shear off, whereas a relatively shallow or high shear key fails in the corners (See Figure 2.27 for failure modes). The capacity of the joint seems to be reduced in case of higher shear keys (Hansen, et al., 1976), suggesting that failure by complete shear off requires a larger load.

However, by increasing the height of the shear keys the total key area in the joint is larger. This results in a larger capacity and cracking load. This holds until the element keys (projecting tooth of the precast element) are too small and start to fail prior to the shear key itself (Hansen, et al., 1976).

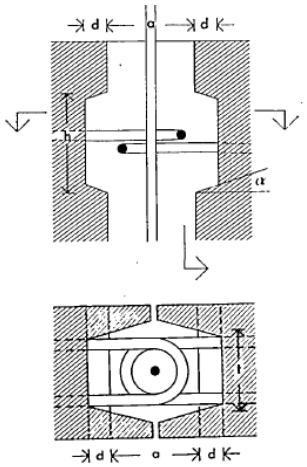

Figure 2.38 Key dimensions (Hansen, et al., 1976)

2.3.5.3 Amount of keys in the joint

The amount of shear keys in the joint has an effect on its capacity. However, a joint with six keys is not necessarily twice as strong as a joint with three keys. The shear force is not necessarily equally distributed over the shear keys either. The papers by Hansen and Cholewicki describe the parabolic stress distribution over the length of the joint (Cholewicki, 1971; Hansen H. , 1967). According to this distribution the shear stress is greatest at the top and bottom of the joint for relatively long joints. So the relation between capacity and amount of keys isn't trivial.

The research by Rizkalla et al. is especially relevant since it covers tests on unreinforced mortar joints, like those developed by Van Keulen. Two joints with a different shear key geometry were tested. The results of these tests are shown in Figure 2.39. The smaller key is applied four times and the large key is applied 2 times. So the joint with the smaller key has a larger key density,

leading to more compression diagonals per length of the joint. It was concluded that the joint's behaviour was insignificantly affected by the change in shear key design. The variation in shear capacity between the two designs was for each loading condition less than 15 percent (Rizkalla, Serrette, Scott Heuvel, & Attiogbe, 1989). However, another research by Chakrabarti et al. investigated the effect of key density as well, this time on reinforced joints. In this research the shape of the keys is the same for all specimens, but for some six keys are applied and for others just three. A relevant increase in capacity was found in these test series (Chakrabarti, Nayak, & Paul, 1988).

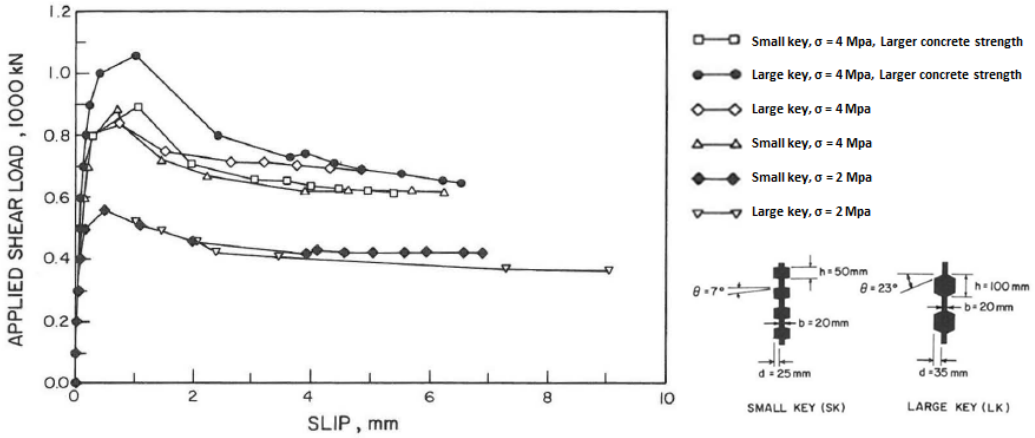

Figure 2.39 Effect of key size and normal pressure on shear slip relation (Rizkalla, Serrette, Scott Heuvel, & Attiogbe, 1989)

A second research by Abdul-Wahab investigated the effect of the number of shear keys on the capacity of the joint by just elongating the joint. Thereby the density of the shear keys is equal for all specimens. The joint area is enlarged. The test results show that the capacity is largely influenced by the number of shear keys. An increase in number of keys directly leads to an increase in capacity. The capacity of a joint with 4 keys is even more than two times larger than the capacity of a joint with 2 keys (Abdul-Wahab, 1986).

However, this research was performed on reinforced profiled concrete joints and attention was paid on the dowel action of the transverse reinforcement specifically. So for the results of coming research on a joint with concentrated reinforcement can differ from those of the tests by Abdul-Wahab. His conclusions should therefore only be seen as background information to get some idea of the possible scale effect and cannot be used form a base for conclusions.

The SBI97 report does also mention the increase of the ultimate and cracking load for a larger relative key area (key density) in the joint (Hansen, et al., 1976).

2.3.5.4 Normal pressure in the joint

The capacity of the joint is increased when a compressive stress normal to the joint is present. This effect is also investigated during the tests performed by Rizkalla et al. During these tests, some specimens were loaded with a normal stress of 2 MPa and others with 4 MPa. The comparison is made with the results of Figure 2.39. The capacity and residual strength of the large key joints are increased by 60 and 80 percent respectively, when the normal stress is 4 MPa instead of 2 MPa. For the joint with small keys the residual strength is around 50 percent larger when a higher normal stress is applied. The larger capacity is a result of *"increase in*

confinement and consequently the tensile resistance of the drypack, provided by the higher stress normal to the connection" (Rizkalla, Serrette, Scott Heuvel, & Attiogbe, 1989).

The results show that an increase of the normal pressure by 100 percent leads to a much smaller increase in capacity. If the behaviour could be described by shear friction theory only, the increase in the capacity would be the same as the increase in stress, as the paper suggests (Rizkalla, Serrette, Scott Heuvel, & Attiogbe, 1989). So besides shear friction, another mechanism is contributing as well.

2.3.5.5 Properties of the reinforcement, joint and element material

It is rather obvious that an increase in strength of the reinforcement, joint and element material increases the shear capacity of the joint. Especially the properties of the joint material have a large influence on the connection's behaviour (Hansen, et al., 1976; Cholewicki, 1971). A higher reinforcement ratio and yield strength increase the capacity of the joint. The effect of the yield strength on the capacity is larger for joints with a high reinforcement ratio. A larger residual strength and therefore ductility is obtained for joints with a higher reinforcement ratio according to tests by Pommeret on joints with distributed reinforcement (Hansen, et al., 1976).

2.4 Conclusion

The literature study on connections in precast concrete first of all provided general principles of connection design. Besides structural aspects, aspects concerning the construction process are very important to consider while developing connections. Evaluating these construction aspects reveals that the developed profiled mortar connections correspond well to the design principles. This supports the relevance of Van Keulen's research and this thesis.

Connections make use of several mechanisms in order to transfer forces between precast elements. These mechanisms were discussed in paragraph 2.2. The principles of compression force transfer are in the context of this research probably just useful as background information, to have some understanding about the way the horizontal connections between precast wall elements and the support of floor slabs on the wall elements work.

For the profiled mortar connections that are analysed in this master research transfer of tensile and shear forces is more important. The principles of tensile force transfer are applied in the way the concentrated transverse tying reinforcement behaves. This reinforcement avoids separation of the two connected wall elements. Adhesion, shear friction, dowel action and shear lock are the mechanisms that transfer the shear force over the mortar joint. While adhesion is used for small shear forces only, the other three mechanisms act simultaneously in the phase where the transferred shear force is larger than the debonding limit. The contribution of adhesion may only be taken into account if the contact surface between precast concrete and joint material is intact. Shrinkage of the joint material is the main reason why this contact is disturbed.

Based on what is known about shear lock, dowel action and shear friction, the interaction between these mechanisms is described. It is expected that most of the shear force is transferred over the vertical profiled mortar connection by shear locking, since this mechanism behaves stiffer than the other two. Shear friction would take place between the two precast wall elements and the joint material, but this would require a sufficient lateral compression. Dowel action of the transverse reinforcement in the horizontal wall joints might also contribute to the transfer of shear forces over the vertical joint. However, the activation of dowel action requires a large shear displacement over the joint compared to shear friction and shear locking.

Other characteristics of the profiled shear connection in general have been described as well. Such as the effect of shrinkage, profile geometry and the application of concentrated reinforcement on the connection's behaviour. These results of previous research are useful to formulate expectations of coming research results.

3 Literature study: Precast concrete shear walls

The precast concrete stability structure of a high-rise building consists of several shear walls oriented in different directions that carry the weight of the structure and transfer the horizontal loads to the foundation. The structure can be analysed by Finite Element calculations that define the flow of forces and deformations of the wall in detail. However, a simple hand calculation is very useful as well.

The easiest way of modelling a high-rise structure is by using the model of a clamped cantilever beam (See Figure 3.1). This beam schematizes the whole stability structure with a certain given bending stiffness EI, shear stiffness GA and axial stiffness EA. The model is useful to define a first estimate of the reaction forces, deformations and required structural dimensions. This simple analysis is also used to validate the outcome of more detailed analyses performed in later phases.

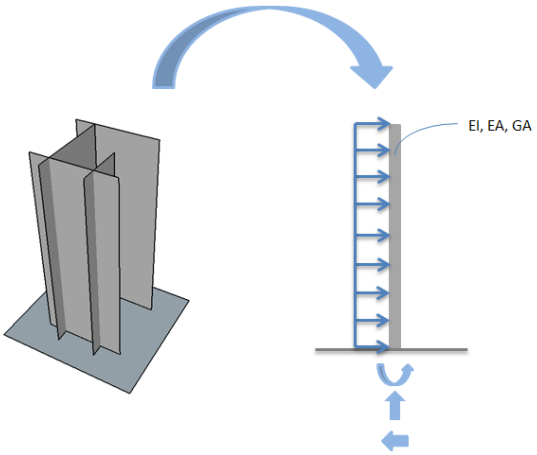

Figure 3.1 Schematisation of a stability structure into a cantilever beam

This chapter discusses the behaviour of a shear wall. The first paragraph explains the two most important beam theories that are used to analyse shear walls. In the second paragraph the general behaviour of shear walls is described and that of precast concrete shear walls in particular. The third paragraph addresses some of the research that has been done on the performance of precast concrete shear walls compared to monolithic walls.

3.1 Beam theories

In the past several beam theories to analyse mechanical problems were developed. When a simple calculation on the clamped beam model, but also when a more complicated finite element analysis is performed a decision must be made on the beam theory the calculation is based on. For the finite element method different elements are produced, some according to one theory and some according to the other. The structural engineer should decide which element to use according to the goal of the analysis keeping in mind the limitations of each theory. The most common beam theories are those developed by Euler-Bernoulli and Timoshenko. The main difference between the theories is whether they take into account only bending or shear deformations or both. The total deformation of a structural element is always a combination of

both types of deformations. However, their relative contribution depends on the geometry of the structural element that is analysed. The two theories are explained in this paragraph

3.1.1 The Euler-Bernoulli Beam Theory

The following section is based on the lecture notes "An introduction to the analysis of slender structures" by A. Simone (Simone, 2011).

The beam theory developed by Euler and Bernoulli only takes into account bending deformations. Any shear strain and deformation is neglected and set to zero. This is a direct consequence of applying Bernoulli's hypothesis to the beam model. The hypothesis states:

"*Plane cross-sections remain planar and normal to the beam axis in a beam subjected to bending"* (Simone, 2011)

The same hypothesis is mentioned in the book by Hartsuijker, when explaining the "Fibre model" (Hartsuijker, 2001). This model assumes a beam to consist of an infinite number of parallel fibres in longitudinal direction of the beam and perpendicular to these fibres an infinite number of cross-sections. According to Bernoulli's hypothesis the angle between the cross-sections and the fibres remains 90 degrees after deformation of the beam. This principle is illustrated in Figure 3.2.

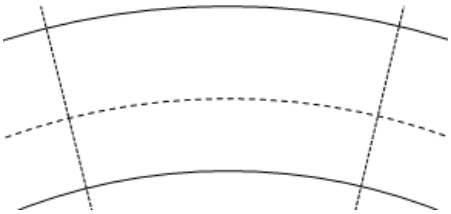

Figure 3.2 Fibres and cross sections remain under an angle of 90 degrees during deformation

For slender elements the deformations caused by shear are small compared to bending deformations and can therefore be set to zero. So in this case Bernoulli's hypothesis is applicable and therefore the equations derived by the Euler-Bernoulli beam theory can be used. Furthermore the theory assumes that the deformations of the structural elements are small compared to their dimensions. Both assumptions result in specific kinematic relations that hold for this beam theory.

The derivation of the differential equation describing the behaviour of a beam according to Euler and Bernoulli can be found in many books on structural mechanics, since it is one of the most important principles used in the working field. For example Simone and Hartsuijker provide this derivation (Hartsuijker, 2001; Simone, 2011). It seems sufficient to refer to these sources instead of repeating the whole derivation in this report. The finally resulting differential equation for the Euler-Bernoulli beam theory relates the load q with the deflection of the beam v, as depicted below. Together with four boundary conditions, two on each end of the beam, the equation can be solved for any problem specifically, whereby the whole displacement-field is known. Consequently, the bending moment and shear force distribution can be found, using the kinematic and constitutive relations.

$$q = EI * \frac{d^4 v}{dx^4}$$

3.1.2 Timoshenko's beam theory

Timoshenko developed a beam theory that also takes into account the deformations caused by a shear force. Before this theory is discussed, the relations for a beam with only shear deformations are considered. The following section is also based on the lecture notes "An introduction to the analysis of slender structures" by A. Simone (Simone, 2011).

3.1.2.1 Pure shear beam

The deformations caused by a shear force V are indicated in Figure 3.3. The shear deformation gamma is the angle between the contours of the original and the distorted shape of the beam. The deformation is schematised as a vertical deflection of one end of a beam part, parallel to the face of the other end. As a result the centre line of the beam is inclined with angle gamma, but the cross-sections remain vertical.

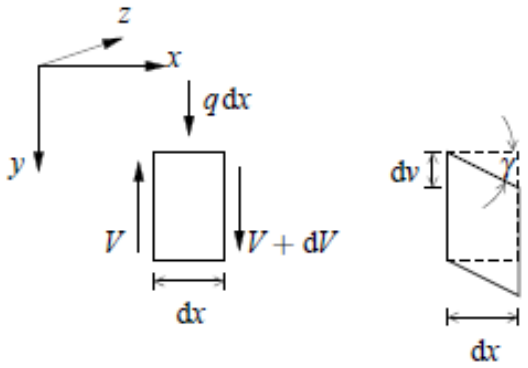

Figure 3.3 Shear deformations (Simone, 2011, p. 17)

Using Figure 3.3, the following kinematic, constitutive and equilibrium relations are found:

$$\gamma = \frac{dv}{dx}\ ;\ \tau = G * \gamma\ ; \tau = \frac{V}{A_s}\ ;\ \gamma = \frac{V}{GA_s}\ ; q = -\frac{dV}{dx}\ ; \frac{dM}{dx} = V$$

Whereby the differential equation for the shear beam is formulated as:

$$q = -GA_s \frac{d^2v}{dx^2}$$

Hereby Hook's law is used with so called shear-modulus G relating the shear stress τ and shear deformations γ. Furthermore it is assumed that the shear stresses are uniform over the shear effective part of the cross section A_s. The resulting differential equation can be used to determine the shear deflections of a beam as a consequence of distributed load q. Consequently the shear forces and bending moments can be determined using the other derived relations.

3.1.2.2 Timoshenko's beam theory

The beam theory developed by Timoshenko combines the bending and shear deformations of the two theories above. Timoshenko introduces two degrees of freedom: a vertical displacement v and a cross section rotation φ. These degrees of freedom are illustrated in Figure 3.4.

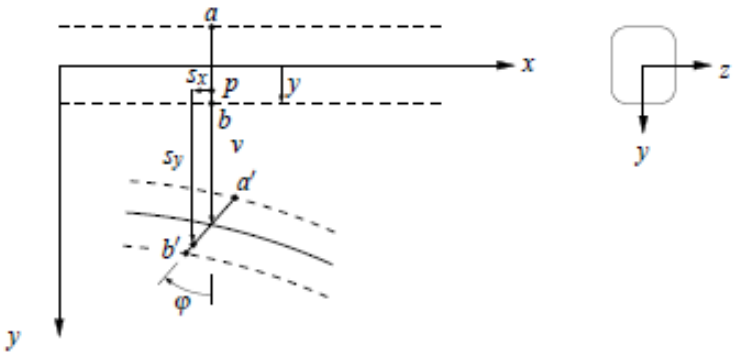

Figure 3.4 Degrees of freedom in Timoshenko's beam theory (Simone, 2011, p. 26)

The deflection v contains a part caused by shear and a part caused by bending.

$$v_{tot} = v_{bending} + v_{shear}$$

Since in Timoshenko's theory the shear deformation is included as well, the angle phi is not equal to the derivative of the deflection. The total rotation of the cross-section consists of a part caused by bending and a part caused by shear. The following relation holds:

$$\frac{dv}{dx} = \gamma + \phi$$

Using kinematic and constitutive relations the shear force and bending moment in the beam can be expressed in the degrees of freedom:

$$V = GA_s\gamma = GA_s(\frac{dv}{dx} - \phi)$$

$$M = \int E * \epsilon * y \, dA = \int -E * y^2 * \frac{d\phi}{dx} \, dA = -EI * \frac{d\phi}{dx} \qquad \neq -EI * \frac{d^2v}{dx^2}$$

The use of two degrees of freedom leads to a system of two differential equations describing the distribution of mechanical quantities over the length of the beam. Both differential equations are obtained by using the equilibrium equations for a small part of the beam. The first equation simply states that the shear force determined by the equation given above is equal to the shear force obtained by taking the derivative of the bending moment. The second equation is composed under the condition that the derivative of the shear force is equal to the negative value of the line load.

$$EI\frac{d^2\phi}{dx^2} + GA_s\left(\frac{dv}{dx} - \phi\right) = 0$$

$$GA_s\left(\frac{d^2v}{dx^2} - \frac{d\phi}{dx}\right) = -q$$

Solving the system of equations results in an expression for the beam deflection that is exactly equal to the summation of the results of the Euler-Bernoulli and shear beam theory. The relations found for the bending moment and shear force distribution over the beam length are the same for all three theories. This is makes sense, since their distribution is a direct consequence of equilibrium conditions, which are the same for all three theories.

3.2 Shear wall behaviour

The behaviour of a shear wall can be described using the beam theories of paragraph 3.1. This paragraph starts with an explanation of the general behaviour of a shear wall. The second part of this paragraph discusses the typical behaviour of the precast concrete shear wall.

3.2.1 General shear wall behaviour

When the beam theories are applied to the basic model of a shear wall, the distribution of the lateral deformation over the height of the wall is as indicated in Figure 3.5.

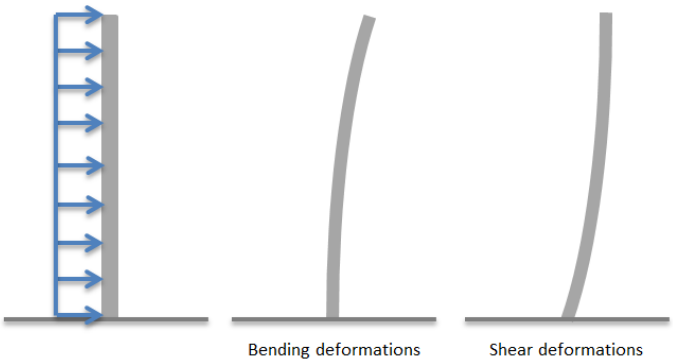

Figure 3.5 Deformations of a shear wall

The total deformation of the wall is the summation of both types of deformation. The relative contribution of each depends on the slenderness of the structure. For a very slender wall, the contribution of shear deformations is minimal and can be neglected. Therefore the Euler-Bernoulli beam theory could be applied for these walls. For a slenderness ratio (height/width) larger than 4, the contribution of shear deformation is less than 5 percent (Straman, 1988, p. 35). The bending deformations are insignificant, for a compact wall with a small slenderness ratio. So in that case a shear beam model is applicable. However, the absolute value of the horizontal deflection is always small for compact walls. The Timoshenko theory gives the most accurate result in any case since it includes both types of deformation. In most cases, the slenderness ratio of a wall is large enough to justify the use of the Euler-Bernoulli beam theory.

The theoretical stress distribution over the shear wall calculated with the Euler-Bernoulli method is equal to that found for a beam. The stress distribution of normal stress and horizontal shear stress is illustrated in Figure 3.6, theory about these distributions can be found in the book by C. Hartsuijker (Hartsuijker, 2001). However, the effect of shear lag on the stress distribution in the wall can be rather significant for slender structures. Much research has been performed on this phenomenon.

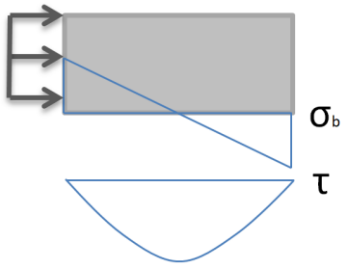

Figure 3.6 Stress distribution in a monolithic shear wall according to Euler-Bernoulli beam model

Shear lag is the deviation of the actual stress distribution in a structural element consisting of webs and flanges from the distribution obtained from the Euler-Bernoulli Beam Theory and is caused by the effect of shear deformations. This theory disregards shear deformations. However, a structural element will never have an infinite shear stiffness. As Kwan states, when the shear stiffness is finite and shear deformations occur, the longitudinal deformations close to the intersection of webs and flanges become larger and those more remote from these intersections become smaller than the Euler-Bernoulli beam theory predicts. This may increase the longitudinal stresses and lateral deflections of the structural element (Kwan, 1996). It is shown in Figure 3.7. Since the longitudinal stress distribution isn't linear anymore, shear lag also results in warping of the floor slabs (Coull and Bose, 1971 cited by (Singh & Nagpal, 1994)). The effect of shear lag occurs in core and tube structures, but also in box girders or T-beams. It is the reason why for these sections an effective flange width is taken into account for the bending stiffness instead of the whole width of the flange.

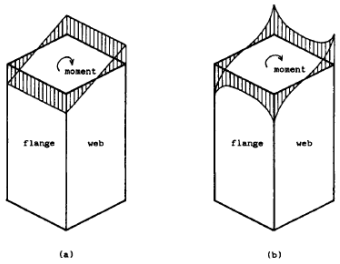

Figure 3.7 Positive shear lag in a core structure (Kwan, 1996)

According to Kwan, the shear lag is larger for structures with a smaller shear stiffness, such as framed tubes. Furthermore, the slenderness of the structure plays a role. A structure with relatively wide webs and/or flanges experiences a larger shear lag effect (Kwan, 1996). This seems logical since shear deformations and shear stiffness are relatively more important for less slender structures. The same relation with slenderness was obtained in Hummelen's research (Hummelen, 2015, p. 41). Kwan states that for a non-slender structure with a uniformly distributed horizontal load, the maximum normal stress can be 2 times larger than calculated with an Euler-Bernoulli beam approximation and that the effect of shear lag becomes insignificant for a slenderness ratio above 20 (Kwan, 1996).

Tube structures have a load bearing facade consisting of rigidly connected columns and beams. The effect of some specific parameters for example the beam and column dimensions on shear lag has been investigated by Lee et al. (Guan, Loo, & Lee, 2000). The conclusion of this analysis corresponds with Kwan's findings. When the shear stiffness is increased, the shear lag effect reduces.

Kwan observed that the effect of shear lag on the bending stresses is larger near the base of a core structure. The effect on the lateral displacement is considerably smaller than the effect on the stresses (Kwan, 1996). The effect of shear lag over the height of the structure is also investigated in later research, for example in a research on shear lag in Tube(s)-in-Tube structures (Guan, Loo, & Lee, 2000; Lee, Loo, & Guan, 2001). This paper also mentions the effect of negative shear lag. The shear lag distribution over the height according to this research is as indicated in Figure 3.8. Above a height of approximately a quarter of the building height, the shear lag effect is negative. This results in a reduction of stresses in corner columns and an increase in centre columns of the tube as illustrated in Figure 3.9.

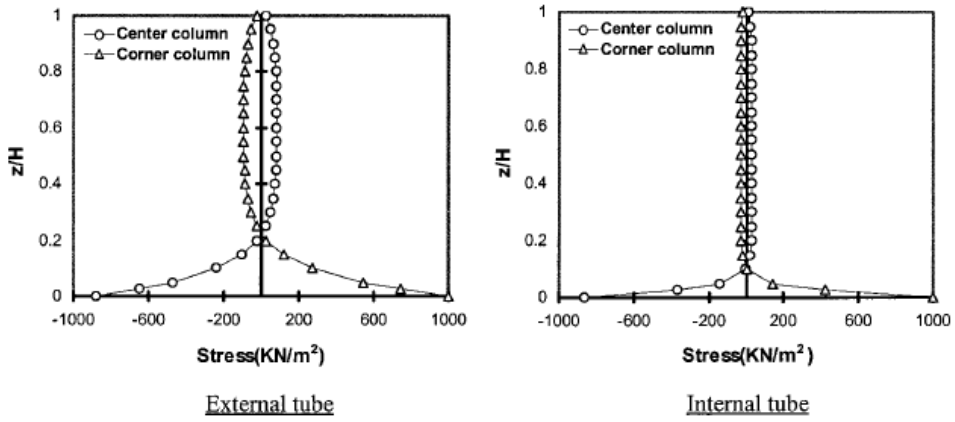

Figure 3.8 Distribution over the height of the building of extra axial bending stress in the columns of the tubes (Lee, Loo, & Guan, 2001)

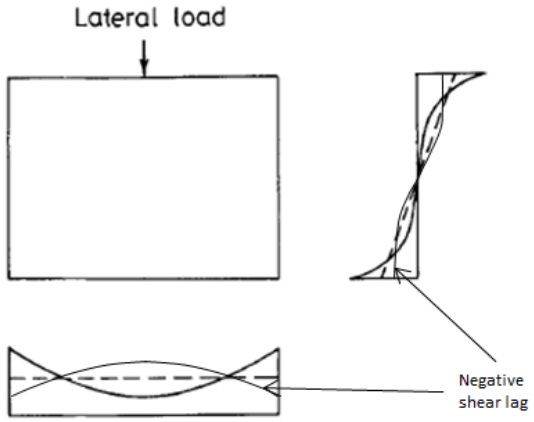

Figure 3.9 Positive and negative shear lag (modification of figure (Singh & Nagpal, 1994))

The effect of negative shear lag and its cause are explained in the paper by Singh and Nagpal (1994) using Figure 3.10. The explanation also clarifies the varying shear lag effect over the height of the structure. In order to explain the phenomenon, a framed tube structure is split into two modes above the j^{th} floor. One mode describes the behaviour of the structure under the applied horizontal load with fixed supports at the j^{th} floor. Due to this load, the structure deforms. Since the shear rigidity is not infinite, the normal stresses in the corner columns will be larger than in the centre columns. This is the positive shear lag as described before. The second mode describes the behaviour of the structure due to the deformations at the j^{th} floor. These deformations due to positive shear lag are larger than at the $(j+1)^{th}$ floor. This results in a stress distribution over the columns, which has the shape of the negative shear lag effect. As Singh and Nagpal state, the negative shear lag effect is a consequence of positive shear lag. When there isn't any positive shear lag, the negative shear lag is absent as well (Singh & Nagpal, 1994). The final stress distribution over the columns is the sum of the two resulting distributions. Beyond a height of approximately one quarter of the total height of the building the negative shear lag is greater. However, when the shear lag effect is larger due to for example a lower shear stiffness, this so called point of shear lag reversal is shifted upwards (Singh & Nagpal, 1994).

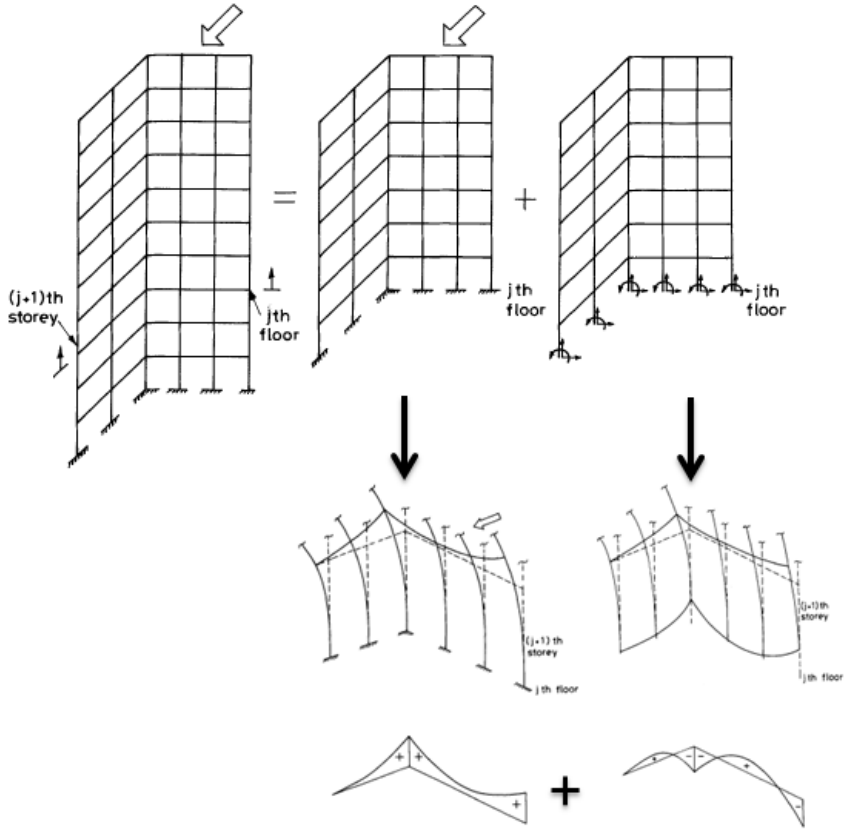

Figure 3.10 The negative shear lag effect explained (Singh & Nagpal, 1994)

J.C. Hummelen analysed the shear lag effect for a TU Delft Master Thesis. The most important conclusions were (Hummelen, 2015):

- The shear lag effect is affected by a changing aspect ratio (the ratio between the depth and width of the core). The best aspect ratio is 1.0, but the difference in shear lag effect with other ratios is minimal.
- A structure approaching the shape of a circle experiences a smaller shear lag effect than a rectangular structure.
- The effect of sharp corners in a structure on shear lag is negligible.
- Making structural vertical joints in a masonry configuration doesn't have any influence on the present shear lag effect in a core structure.
- The shear lag effect in slender structures is smaller.

It can be concluded that the schematisation of a stability structure into a clamped bending beam provides a sufficient first estimate for the structural behaviour. However, if the shear deformations are ignored, the predicted deformations and stress distributions deviate from reality. In any case a larger shear stiffness or a higher slenderness of the structure makes the Euler-Bernoulli approximation more valid and reduces the shear lag effect and the relative contribution of shear deformations.

3.2.2 Behaviour of precast concrete shear walls

For a precast shear wall with a stacked element configuration, the beam model must take the shear stiffness of the longitudinal joints into account in order to describe the full behaviour of the wall. This shear stiffness determines the coherence of the wall. Shear forces cannot be

transferred over a joint without any stiffness. In that case the wall can basically be modelled as two separate beams, resulting in large deflections and stresses in the cross section. If the shear stiffness of the longitudinal joint is infinitely large, the wall is monolithic. A precast wall will behave between these two limits, since the vertical shear connections will have a limited shear stiffness and are therefore able to transfer some longitudinal shear forces from one column of elements to the other. The effect is illustrated in Figure 3.11. Possible vertical wall to wall connections are discussed in chapter 2.

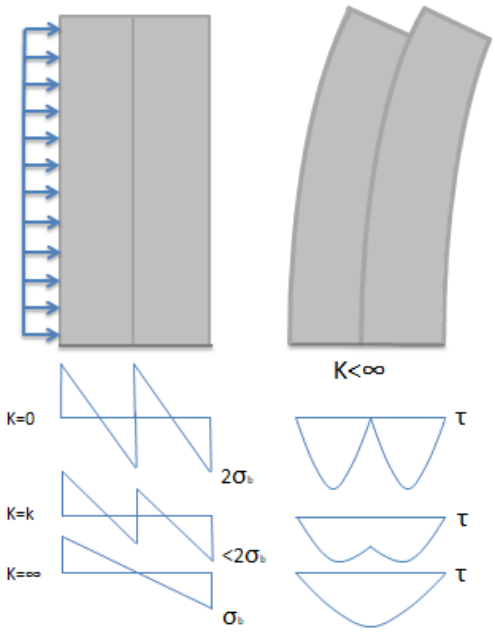

Figure 3.11 Effect of longitudinal joints

In order to have a better understanding of the behaviour of a precast shear wall, the longitudinal shear stresses are analysed in more detail. Sticking to the introduced beam model, a theoretical distribution of the longitudinal shear stress is found in beam theory as well. The book by C. Hartsuijker describes how to derive an expression for the magnitude of the shear stresses in a longitudinal section of a prismatic beam (Hartsuijker, 2001).

As described before, the longitudinal shear stresses in the joints of the wall create a coherent structure of the vertically stacked precast elements. The same holds for a beam consisting of two elements placed on top of each other.

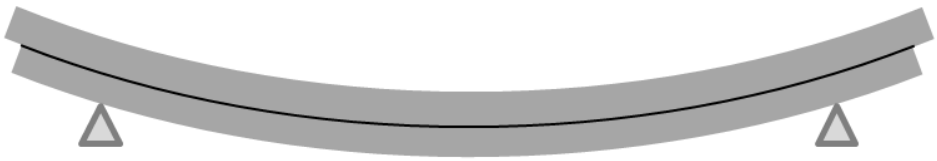

Figure 3.12 Slip between two beam sections without shear transfer in the longitudinal joint

When a part at the bottom of the beam is taken out in order to analyse the state of equilibrium, it can be seen that a longitudinal shear force along the cutting surface s^a_x makes equilibrium with the inconstant normal force (See Figure 3.13).

$$\Sigma F_x = -N^a + (N^a + \Delta N^a) + s_x^a * \Delta x = 0 \rightarrow \; s_x^a * \Delta x = \Delta N^a \quad [3.1]$$

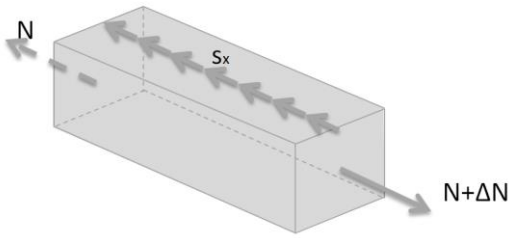

Figure 3.13 Forces on the lowest part of a beam (based on (Hartsuijker, 2001))

The normal force at one end is not equal to the force at the other end since the normal stress caused by bending varies over the length of the beam. The change in normal stress is described in the following way for a prismatic beam:

$$\frac{d\sigma(y)}{dx} = \frac{1}{A} * \frac{dN}{dx} + \frac{y}{I_z} * \frac{dM_z}{dx} \quad [3.2]$$

For the case of the beam, the normal force is constant, whereby the change in normal stress can be described as:

$$\frac{d\sigma(y)}{dx} = \frac{y}{I_z} * \frac{dM_z}{dx} = \frac{V_y * y}{I_z} \quad [3.3]$$

This relation is only valid for structural elements that can be considered as a slender beam and are therefore modelled with the Euler-Bernoulli beam theory.

The normal force in the plane is equal to:

$$N^a = \int \sigma(y) dA \quad [3.4]$$

This combined with the equilibrium equation [3.1] gives:

$$s_x^a = \frac{\Delta N^a}{\Delta x} = \int \frac{d\sigma(y)}{dx} dA = \frac{V_y}{I_z} * \int y \, dA = \frac{V_y * S_z^a}{I_z} \quad [3.5]$$

Looking at this equation, it appears that the longitudinal shear stress is dependent on the transversal shear force acting in a cross section. For a clamped beam under a uniform q load, the shear force diagram is linear and so is the theoretical longitudinal shear stress diagram.

The total shear force in the longitudinal joints is the integral of the shear force per length s_x^a over the length of the joint.

$$R_{x_s}^{\ a} = \int_l s_x^a dx = \frac{M_z * S_z^a}{I_z} \quad [3.6]$$

For calculating the shear force over a certain part of the joint, the difference in bending moment ΔM_y must be inserted in above relation.

Using the derived formulas for calculating the distribution of shear stresses in a longitudinal joint over the height of a shear wall, results in a sufficient indication of the real stresses that develop. However, especially for the lowest and highest part of the joint the result will deviate from the actual behaviour.

Several sources mention the effect of shear deformations of wall panels and vertical joints on the longitudinal shear stress distribution in the vertical joints (Hansen, et al., 1976; Straman, 1988). As Straman explains, the shear stresses in the finitely stiff joints induce a shear deformation. This shear deformation results in a relative displacement between the two sides of the joint and consequently the two adjacent elements. The distribution of displacements is indicated in the lower image of Figure 3.14. As a result of this relative displacement, a horizontal cross-section of the wall isn't plane anymore, whereby Bernoulli's Hypothesis isn't valid anymore. The distribution of longitudinal shear stress over the height of the wall deviates from the linear distribution calculated with the relations derived before, as shown in Figure 3.14. The most important difference is in the magnitude and location of the maximum shear stress. As the figure indicates, this maximum occurs somewhat above the base line of the wall and is generally smaller than the maximum value calculated with the Euler-Bernoulli beam theory.

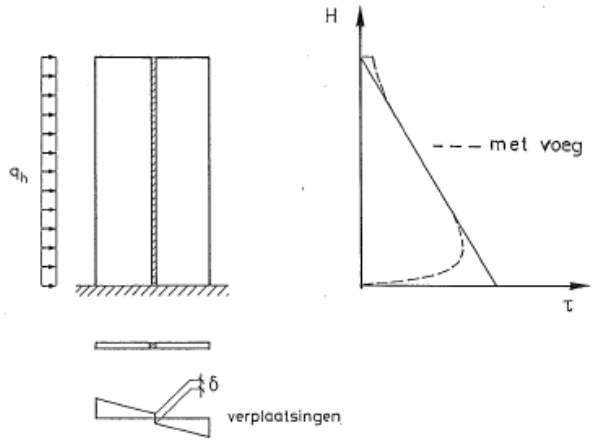

Figure 3.14 Longitudinal shear stress distribution in vertical joint over the height of the wall (Straman, 1988)

Hansen et al. do not only describe the effect of shear deformations of the joints on the vertical shear stress distribution, but also describe the effect of shear deformations of the wall elements separately (Hansen, et al., 1976). The effects on normal, horizontal and longitudinal shear stress are illustrated in Figure 3.15.

The figure shows for the normal stresses the theoretical linear distribution of an Euler-Bernoulli beam when shear deformations are not included at all. When shear deformations of the wall panels is included, the shear lag effect is clearly visible by the peak stresses at the outer fibres. When shear deformations of the joint are included as well, the finite joint stiffness introduces the jump that has been described before. Note that tensile stresses do not necessarily occur, because the vertical load is included in the analysis.

The longitudinal shear stress distribution shows that the deviation of the shear stress at the top is caused by the limited shear stiffness of the joints and the reduction of the maximum is a consequence of both types of shear deformations.

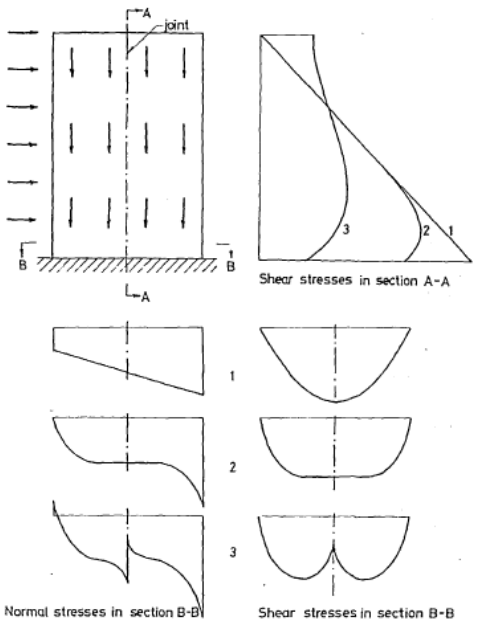

Figure 3.15 Effect of shear deformations on stress distributions 1. No shear deformations 2. Shear deformations in panels only 3. Shear deformations in panels and vertical joints (Hansen, et al., 1976)

Straman investigated the effect of vertical joints on the behaviour of the shear walls. In this research he focused among other things on the deflection of the wall, the normal stresses that develop due to bending and the vertical shear stress distribution in the joints. He concluded that the effect of vertical joints in shear walls on the deflection and bending stresses is the smallest if the joints are located close to the outer fibres of the wall. A joint exactly in the neutral axis results in the largest increase of bending stresses and deformations compared to a monolithic wall. Furthermore, the magnitude of the influence of vertical joints doesn't depend on their stiffness exclusively, but on the ratio between their stiffness and the stiffness of the wall material (Straman, 1988). A joint with a certain stiffness applied in a very stiff wall affects the wall deflection and bending stresses to a larger extend, than when the wall and joint stiffness are comparable. A wall containing joints with a stiffness almost equal to the element stiffness is after all almost monolithic, even if the stiffness of both is considerably small.

3.3 Performance of precast concrete shear wall structures

The wall elements in a precast shear wall are usually rather stiff and are therefore not inferior to cast in place elements. The joints however, reduce the stiffness of the wall compared to monolithic walls. This has been the major disadvantage of using precast concrete shear walls as stability structure for high rise buildings. This paragraph describes the results of previously performed studies on the parameters affecting the behaviour of precast concrete shear walls. These studies quantify the difference in behaviour, mainly stiffness, between the monolithic and the precast shear wall.

3.3.1 Effect of joints on the stiffness of shear walls

In the past research has been done on the parameters affecting the stiffness of precast stability walls (Migayrou, 2016; ten Hagen, 2012; Falger, 2003; van Keulen & Vamberský, 2012; van Keulen, 2010). These researches indicate the sensibility of the stiffness of the wall to different design parameters. Furthermore it compares the horizontal deflection of the precast shear wall to the deflection of a monolithic wall for a certain applied load, a very important comparison, since for high-rise structures the stiffness requirements determine the structural dimensions in most cases.

First of all, the relation between the type of connection between the precast elements and the behaviour of the stability wall was analysed by Falger (Falger, 2003). This research focused on the relative performance of walls with a masonry configuration and open joints compared to that of monolithic walls and walls with common connection types. Falger's goal was to illustrate the possibilities of the masonry configuration with open joints, whereas the goal of this study will be to illustrate the possibilities of the stacked configuration with the newly developed profiled mortar connections.

Falger analysed the wall's deformations and force and stress distributions for four different types of stability walls all with the same outer dimensions (slenderness ratio of 6): a fully closed wall, a wall with on each floor one opening on the central axis, a wall with six openings per floor and a wall with eight openings per floor. So the wall's in-plane stiffness varies over the types of structure. With six different types of connections and four types of walls, in total 24 analyses were performed. The results show that the stiffest designs besides a monolithic wall are the open joint with masonry configuration and the reinforced profiled shear joint with a stacked configuration.

Joint/Type of wall	No openings	1 opening per floor	6 openings per floor	8 openings per floor
Monolithic	100	100	100	100
Open joint masonry	105.3	108	106.1	106
Reinforced profiled joint	107	110.3	106.8	105.7

Table 3.1 Resulting top deflection of stability walls (Falger, 2003, pp. 75-76)

Two conclusions Falger made from these results are: the deflection of both connection types are always of the same order of magnitude and for the open joints the increase in deflection compared to a monolithic wall seems independent of the structural stiffness, since for all wall types the index is around the same value (Falger, 2003, p. 79). Combining these two conclusions would suggest that also for the reinforced profiled shear joint the increase in deflection

compared to a monolithic wall is independent of the structural stiffness. The results in the table above do not exclude this statement. In line with these results, the same behaviour for an unreinforced profiled mortar shear joint might be expected.

The larger relative deflection of the reinforced profiled joint for the structure with one opening is due to the location of the connection. The element division is such that on each floor a joint is present in the lintel above the opening. The shear stresses in these joints are larger due to the shorter length and in some the shear capacity is even reached, whereby plastic deformation in these joints and redistribution to other joints occur, all resulting in a larger deflection of the structure (Falger, 2003, p. 80). This indicates that the element division should be such that no joints are present at a section with an opening.

Falger also concludes that the deflection of the wall is more sensible to a variation in lower values for the connection stiffness than a variation in high stiffness values. This means that it is very effective to improve the stiffness of connections with a relatively small stiffness, but the effect on the lateral displacement of the wall of making stiff connections even stiffer is rather small. From this it can be concluded that an extensive optimisation of the connection stiffness isn't useful.

Continuing on Falger's study, Van Keulen investigated the separate contributions of horizontal and vertical joints to the decreased wall stiffness. He tested only the fully closed wall and the wall with one centre opening, both executed with different masonry element configurations. In the first step the walls were modelled with open vertical joints and horizontal joints with a monolithic stiffness. The resulting deflections were larger than for a monolithic wall purely due to the open vertical joints. In case of a closed wall, the increase of deflection caused by the open vertical joints has a maximum of 3.8 percent compared to a monolithic wall. In case of a wall with centre openings, the increase is 4.1 percent at most. In the second step the stiffness of the horizontal joints was changed into a value related to a common connection type (horizontal mortar joints with pin reinforcement). The resulting deflections were larger than for a monolithic wall and for a wall with only open vertical joints. The increase compared to a monolithic wall was at most 8.3 percent for a closed wall and 10.2 percent for the wall with centre openings. According to these results, the deflection increase of a precast wall with a masonry configuration compared to a monolithic wall is for a larger part caused by the presence of horizontal joints between the elements (van Keulen, 2010). The results of Van Keulen's study are not one-to-one applicable to the intended design with a stacked configuration and vertical profiled mortar joints. However, if they indicate the significance of the contribution of the horizontal joints for the designed shear wall, it must be kept in mind that even when an optimally stiff vertical connection is used, the deformation of the wall is still considerably larger than for a monolithic wall due to the horizontal connections.

Although the shear stiffness of horizontal joints appears to play a significant role for the total top deflection of the shear wall, Migayrou showed that the normal stiffness of these joints has a minor influence on the deformations. This is due to the small thickness of the horizontal joints compared to the height of the wall elements (Migayrou, 2016, p. 30).

According to Vamberský and van Keulen, the increase of the horizontal deflection of the precast wall compared to a monolithic wall is larger for smaller slenderness ratios. Since the shear deformation is the largest for less slender walls, it is shown that the joints in a precast wall

mainly affect the shear deformations and hardly increase the bending deformations (van Keulen & Vamberský, 2012). As a result all the relations between the horizontal deflection and a design parameter show a larger deflection increase for lower slenderness values. So when the slenderness of the structure is known, the consequence of a precast design can already be estimated. Test results in the Bachelor Thesis of Migayrou showed the same relation between the deflection increase and the slenderness ratio (Migayrou, 2016, pp. 24-38).

Test results show that the size and configuration of the concrete elements have an effect on the wall's stiffness (van Keulen & Vamberský, 2012). These effects are always the largest for less slender walls, as explained above. Van Keulen and Vamberský concluded that the use of larger elements reduces the amount of joints and will therefore increase the wall's stiffness. The effect of the element configuration for a couple of options is shown in Figure 3.16. The vertical joints in a masonry configuration were kept open for this analysis. The vertical joints in the stacked configuration were modelled as unreinforced profiled mortar joints with a shear stiffness of $5.0 \cdot 10^5$ kN/m/m. This stiffness is said to be rather low. The results show the relatively high performance of the masonry configuration with open vertical joints (a) and the stacked configuration with profiled joints (e). Falger observed small deviations between the results for an open vertical joint and a reinforced profiled joint (Falger, 2003, p. 75). This illustrates the potential of the idea to create stability walls with the stacked configuration and the proposed mortar joints. Another observation in this test is the relatively better performance of structures with a horizontal element configuration compared to a vertical one. Based on this observation, Van Keulen and Vamberský conclude that a horizontal configuration is always preferred.

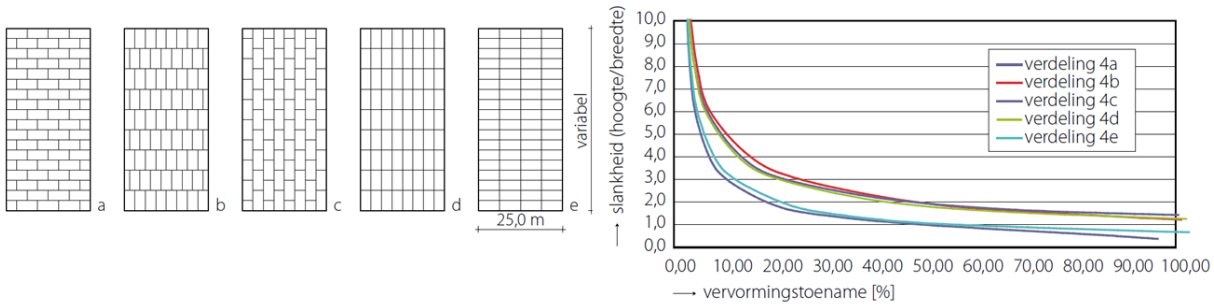

Figure 3.16 Relation between element configuration and increase in top deflection of the stability wall (van Keulen & Vamberský, Vervormingen prefab wandconstructies, 2012)

The shear stiffness of joints depends on the normal stress in the joint. The variation in normal stress over the different vertical joints in the building is not that large, but for the horizontal joints this is not the case. A horizontal joint on the lower stories is subject to a far larger normal stress than a joint at one of the highest stories. The normal stress even varies over the width, due to bending deformations of the wall. Falger investigated the need of doing an iterative analysis, whereby first the normal stress in the horizontal joints is calculated and then the shear stiffness is updated accordingly. According to this study, a shear stiffness based on a first estimate of the normal stress in the joint is sufficient (Falger, 2003, p. 69). For a feasibility study of a high-rise structure in precast concrete Ten Hagen evaluated this outcome and concluded that even a model with the same shear stiffness for all the horizontal joints in a shear wall gave sufficient results (ten Hagen, 2012, p. 88).

3.3.2 Effect of joints on the force distribution in shear walls

Falger and Ten Hagen also evaluated the force distribution in the shear walls. Although Ten Hagen only focused on the masonry configuration with open joints, Falger considered other types of connections as well.

Some important conclusions on the force distribution according to Falger's research (Falger, 2003, pp. 80-100):

- The maximum compression stress in the wall elements increases when a connection type with a lower shear stiffness is used. This is a result of a decreasing uniformity of the wall with a decreasing shear stiffness of the vertical joints. The effect is in accordance with the theory of section 3.2.2.

- The distribution of the normal stress over the width of the structure (a horizontal section) shows "jumps" at the locations of the vertical shear joints. This jump is larger for a smaller shear stiffness of the vertical joints. This is in accordance with the theory explained in paragraph 3.2.2.

- The horizontal shear stress in the elements drops at the location of a vertical shear joint.

- In a wall with openings the shear forces and bending moments in wall sections between the openings with a vertical shear joint are smaller than those for wall sections without a vertical shear joint. Since wall sections without a vertical joint are stiffer than sections with a vertical joint, they will take up a larger part of the loads.

- A wall with open vertical joints has a specific shear stress distribution. The shear forces flow through the elements around the gaps created by the open joints. This results in considerably higher shear stresses compared to a monolithic wall. Furthermore the increase of moments and shear forces in the wall may be up to 45 percent. So although the profiled and open joint designs show quite similar deformation results, this is not the case for the force distribution.

- The overlap between wall elements in a masonry configuration must be at least 25 percent of the element width in order to obtain the desired behaviour.

Ten Hagen studied the effect of making structural vertical joints instead of open joints in a masonry configuration. The effect on the top deflection of the wall appeared to be minimal. However, the shear stress distribution changed due to the improved continuity of the wall. It approached the distribution of a monolithic wall (ten Hagen, 2012, pp. 89-91).

3.4 Conclusion

Different types of connections can be compared on the scale of the connection itself. In that sense the properties as stiffness, capacity and ductility of the connection are discussed in a qualitative or quantitative way. However, as mentioned multiple times in this report, the influence of the connections on the behaviour of the complete structure is of major importance. In that sense the context must be considered as well.

In this case this context is given by the shear wall in which the vertical profiled mortar connections will be applied. This wall can be slender or compact, with many openings or closed. The influence of the connections on the shear walls behaviour varies along all these type of shear walls.

In order to gain insight in the effect of connections on the displacement and stress distribution in a shear wall, the theoretical methods that can be applied were discussed in paragraph 3.1. These theories were subsequently translated to the case of a shear wall in paragraph 3.2. In this paragraph the difference between a monolithic and precast shear wall was discussed. The connections in a precast wall cause an increase in lateral deflection and an altered normal and shear stress distribution.

Previous research on the behaviour of precast compared to monolithic shear walls indicated the differences in stiffness and stress distribution. This was discussed in paragraph 3.3. The relative difference in stiffness between these two kinds of walls is promising for the purpose of this master research. The difference depends on the slenderness ratio of the wall and the type of connection that is used. The stiffness reduction caused by joints is smaller for more slender walls. In case of reinforced profiled connections this is quite soon less than ten percent. So this result is positive for the application of vertical profiled mortar connections in high rise buildings, where the slenderness is generally quite large.

The influence of the vertical profiled mortar connections in a shear wall with stacked element configuration will be analysed in this research. This will be analysed by comparing the wall's stiffness and stress distribution with that of a monolithic wall. The obtained behaviour of this shear wall can also be compared to what is theoretically expected and expected by former research, based on the information presented in this chapter.

4 Literature study: Tests on the vertical profiled mortar connections

This chapter summarizes the relevant results of the tests on profiled mortar connections performed by Van Keulen. The whole chapter is based on Van Keulen's report that describes the most important test results (van Keulen, 2015). Van Keulen developed the four types of profiled mortar joints that are shown in Figure 4.1. From left to right: the staggered shear key joint, the aligned shear key joint, the roughened serrated joint and the joint with aligned small keys. A roughened plain joint was considered as well, but this project will only focus on profiled joints.

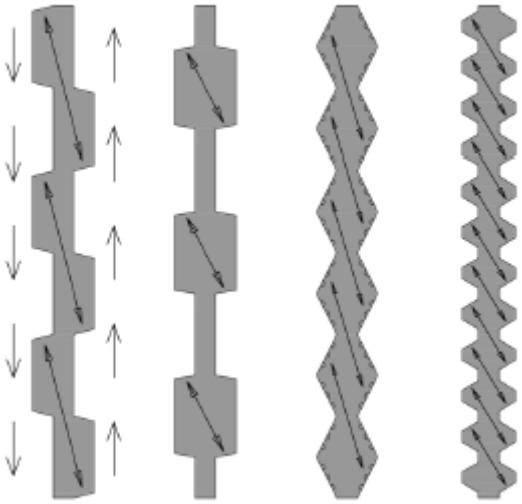

Figure 4.1 Profiled joints developed by Van Keulen (van Keulen, 2015)

The figure indicates the intended compressive diagonals that develop in the joints. The test results should reveal whether the diagonals will indeed be oriented in this way or set according to a different configuration. The geometry of the joints is designed in such a way that failure by type B or D doesn't occur (See Figure 2.27). As will be clear, the joints will fail according to failure mode C.

Figure 4.2 shows the test setup that is used by Van Keulen in order to test the profiled mortar connections. The length over which the joint was applied is 600 mm. The thickness of the concrete elements is 200 mm. Above and below the joint steel bars are used that function as concentrated reinforcement. The steel bars are slightly prestressed to keep all the elements together. Some test specimens were prestressed by a larger initial force. The connection is loaded by a displacement controlled shear force that is applied with a speed of 0.2 mm/min.

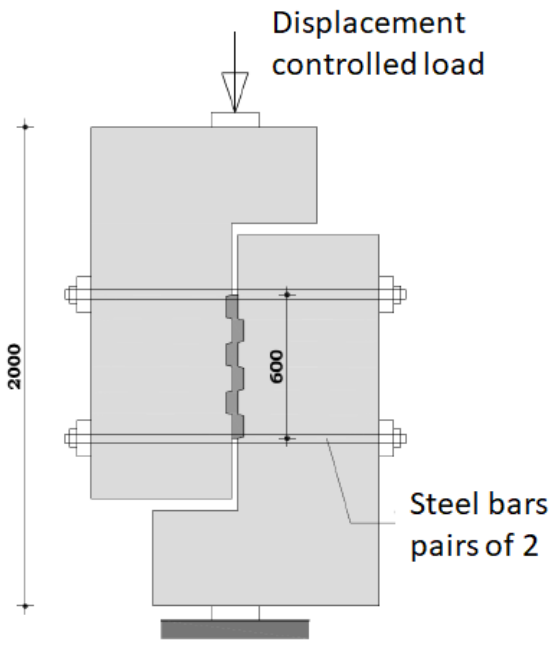

Figure 4.2 Classical shear test used by Van Keulen (van Keulen, 2015)

This chapter describes the results for all four developed joint geometries of Figure 4.1. The first paragraph describes the shear-slip relations, the second discusses the relation between shear and lateral force and in the third paragraph a comparison between the four joints is made. Paragraph 4.4 contains some concluding remarks.

4.1 Shear-slip behaviour of the joints

Different aspects of the joints' behaviour are of importance. The most important aspect is their shear-slip behaviour, from which the shear stiffness and capacity can be determined.

4.1.1 Shear-slip relation for the staggered key joint

Figure 4.3 shows the shear-slip behaviour of this type of joint that is obtained during the tests. It is concluded that the behaviour corresponds to the one discussed in section 2.3.3. In stage A bond in the interface enables an infinite amount of compression diagonals to develop until debonding of the interface takes place at point B, where after the main diagonals predefined by the geometry take over the force transfer. After point C the first cracks develop parallel to the compression diagonal as a result of exceedance of the mortar's tensile strength. This failure by type A isn't fatal. The capacity is reached just before failure by type C occurs. The shear keys shear off by the formation of a vertical crack. A residual capacity which is equal to the frictional capacity of the crack surface is left. In stage A shear is transferred by adhesion, whereas in stage B till D shear lock is the major transfer mechanism. The results presented in Figure 4.3 are obtained for a joint executed with regular K70 mortar and prestressed in the direction normal to the joint with a compressive stress equal to 2 MPa.

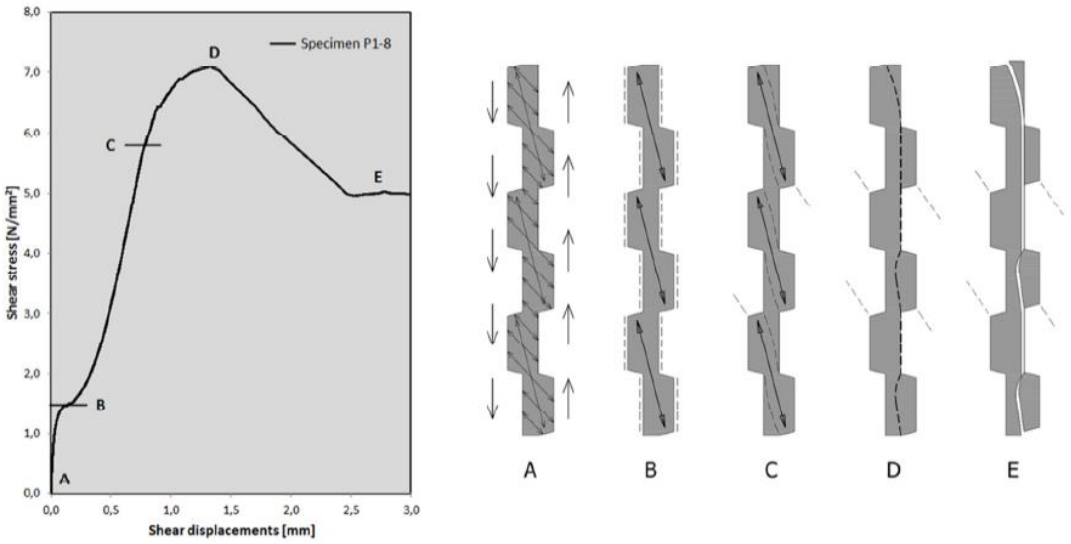

Figure 4.3 Shear-slip behaviour of the staggered shear key joint (van Keulen, 2015)

4.1.2 Shear-slip relation for the aligned shear key joint

The joint profile with aligned shear keys shows a behaviour corresponding for a large part with the staggered joint. However, these joints show some more ductility after reaching their capacity. This is caused by the formation of extra kinked diagonals that reach from one key to the other. After the capacity is reached in point C, cracks develop in each shear key. Thereby the small diagonals disappear, but the kinked diagonals are still able to transfer a shear force until in point D a vertical crack occurs shearing of all the shear keys. The capacity in point D is somewhat lower than in point C, but the kinked diagonals prevent a sudden decrease to the residual strength. It must be noted that the results in Figure 4.4 belong to a joint which is executed with fibre reinforced mortar and a normal compressive prestress of 2 MPa.

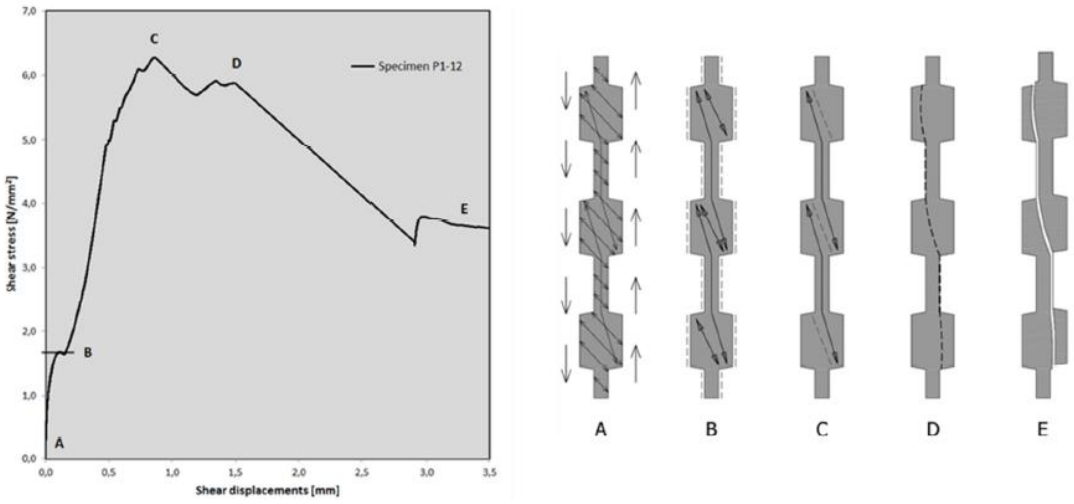

Figure 4.4 Shear-slip behaviour of the aligned shear key joint (van Keulen, 2015)

4.1.3 Shear-slip relation for the roughened serrated joint

The shear-behaviour of the serrated joint with a roughened surface, fibre reinforced mortar and prestressed with 2 MPa is shown in Figure 4.5. The major difference with the two other joints is its large initial stiffness and debonding capacity. This makes the joint very compatible with a

monolithic design if the adhesion in the interface can be guaranteed and the load is smaller than the debonding capacity.

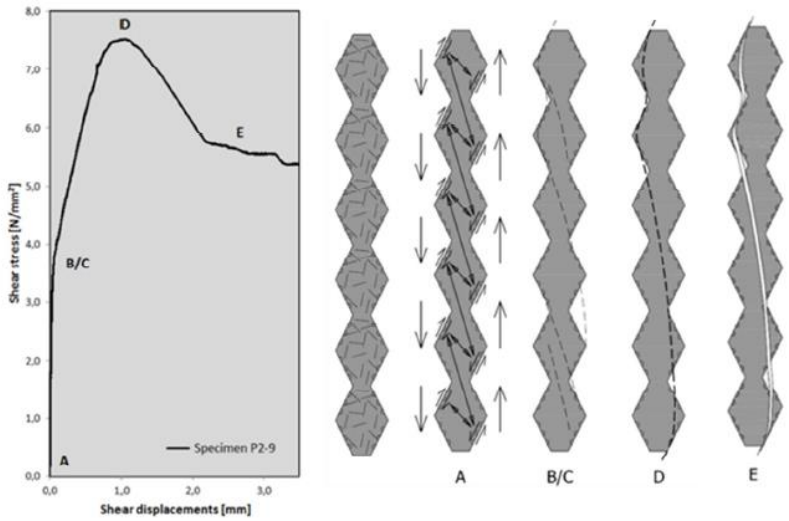

Figure 4.5 Shear-slip behaviour of the roughened serrated joint (van Keulen, 2015)

4.1.4 Shear-slip relation for the joint with aligned small shear keys

Figure 4.6 shows the shear-slip behaviour of the fourth type of joint. The results are obtained for a joint that is executed without any lateral prestress and with regular K70 mortar. This joint shows a large ductility after the capacity is reached in point D. The joint shows behaviour similar to that obtained for other joints.

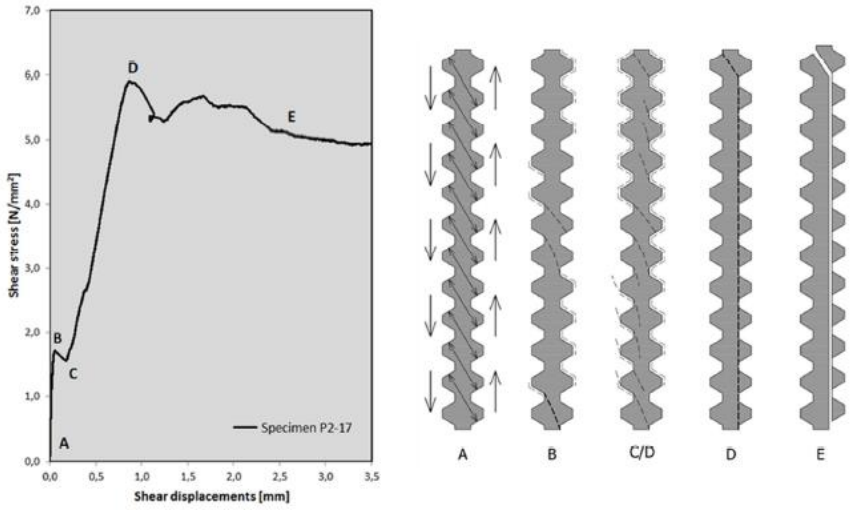

Figure 4.6 Shear-slip behaviour of the joint with aligned small shear keys (van Keulen, 2015)

4.2 The relation between the shear and lateral force

Another important aspect of the behaviour of the shear joints is the development of horizontal forces during loading. As explained in section 2.3.1, a horizontal force appears as a consequence of the transfer of the vertical shear force by an inclined compressive strut in the shear keys. This horizontal force must be resisted by either a lateral compressive prestress or a sufficient lateral stiffness provided by the in-plane stiffness of the adjacent precast elements. A combination of both is also possible, as will be supported by the following results. The important observations are discussed with use of the results for a staggered shear joint.

Figure 4.7 shows the test results for the staggered shear joints. The left diagram shows the shear stress-slip relation and the right shows the relation between shear force and horizontal reaction. The initial lateral prestress of 2 MPa in specimen P1-8 is deduced from the starting point of the V-H relation for specimen P1-8, which is at a force H of significant magnitude.

The different phases in the development of the horizontal force coincide with those of the developing shear force. In the first stage the shear forces are still transferred by adhesion instead of shear lock, whereby the horizontal reaction isn't increasing yet. The lateral force even appears to reduce slightly. This effect is best visible for specimen P1-8. The cause of this reduction is found in the deformation of the joint in this stage, which is shown for a small part of the joint in Figure 4.8. Both the shear deformation and a possible extensional deformation as a result of lateral prestress cause the small element to shorten in lateral direction. This results in a reduction of strain in the lateral steel bars and therefore a reduction in lateral force.

In the stage after debonding, the shear force is mainly transferred by the compression diagonals in the shear keys. This will increase the lateral force. The slope of the V-H relation reveals that the shear force that is transferred increases faster than the horizontal force that is required.

When the first cracks start to develop, certain ratios for V_s/H_s are found. These are given in Table 4.1. For the moment of failure the ratios are determined as well. For most specimens it appears that, based on a comparison of these ratios, the lateral force increases more than the shear force in the stage after cracking of the mortar.

After the capacity is reached, the shear lock mechanism fails. Therefore the horizontal force decreases to a certain value it keeps having in the residual strength stage of the connection.

The relation of specimen P1-8 shows that the horizontal force doesn't increase significantly up to a relatively large value of the shear force. In order to understand this effect, a closer look on the composition of the lateral force H must be taken. This force is formed by the summation of two contributions: the prestress force and the lateral stiffness force F_k. For the first three specimens, a small prestress is applied, whereby the lateral force H is almost completely provided by the force induced by the resistance of the surrounding elements to lateral displacements F_k. Specimen P1-8 is significantly prestressed and this force is for a long time sufficient to provide resistance to the horizontal component of the diagonal compressive force. Only when the full prestress force is "used", the lateral stiffness starts to play a role. The table results show that the lateral force caused by lateral stiffness at the moment of cracking is just 3 kN. When failure finally occurs, the lateral stiffness has a significant contribution to the lateral force, since $F_{k,u}$ is 90 kN and H_u is 334 kN.

Type	Prestress MPa	Lateral stiffness	Type of mortar	V_s	H_s	$F_{k,s}$	V_s/H_s	V_u	H_u	$F_{k,u}$	V_u/H_u
P1-5	0.1	M24	K70	427	85	46	4.2	597	141	120	4.2
P1-6	0.1	M24	Fibre	504	106	86	4.8	608	141	121	4.3
P1-7	0.1	M38	K70	401	76	56	5.3	673	162	142	4.2
P1-8	2	M38	K70	700	247	3	2.8	851	334	90	2.5

Table 4.1 Results for the staggered shear joint at moment of cracking s and ultimate capacity u (van Keulen, 2015)

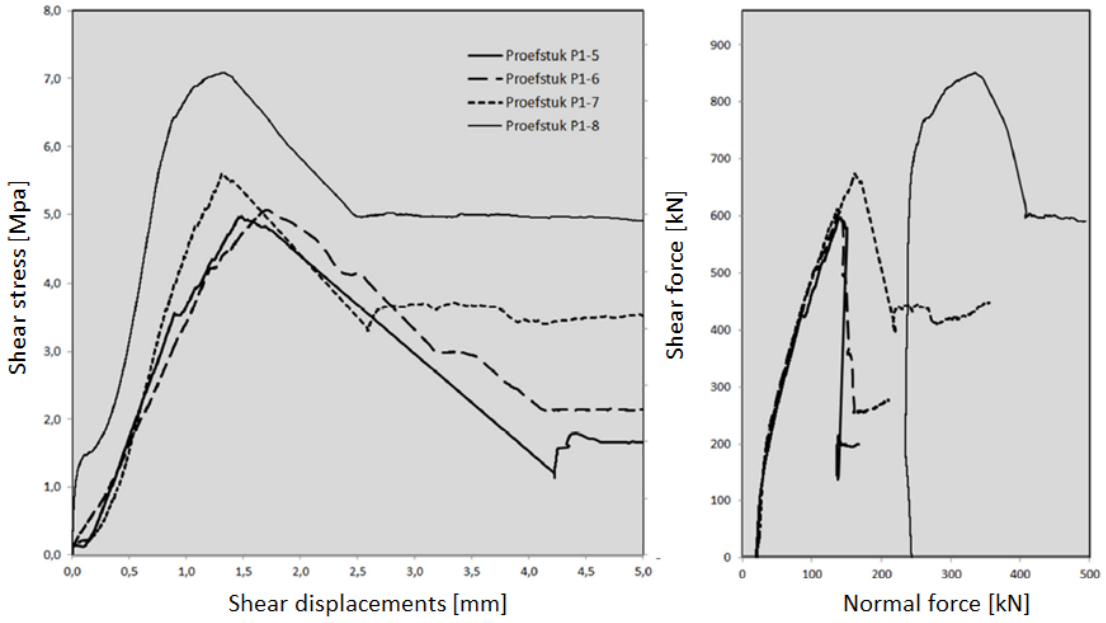

Figure 4.7 Shear-slip and V-H relation for the staggered shear joint (van Keulen, 2015)

The ratio between V and H is closely related to the angle alpha between the compression diagonal and the vertical axis. According to the equilibrium diagrams presented in section 2.3.1, the angle alpha is not exactly defined by V/H. However, since the contribution of the frictional force is likely to be very small, the ratio is a good approximation for the angle of the diagonal force.

The geometry of the profiled joint tries to predefine the direction of the compression diagonals. However, the angle of the diagonal won't be exactly as the geometry defines and will change during the loading process. In the first stage of the loading process the deformation of the joint material (Figure 4.8) contributes to a decrease of the angle between the diagonal and the vertical axis, alpha. Purely based on the joint's geometry, this ratio should be 4:1. The results in Table 4.1 show that the diagonal is steeper.

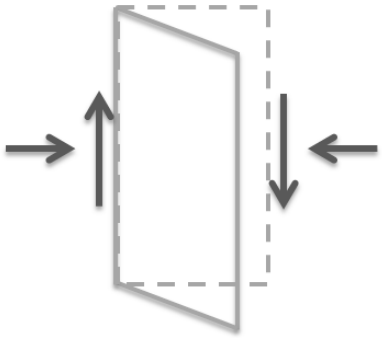

Figure 4.8 Deformation of the joint in initial stage

After cracks occur in the joint material, the angle increases. In this stage the increase of the horizontal force H becomes larger than the increase in vertical shear force V. The stiffness of the joint is reduced, whereby its deformations increase. The result is a rotation of the compression diagonal to a flatter orientation, resulting in a relatively larger horizontal component of the diagonal force, indicated by a smaller ratio for V/H.

Based on the comparison between the four tested joints, two important conclusions can be made with respect to the lateral stiffness and prestress.

- A connection with a larger lateral stiffness will have a larger shear capacity
- A connection prestressed in lateral direction will have a larger shear capacity

Although the report doesn't explicitly mention an increase in shear stiffness as a result of a larger prestress or lateral stiffness, the diagrams in Figure 4.7 indicate this dependency.

Another conclusion drawn in the report, based on results not presented here, is that the capacity of a connection with a narrow joint is larger than with a wide joint. The predefined angle of the diagonal is smaller for a narrow joint, resulting in a smaller diagonal force and horizontal component for the same transferred shear force. This increases the ultimate capacity of the connection.

Furthermore the effect of applying fibre reinforced mortar in some of the joints is investigated, but the small amount of tests with this mortar cannot provide confidential results. It is expected that the fibres will increase the joint's capacity, since they will increase the tensile strength of the mortar. Furthermore the residual capacity can be improved by the fibres, since they prevent one major crack to occur.

4.3 Comparison between the four types of joints

Figure 4.9 shows the shear-slip and V-H relation for the four types of vertical mortar joints. Based on these results, a comparison between the four options can be made.

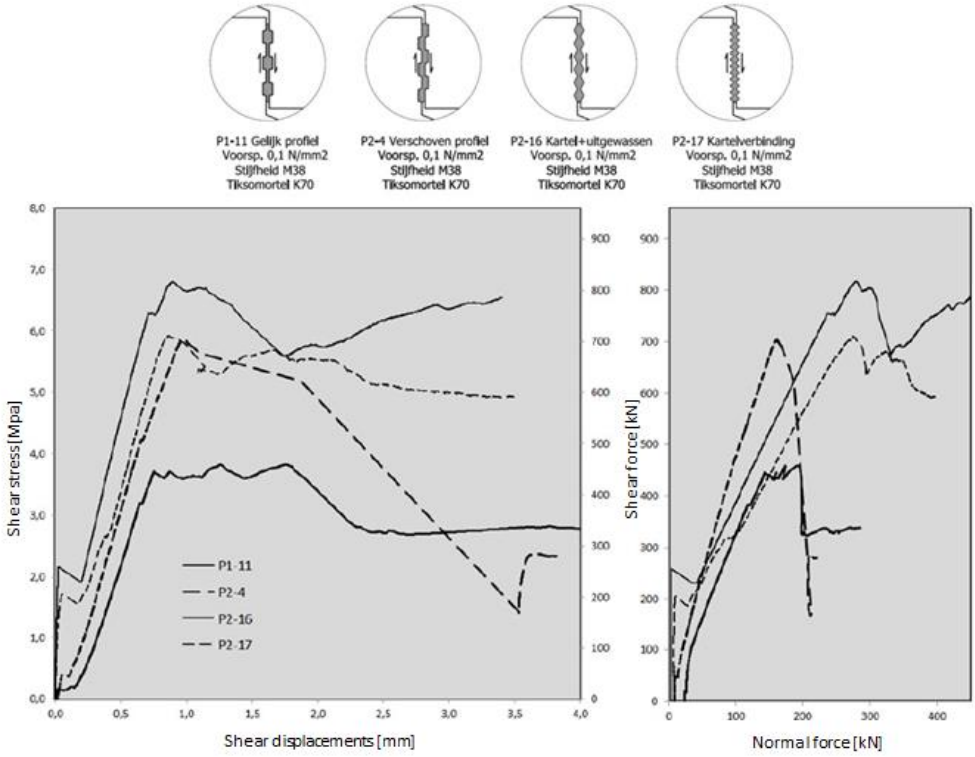

Figure 4.9 Comparison of vertical mortar joints (van Keulen, 2015)

From the left graph the shear capacity can be read. The roughened serrated joint has the largest capacity. The joint with small keys has the second largest capacity and the capacity of the joint

with staggered profile is slightly smaller. The joint with aligned profile has a considerable smaller capacity. The amount and angle of the compression diagonals determine the capacity of the joint. Joint P2-16 has steep diagonals and P2-17 has many diagonals, whereby their capacities are the largest.

The angle of the diagonals also determines the V-H relation. The steepest diagonals develop in joint P2-4, whereby for the same shear force transfer a smaller horizontal appears. Therefore this joint requires the smallest lateral stiffness of the adjacent elements. This is especially an advantage for application in wall sections with large openings.

Considering the shear stiffness of the joints, the largest differences are found in the phase before debonding of the interface. By roughening the surface of joint P2-16 cracking of the interface is postponed, resulting in a large initial stiffness with considerable debonding capacity. Joint P2-17 also appears to be rather stiff in the first phase. In the other two joints the interface cracks rather soon, whereby the shear lock mechanism is called upon earlier, resulting in larger shear deformations. However, the stiffness of all joints after debonding doesn't differ much. This is observed by considering the four shear-slip relations which are approximately parallel in this phase.

In each case another joint type can be the best option. The roughened serrated joint has the largest capacity. But roughening the surface is a laborious process sensible to deviations and mistakes. Furthermore the provided capacity can in many cases be way larger than required. Therefore the small keyed joint or the joint with staggered profile might be a better option. The joint with staggered profile sets lower requirements on the lateral stiffness, whereas the joint with small keys has a larger initial shear stiffness. These are two aspects to weigh. Based on the comparison a joint with aligned profile is in many cases not preferred.

4.4 Conclusion

The study on the previous research on profiled connections in paragraph 2.3 provided information on the shear-slip behaviour with its different characteristic stages, and parameters that influence this behaviour. The behaviour that is obtained by Van Keulen shows a lot of similarities with the information of paragraph 2.3. Van Keulen already considered the effects of joint geometry presented in section 2.3.5 while developing the four types of profiled joints. The results of this chapter showed that besides the parameters known from literature, the lateral stiffness and prestress have a large influence on the connection properties as well. A larger laterals stiffness and/or lateral prestress increases the shear capacity and stiffness of the connection.

5 Overview of the research topic

An overview of aspects that play a role in the behaviour of the vertical profiled mortar connections can be produced, based on the information presented in previous chapters. The first paragraph of this chapter describes this overview, that provides insight in all the aspects that could or should be investigated in order to be able to model the vertical profiled mortar connections in a shear wall. Since this research aims on developing a modelling approach for practical situations, not all identified effects that determine the connection's behaviour are included. So in the second paragraph the scope of this research is set by excluding some of the effects from this research. The third paragraph concludes with an enumeration of the specific research questions that are discussed in the remaining part of this report.

5.1 An overview of possible research aspects

The problem statement of this thesis has been formulated in chapter 1. This problem statement can be rephrased in a more general way:

"How can the vertical profiled mortar connection be modelled?"

In order to answer this question completely, many aspects that are involved in modelling the connection must be investigated. This paragraph attempts to identify these research aspects in a structured way, in order to gain insight in the complexity of modelling the vertical profiled mortar connection. The overview in this paragraph is composed with the current knowledge. It is therefore not necessarily complete.

5.1.1 Required knowledge to model the vertical profiled mortar connections

Modelling the shear connection comprises two main aspects:

- choosing the way of modelling that is applied;
- determining the connection properties that are required as input for this model.

The chosen modelling technique determines the connection properties that are required as an input. On the other hand, the importance of certain connection properties, for example a non-linear shear slip relation, determines the chosen modelling technique as well. So these two aspects need to be aligned.

So research must be done on the different modelling techniques that are feasible for the developed vertical profiled mortar connections. Questions to answer here concern for example the working of different finite elements and the possibilities within different software packages. Connection properties are for example:

- The shear stiffness;
- The shear capacity;
- The residual capacity;
- The nonlinear behaviour after cracking;
- The adhesive capacity;
- The adhesive stiffness.

These properties all concern the shear slip behaviour of the connection. Another property can also be the relation between the transferred shear force and the induced horizontal force by shear locking in the joint.

Research on the way the connection properties are determined contains more aspects to analyse. So this research is subdivided further in the remaining of this paragraph.

5.1.2 Determination of the connection properties

The connection properties are determined by a combination of different structural effects. According to the current knowledge, these effects are:

- Shrinkage of the joint mortar;
- Nonlinear behaviour of the materials;
- Dowel action of the transverse reinforcement in horizontal joints;
- The influence of normal stress in the joint;
- The influence of lateral stiffness obtained from the surrounding structure;
- The influence of joint properties on the behaviour of the mortar.

First of all, the behaviour of each effect should be analysed. What this analysis into the effects entails, is briefly discussed in the next section.

Secondly, when this knowledge is provided and each effect can be fully described and quantified, it is not yet known in which manner these effects influence the connection's properties. For example, when the magnitude of the lateral stiffness is known, it is not yet known to which shear stiffness this will lead. Or when the effect of dowel action of the reinforcement is described, it is not yet known how the dowel action cooperates with the shear transfer in the mortar joints. So the relations between each structural effect and the connection properties they influence must be investigated.

Lastly, multiple effects will have influence on the same connection property. For example, the lateral stiffness influences the shear stiffness of the mortar joint, but the joint properties, such as the type of profile that is used, will also partly determine this shear stiffness. So it should be known in which way all these effects combined determine one single connection property.

Based on the analysed combined relations, the influence of each effect relative to the others can be obtained. In this way the relevance of each effect is indicated. For the development of a practical way of modelling this is very important, since certain effects may be neglected in the modelling approach based on their relevance. Furthermore, knowing the relevance of each effect can be very useful for the structural designer in early phases of the design process. It gives insight into which effects to focus on while making important decisions when detailed analyses have not yet been performed.

5.1.3 Description of structural effects

If all the enumerated structural effects are quantified and their combined influence on the connection's properties is known, the connections can be modelled in a shear wall model according to the intended modelling approach. However, the magnitude of the structural effect is in most cases determined by many parameters, which are mostly dependent on design decisions. So in order to quantify each structural effect, research is required into these effects and the way

their magnitude is influenced by design parameters. This section contains a short explanation of these researches.

Since the magnitude of each structural effect may depend on multiple parameters, the relative influence of each parameter in determining the magnitude of each effect and especially the relevant effects is of interest. This indicates the relevance of each parameter. Irrelevant parameters may be ignored in the quantification of certain structural effects. Furthermore the structural designer can base decisions in early phases of the design process on the known relevance of all parameters. If for example the structural designer is aware of the fact that the lateral stiffness is a relevant structural effect that is largely determined by the distance between the mortar joint and the location of wall openings, he or she will emphasise this in the façade design.

5.1.3.1 Shrinkage of the joint mortar

As discussed in paragraph 2.3.4, the shrinkage of the applied joint material may lead to loss of adhesion in the concrete joint interface. However, the provided information was based on older types of mortar. Nowadays mortars are developed that hardly shrink. So is it still valid to state that adhesion may not be relied upon?

Furthermore, the effect of lateral expansion of the wall elements might also mitigate the effect of shrinkage. Figure 5.1 illustrates this effect. The precast wall elements are vertically loaded by dead load of the stories above the observed level. This vertical load will lead to a lateral expansion of the elements, what narrows the vertical joints between the elements. This effect may mitigate the effect of shrinkage, whereby the adhesive capacity of the concrete mortar interface is still present.

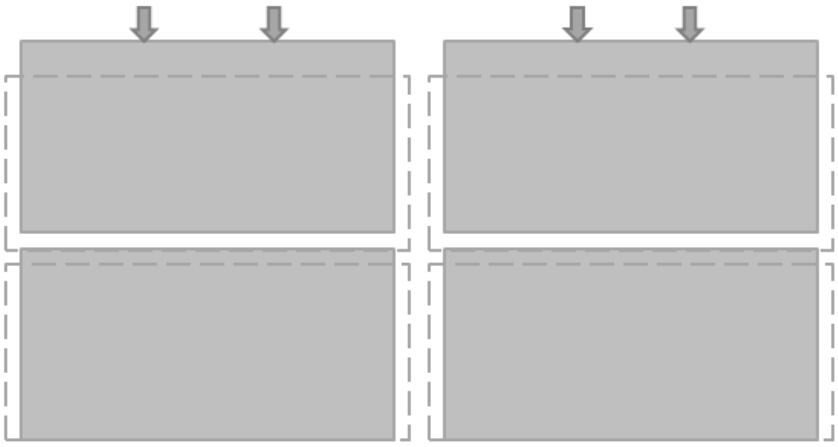

Figure 5.1 Lateral expansion of the wall elements

The effect is similar to what has been described in section 2.2.1 for compressive connections. The influence of the horizontal joints between the wall panels will be significant, according to what has been presented in that section. The properties of the horizontal joint filling and the possible application of starter bars in these joints determine to what extend the illustrated deformations are prevented.

If the effect of shrinkage is significant, this will result in a shear slip-shear stress relation for the vertical connections that differ from the ones found by Van Keulen. As has been discussed in section 2.3.4, shrinkage leads to a successive development of shear force transfer due to the gap

in the interface that has occurred. Dowel action of the transverse reinforcement is the first mechanism that transfers shear forces over the vertical joint, until contact between the precast wall elements and the joint mortar is restored and shear locking and shear friction take over the force transfer.

5.1.3.2 Nonlinear behaviour of the materials

The different stages of the shear slip-shear stress relation were described in paragraphs 2.3.3 and 4.1. What is seen is a non-linear relation between the shear slip and shear stress. The relation might be approached by a linear relation until the point of ultimate capacity. However, after first cracks occur in the mortar or the precast elements, the stiffness reduces gradually and after reaching the ultimate capacity, the capacity drops to a residual value.

As discussed in paragraph 2.1 ductility and deformation capacity are important properties for connections applied in precast concrete. Insight into which parameters determine the post cracking behaviour of the connection and therefore properties as ductility and deformation capacity, but also residual capacity and moment of cracking is important to be able to ensure proper connection behaviour.

5.1.3.3 Dowel action of the transverse reinforcement

The vertical profiled mortar connections make use of transverse reinforcement that is applied only in the horizontal joints between precast wall elements that are regularly present at the height of each floor slab in the building. The main purposes of the reinforcement are to provide lateral resistance against dilatation of the vertical profiled mortar joint, to take up tensile forces as a result of diaphragm action in the floor slabs and to provide structural integrity by transferring forces to an alternative load path.

The application of these horizontal reinforcement bars basically creates reinforced mortar beams at each floor. A possible side effect of these beams is that they are transferring vertical shear forces in the wall by dowel action. The transfer mechanism of dowel action is discussed in section 2.2.3. The contribution of dowel action of these beams is explicitly discussed in section 2.3.4.

Figure 5.2 gives a schematic illustration of the dowel action that takes place. The stiffness and capacity of this structural effect depend among others on the material properties of the reinforcement steel and the mortar in the horizontal joints, the dimensions of the horizontal mortar joints, the amount of reinforcement that is applied and the bending stiffness and capacity that is obtained with this combination. Furthermore, the way the horizontal joints are executed will be of influence as well. Figure 2.2 showed two possible variants for the horizontal connection between the wall elements and the floor that is also supported at the location of the horizontal joints. Whether the floor is supported by a corbel or integrated in the wall determines the location of the transverse reinforcement with respect to the wall elements and will therefore also influence the contribution of dowel action of this reinforcement to the transfer of vertical shear forces in the wall.

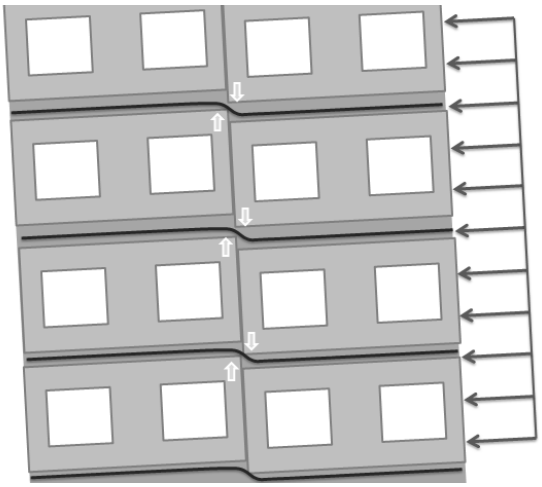

Figure 5.2 Dowel action of transverse reinforcement

All the parameters that are mentioned are known from design. So if the relation between the dowel action and these parameters is known, the magnitude of the effect of dowel action can be identified in early design stages. The relative contribution of dowel action to the properties of the vertical profiled mortar connection determines whether this effect is really relevant to take into account while designing a precast shear wall with this type of connections.

5.1.3.4 Normal stress in the joint

The test results of Van Keulen indicated the influence of a compressive stress perpendicular to the joint interface (paragraph 4.2). The presence of normal stress increased the shear capacity and stiffness of the joints. Especially for horizontal joints this normal stress is important, since these joints are compressed by dead loads. This doesn't hold for vertical joints between the wall elements. So the importance of this effect for the specific case of vertical profiled mortar joints may be rather insignificant. However, if it does occur it can be of major influence, as the test results indicated. Therefore this effect cannot be missing from this list.

5.1.3.5 Lateral stiffness

Van Keulen's tests also indicated the effect of lateral stiffness. The lateral stiffness is a measure for the resistance to dilatation of the joint provided by the surrounding precast elements in combination with the transverse reinforcement. This dilatation is caused by the horizontal force component of the compressive force that develops in the joint mortar as a result of shear locking. The effect is discussed in section 2.3.2 and illustrated in Figure 2.29.

The lateral stiffness is determined by many parameters, among which the axial stiffness of the transverse tying reinforcement, the Young's modulus of the precast concrete and the presence, size and location of wall openings.

The results discussed in chapter 4 demonstrated that the lateral stiffness increases the shear stiffness and capacity of the connection. The exact relation between the lateral stiffness and these two connection properties must be investigated, as explained in section 5.1.2. This relation compared to those between the other effects and the connection properties determines the relevance of the lateral stiffness.

5.1.3.6 Joint properties

The behaviour of the vertical joint also depends on the material properties of the mortar, the profile geometry and the treatment of the concrete-mortar interface, such as roughening or use of a bonding agent. Furthermore executional aspects, such as the filling ratio of the joint play a role as well.

The joint properties determine for example the stiffness of the compression diagonal that develops, the adhesive capacity, the cracking pattern that develops in the mortar and the failure mechanism that determines the ultimate shear capacity of the joint. So besides the linear properties of the connection, they are also linked to nonlinear properties. The distinction between the nonlinear effects and the joint properties won't therefore not always be clearly defined.

After debonding of the interface, shear transfer in the joint is partly provided by shear locking and partly by shear friction in the interfaces between concrete and mortar. The joint properties will also influence the relative contribution to the force transfer of these two mechanisms.

5.1.4 Summary of the possible research aspects

This paragraph discussed the overview of the research topic. All aspects that could be investigated were enumerated. The following list gives a simple overview of these research aspects:

- Research on modelling the vertical profiled mortar connection
    - Research on modelling techniques in FEM software
    - Research on the influence of different structural effects on the connection properties that are part of the model input
        - Research on the working principles of all structural effects
            - Shrinkage of the joint mortar
                - Research on the combination of parameters influencing this effect
            - Nonlinear behaviour of the materials
                - Research on the combination of parameters influencing this effect
            - Dowel action of the transverse reinforcement in horizontal joints
                - Research on the combination of parameters influencing this effect
            - The influence of normal stress in the joint
                - Research on the combination of parameters influencing this effect
            - The influence of lateral stiffness obtained from the surrounding structure
                - Research on the combination of parameters influencing this effect
            - The influence of joint properties on the behaviour of the mortar
                - Research on the combination of parameters influencing this effect
        - Research on the influence of each structural effect on the connection properties

- Research on the way a the combination of all effects influences the connection properties
    - Indicating the relevance of each effect. What can be ignored in modelling the connection's behaviour?

If all this research is performed a modelling approach that includes all connection properties and relevant effects can be constructed. Figure 5.3 shows schematically in a flow-diagram the setup of this modelling approach.

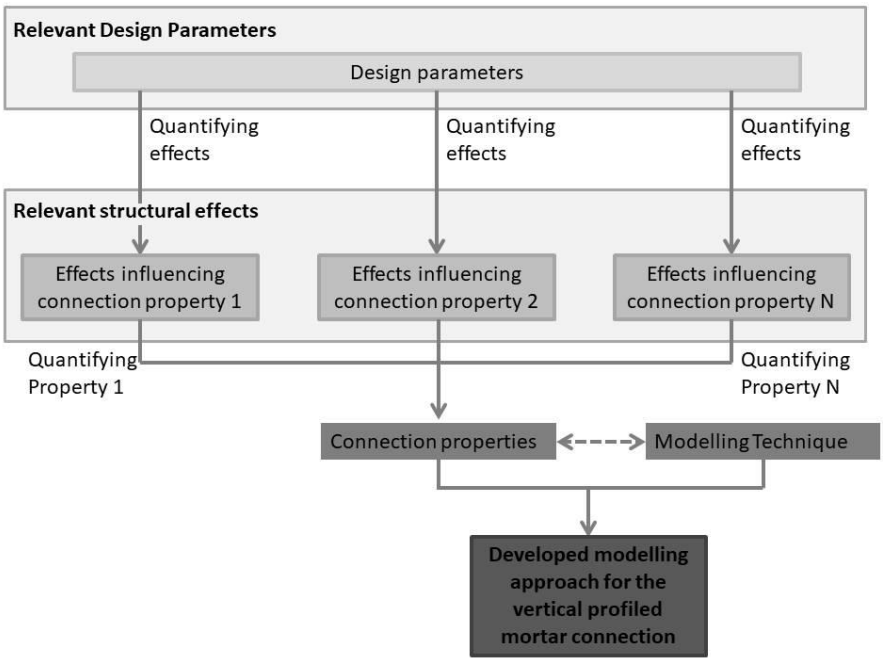

Figure 5.3 Schematic representation of the process of modelling the vertical profiled mortar connections

It all starts with determining the magnitude of all relevant design parameters that are involved in defining the connection properties. With use of the known design parameters the relevant structural effects are quantified. In Figure 5.3 there are N relevant structural effects, since all effects are included in this general scheme. When the magnitude of all the relevant structural effects is known, the discovered relations between the combination of these effects and the connection properties are used to determine the connection properties. These properties are input for the chosen modelling technique. This can for example be a linear or nonlinear interface element, discrete springs or a volumetric element. The choice for a certain modelling technique depends on the goal of the analysis that is performed with the complete structural model. As mentioned previously, the chosen modelling technique determines the required property input, but the important properties on the other hand set requirements and constraints to the modelling techniques that could be applied. The defined connection properties in combination with the chosen modelling technique form the way of modelling that is used for the vertical profiled mortar connection in a precast shear wall with stacked element configuration.

5.2 Scope and Simplifications

Previous paragraph gave a broad overview of the parameters and effects that influence the behaviour of the connection. Not all the addressed research topics can be considered in this thesis. So some topics must be analysed in further research. This paragraph defends the scope defined for this thesis. This inevitably leads to multiple simplifications to the connection's behaviour, which are discussed as well.

5.2.1 Excluded structural effects

At the beginning of paragraph 5.1 the problem statement of chapter 1 was rephrased in a more general way and the overview of previous paragraph was based on this general problem statement. The original problem statement of this thesis defined in chapter 1 is:

"How can the vertical profiled mortar connection be modelled in practical situations?"

Keeping this in mind, the relevance of some structural effects for these practical design situations is reassessed. Nonlinear behaviour of structural elements or materials is for example often not relied upon in design. Furthermore, in practical situations a conservative approximation is often desired. These considerations led to the exclusion of several structural effects from this master research.

5.2.1.1 Exclusion of nonlinear effects

The real behaviour observed during previous tests on profiled shear connections is described in section 2.3.3. The shear slip relation is characterised by its different phases: force transfer by adhesion, force transfer by compression diagonals, crack development in the mortar and the post cracking phase where the residual capacity is provided by shear friction in the main crack.

The effects of adhesion, crack development and residual capacity are not taken into account. In most design calculations it will probably be required that the connections will remain uncracked. So the post-cracking behaviour is not directly important for the purpose of a practical way of modelling. The effect of adhesion is in most cases obstructed by shrinkage of the mortar, based on tests on older types of mortar. Although adhesion might occur with modern mortar types, the effect is neglected in the parameter study, since it is likely to be neglected in practical situations. If this isn't the case because of shrinkage, then it will be because of executional aspects, such as the cleanliness of the interface. Excluding the relatively stiff adhesive force transfer is a conservative approximation.

Figure 5.4 shows schematically the simplification of the shear slip- shear stress relation that is obtained by applying the proposed exclusion of nonlinear effects. A linear relation is obtained where the only unknown is the shear stiffness that is given by the angle of the relation. Since a linear modelling is applied, even a capacity is lacking. Thereby the relation continues till infinitely large values of the shear slip and shear stress in the joint. For this reason the resulting shear stress that is obtained from the model should always be compared to the capacity that was found in the test results presented in chapter 4.

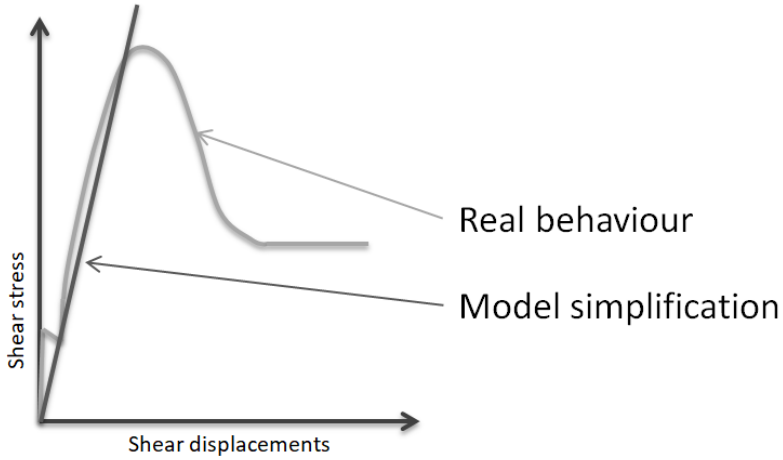

Figure 5.4 Model simplification of the connection's shear slip- shear stress relation

5.2.1.2 Exclusion of shrinkage

As described in section 2.3.4, shrinkage will result in a gap between the precast concrete elements and the joint mortar. As a result, the shear forces are initially transferred by dowel action of the floors and transverse reinforcement. The mortar joint is only activated when contact with the precast elements is restored due to shear deformations.

This successive behaviour is not considered in this thesis. Here it is assumed that the compression diagonals take up shear forces from the start, when the shear displacements are still equal to zero.

The modelled situation in total with respect to shrinkage can be described as a situation where a modern shrinkage poor mortar is applied, that shrinks just enough to loose contact in the interface, whereby adhesive forces are cancelled out but the mortar can still transfer shear forces directly.

5.2.1.3 Exclusion of dowel action of the tying reinforcement

Since the consecutive behaviour as a result of shrinkage is not taken into account, any dowel action of the transverse reinforcement only takes place simultaneously to the shear transfer by shear locking and shear friction in the mortar joint. In chapter 2 it has been explained that the shear stiffness obtained from dowel action is considerably lower than the stiffness obtained by the other mechanisms, because dowel action is activated only with a relatively large shear slip over the joint.

For this reason the contribution of dowel action to the shear stiffness of the connection is assumed to be relatively small. If this contribution is small, it is reasonable to model the transverse reinforcement by truss elements that can only transfer axial forces. Hereby the shear transfer is fully taken by the mortar joint, which enables investigation of the behaviour of the joint exclusively.

5.2.1.4 Exclusion of the effect of normal stress

Since the research is focused on the application of the profiled shear connection in vertical joints between precast concrete wall elements, the influence of stress normal to the connection is not considered. The application of profiled shear connections in horizontal joints is not part of this research.

5.2.2 Included effects

The effects that are included in this research are the effect of lateral stiffness and the joint properties. Since the nonlinear properties of the connection are not included, only the relation between these two effects and the shear stiffness of the connection is investigated.

Since shear locking is seen as the most contributing shear transfer mechanism and this induces lateral forces on the joint's environment, the effect of the lateral stiffness is important to investigate.

Furthermore, the joint properties such as the mortar properties and the profile geometry are expected to have a significant contribution to the linear shear stiffness of the connection.

5.3 Content of the master research

The schematic model workflow that was presented in paragraph 5.1 can be adjusted to the scope that is defined in previous paragraph. Figure 5.5 shows the adjusted model scheme.

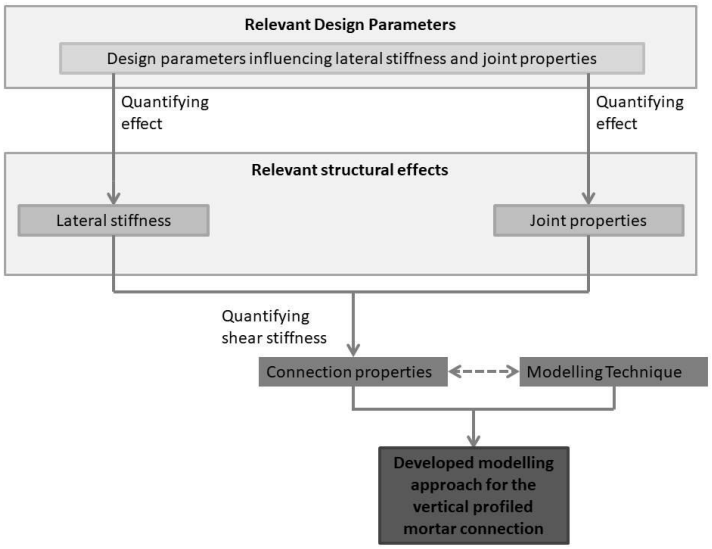

Figure 5.5 Schematic representation of the modelling method according to this research

Due to the exclusion of several effects and the restriction to linear behaviour, the only unknown connection property is its shear stiffness that is related to shear transfer in the mortar joint. The scheme illustrates in which way this property is defined.

Several design parameters influence the two effects that are considered: The influence of lateral stiffness and joint properties. In sections 5.1.3.5 and 5.1.3.6 some of these design parameters were mentioned. The relation between the combination of these design parameters and the magnitude of the two effects will be analysed. For the step "quantification of effects" three important questions arise:

- In which manner does each single design parameter influence the magnitude of the lateral stiffness and/or the joint properties?
- Which design parameters contribute insignificantly and may be ignored in defining the magnitude of the lateral stiffness and the joint properties?
- In which manner does the combination of multiple design parameters determine the magnitude of the lateral stiffness and/or the joint properties?

The next step is defining the connection property with the known lateral stiffness and joint properties. This step of quantification of the shear stiffness comprises the following questions in this master research:

- In what way does a combination of lateral stiffness and joint properties determine the shear stiffness of the connection?
- What is the relative contribution of both effects to the shear stiffness of the connection?

By answering these five questions, it must be possible to develop a linear modelling approach for the vertical profiled mortar connections, that takes into account the effect of lateral stiffness and varying joint properties. This approach is then applicable for practical situations where the conservative assumption is made that adhesion doesn't occur and none of the mortar joints is loaded beyond their ultimate capacity in order to be able to disregard nonlinear behaviour.

The remaining of this report describes the research that is performed in order to answer these five questions. The first step in this research is to develop a model that can be used to analyse the relations between the defined parameters, effects and properties. In chapter 6 the translation from Van Keulen's test setup to a finite element modelling approach is described. Chapter 7 describes the analysis that has been performed on a finite element model of the test setup, using the modelling approach developed in chapter 6.

Subsequently the model is expanded to a larger scale in order to perform a parameter study, in which several design parameters are varied over a certain range, while recording the resulting lateral and shear stiffness. This study is executed in order to find answers to the first and second formulated question. The parameter study of chapter 8 is not sufficient to describe in which manner the combination of parameters determines the connection's shear stiffness. So in order to formulate a more complete answer to the third question, more research is required. This is described in chapter 9, where also a start is made in answering the last two questions.

In chapter 10 analytical relations between the structural effects and the shear stiffness are derived, based on the results presented in chapter 8 and 9. These relations will provide a complete answer to the last two questions. Thereafter it is tried to develop a practical way of modelling, which is based on the derived relations, that can be used in a structural model of a complete building. This way of modelling is subsequently evaluated on a shear wall model, which is described in chapter 11.

6 Principles of the applied bar model

In chapter 5 an overview of research aspects was given and the scope of this thesis was set. The focus of this thesis is on the effect of lateral stiffness and varying joint properties on the linear behaviour of the vertical profiled mortar connection. Since a linear analysis is performed, the shear stiffness is the only unknown connection property. A model setup must be developed that can be used to analyse the influence of different design parameters on the lateral stiffness, relevant joint properties and the linear shear stiffness of the connection. In this chapter a description of the model setup is provided. This model setup is feasible for the indicated research goals but is not necessarily feasible for practical situations. In the first paragraph the translation of the test setup to the finite element model is discussed. The second paragraph focusses on the way the output of the model is processed.

Using the model setup that is explained in this chapter, a finite element model with the same layout as the test setup is analysed in chapter 7, in order to be able to compare the finite element results to Van Keulen's test results. For the parameter study in chapter 8 the finite element model is further expanded to a larger scale of a complete shear wall. Taking this step immediately would be too fast, wherefore the intermediate analysis of chapter 7 is necessary.

6.1 Translation of test setup to FE model

This paragraph discusses the translation of Van Keulen's test setup to the finite element model that is used for this research.

6.1.1 Description of the test setup

The test setup is shown in Figure 6.1. The connections are tested by means of a shear test. For this purpose two L-shaped concrete elements are produced. In between these elements the joint is applied over a length of 600 mm, resulting in three compression diagonals that develop. The thickness of the concrete elements is 200 mm. Above and below the joint external steel bars are used that function as concentrated reinforcement. The steel bars are slightly prestressed to keep all the elements together. Some test specimens were prestressed by a larger initial force, in order to simulate lateral compression of the joints.

A displacement load is applied on top of the upper L-shaped element. The support is placed on the lowest L-element exactly underneath the point of load application in order to avoid moments in the test specimens. The induced load on the specimen is transferred via the mortar joint from the upper concrete element to the other. The right picture of Figure 6.1 shows the sensors that are used to measure the horizontal and vertical displacement differences over the mortar joint that occur as a result of the shear force.

Figure 6.1 Van Keulen's test setup (van Keulen, 2015)

6.1.2 The combination of shear friction and shear locking in Van Keulen's joints

The whole of the connection consists of a profiled mortar joint and concentrated transverse reinforcement at the height of each floor level. The transfer of the vertical shear forces that develop in the shear wall is provided by a combination of adhesion, shear friction, dowel action and shear lock. However, as already explained in paragraph 5.2, the contribution of adhesion and dowel action are excluded. Remaining are shear friction and shear locking.

The combination of these two effects in a profiled mortar joint is described in section 2.3.1. If enough shear friction can take place in the concrete mortar interface, it will provide force equilibrium without the need for an extra horizontal force provided by transverse tying reinforcement, as Figure 2.24 illustrates. In this situation the contribution of the shear friction to the direct transfer of the vertical shear force is limited, since its vertical force component is rather small.

However, the test results in chapter 4 (Figure 4.7 and Table 4.1) clearly show the need for an extra horizontal force that makes equilibrium with the horizontal force component of the compression diagonal force that develops due to shear locking. The contribution of shear friction seems limited, especially for the developed profiles with a smooth concrete-mortar interface. The force equilibrium of the joint is therefore more similar to the principle sketches of Figure 2.25.

The ratio V/H that is calculated by Van Keulen for the point of initial cracking and ultimate capacity, will approach the angle of the compression diagonal that developed in the mortar (Table 4.1). The error between this calculated and real value of the angle depends on the relative contribution of shear friction. This can be seen from Figure 2.25. If the force $F_{friction}$ is very small, the force diagram approach a normal triangle, where $F_{diagonal}$ is only defined by the forces V an H.

It is possible to estimate the separate influence of shear friction and shear locking based on the assumption that the compression diagonal in the mortar will develop with an angle equal to that of the line that connects the midpoints of two opposite inclined surfaces. This principle is illustrated for the staggered joint in Figure 6.2.

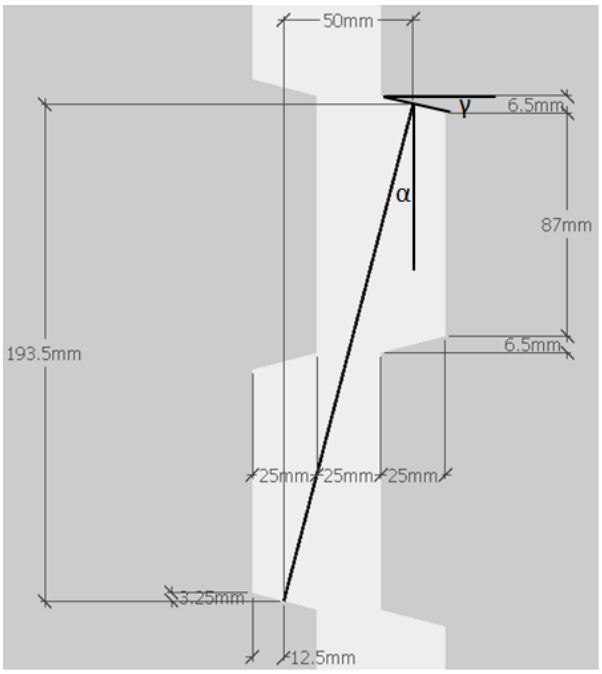

Figure 6.2 Profile geometry of the staggered joint

According to this geometry, the angles of the diagonal and the inclined surface are given by the following ratios:

$$\alpha = \frac{193.5}{50} = 3.87 \qquad \gamma = \frac{6.5}{25} = 0.26 \ (\frac{1}{\gamma} = 3.84)$$

The diagonal and the inclined surface are almost perpendicular. For now it is assumed they are exactly perpendicular. Therefore the equilibrium of forces must be according to Figure 6.3. According to Table 4.1, the ultimate capacity of for example specimen P1-5 is 597 kN and the accompanying H is 141 kN. The diagonal force has a slope of 3.87 and therefore the total horizontal force (H plus the horizontal component of $F_{friction}$) must be equal to:

$$F_{h,total} = \frac{597}{3.87} = 154\ kN \rightarrow F_{friction,h} = 154 - 141 = 13\ kN$$

The vertical force component of the friction force in the inclined concrete mortar interface is:

$$F_{friction,v} = F_{friction,h} * \gamma = 13 * 0.26 = 3.4\ kN$$

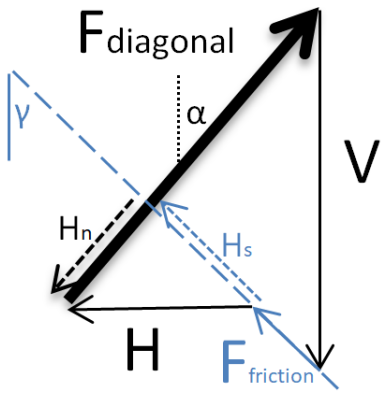

Figure 6.3 Force equilibrium in case of a perpendicular diagonal force and shear friction

The found vertical component of the shear friction must be subtracted from vertical shear force V to find the part of the shear force that is transferred by shear lock. Then an iteration is required to find a new estimation of $F_{h,total}$, $F_{friction,h}$ and $F_{friction,v}$

$$V_{shearlock} = V - F_{friction,v} = 597 - 3.4 = 593.6\ kN$$

$$F_{h,total} = \frac{593.6}{3.87} = 153.4\ kN \rightarrow F_{friction,h} = 153.4 - 141 = 12.4\ kN$$

$$F_{friction,v} = F_{friction,h} * \gamma = 12.4 * 0.26 = 3.22\ kN$$

After some iterations the following stable value is found: $F_{friction,v}$= 3.24 kN. This means that the direct contribution of shear friction in the inclined interface to the transfer of the shear force V is:

$$\frac{3.24}{597} = 0.54\%$$

The estimated contribution of shear friction in the transfer of the shear force is very low. It is unfortunately not possible to accurately distinguish the contributions of shear locking and shear friction from the provided test results. This estimation is done under the assumption of a diagonal force perpendicular to the inclined surface and shear friction that only takes place along the inclined interface and not along the vertical concrete-mortar interface of the profiled joint.

For this research especially the role of the lateral stiffness that must provide the force H is of interest. For this reason it is decided to simply ignore the contribution of shear friction. This results in simple relations between the shear force V, the horizontal force H and the compressive diagonal force F_d. The angle of the diagonal is then simply found by the ratio V/H. The whole is illustrated in the force diagram of Figure 6.4.

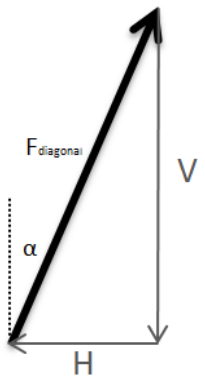

Figure 6.4 Force equilibrium without shear friction

6.1.3 Compression diagonals modelled as bar elements

Since the contribution of shear friction is ignored, only shear locking transfers the vertical shear force. This takes place by axial compression in the mortar that occurs in a compression diagonal between the two opposite inclined surfaces of the joint profile.

This behaviour is simply modelled by diagonal bar elements that represent the compressive struts that develop when the connection is loaded in shear. Figure 6.5 presents the applied

schematisation. The left image shows schematically the presence of the mortar and the direction of the principle stresses that develop. The model simplifies this behaviour by a diagonal bar with a Young's modulus equal to that of the mortar and a cross-sectional area that represents the dimensions of the compression diagonal in the mortar. This bar is executed as truss element that can only transfer axial forces.

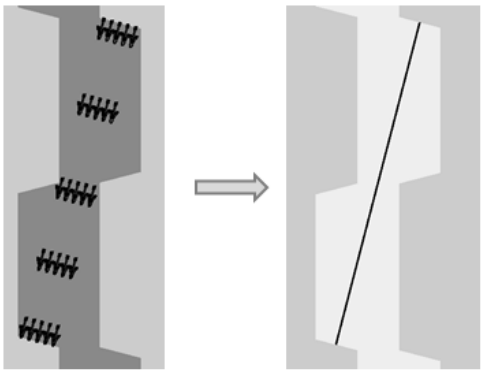

Figure 6.5 Schematisation of the compression diagonal

The bars require a certain cross-sectional area, E-modulus and slope as input. The E-modulus is based on provided information about the type of mortar used during the tests (Van Keulen, 2013). The cross sectional area and slope are not known exactly, but they are bounded by the chosen profile geometry. Values for both are chosen based on an educated guess. Both parameters are investigated during the study, whereby their influence on the connection's behaviour is indicated by a resulting upper and lower limit.

Figure 6.6 presents the schematisation of the bar model. Each single diagonal is modelled by a bar element. This element is on one side loaded with a shear force V and on the other side "supported" by the concrete element where the force is transferred to. This force V induces a horizontal force H that is solely defined by V and diagonal angle alpha, as a result of ignoring the contribution of shear friction. The bar element is on both sides horizontally supported by a spring. This set of support springs illustrates the lateral stiffness that is provided by the two surrounding concrete elements in combination with the applied transverse tying reinforcement.

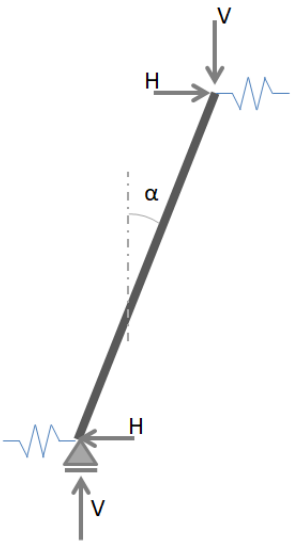

Figure 6.6 Schematisation of the bar model

The rotation of the compression diagonals during loading, that is described in paragraph 4.2, is not taken into account. Since the analysis is geometrically linear, the angle under which the bars are modelled remains constant. Doing a geometrical nonlinear calculation may be a way to include the effect of a rotating diagonal. However, since there are more factors influencing the angle of the diagonal that cannot be modelled, it is not sure whether a nonlinear analysis is able to describe the effect in a correct way. The slope of the diagonal is one of the parameters that is varied during the study. Therefore it is possible to draw conclusions on the relevance of this effect and the need of taking it into account.

By modelling diagonal bars, there are only two joint properties included in the model:

- The diagonal stiffness;
    - This is determined by the E-modulus of the mortar, the cross section of the diagonal bar that is used and the length of the bar elements.
- The angle of the diagonal bars;
    - This is determined by the profile geometry.

The relation between these joint properties and design parameters they are influenced by (such as profile geometry) cannot be investigated with the bar model. This is because the orientation of the bars and their properties are manually inserted input of the model. So only the relation between these two joint properties and the connection's shear stiffness is analysed. This means that the modelling scheme of Figure 5.5 is not analysed thoroughly. Figure 6.7 indicates the relation that isn't taken into account by using the bar model. If the outcome of the parameter study will show that the joint properties are relevant, it can be very useful to perform a more in depth research on the relation between the design parameters and the joint behaviour.

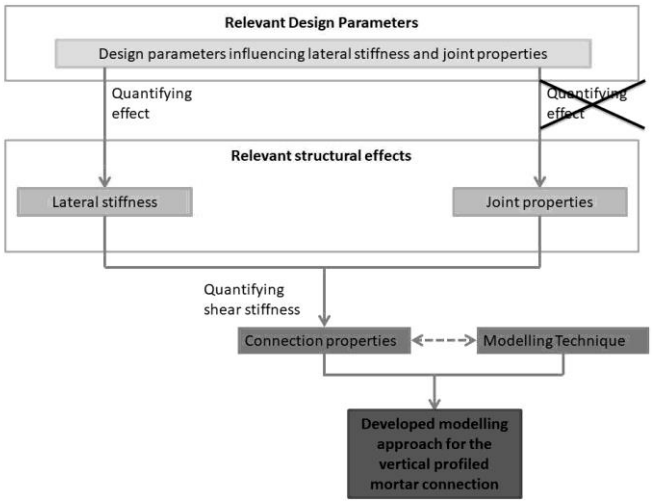

Figure 6.7 Due to the application of the bar model, the relation between design parameters and joint properties is not analysed.

The developed bar model is a way to model the vertical profiled mortar connections, however it is not feasible for practical situations. Application of the bar model requires a discrete bar element for each compression diagonal that develops in the mortar joint. That means that for a single floor high joint approximately fifteen diagonal bars must be modelled. If a complete building consisting of multiple shear walls is analysed, the model would contain thousands of bar elements that are inserted manually. So the bar model is useful for the purpose of this

research, but not for practical situations and is therefore not a proper answer to the problem statement of this research.

6.1.4 Analysed profile type

As addressed in chapter 4, Van Keulen developed and tested four profiled mortar joints. However, this research only considers connections with a staggered profile.

The profiles with aligned shear keys are harder to model, because of the consecutive interaction between the compression diagonals within one key and the kinked compression struts between two keys. This interaction cannot be modelled in a linear analysis with bar elements representing the diagonals. The proposed linear bar model is also not capable of taking the effect of a roughened surface of the serrated waterjetted profile into account. Furthermore it was concluded by Van Keulen that the profile with small keys performs less favourable compared to the staggered profile. For these reasons the staggered profile was chosen to analyse first. In later research the a model for the other profiles can be developed.

6.1.5 The finite element model of the test setup

In order to develop the finite element bar model of the staggered joint, the geometry of the mortar joint is translated to the corresponding bar model geometry. This is illustrated in Figure 6.8.

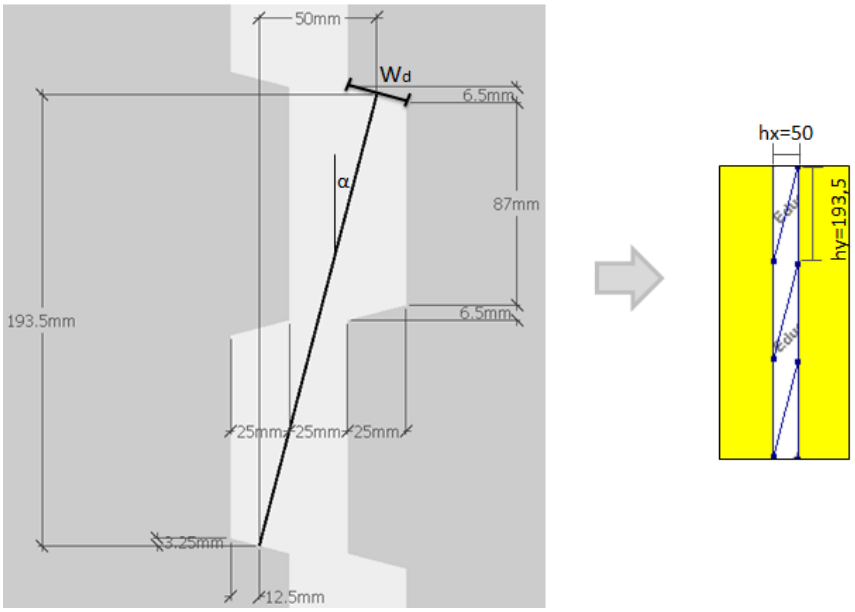

Figure 6.8 Translation of joint geometry to bar model

The orientation of the bars is defined by the orientation of the line between the midpoints of two opposite inclined surfaces. According to the geometry of the staggered joint, the vertical and horizontal distance between the bar's begin- and endpoint is 193.5 and 50 mm respectively. Hereby the diagonal angle alpha is determined.

The stiffness of the diagonal bars depends on the mortar's Young's modulus, the diagonal cross section and the length of the bar element. The last is fixed by the definition of alpha. The Young's modulus is based on material properties provided by Van Keulen (Van Keulen, 2013). The cross-sectional area is defined as:

$$A_{d,i} = W_d * t$$

A_d is the bar's cross section. W_d is the width of the compression diagonal that is assumed to be equal to the length of the inclined surface (See Figure 6.8) and t is the thickness of the concrete elements. The stiffness of a single diagonal bar, the diagonal stiffness is defined by:

$$k_{d,i} = \frac{A_{d,i}E_d}{L_d} \; where \; L_d = \sqrt{h_x^2 + h_y^2} \quad [6.1]$$

As indicated in Figure 6.8, the profiled surface is not included in the finite element model. The effect of the profile is already taken into account in defining the bar's properties. Modelling the profile is not contributing to better results and is also very laborious.

Figure 6.9 shows the developed finite element model that is used to simulate the test setup. As can be seen, the bar model is applied for the three diagonals that develop in the joint, the input of this model is according to Figure 6.8, Resulting in a gap between the two L-elements of 50 mm, instead of 25 for the test setup.

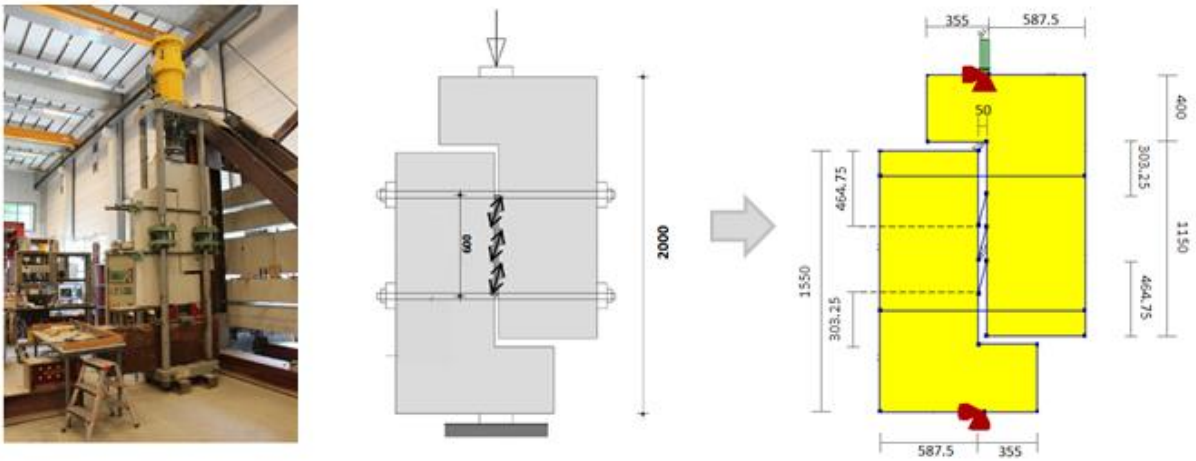

Figure 6.9 Translation from test setup to finite element model (van Keulen, 2015)

Just like for the test specimen, a displacement load is placed on top. The vertical support is placed on the bottom under the point of loading. The horizontal supports are required to keep the model stable. Since a point load or support results in the occurrence of a singularity, both are applied over a certain small length.

The dimensions of the L-shaped elements are equal to those of the test setup. Therefore the modelled transverse bars have equal length as well, resulting in the same axial stiffness.

6.2 Processing of model output

During the performed tests, the applied force and the displacements over the mortar joint were measured continuously. Figure 6.10 shows the measuring equipment that was used to measure the displacements over the joint. Together with the measured applied shear force, the diagram of Figure 6.10 is created. This diagram is discussed in paragraph 4.1. The test results showed a correlation between the shear stiffness of the connection and the lateral stiffness that was provided. The relation between the specimen's shear stiffness and the properties of the mortar has not been quantified by Van Keulen's tests.

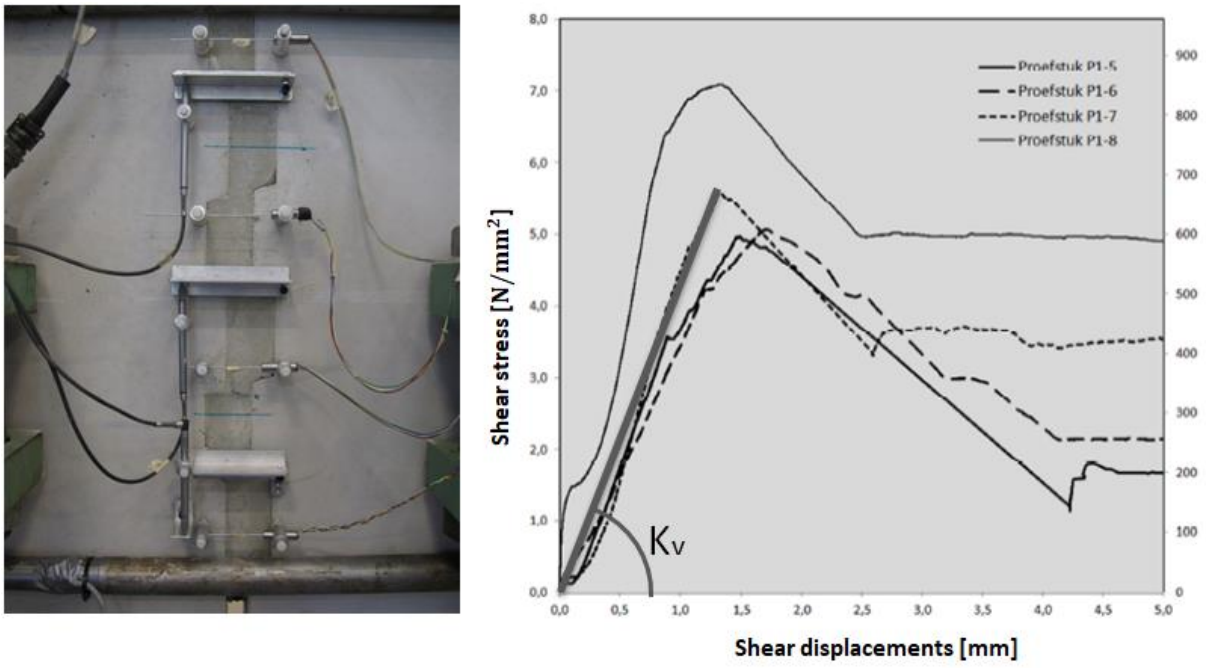

Figure 6.10 Test results with indication of the secant shear stiffness K_v that must be modelled by the bar model. (van Keulen, 2015)

The finite element model of the connection is developed in DIANA 10.2. The applied linear bar model should approximate the shear stiffness, that is obtained from the tests, by a secant shear stiffness K_v. This stiffness is indicated for test specimen P1-7. The secant shear stiffness depends on the lateral stiffness K_h and the diagonal stiffness K_d, which is defined by equation 6.1.

The magnitude of the shear and lateral stiffness must follow from the model results. The processing of model output into these stiffness quantities is illustrated in Figure 6.11.

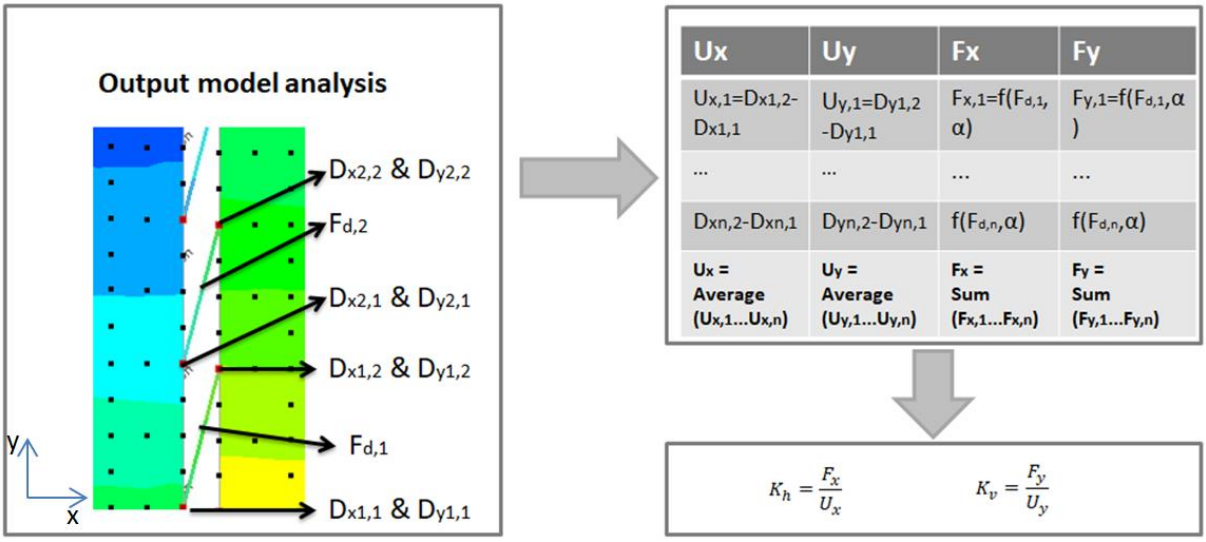

Figure 6.11 Processing of model output

The displacements D_x and D_y in the end points 1 and 2 of each diagonal 1 till n and the axial force F_d in each diagonal bar 1 till n is taken as output from the analysis. These values are stored in a table and subsequently the quantities U_x, U_y and F_x and F_y are calculated.

F_x and F_y are respectively the summation of all horizontal and vertical components of each axial diagonal force. So F_y is equal to the shear total shear force that is transferred by the connection and F_x is the total lateral force that is induced to the surrounding concrete elements. As indicated in Figure 6.11, these quantities are a function of each individual axial diagonal force and the angle of the diagonals α. This is in correspondence with the force equilibrium of Figure 6.4.

Subtracting $D_{x1,1}$ from $D_{x1,2}$ results in the dilatation $U_{x,1}$, which is the horizontal dilatation of the joint at the location of diagonal number 1. Similarly, subtracting $Dy_{1,1}$ from $Dy_{1,2}$ gives the shear slip over the joint at the location of diagonal number 1, $U_{y,1}$. These two values are often referred to as the local horizontal and vertical displacement difference. U_x and U_y are the average of all the local displacement differences. Figure 6.12 illustrates the quantities U_x an U_y, where U_x is the summation of par 1 on the left side and part 2 on the right side of the joint.

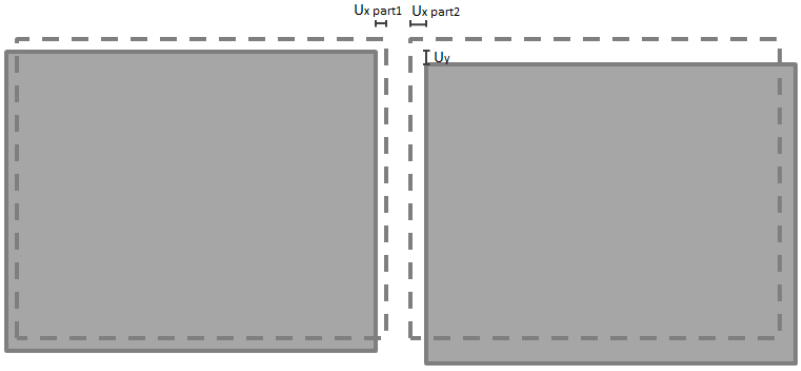

Figure 6.12 Indication of Ux and Uy

The shear and lateral stiffness are then defined as:

$$K_v = \frac{F_y}{U_y} \qquad K_h = \frac{F_h}{U_x} \quad [6.2]$$

So the shear stiffness is the total transferred shear force divided by the average slip over the joint. This stiffness is a secant stiffness that should approximate the secant stiffness of the test results as indicated in Figure 6.10. The lateral stiffness is the total horizontal force induced on the surrounding divided by the average dilatation of the joint.

The stiffness quantities can also be defined for an individual diagonal:

$$k_{v,i} = \frac{F_{y,i}}{U_{y,i}} \qquad k_{h,i} = \frac{F_{h,i}}{U_{x,i}} \quad [6.3]$$

Another quantity that is used is the shear and lateral stiffness per diagonal, the average shear and lateral stiffness, which is simply the total stiffness value divided by the amount of diagonal bars in the connection:

$$k_v = \frac{K_v}{\#diagonals} \quad k_h = \frac{K_h}{\#diagonals} \quad [6.4]$$

This quantity is used to compare models with an unequal amount of diagonals. For example to compare the model of the test setup that is created with the model that is used for the parameter study.

6.3 Conclusion

This chapter discussed the development of the bar model that is used to do research on the vertical profiled mortar connections. The bar model can be applied by neglecting the effects that were discussed in paragraph 5.2 together with the assumption of a small shear friction contribution.

The model is useful to investigate the influence of a varying lateral stiffness, due to varying design parameters, on the shear stiffness of the connection and the influence of the size and angle of the compression struts that develop in the mortar joint. As explained, the model doesn't take into account the way in which these two properties of the diagonal struts are determined by design parameters. The reason for this is the fact that the properties of the diagonal struts must manually be given as model input. The consequence for the developed modelling scheme has been indicated in Figure 6.7. Further research on this relation might be necessary.

The developed bar model is a way to model the vertical profiled mortar connections, however it is not feasible for practical situations and is therefore not a proper answer to the problem statement of this research.

7 Analysis of a small vertical profiled mortar connection

In the previous chapter the bar model is discussed. This bar model is developed to create a finite element model of the test specimens that were tested by Van Keulen (Figure 6.9). Before further research on the connection can take place on a large scale, it is wise and interesting to analyse this model of the test specimen. This chapter describes this analysis.

The goal of doing an analysis on a finite element model of the test setup is to validate the use of the bar model for the vertical profiled mortar connection. This is done by analysing the model's behaviour compared to the test specimens. Besides a qualitative comparison, also a quantitative evaluation is done. This quantitative evaluation is based on the resulting values for the shear stiffness of the connection. The qualitative and quantitative comparison form the link between the test results and the results of the model research of this thesis.

Besides an analysis of a model with the same geometry as the test specimens, also an enlarged model is analysed in order to investigate the effect of creating a larger connection. This step is important for the switch from a model with the size of the test specimen to a model as large as a shear wall.

The first paragraph provides an overview of the input of the finite element model. The second paragraph discusses the results of the analysis on the small model with the geometry equal to the test setup. The results obtained from the larger model and an evaluation of the difference between the two models are part of the third paragraph of this chapter. As the results will show, the magnitude of the shear stiffness in the FE model is larger than the test results indicate. In the fourth paragraph this quantitative difference is examined and possible causes are addressed.

7.1 Model input

The test setup is modelled in DIANA 10.2. The small model, as shown in Figure 7.1, contains two L-shaped concrete elements. The dimensions of these elements are equal to those of the test specimens (Van Keulen, 2018). These elements are connected by three diagonal bars, corresponding to the applied joint profile during the tests with three compression diagonals. The two concrete elements are kept together by two transverse steel bars that are connected to the outer edges of both concrete elements. The model is loaded by a prescribed downward displacement of 1mm at the top, located right above the center line of the joint. The supports at the bottom are also located on this center line in order to avoid eccentricities. In order to prevent peak stresses, forces and displacements, the prescribed displacement and the support are applied along a small stiff line segment.

In a second analysis the model is enlarged by a factor 1.5 along the diagonal, making all outer dimensions of the L-shaped elements 1.5 times larger. This model contains six diagonal bars, as can be seen in Figure 7.2. Applying six bars resulted in approximately the same distance between the end points of the outer bars and the edges of the vertical joint.

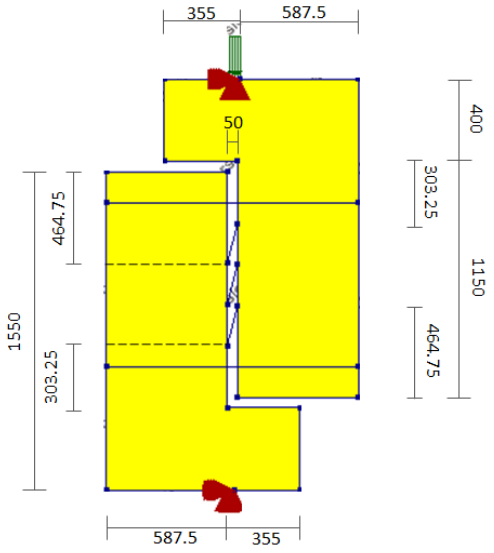

Figure 7.1 Dimensions of the small test setup model

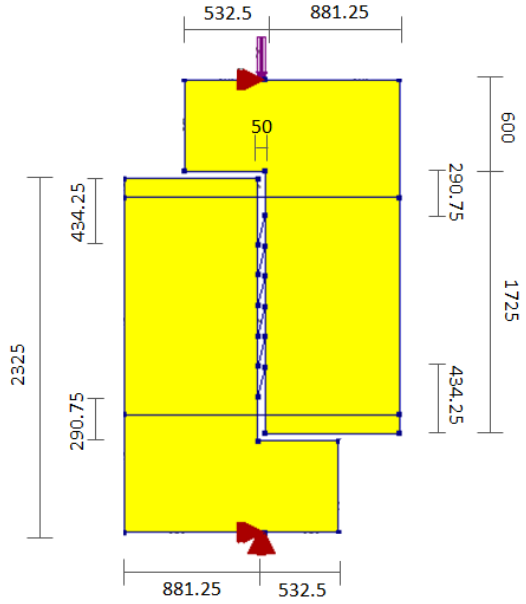

Figure 7.2 Dimensions of the enlarged test setup model

The dimensioning of the diagonal bars is discussed in section 6.1.5 and illustrated in Figure 6.8. The assumed width of the compression diagonal that is illustrated in this figure and the thickness of the elements and joint of 200 mm result in a cross sectional area of 5166 mm^2.

During the tests, Van Keulen applied M16, M24 or M38 bars. These were applied above and below the connection in pairs of two. In order to test the dependency of K_v in the finite element model, the same variation is performed by varying A_R. Table 7.1 shows the properties that are used in the model.

The mesh is built up of rectangular quadratic elements with a size of 50 mm. A mesh sensitivity analysis was performed on the small model in order to define an adequate mesh size and to test if the model is free of singularities that disturb the generated output. Furthermore some sanity checks were performed to validate the model. Appendix B contains the mesh sensitivity analysis and the sanity checks.

L-shaped Elements	
Plane stress elements CQ16M	
Thickness t	200 mm
E-modulus E_c	35000 N/mm^2
Poisson's ratio v	0.2
Diagonal bars	
Regular truss elements L2TRU	
Length	199.86 mm
h_x	50 mm
h_y	193.5 mm
α	3.87
Cross-sectional area A_d	5166 mm^2
E-modulus E_d	25000 N/mm^2
Diagonal stiffness k_d	646.202
Poisson's ratio v	0.2
Reinforcement bars	
Regular truss elements L2TRU	
Cross-sectional area A_R	402/905/ 2268 mm^2
E-modulus E_s	210000 N/mm^2
Poisson's ratio v	0.3

Table 7.1 Model input

7.2 Results of the small test setup model

This paragraph gives an overview of the results from the analysis on the small test setup model. Besides analysing the behaviour of the model, a small parameter study is done by varying the cross-sectional area of the transverse reinforcement bars, as explained in previous paragraph. Most of the results concern the consequences of this variation of quantity A_R. Each section shows some of the results and provides a short discussion.

7.2.1 The displacement field

Figure 7.3 shows the deformations of the model under a vertical displacement applied at the top. Due to the vertical translation, the diagonals are compressed, which results in a horizontal force component that pushes the concrete elements apart. The curved load path through the L-shaped elements, that can be seen in Figure B.2 causes bending of the concrete elements. The way the elements bend corresponds to the applied combination of loads and supports. The results are exactly point symmetric in the centre point of the model, which is must hold, since the geometry is symmetric in the centre point as well.

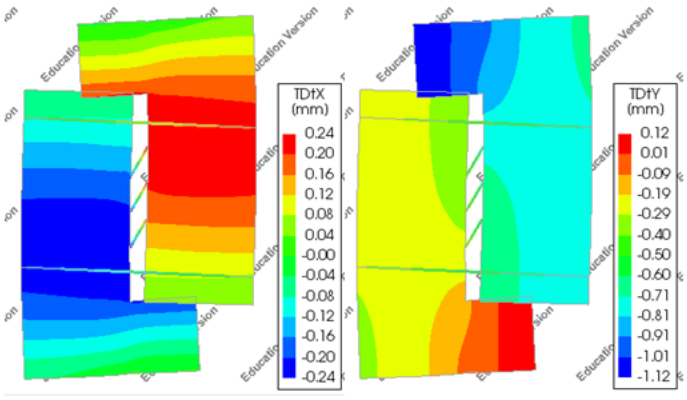

Figure 7.3 Deformation of the model (M24)

7.2.2 $K_v - A_R$ relation

Figure 7.4 shows the outcome of the variation study of A_R. The cross-sectional area of the transverse reinforcement, A_R, is the area of reinforcement that is given to each of the two transverse bars. It is clear that the shear stiffness is dependent on the type of bars that is applied. A connection with M16 bars behaves less stiff in shear than a connection with M38 bars. It must be noted that the $K_v - A_R$ relation is only valid when values given in previous paragraph for the input properties, E_d, A_d, E_c, E_s and α, are used. This is because the relation will be different when another value for the diagonal bar stiffness, K_d, is applied or when the lateral stiffness is varied by changing other design parameters such as the Young's modulus of the steel reinforcement bars or concrete L-elements.

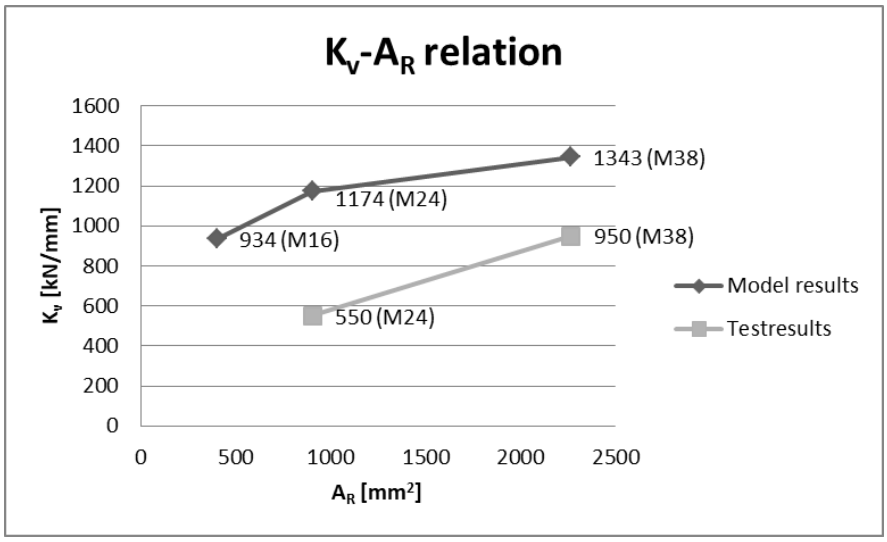

Figure 7.4 K_v-A_R relation

The difference in shear stiffness that occurs due to the variation in A_R is also visible in the obtained relation between the shear force and the shear slip, where the slope of the relation is equal to the found shear stiffness.

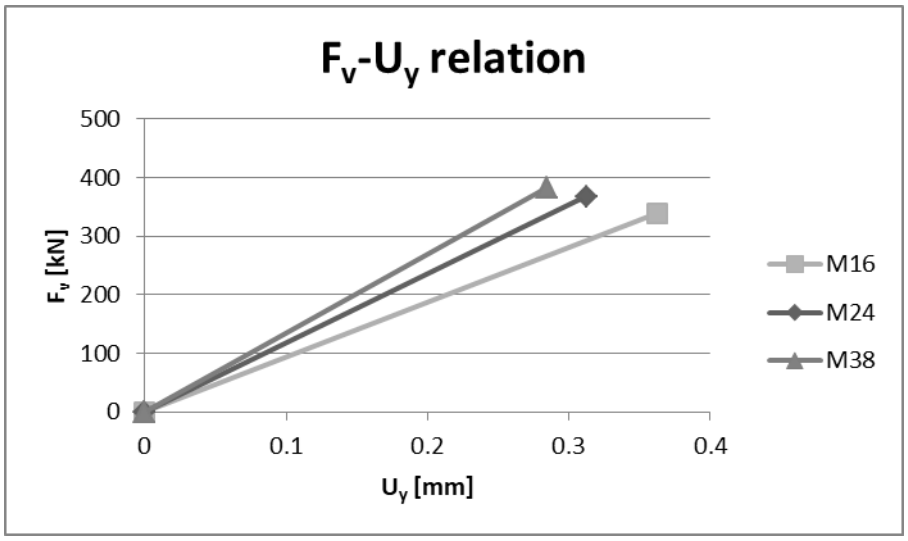

Figure 7.5 F_v-U_y relation

The question is whether the calculated stiffness, K_v, is comparable to the stiffness resulting from the tests. The shear stiffness of test specimens P1-5 (M24) and P1-7 (M38) is estimated from the resulting shear slip- shear stress relation. The tangent stiffness is determined in the phase where compression diagonals take most of the load, as shown in Figure 7.6. Note that the estimated tangent stiffness of the test specimens is even larger than their secant stiffness that the model should approximate. The resulting test specimen stiffness values were also indicated in Figure 7.4, where it is clearly seen that the finite element model acts stiffer. The cross-sectional area of the joint is 200 by 600 mm.

$$K_{v,M24} = \frac{(3.6 - 0.35) * 200 * 600}{0.9 - 0.2} = 557143 \frac{N}{mm} \approx 550 \frac{kN}{mm}$$

$$K_{v,M38} = \frac{(3.9 - 1.1) * 200 * 600}{0.8 - 0.45} = 960000 \frac{N}{mm} \approx 950 \frac{kN}{mm}$$

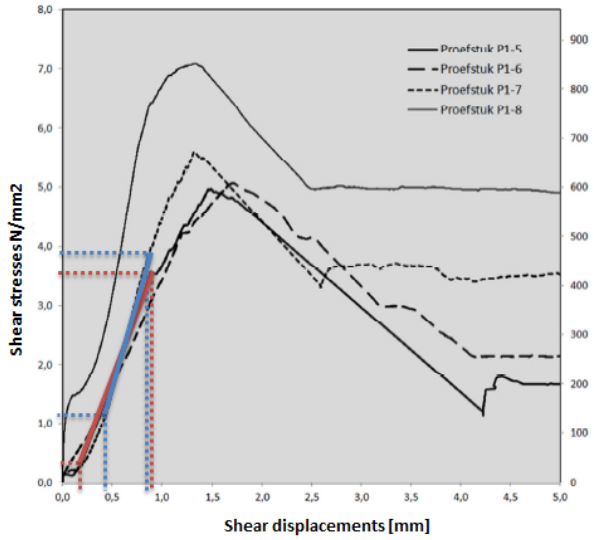

Figure 7.6 Shear slip-shear stress relation obtained from tests (van Keulen, 2015)

The stiffness with M24 bars is 2.1 times larger for the FE model and the stiffness with M38 bars is 1.4 times larger. The way the stiffness varies between the two specimens is also different. The stiffness of a test specimen increases by 70 percent when M38 is applied instead of M24, for the models this increase is just 15 percent. Paragraph 7.4 discusses the numerical difference in more detail.

7.2.3 K_h – A_R relation

Figure 7.7 shows the relation between the cross-sectional area of the reinforcement, A_R, and the lateral stiffness K_h. As one would expect, the lateral stiffness increases with a larger cross-sectional area of the reinforcement. However, due to the limited stiffness of the concrete L-elements, the lateral stiffness will never get infinitely large by using a lot of reinforcement. The whole can be thought of as a series of springs, containing one spring simulating the stiffness of the transverse bars and one simulating the stiffness of the concrete elements. When one spring is infinitely stiff, while the other spring has a finite stiffness, the series as a whole will always have a finite stiffness. Due to this effect the relation between A_R and K_h is asymptotic. If A_R is in this case larger than approximately 5000 mm^2, the lateral stiffness hardly increases for an increased A_R.

With the same springs in series analogy it can also be reasoned that the influence of A_R depends on the magnitude of other parameters that define the lateral stiffness, such as the stiffness of the concrete elements. Therefore it must be noted that the relation of Figure 7.7 is only valid when the input geometry and properties for, E_d, A_d, E_c, E_s and α, given in previous paragraph are used.

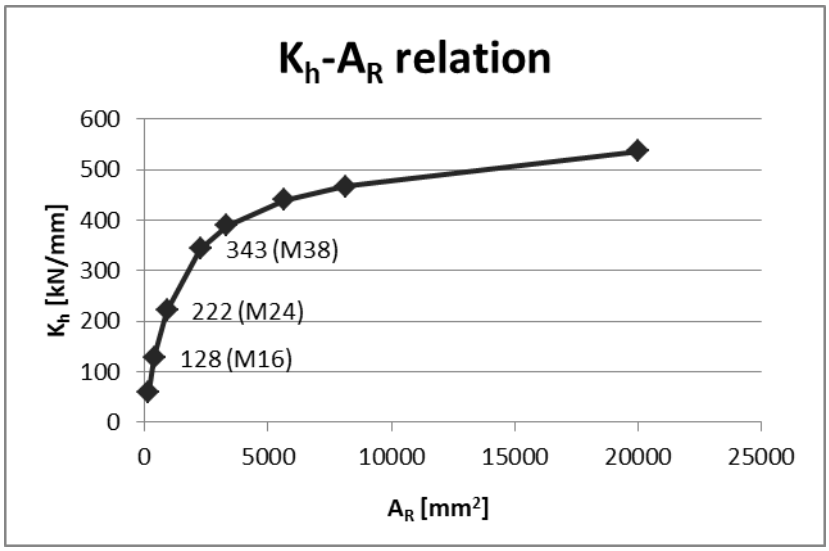

Figure 7.7 K_h-A_r relation

7.2.4 k_v – k_h relation

The previous results can be combined to form the relation between the lateral stiffness and the corresponding shear stiffness of the connection. Table 7.2 gives an overview of the corresponding stiffness values for the three different types of reinforcement bars. The results show that the shear stiffness increases for larger values of the lateral stiffness.

	M16	M24	M38
K_v [kN/mm]	934	1174	1343
K_h [kN/mm]	128	222	343

Table 7.2 Corresponding shear- and lateral stiffness for each type of reinforcement

These are just three points of the relation between the two quantities. If more points are generated, a more detailed relation between the shear and lateral stiffness can be defined.

Figure 7.8 shows the relation between the average shear and lateral stiffness (the total values divided by three diagonals). The average stiffness values are plotted in order to be able to easily compare this result with the coming result of the larger model. The relation contains one unique value for the shear stiffness for each value of the lateral stiffness.

When the lateral stiffness is equal to zero, the shear stiffness must be zero as well. In this case the modelled diagonal bars in the joint can freely rotate, because they aren't constrained in horizontal direction. The model has become a mechanism that cannot take any load. Therefore the shear stiffness must be zero in this case.

The relation is also asymptotic. This means that even for an infinitely large lateral stiffness the shear stiffness is still limited. The shear stiffness will never exceed a certain limit value. In this case the limit is around 600 kN/mm. This behaviour appears reasonable, since the shear stiffness is also partly determined by the joint properties. These are the diagonal stiffness K_d and

the diagonal angle α. In case the lateral stiffness is infinitely large, the shear stiffness is completely determined by these two joint properties, which therefore define the limit value of the asymptote.

So the diagram shows that the shear stiffness is indeed defined by a combination of the lateral stiffness and the applied joint properties, as is discussed in chapter 5. For this reason the relation of Figure 7.8 is only valid for the specific input properties of A_d, E_d, h_x and h_y that are indicated in Table 7.1. The limit of the relation and the way the relation converges to this limit alter, when other values for the joint properties are used.

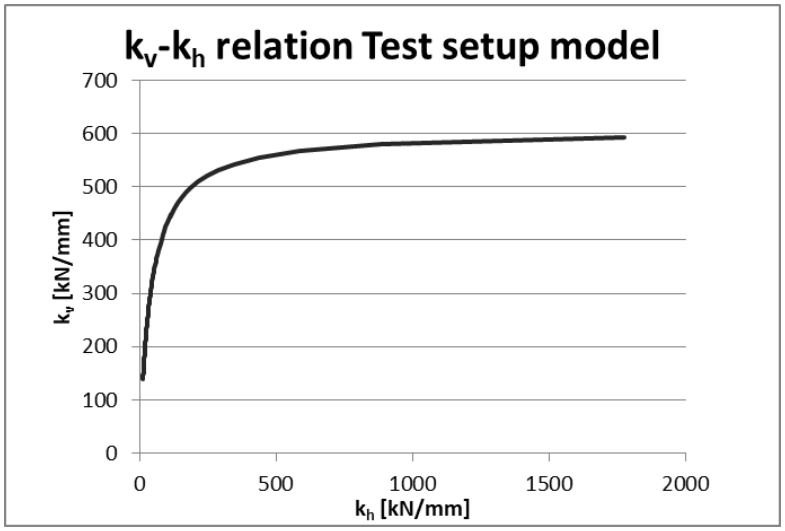

Figure 7.8 Relation between the average shear stiffness and the average lateral stiffness

The relation between the shear and lateral stiffness indicates the relevancy of the lateral stiffness in this model. The range in which the average lateral stiffness is varied by the use of different reinforcement (43-115 kN/mm) is in the range where the influence of the lateral stiffness on the shear stiffness is very large. Due to the asymptotic behaviour the influence of the lateral stiffness gradually decreases as its absolute value increases.

7.2.5 K-U and K-F relations

According to the definitions presented in paragraph 6.2, an increase of the shear or lateral stiffness can either be caused by a decrease of the displacement difference U, an increase of the transferred force F or a combination of both. Table 7.3 presents an overview of the values for the stiffness quantities, the deformation differences and the force components for each of the three analysed models. The results indicate that an increase in lateral stiffness caused by application of larger reinforcement bars leads both to an increase of the transferred forces and a decrease of the displacement difference over the joint.

	M16	M24	M38
K_v [kN/mm]	934	1174	1343
K_h [kN/mm]	128	222	343
U_x [mm]	0.68	0.43	0.29
U_y [mm]	-0.36	-0.31	-0.28
F_x [kN]	-87	-95	-99
F_y [kN]	-336	-364	-376

Table 7.3 Stiffness, forces and displacement difference values

A positive value for U_x indicates a dilatation of the joint and a negative value of U_y indicates that the loaded L-element displaces downwards relative to the supported L-element. Force components are negative since a compressive force occurs in the diagonal bars. The lateral stiffness is given as absolute value.

The asymptotic behaviour that has been described is also obtained in the relation between the two stiffness values and the displacement differences. Figure 7.9 shows the relation between the two stiffness values and the horizontal displacement difference over the joint, the dilatation. In order to let U_x be zero, an infinitely large lateral stiffness is required. In that case, the shear stiffness has the limited value of approximately 600 kN/mm that was found before. From Figure 7.10 it is also observed that the shear slip U_y cannot be smaller than approximately -0.24 mm. The limit is defined by the specific input that is given for K_d and α.

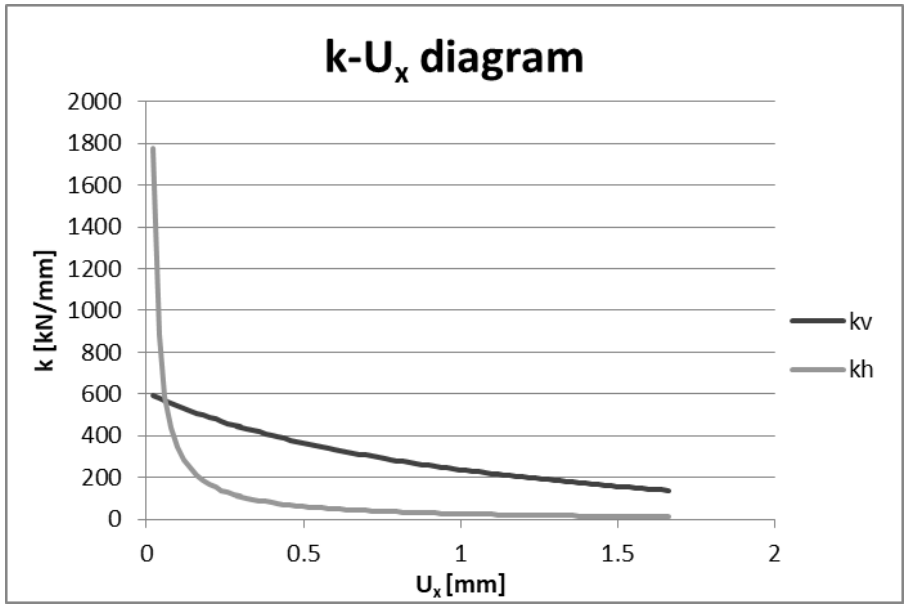

Figure 7.9 Relation between the two stiffness values and the horizontal displacement difference

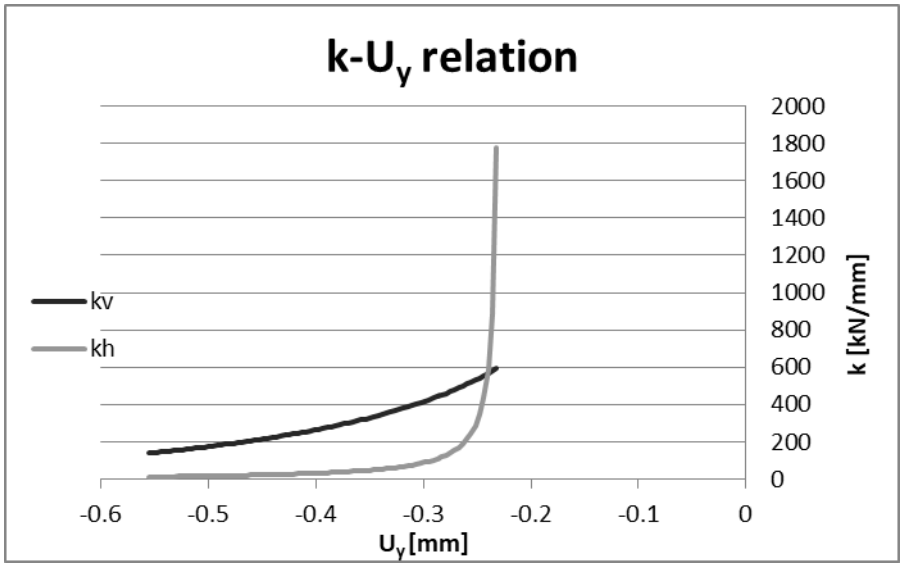

Figure 7.10 Relation between the two stiffness values and the vertical displacement difference

7.2.6 U_x-U_y relation

The behaviour of the bar model that is used to model the compression diagonals in the mortar joint can better be understood by studying the U_x-U_y diagram. Figure 7.11 shows this diagram that can be used as a graphical tool to illustrate the behaviour of the diagonal bars.

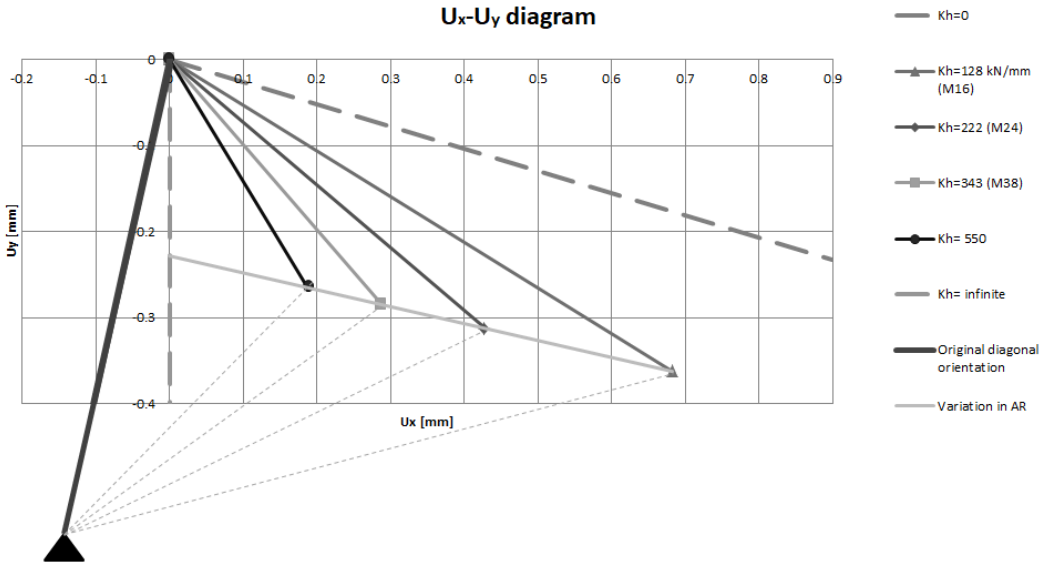

Figure 7.11 The Ux-Uy diagram

The origin of this diagram forms the initial location of the endpoint of the diagonal. The other endpoint is illustrated as a hinge support (Note that the length of the diagonal in Figure 7.11 is not to scale with the displayed results). The original orientation of the diagonal is illustrated by a line between the two endpoints.

The diagram shows multiple lines starting from the origin that illustrate a certain relation between U_x on the horizontal axis and U_y on the vertical axis. The dashed line illustrates the behaviour of a model where the lateral stiffness is equal to zero. In that case the diagonal only rotates around the hinge support, which results in a displacement of the free endpoint along this dashed line perpendicular to the original diagonal orientation. Small displacements are assumed, whereby the dashed line can be drawn straight instead of circular.

In the other limit case, the lateral stiffness is infinitely large. In that situation the free endpoint of the diagonal can only move downwards, whereby the dilatation U_x remains zero. This limit is illustrated by the dashed line along the y-axis of the diagram.

Application of M16, M24 or M38 reinforcement bars results in a lateral stiffness between zero and infinity. In case M16 is applied for example, the free endpoint of the diagonal translates over the M16 line. The magnitude of the load in the performed analysis results in a new location of the diagonal's free end point, which is indicated by the triangle. If a smaller load was applied, the resulting endpoint would still be on the M16 line, but closer to the origin. The thin dashed lines between the support and the resulting endpoints for different values of K_h illustrate the deformed orientation of the diagonal.

The line for K_h=550 kN/mm is the maximum value of the lateral stiffness that is obtained by using a lot of reinforcement. If the lateral stiffness must be greater than this value, other design parameters, such as the E-modulus of the concrete, must be given stiffer values.

It appears that for each value of the lateral stiffness a unique line, like the M16 line, can be drawn in this diagram. So for each value of the lateral stiffness, a unique ratio U_x/U_y is found.

The shear force that is transferred depends on the shortening of the diagonal bar that occurs, since the following relation holds for the diagonal bar: $F_d = E_d A_d * \frac{\Delta L}{L}$. If Kh is zero the bar only rotates, which doesn't result in any strain in the bar and therefore leads to a transferred force equal to zero. In any case where the found combination of U_x and U_y doesn't lead to a point on the K_h=0 line, the diagonal shortens and therefore transfers a shear force. The perpendicular distance between the found point and the K_h=0 line indicates the magnitude of the shortening of the diagonal bar. A larger distance means a larger shortening which results in a larger transferred force. As can be seen in Figure 7.11, the point of M16 lies closer to the K_h=0 line than the points of M24 and M38, therefore a smaller force is transferred in case M16 bars are used. The results in Table 7.3 show that this is indeed true.

The analysis of the U_x-U_y diagram shows that the behaviour of the diagonal bars can be visualised according the model of Figure 6.6. In the diagram of Figure 7.11 the separate horizontal displacements of the lower and upper end point of the bar are lumped into the value U_x.

7.2.7 Evaluation of the results

The presented results indicated that the finite element model that is constructed acts similar to the test specimens in the sense that the dependency of the shear stiffness on the lateral stiffness show similar behaviour. However, the resulting stiffness values of the FE model differ numerically from the stiffness values found for the test specimens. This numerical difference is further analysed in paragraph 7.4.

The relation between the applied reinforcement cross section and the lateral stiffness provides insight in the influence of the design parameter A_R. The relations between the shear and lateral stiffness and the dilatation U_x and shear slip U_y provide insight in the way the quantities K_d and K_h influence the shear stiffness of the connection, K_v.

7.3 Results of the large test setup model

This paragraph discusses the results of the analysis on a model that is 1.5 times larger than the test specimen model and has 2 times more diagonals. The cross-sectional area of the transverse steel bars is given the same values as for the small model. Each section shows some of the results and provides a short discussion. Especially the difference with the previous model is of importance.

7.3.1 The displacement field

Figure 7.12 shows the displacements in x- and y-direction for the large model. The same symmetric behaviour as for the small model is observed. The elements move away from each other and are bending a bit due to the eccentricity of the load with respect to the shear centre of the elements. The two bars keep the whole together, functioning as a kind of supports for the bending elements.

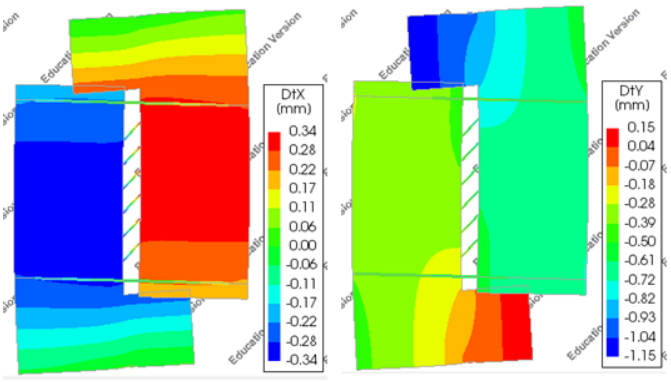

Figure 7.12 Displacement in x and y-direction for the large model (M24).

7.3.2 K – A_R relation

Figure 7.13 shows the relation between the shear stiffness and the cross-sectional area of the transverse reinforcement per side of the connection. When the relation is compared to the one obtained from the small model, it is concluded the behaviour is similar. The difference between the largest and smallest value is a factor 2. This indicates that the influence of a variation of A_R on the shear stiffness of the connection is greater than in the small model.

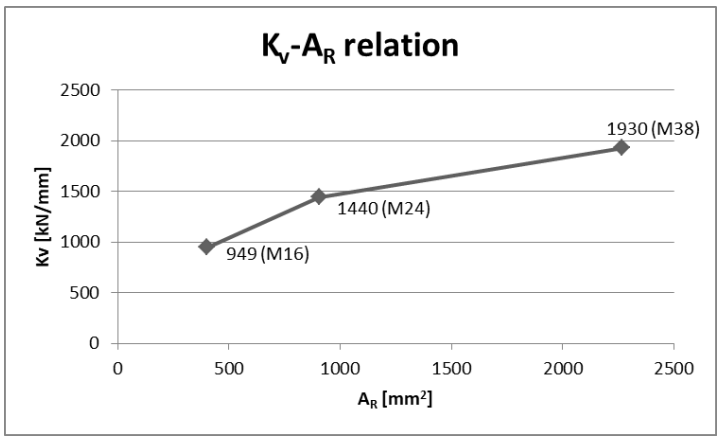

Figure 7.13 Relation between the shear stiffness and the amount of transverse reinforcement (large model)

Figure 7.14 shows the relation between the lateral stiffness and the cross-sectional area, A_R. This relation shows that the large model also behaves similarly to the small model concerning this aspect.

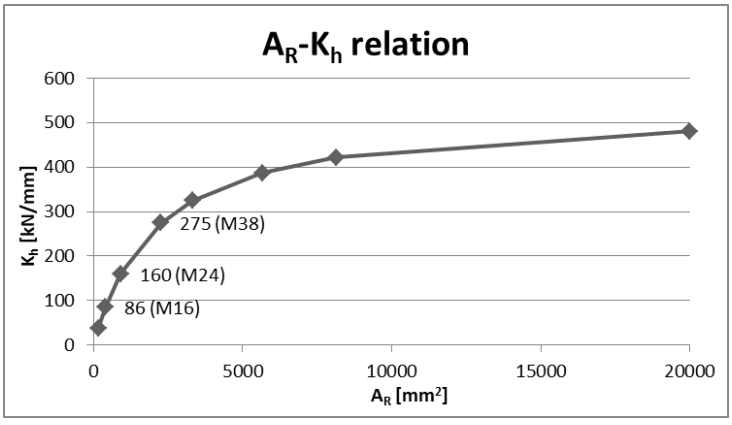

Figure 7.14 Relation between the lateral stiffness and the amount of lateral reinforcement (large model)

7.3.3 Comparison of the two models

Table 7.4 shows for the small and the large models the values for the shear and lateral stiffness and the average displacement differences in both directions. So far it is concluded that the global behaviour of both models is similar. Looking at the numerical values, some interesting facts can be seen.

		M16	M24	M38	Same K-bars (M24 small)
D	[mm]	16	24	38	-
A_R	[mm^2]	402	905	2268	1339
K-bars large	[kN/mm]	46	104	262	155
K-bars small	[kN/mm]	68	155	388	-
K_h-large	[kN/mm]	86	160	275	206
K_h-small	[kN/mm]	128	222	343	-
K_h Ratio	-	0.67	0.72	0.80	-
K_v-large	[kN/mm]	949	1442	1930	1670
K_v-small	[kN/mm]	934	1174	1343	-
K_v Ratio	-	1.02	1.23	1.44	-
U_x large	[mm]	1.02	0.63	0.40	0.51
U_x small	[mm]	0.68	0.43	0.29	-
U_y large	[mm]	-0.36	-0.27	-0.22	-0.24
U_y small	[mm]	-0.36	-0.31	-0.28	-

Table 7.4 Comparison between the large and small model

First of all, the lateral stiffness of the large connection with the same type of bars appears to be smaller than that of a small connection. There are two reasons for this. The first and most important reason is that with the same cross sectional area of the bars, the bar stiffness is lower in the large model. According to the definition K-bar is EA/L, the longer bar length in the large model reduces the bar stiffness. The difference is clearly seen by comparing the values for K-bars large and small in the columns for M16, M24 and M38 bars. In order to exclude this effect, a large model with a bar stiffness equal to that of the M24 bars in the small model is analysed. The results of this analysis are shown in the last column of Table 7.4. It can be seen that the lateral stiffness of this model (206 kN/mm) is still smaller than the lateral stiffness of the small model with M24 bars (222 kN/mm). So there is a second reason for the difference in lateral stiffness, namely the smaller relative in-plane bending stiffness of the concrete L-shaped elements. Increasing both the length and width by a factor 2 for example, results in larger deformations of the L-shaped elements. This is illustrated by comparing the elements with simply supported beams (see calculation below). In this case the horizontal components of the diagonal forces are represented by the line load q. The transverse bars are represented by the supports.

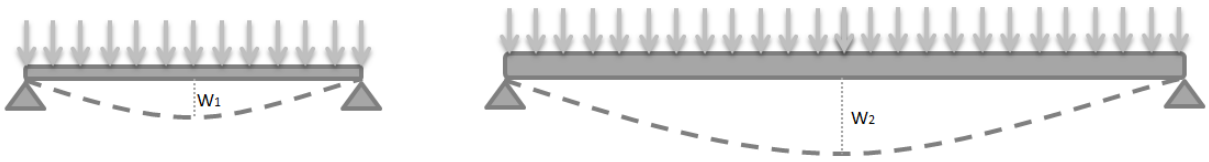

Figure 7.15 Simply supported beam model

$$W_1 = \frac{5}{384} * \frac{q * l^4}{E * \frac{1}{12} * w * h^3}$$

$$W_2 = \frac{5}{384} * \frac{q * (2l)^4}{E * \frac{1}{12} * w * (2h)^3} = \frac{2^4}{2^3} * \frac{5}{384} * \frac{q * l^4}{E * \frac{1}{12} * w * h^3} => W_2 = 2 * W_1$$

From these observations it must be concluded that a model with larger dimensions requires more transverse reinforcement in order to limit the lateral stiffness reduction compared to a small model. Applying a large enough value of A_R results in a lateral stiffness reduction that is only caused by the difference in in-plane bending stiffness of the concrete elements.

Secondly, although the lateral stiffness of the large connection is smaller, its shear stiffness is larger. Since the large model contains 2 times more diagonal bars, with unchanged E_d, A_d, L_d and α with respect to the small connection, the total shear stiffness is larger. However, since the total shear stiffness is not increased by a factor 2, the shear stiffness per diagonal appears to be smaller in the larger connection. Since the average vertical deformation difference is smaller for the larger connection according to the results in Table 7.4, it must be that the force taken per diagonal is smaller in the large connection. Section 7.3.5 discusses the force per diagonal in more detail.

Finally, in cases where small reinforcement bars are applied, it can be that the total shear stiffness of the large model is smaller than that of the small model. In that case it holds that the lateral stiffness of the large model is relatively so low, that the shear stiffness per diagonal is more than two times smaller than occurs in the small model. The results for M16 in Table 7.4 show that for this cross section the total shear stiffness of the large model is still slightly larger than for the small model (2 percent). Table 7.5 presents the stiffness values of a large and small model where bars with a diameter of 10 mm are applied. In this case it appears that the total shear stiffness of the large model is just 81 percent compared to what is found for the small model. Figure 7.16 shows the normalised total shear stiffness as a function of the cross-sectional area of the transverse reinforcement. A normalised shear stiffness of for example 1.6 indicates that the total shear stiffness of the large connection with given A_R is 1.6 times larger than that of the small connection with the same A_R. It appears that if A_R is smaller than approximately 400 mm^2, the total shear stiffness of the large model is smaller than that of the small model with the same A_R, resulting in a normalised shear stiffness smaller than 1.

	Large connection	Small connection	Ratio
D	10	10	-
K_h [kN/mm]	38	60	0.63
K_v [kN/mm]	490	602	0.81

Table 7.5 Comparison of a large and small connection with small amount of reinforcement

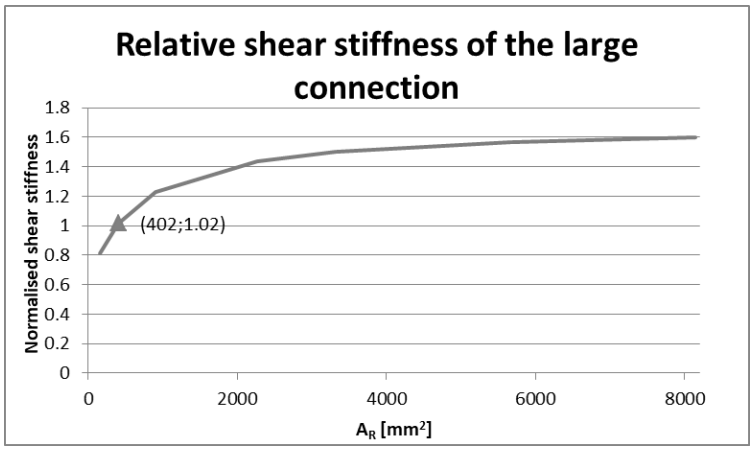

Figure 7.16 Relative shear stiffness of the large connection

7.3.4 k_v-k_h relation

The k_v-k_h relation indicates an important characteristic of the scale effect that occurs between the two models. The diagram is shown in Figure 7.17. It appears that this relation is exactly the same as the relation found for the small model in section 7.2.4. This means that a certain lateral stiffness per diagonal will in both cases lead to the same shear stiffness per diagonal. In this case this would mean that, compared to the small model, the large connection with a two times more diagonal bars and a two times larger total lateral stiffness has the same lateral stiffness per diagonal and therefore the same shear stiffness per diagonal, which leads to a two times larger total shear stiffness of the connection.

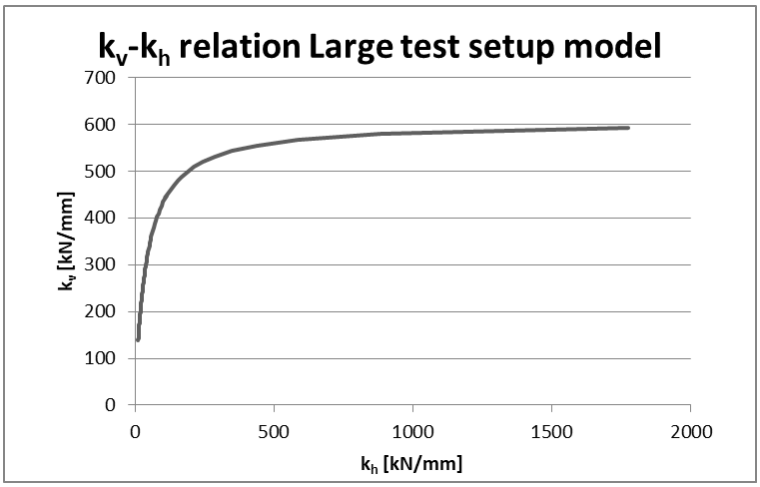

Figure 7.17 Relation between the vertical and lateral stiffness per diagonal for a large connection

7.3.5 Diagonal force distribution

Figure 7.18 shows the diagonal force distribution of the large and small model. This distribution illustrates the shear force distribution. Two conclusions can be drawn. First, the force distribution is in both cases symmetric with respect to the centre of the joint. The upper diagonals take the largest force, the middle diagonals the smallest. Second, the force per diagonal in the large model is significantly smaller than in the small model. In previous section it was already concluded this should be the case, since the average vertical displacement difference of the large model is smaller, while the total shear stiffness is smaller as well.

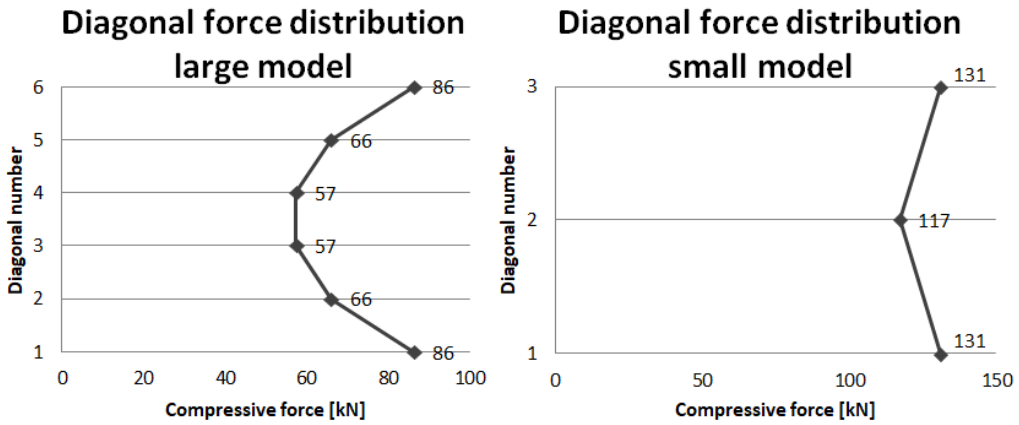

Figure 7.18 Diagonal force distribution of large and small model compared

7.3.6 Evaluation of the results

The most important conclusions that can be drawn from the comparison between the large and the small test setup model are:

- The lateral stiffness of a larger model may be smaller. This is partly caused by the lower axial stiffness of the longer transverse reinforcement bars and partly by a possible reduced in-plane bending stiffness of the surrounding concrete elements.
- The k_v-k_h relation is for both models the same, which means that if the obtained lateral stiffness per diagonal in two cases is equal, the corresponding shear stiffness per diagonal is equal. The amount of diagonals in the connection determines which connection has a larger shear stiffness.
- The force distribution over the diagonals and thereby the shear force distribution over the joint is similar in both cases. The middle diagonals transfer the smallest force and the distribution is symmetric.

7.4 The numerical difference between test results and FE model

In section 7.2.2 the resulting shear stiffness for the small model corresponding to the different values of A_R has been discussed. A comparison with the shear stiffness resulting from the tests showed that the finite element model reacts a lot stiffer than the test specimens. In this paragraph possible causes of the numerical difference are addressed and a calibration of the model is executed. In the parameter study the calibration is ignored again, since the calibrated properties are varied to investigate their influence. However, in chapter 11 when a shear wall with vertical profiled mortar connections is compared to a monolithic wall, the calibrated values are used as input in order to obtain realistic results.

7.4.1 Possible causes of the numerical difference

The numerical difference in results of the finite element analysis and the tests can have multiple causes. Some of these causes are mentioned in this section.

First of all, the test specimens are manually produced whereas the finite element model represents a perfect representation. Executional aspects such as the filling ratio of the mortar joint or imperfections of the concrete elements or mortar joint have influence on the test results. Van Keulen made notes of the test specimens that were damaged or where complications occurred during the tests. Although the specimens that are used to evaluate the finite element

model do not contain such remarks, they still aren't perfect. The finite element model would therefore have a greater shear stiffness than the test specimen.

Secondly, the lateral stiffness of the test specimen is not only provided by the concrete elements and the transverse bars, but also by the steel plates connecting the bars to the concrete elements. This last aspect is not taken into account in the finite element model. Therefore the lateral stiffness of the finite element model with for example M24 bars is larger than that of the test specimen with M24 bars, resulting in a larger shear stiffness as well.

Another reason for the deviation is the assumed value for the stiffness of the diagonal bars that model the mortar. For these bars an E-modulus of 25000 N/mm^2 and a cross-sectional area of 5166 mm^2 are used. The E-modulus is based on tests on the applied mortar, the area is based on an assumption (See Figure 6.8). The mortar may, although not yet visible, be cracked, whereby the E-modulus could be considerably smaller than assumed. Furthermore the width of the diagonal for example could be a lot smaller than assumed, resulting in a lower diagonal stiffness as well. The angle of the compression diagonal is also roughly estimated.

Other reasons for the numerical deviation of the results can be small deviations in the loading and support conditions of the finite element model. For example the infinitely stiff horizontal supports that are applied in the finite element are required to obtain a stable model. In the test setup the specimens are not infinitely stiff supported at these locations.

7.4.2 Calibration of the joint properties

Based on the mentioned causes of deviation, the finite element model will be calibrated to better correspond to the test results. This calibration considers the deviating lateral stiffness and the assumptions on the variables that determine K_d. The method that is applied is as follows:

1. The secant stiffness of the test result is determined
2. The band width of the lateral stiffness of the test specimen is determined
3. The lateral stiffness of the model is adjusted to this bandwidth by adjusting the transverse bar cross section A_R:
    a. One model is created with minimum lateral stiffness
    b. One model is created with average lateral stiffness
    c. One model is created with maximum lateral stiffness
4. The K_d value's for which each model has a total shear stiffness, equal to the secant stiffness, is searched.
5. The found K_d values are subdivided into an estimation of the E-modulus and cross-sectional area of the diagonal bars.

The calibration method considers the diagonal stiffness as the unsure variable that needs calibration. The angle of the diagonal is not calibrated. In order to do the calibration properly, the lateral stiffness of the test setup model should correspond to that of the test specimen that is compared. The described method is applied for the calibration of the finite element results for the connection with M38 reinforcement bars.

7.4.2.1 Determination of the test specimen's secant stiffness

The secant shear stiffness of the test specimen is determined from the relation between the shear displacements and the shear force. The secant shear stiffness is the slope of the straight

line between the origin of the diagram and the point of the ultimate shear force with corresponding shear displacement. Figure 7.19 illustrates the way this stiffness is determined.

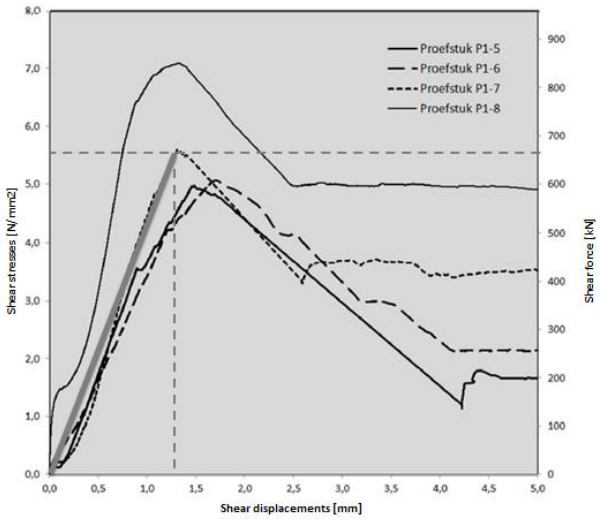

Figure 7.19 Determination of the secant shear stiffness (van Keulen, 2015)

$$K_{v,test} = \frac{F_{v,ultimate}}{U_{y,ultimate}} \approx \frac{670\ kN}{1.3\ mm} = 515\,\frac{kN}{mm}$$

7.4.2.2 Determination of the test specimen's lateral stiffness

The lateral stiffness of the test specimens is determined from the relations between the summed normal force and the normal displacements over the joint. Since these relations show a nonlinear lateral stiffness, it is hard to give a good estimation of the linear lateral stiffness that should be inserted in the finite element model. For this reason an minimum, average and maximum value of the lateral stiffness are determined. This will result in a bandwidth of the diagonal stiffness that must be applied in the finite element model. The largest lateral stiffness will give the smallest required diagonal stiffness K_d in order to let the model correspond with the determined secant shear stiffness.

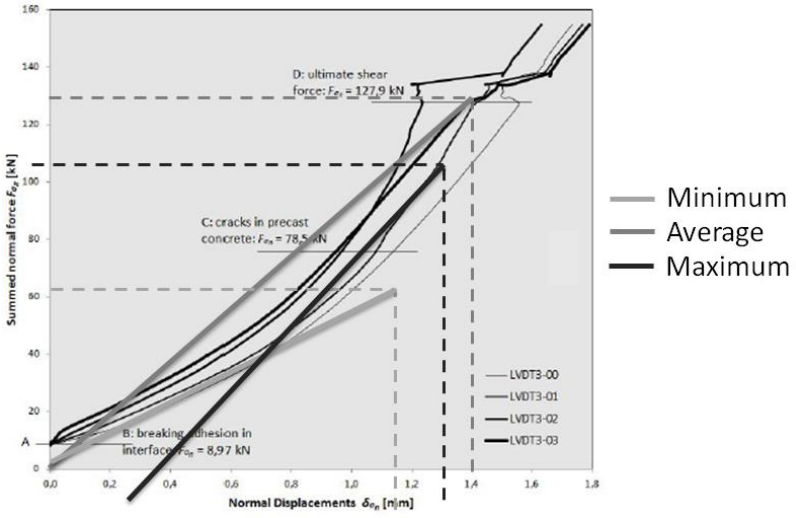

Figure 7.20 Determination of the lateral stiffness (Van Keulen, 2018)

$$K_{h,test,min} = \frac{F_h}{Ux} \approx \frac{(70-9)kN}{1.15\ mm} = 53\frac{kN}{mm}$$

$$K_{h,test,average} = \frac{F_{h,ultimate}}{U_{x,ultimate}} \approx \frac{127.9\ kN}{1.4\ mm} = 91\frac{kN}{mm}$$

$$K_{h,test,max} = \frac{F_h}{Ux} \approx \frac{113\ kN}{(1.32-0.28)\ mm} = 109\frac{kN}{mm}$$

7.4.2.3 Adjustment of the lateral stiffness in the finite element model

The estimated values of the lateral stiffness must be inserted in the finite element model. The easiest way to do this, is to adjust the axial stiffness of the transverse bars into a fictitious value that results in a total lateral stiffness corresponding with one of the three determined values. In this way three models are considered: one for the minimum, one for the average and one for the maximum lateral stiffness. In order to obtain a lateral stiffness close to 91 kN/mm for example, the inserted value for A_R must be approximately 265 mm^2. This leads to a lateral stiffness of the finite element model of 92.7 kN/mm.

7.4.2.4 Calibrated values for the diagonal stiffness

The three models with the correct lateral stiffness are now ready to use for calibration of the diagonal stiffness to the test result. The shear stiffness of the model must be 515 kN/mm. The resulting calibrated values of the diagonal stiffness are found in Table 7.6. The largest diagonal stiffness is required in the model with a minimal lateral stiffness and vice versa. The found values are valid for a joint thickness of 200 mm. If this thickness is changed, the diagonal stiffness values must be changed accordingly, since another thickness will lead to a changed cross-sectional area of the diagonal bars and thus a changed diagonal stiffness.

Model	K_h [kN/mm]	K_v [kN/mm]	K_d [kN/mm]	k_d [kN/mm]
Minimum	53	515	1560	520
Average	91	515	880	293
Maximum	109	515	800	267

Table 7.6 Calibrated diagonal stiffness values (for t=200 mm)

7.4.2.5 Bandwidth of the diagonal properties

The calibrated values of the diagonal stiffness can be subdivided in an applicable E-modulus and cross section of the bar elements. Previously an E-modulus of 25000 N/mm^2 was used, since this corresponds to the mortar that is modelled by the bar elements. However, the mortar may be cracked, whereby it's stiffness could be reduced with 50 percent for example.

The assumption was made that the width of the compression diagonal, W_d, is equal to the width of the inclined surface of the profile (Figure 6.8). It is interesting to compare the diagonal width resulting from the calibration with this assumption. In this case it is still assumed that the thickness of the compression diagonal is equal to the thickness of the concrete elements and the joint (t=200 mm). When a cracked and uncracked value for the E-modulus are considered, together with three estimated K_d values, this results in six values for the width of the compression diagonal. Note that the value K_d is the total diagonal stiffness (for three diagonals) and the values for A_d and W_d are given per diagonal.

Model	K_d [kN/mm]	A_d (cracked) [mm²]	W_d (cracked) [mm]	A_d (uncracked) [mm²]	W_d (uncracked) [mm]
Minimum	1560	8325	41.6	4160	20.8
Average	880	4695	23.5	2350	11.7
Maximum	800	4285	21.4	2140	10.7

Table 7.7 Calibrated values of A_d and W_d

The width of the inclined surface is 25.8 mm. So a compression diagonal width of 41.6 mm is not very realistic. However, the other values for W_d are reasonable with respect to the width of the inclined surface.

7.4.2.6 Conclusion of the calibration

The most important conclusion that can be drawn from the resulting values for W_d is that the bar model can give realistic values for the shear stiffness of the connection when realistic values for the diagonal stiffness are given as an input. This conclusion substantiates the feasibility of the bar model as a way of modelling to approximate the behaviour of the vertical profiled mortar connection.

The maximum and minimum value that are found for the diagonal stiffness provide the limits within which a value can be chosen in order to let the model results be realistic, compared to the test results. These limits hold for the case where the thickness of the joint is 200 mm. The found limit values for W_d are independent of the joint thickness, t.

7.5 Overview of the results

This chapter discussed the analysis that was performed on a model that approximates the test setup and its behaviour as observed during Van Keulen's tests. The first model had equal dimensions, whereas the second model was enlarged by a factor 2 in order to observe the effect of scaling the connection. The following general conclusions can be drawn based on the results presented in this chapter:

- The finite element model behaves similar to test specimens of this shape, with respect to force flow and displacement field.
- An increase in lateral reinforcement leads to an increase in lateral and shear stiffness subsequently. This was also observed in Van Keulen's test results.
- The relation between the cross-sectional area of the transverse reinforcement and the lateral stiffness is asymptotic, since an infinitely large A_R does not lead to an infinitely large lateral stiffness, since the last is also determined by the in-plane bending stiffness of the concrete elements.
- The relation between the lateral stiffness and shear stiffness is also asymptotic. Due to the limited diagonal stiffness, an infinitely large lateral stiffness won't lead to an infinitely large shear stiffness.
- The influence of A_R on the lateral and shear stiffness of the connection is dependent on the chosen values of other design parameters. This holds, because the lateral stiffness is defined by other properties besides A_R, such as the E-modulus of the concrete.
- The influence of the lateral stiffness on the shear stiffness of the connection depends on the magnitude of the diagonal stiffness and the angle of the diagonals. Since these two joint properties together with the lateral stiffness determine the magnitude of the shear stiffness. This was already indicated in chapter 5.

- The resulting relations from the finite element model are thus only valid in this specific case, with this specific combination of input properties.
- Evaluation of the results, especially the U_x-U_y diagram, indicated the applicability of the model schematization for the bar model that was presented in Figure 6.6.
- The values for the shear stiffness resulting from the finite element model are greater than those resulting from the tests. Calibration of the assumed variables that determine the diagonal stiffness, such as the mortar E-modulus and diagonal cross section, showed that comparable stiffness values can be obtained within realistic limit values of the analysed variables. These calibrated design parameters are used in Chapter 11.

The following specific conclusions can be drawn from the comparison between the small and large model of the test setup:

- The large connection shows similar behaviour compared to the small connection and the test specimens with respect to the force flow and displacement field.
- The lateral stiffness that is obtained for a large connection is generally lower for the same value of A_R, due to the smaller in-plane bending stiffness of the larger L-shaped elements and the smaller axial stiffness of the reinforcement bars with equal cross-section but greater length.
- So if a larger connection is used attention must be paid to the provided lateral stiffness that tends to decrease as a result of larger structural dimensions. A larger connection will therefore require a larger amount of transverse reinforcement.
- Despite a possible lower lateral stiffness, the shear stiffness of the large connection is in most cases larger than for the small one. This is the result of the larger amount of compression diagonals that are present. These diagonals all contribute to the shear stiffness as parallel springs.
- The influence of a variation of the cross-sectional area of the transverse reinforcement on the shear stiffness of the connection is larger in case of a large connection.
- The relation between the average lateral and shear stiffness for the large connection is equal to that relation for the small connection.
- So if it is managed to keep the average lateral stiffness of the large connection equal to that of the small connection, the average shear stiffness of the large connection will also be equal to that of the small connection. Therefore the total shear stiffness of the large connection will be for example two times larger if the larger connection contains two times more diagonals than the small one.

The analysis of the finite element model of the test setup showed that if the bar model is used to model the vertical profiled mortar connections, the resulting behaviour is realistic and provides insight in the influence of the lateral stiffness and diagonal stiffness on the shear stiffness of the connection.

The bar model will therefore be used in the next phase where a parameter study is performed in order to analyse the influence of design parameters that determine the magnitude of the lateral stiffness and the influence of the joint properties K_d and α on the shear stiffness.

8 The parameter study

The previous chapters discussed the development and analysis of the bar model that is used to investigate the behaviour of the vertical profiled mortar connections in terms of its linear shear stiffness. This stiffness is dependent on the lateral stiffness, that is provided by the surroundings of the connection, and the properties of the compression diagonals that develop in the mortar in the joint.

The magnitude of the lateral stiffness is determined by multiple design parameters. The design parameters that are considered in this study are:

- The stiffness of the transverse reinforcement: K_s
- The Young's modulus of the precast concrete elements: E_c
- The height of window openings close to the joint: h
- The width of the column between the joint and these window openings: a

The parameter study that is reported in this chapter tries to quantify the influence of each individual parameter on the lateral stiffness. Furthermore the influence of the two diagonal properties, K_d and α, on the shear stiffness is investigated as well.

Based on the results of the parameter study, the goal is to gain insight into the following aspects, related to the questions formulated in paragraph 5.3:

- The relevance of each design parameter that partly determines the lateral stiffness, based on their influence on the lateral and shear stiffness of the connection.
- The relevance of the two investigated diagonal properties, based on their influence on the shear stiffness of the connection.
- The relevance of the lateral stiffness, based on its influence on the connection's shear stiffness
- The relation between the design parameters and the lateral stiffness
- The relation between the lateral stiffness, diagonal stiffness, diagonal angle and the connection's shear stiffness.

The relevance of design parameters and diagonal properties indicates which of them must be included in a practical modelling approach that is developed and if some may be ignored. Furthermore the relevance indicates for which factors further research is useful and which factors must be taken into account from the beginning of the design process. If for example the joint properties appear to be very relevant, it may be valuable to develop another model that can investigate the relation between design parameters and joint properties. As explained in paragraph 6.1, the bar model cannot be used for this purpose. If the location of the openings appears to be very relevant, it is a good idea to take this into account from the beginning of the design process.

Insight in the relations between the considered factors is used to develop the modelling approach for practical situations that is aimed at in this thesis.

The first paragraph of this chapter discusses the development of the model that is applied for the parameter study. The input properties and methodology are discussed in the second paragraph. The third paragraph provides an overview of the results. Paragraph four enumerates and discusses the most important conclusions.

8.1 Development of the model

Three different models were developed that could be used for the parameter study. One model consists of a complete shear wall, the other two contain just a part of a shear wall. This paragraph describes the setup of the three models and the comparison between them, which gives insight in the feasibility of the models. Each model can have different advantages and disadvantages or might even be invalid. The comparison is part of the process to find a model that is suitable for the parameter study and it's also functioning as a validation of the structural behaviour of the three models.

8.1.1 Setup of the three models

The input properties of the model, like material properties and element cross sections, are discussed in the next paragraph. The three models discussed here differ only in terms of geometry and boundary conditions, as is explained in this section.

8.1.1.1 A full wall model

First of all, the parameter study can be performed on a model that contains a complete shear wall. The model is shown in Figure 8.1. This shear wall is loaded by a distributed horizontal force at each floor level, since in real situations the floor slabs distribute the wind loads in the same manner. At the bottom the wall is supported in horizontal and vertical direction. The wall is 10.05 metre wide (joint width is 0.05 metre) and contains 5 stories with a height of 3.2 metres. Therefore the wall is rather compact, whereby the bending deformations and horizontal deformations in general are small. In this manner the deformations resulting from the joint behaviour are more clearly visible. Results of previous research presented in section 3.3.1 showed that the influence of vertical joints with finite stiffness is larger in compact walls. So this wall model should be feasible for analysing the behaviour of the vertical joint.

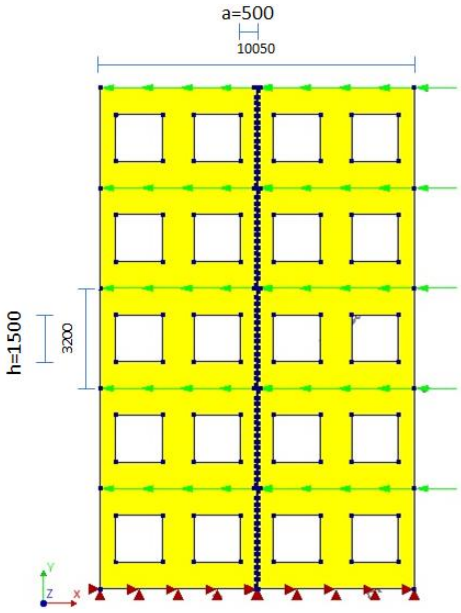

Figure 8.1 Model of a complete shear wall (Model 1)

According to the information provided in section 3.2.2, the load will lead to a vertical shear force that is transferred by the vertical joint between the two columns of wall elements. This joint contains 15 diagonal bars per floor and at each floor level a horizontal bar element, which models the transverse reinforcement.

8.1.1.2 A model loaded in shear

If the parameter study is performed on a smaller model, some advantages with respect to the full wall model may be obtained:

- Varying the geometry of the windows is less laborious.
- The model provides a more detailed view on the deformations and stress distribution that occur around the joint.
- The connection is tested on a typical form of loading; behaviour of the shear wall that influences the joint is excluded from the analysis.

The first argument is an executional benefit that fastens the process. The second argument means that the effect of for example a change of the distance 'a' (See Figure 8.1) is more clearly visible. A change of this width will lead to a different bending deformation of the column between the joint and the window. In a model of a complete shear wall this larger bending deformation is less visible due to the global horizontal deflection of the wall.

The third argument means that the joint can be tested on pure shear, whereas in a complete shear wall the joint is indirectly loaded by vertical shear. The shear behaviour is schematically illustrated in Figure 8.2. The load should directly lead to the slip that occurs over the vertical joint. In case a complete shear wall is modelled according model 1, also other structural behaviour may affect the results.

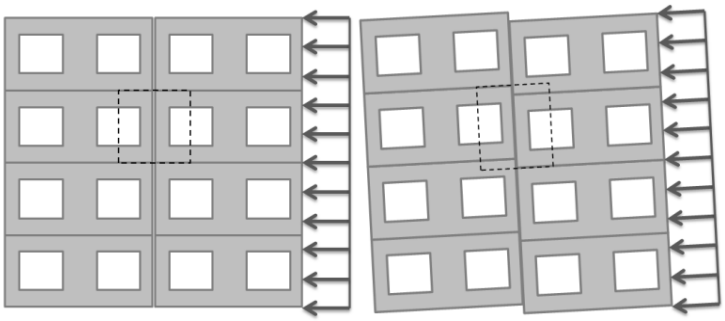

Figure 8.2 Vertical shear in the joint (schematic illustration)

The constructed model is shown in Figure 8.3. The modal contains three stories with a height of 3.2 metres. The standard dimensions of the window openings are the same as in the shear wall model. The same joint is modelled, containing a width of 50 mm, 15 diagonals per floor and 1 transverse bar at each floor level. On the left side, a vertical and horizontal support is applied. On the right side the model is loaded by a vertical shear force and horizontally supported. This horizontal support is required to prevent bending moments in the model. If this support was removed, the model would basically be a clamped beam and a 90 degrees rotation of the previous model. In that situation the joint would be tested as horizontal shear wall joint and the bending moment would result in tensile forces in the joint, which is not in accordance with the conditions that occur in a vertical joint.

A disadvantage of this model is that the horizontal support on the right side will make the contribution of the transverse reinforcement less significant, since the wall elements cannot rigidly translate in horizontal direction.

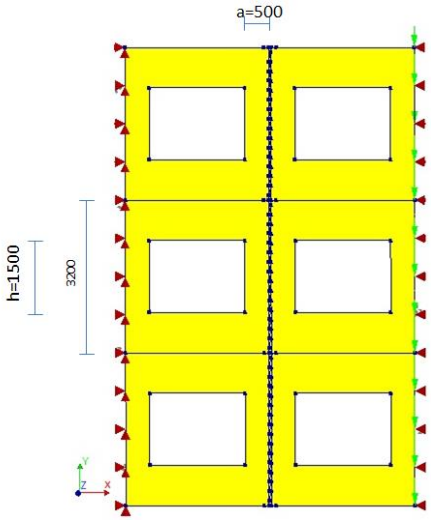

Figure 8.3 Model loaded by a vertical shear force (Model 2)

8.1.1.3 A model of a wall detail

The third model zooms in even further. Its geometry is shown in Figure 8.4. This model includes only the part between the dashed square in Figure 8.2. The behaviour of the surroundings of the joint can very well be analysed in this case. However, the boundary conditions are more complex.

The model is loaded by a vertical deflection of 1 mm at the top right edge and vertically supported along the bottom left edge, resulting in a vertical shear force that is transferred by the vertical joint. The horizontal supports are applied on the left side only. Since the vertical edges on the right side are cuts of the wall element, they must remain straight. Tyings are used for this purpose. The same holds for the upper left and lower right horizontal edges, where the wall elements above and below obstruct non-uniform vertical deformations. Appendix C contains a more detailed description of this model, including its particular behaviour.

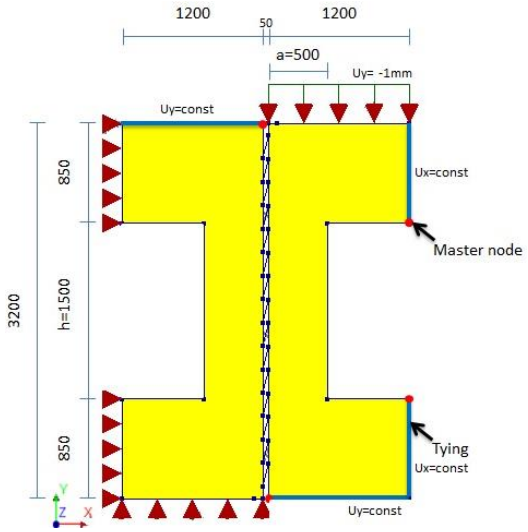

Figure 8.4 Single floor model (Model 3)

8.1.2 Comparison of the three models

The comparison of the three models is based on multiple aspects. First of all the occurring deformations are analysed. Secondly, the stress distribution is considered and finally the distribution of shear force over the joint is compared. The comparison of the behaviour of the models is used to select the model that is used for the parameter study. It must be noted that the load in each model has a different magnitude, whereby the results should not be compared on the exact numerical values of the deformations, stresses and forces.

8.1.2.1 Comparison of the deformations

The following figures give an overview of the deformation fields in X- and Y-direction of the three models. The figures also contain the contours of the undeformed models. The models are from now on referred to as models 1,2 and 3.

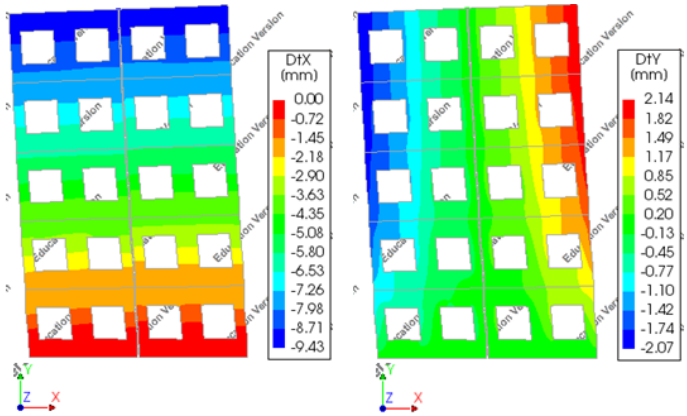

Figure 8.5 Deformation of the shear wall model (Model 1)

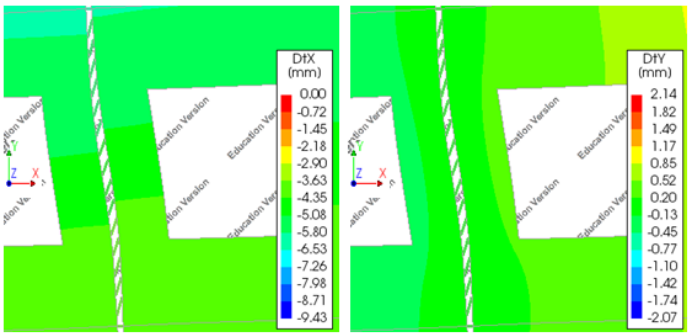

Figure 8.6 Detail of the deformation of the shear wall model (Model 1)

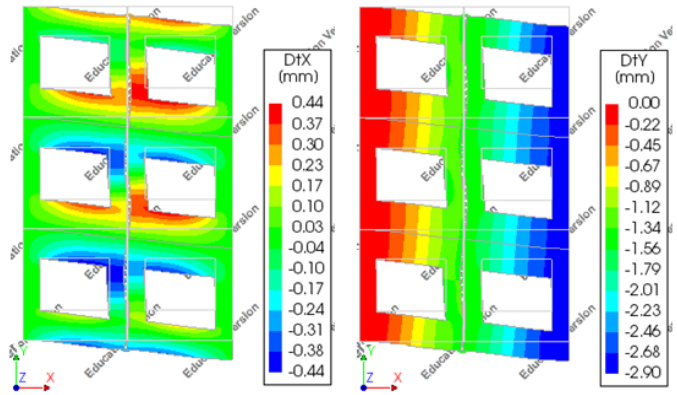

Figure 8.7 Deformation of the shear model (Model 2)

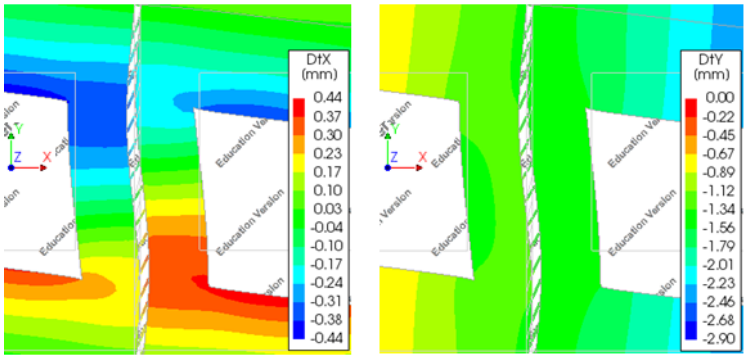

Figure 8.8 Detail of the deformation of the shear model (Model 2)

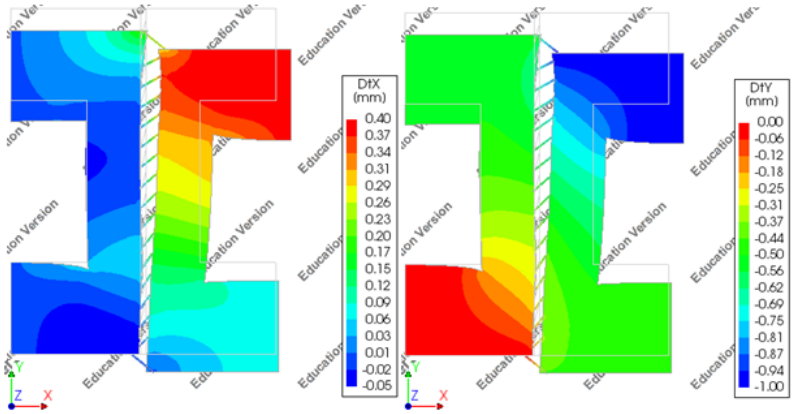

Figure 8.9 Deformation of the wall detail model (Model 3)

The deformation of model 2 shows a shear deformation of the lintels and columns over the entire model. The detail also shows that the joint itself deforms into a sinusoidal shape . This same shape can also be seen in the detail of the joint in model 1. The overview of the deformation of model 1 shows that the shear deformation makes a significant contribution to the total deformation of this wall. This follows from the course of the horizontal displacements over the height of the wall, which is characteristic for a compact wall. In both models, the joint widens over the entire height of the floor, with the largest dilatation occurring halfway the height. In model 3 the joint deforms differently. Although the left element shows a sinusoidal horizontal deformation, the right element deforms in a different way. As a result, the joint between the elements widens most at the top of the floor.

In the vertical direction, it is most clear for model 3 that the elements shift with respect to each other. However, in all three cases the right side of the joint moves downwards relative to the left side. This shows vertical shear occurs over the width of connection. This shear ensures that the diagonal bars of the joint can remain under pressure despite the fact that the ends of the bars move apart in horizontal direction.

8.1.2.2 Comparison of the stress distribution

The following figures show the stress distributions of shear stress Sxy and principle stresses S1 and S2 over the model.

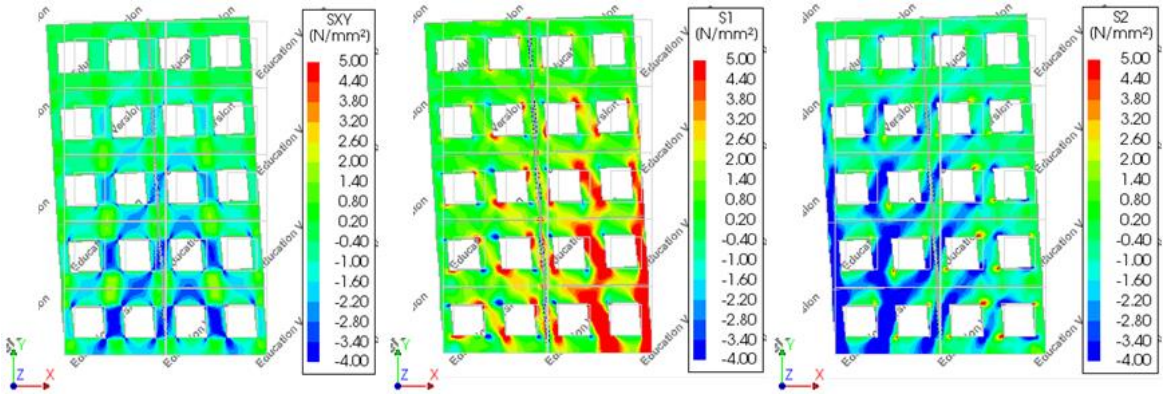

Figure 8.10 Stress distribution in Model 1 (Shear stress Sxy, Principle stresses S1 and S2)

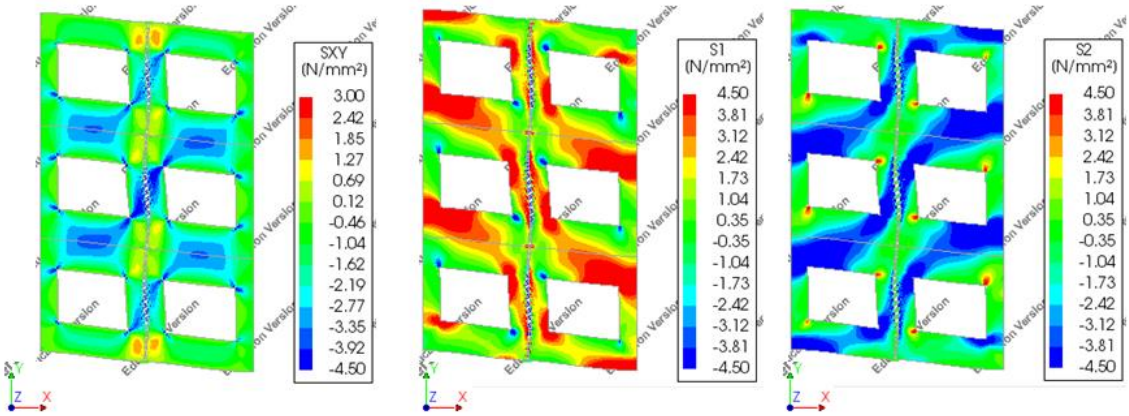

Figure 8.11 Stress distribution in Model 2 (Shear stress Sxy, Principle stresses S1 and S2)

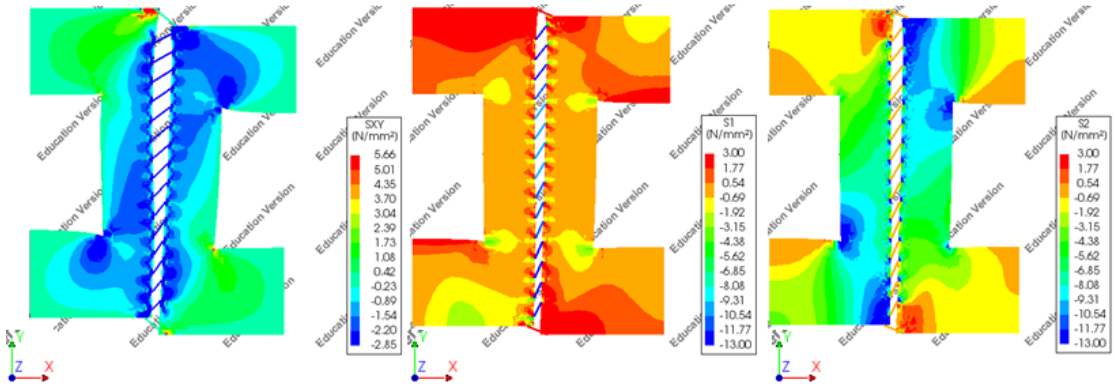

Figure 8.12 Stress distribution in Model 3 (Shear stress Sxy, Principle stresses S1 and S2)

In general, it could be argued that a model that "cuts" a part of the stability wall in a correct way should show a similar stress distribution as what occurs at that location in the entire stability wall. So the stress distribution around the joint in models 2 and 3 should be comparable to that of model 1. The above figures show that in each model a pressure diagonal develops that runs globally from top right to bottom left. For models 1 and 2 it can clearly be seen that there are traction diagonals from the upper left to the lower right. This cannot be seen in model 3.

Appendix D contains an overview of the distribution of the shear stresses Sxy along the contours of the part that is cut out by model 3. The results show that the stress distributions of the first and second model are similar. From this it may be concluded that the cut of the second model resembles the stress state that occurs in a complete shear wall.

8.1.2.3 Comparison of the longitudinal shear force distribution in the joint

Another important aspect regarding the force and stress distribution is the manner in which the shear force is divided over the diagonal bars of the connection. This will have an important effect on the behaviour of the connection. Figure 8.13 shows the distribution of the diagonal forces over the floor height for the three different models. For models 2 and 3 the middle floor has been analysed. Since the magnitude of the load in each model is different, the exact numerical values of the resulting distributions shouldn't be compared. The difference between models 1 and 2 can very well be the result of this unequal load. Two things stand out:

- In model 3, the greatest compressive forces are transmitted through the diagonals at the top and bottom of the floor, in models 1 and 2 this occurs halfway the floor height.
- In models 1 and 2, even tensile forces arise in the upper and lower diagonal / diagonals in the standard situation that is studied. (It should be noted that the profiled mortar connection used cannot transfer any tensile force through the mortar. So in reality the mortar will be detached here and the tensile forces will probably be transferred by the transverse reinforcement.)

In model 3, the distribution of the shear force across the diagonals seems purely determined by the lateral stiffness provided by the surrounding elements. The lateral stiffness must be lower for the part of the joint that is next to the window openings, compared to the part next to the lintels. So for the upper and lower diagonals, which are located at the height of the lintels, the lateral stiffness is locally larger, whereby these diagonals transfer the largest shear force. The found lateral stiffness distribution corresponds to the sketch of Figure 1.3 at the beginning of this thesis. The found force distribution corresponds to the distribution found by H. Hansen (Hansen H. , 1967) and the distribution found for the test setup model.

However, in models 1 and 2 the greatest shear force is transferred half way the floor height. Apparently another effect compensates for the locally lower lateral stiffness, whereby the diagonals halfway carry the largest force. Figure 8.10 and Figure 8.11 show that pressure diagonals develop in the model, as a result of the window recesses. These diagonals cross the joint halfway each floor, leading to a large transferred shear force at this location. Apparently, the pressure diagonal that develops in model 3 doesn't behave in the same manner as those that develop in models 1 and 2.

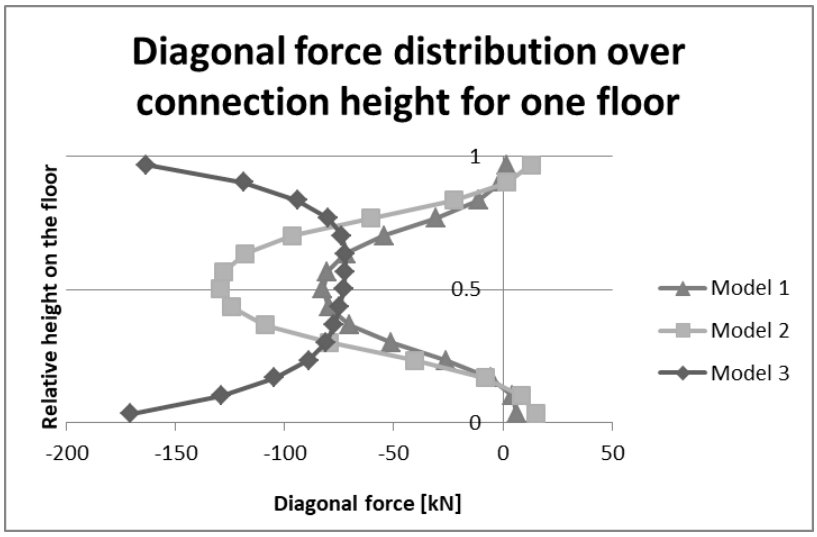

Figure 8.13 Diagonal force distribution over the height of the middle floor

8.1.3 Evaluation of the models

It must be concluded that it appeared to be hard to create a model containing a part of a shear wall. For both models 2 and 3 the boundary conditions cause deviations in the behaviour of the model with respect to model 1.

All three models have advantages and disadvantages. The third model behaves in a completely different manner as the other two. The diagonal force distribution of this model clearly shows the influence of the lateral stiffness, which is positive for a study into this effect. However, the modelled behaviour deviates too much from what happens in a shear wall as the results in this paragraph and appendix D and the model evaluation in appendix C show. The behaviour shows more similarities to a compression instead of a shear test. This deviating behaviour results in essentially different relations for the influence of different parameters, as can be seen by comparing the results in appendix E with the results of paragraph 8.3. For this reason the model is considered not to be applicable for this study.

The second model behaves more like the situation in a shear wall. However, the wall elements cannot translate in horizontal direction, whereby the model is not suitable for a study into the influence of the transverse reinforcement. Based on the comparison with model 1, the second model is assumed to be suitable for analysing the local behaviour of the connection.

The first model is based on the largest scale since it contains a complete shear wall. Therefore full insight in the way the connection is loaded and the structural behaviour of the shear wall that affects the joints behaviour is lacking. So for a more detailed analysis of the connection's behaviour, the model is probably less suitable than model 2. However, it appears to be the best solution for the purpose of this parameter study. The applied boundary conditions are undisputedly corresponding to a real shear wall. Furthermore, the results of the parameter study will show the parameter influence as it occurs in reality, taking into account the shear wall's structural behaviour that might play a role. The results of model 2 would be more theoretical, since the way of loading is more idealised.

The results of the first model are therefore presented in paragraph 8.3. Appendix E also contains the parameter study results obtained with the other models. The similarities in the three results can be seen as a verification of the results of the performed parameter study. The deviations of

the results in appendix E can be assigned to the drawbacks of models 2 and 3. In most cases the influence of parameters in model 2 is similar to that in model 1.

8.2 Input and methodology

This paragraph discusses the input properties and the methodology that is applied in the parameter study. This methodology concerns the way the parameters are varied, the boundaries within this is done and the way the output is processed into comprehensible diagrams.

8.2.1 Overview of parameters and standard input

Figure 8.14 provides an overview of the parameters that are considered in the analysis. These parameters are:

- The stiffness of the transverse reinforcement, K_s
- The Young's modulus of the precast concrete elements, E_c
- The height of window openings close to the joint, h
- The width of the column between the joint and these window openings, a
- The axial stiffness of de diagonal bars, K_d
- The angle of the diagonal bars, α

Three of these parameters need more explanation.

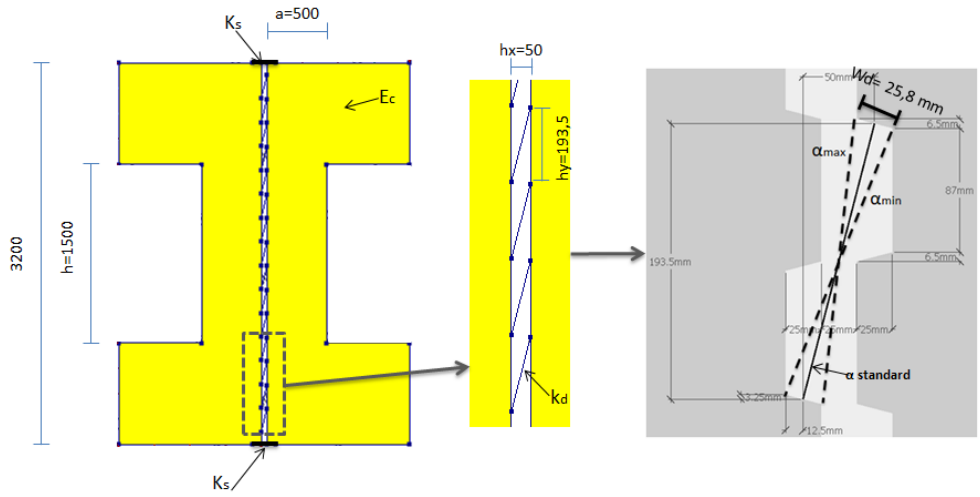

Figure 8.14 Overview of parameters

8.2.1.1 The diagonal angle and stiffness

As Figure 8.14 illustrates, the standard value of the diagonal angle is defined by the line that connects the two midpoints of opposite inclined surfaces. The limits of the variation are determined by the profile geometry as well. They are obtained by creating the lines that connect the endpoints of the inclined surfaces.

The diagonal stiffness is determined by the length of the diagonal, the E-modulus and the cross-sectional area. For the standard value of the cross-sectional area the same assumption is applied as for the test setup model, where the area was equal to the element thickness times the width of the inclined surface. The variation of the stiffness is based on a variation of the width of the diagonal W_d, keeping the length, E-modulus and thickness constant.

8.2.1.2 The transverse spring stiffness

In reality the transverse reinforcement continues over the full length of the shear wall. However, as described in section 2.2.2, an embedded bar in tension transfers most of the tensile forces along the first part of the embedded length. So most of the reinforcement's elongation occurs over this active part. For this reason the reinforcement is modelled along a short distance. The length that is given to the transverse bars is illustrated in Figure 8.15.

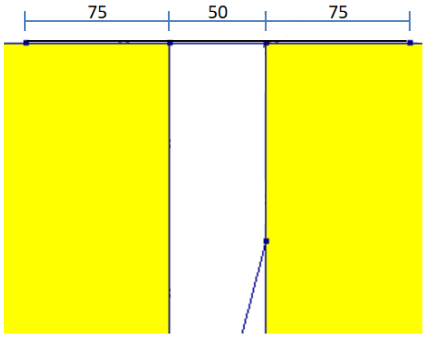

Figure 8.15 Length of the transverse reinforcement bars

The stiffness of the transverse bars in the model contains only the contribution of the axial stiffness. This is fully determined by the bar length, the E-modulus of steel and the applied cross section. This is not in accordance with the real situation.

In reality the transverse reinforcement is applied in the horizontal mortar joints between the wall elements. The figures on page 6 show examples of possible locations of the transverse reinforcement. A transferred horizontal tensile force crosses two interfaces. The force transfer in these interfaces influences the stiffness of the load path.

Figure 8.16 shows this load path. At locations 1, the horizontal force is transferred by friction between the precast concrete elements and the mortar in the joint. At locations 2, the force is transferred by friction between the mortar and the reinforcement. At location 3 the force is transferred by axial tension of the reinforcement bar.

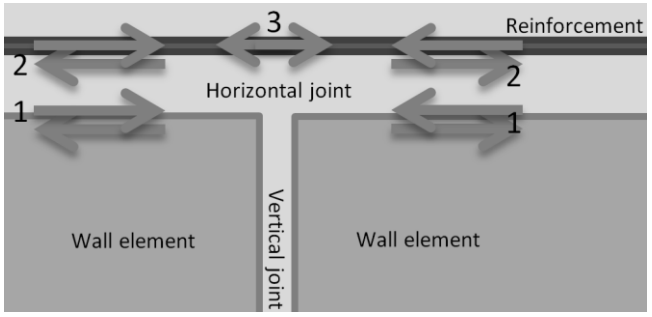

Figure 8.16 Force transfer via the reinforcement. 1. Shear friction between concrete and joint mortar 2. Bond stresses between reinforcement and joint mortar 3. Transfer of axial tensile force in the reinforcement.

All three force transfer mechanisms must be lumped into the stiffness K_s that is assigned to the transverse bars in the finite element model. However, this stiffness is solely determined by the axial stiffness of the bars. If the stiffness of the modelled springs appears to be very important, a more detailed investigation can be done to determine the combined stiffness more precisely.

8.2.1.3 Standard values

Table 8.1 shows the standard values that are used as model input. The total diagonal stiffness that is given is the summed axial stiffness of all fifteen parallel diagonal bars. The transverse spring stiffness is the axial stiffness of a single transverse bar. Both quantities are assigned by a capital "K", which indicates that it is the total stiffness. The total stiffness is always the total value per floor.

Some standard values of parameters are arbitrary. For example the chosen values for h and a. In all cases the window openings are applied around the horizontal centre lines of the floors, resulting in two equally sized concrete lintels above and below the openings. The standard value for the concrete stiffness, E_c, of 35000 N/mm^2 followed from regular material properties for uncracked concrete. The standard value of K_s was hard to determine, since the stiffness of the bars includes more than only the axial stiffness of the reinforcement, as explained in the previous section. Therefore the standard value is determined based on the resulting horizontal displacement difference, which shouldn't be too large compared to other deformations. The standard values of A_d and alpha followed from the profile geometry.

The shear wall model is loaded by a horizontally distributed load of 40 N/mm on each floor level. A quadratic mesh is used with a mesh size of 100 mm. This mesh size has been determined based on a mesh size dependency study that was performed on Model 3. The results of this study are provided in appendix C.

Concrete Elements	
Plane stress elements CQ16M	
Thickness t	200 mm
E-modulus E_c	35000 N/mm^2
Poisson's ratio ν	0.2
Window height h	1500 mm
Column width a	500 mm
Diagonal bars	
Regular truss elements L2TRU	
Length L_d	199.86 mm
Slope [h_y/h_x] α	3.87
Cross-sectional area A_d	5166 mm^2
E-modulus E_d	25000 N/mm^2
Total diagonal stiffness K_d	9693 kN/mm
Poisson's ratio ν	0.2
Amount of diagonals per floor	15
Reinforcement bars	
Regular truss elements L2TRU	
Cross-sectional area A_R	5620 mm^2
E-modulus E_s	210000 N/mm^2
Length L_s	200 mm
Transverse spring stiffness K_s	5901 kN/mm
Poisson's ratio ν	0.3

Table 8.1 Overview of standard input values

8.2.2 Variation of parameters

The standard model is the starting point of the variations. Each time only a single parameter is varied, while keeping the other parameters equal to their standard value. In this way the pure influence of a single parameter is investigated.

Table 8.2 gives an overview of all parameter's standard values and variation values. The standard values are highlighted.

Parameter	Unit	Min							Max
E_c	N/mm^2	10000	25000	30000	**35000**	40000	45000	50000	
K_d	kN/mm	1876	3753	5629	7505	**9693**	11258	13134	
K_s	kN/mm	525	2534	4222	**5901**	6756	8444	13511	
α	$[h_y/h_x]$	2.49	**3.87**	5.25	6.35	7.99			
a	mm	200	300	**500**	600	700	800	1200	
h	mm	700	1000	1200	**1500**	1600	1800	2000	2500

Table 8.2 Variation of the parameters (standard values in bold and underlined)

The limits of alpha are determined by the edges of the opposite inclined surfaces (See Figure 8.14). The maximum theoretical value is 8, the minimum value is approximately 2.5. So a huge variation of alpha is possible within the staggered profile geometry.

The variation of alpha within the profile coincides with a shortening or elongation of the diagonal. This directly influences the diagonal's stiffness. In order to get a pure image of the effect of a variation of alpha, any length variation should be avoided. However, in this parameter study it is decided to investigate the insecurity of the diagonal's orientation as whole. Therefore the angle is varied within the limits indicated in Figure 8.14 and the diagonal length is changed according to the profile edges. For example, in the steepest orientation alpha is $\frac{200}{25} = 8.00$ and the length is set to: $\sqrt{25^2 + 200^2} = 201.56\ mm$, and in the flattest orientation alpha is $\frac{187}{75} = 2.49$ and the length is set to: $\sqrt{75^2 + 187^2} = 201.48\ mm$. As can be seen, also in comparison with the length given in Table 8.1, the length variation is not very large, but does influence the results. In the model, the width of the gap between the wall elements is varied between 25 and 75 mm corresponding to the chosen value of alpha and the orientation of the diagonal.

The parameters K_s and K_d are varied by changing the cross sections A_d and A_R. The values for A_d were determined based on the profile geometry. Because the stiffness K_s contains multiple aspects, as explained in section 8.2.1.2, practical limits are uncertain. Therefore a wide variation of A_R is applied in order to create a wide range of the transverse spring stiffness.

8.2.3 Processing of results

The way the results are processed is in general equal to the approach used for the test setup model. An analysis is performed on the model with for a single parameter X variation value y and for all other parameters the standard value as input. Only the middle floor of the shear wall model is considered while processing the output of the analysis. So the displacements of the fifteen diagonal endpoints and the forces in each diagonal on this floor are exported and stored in a table. From the average displacements and summed forces, the lateral and shear stiffness are calculated. This results in one data point in the relation between parameter X and shear stiffness K_v and one data point in the relation between parameter X and lateral stiffness K_h. Subsequently, the analysis is repeated for another value of parameter X.

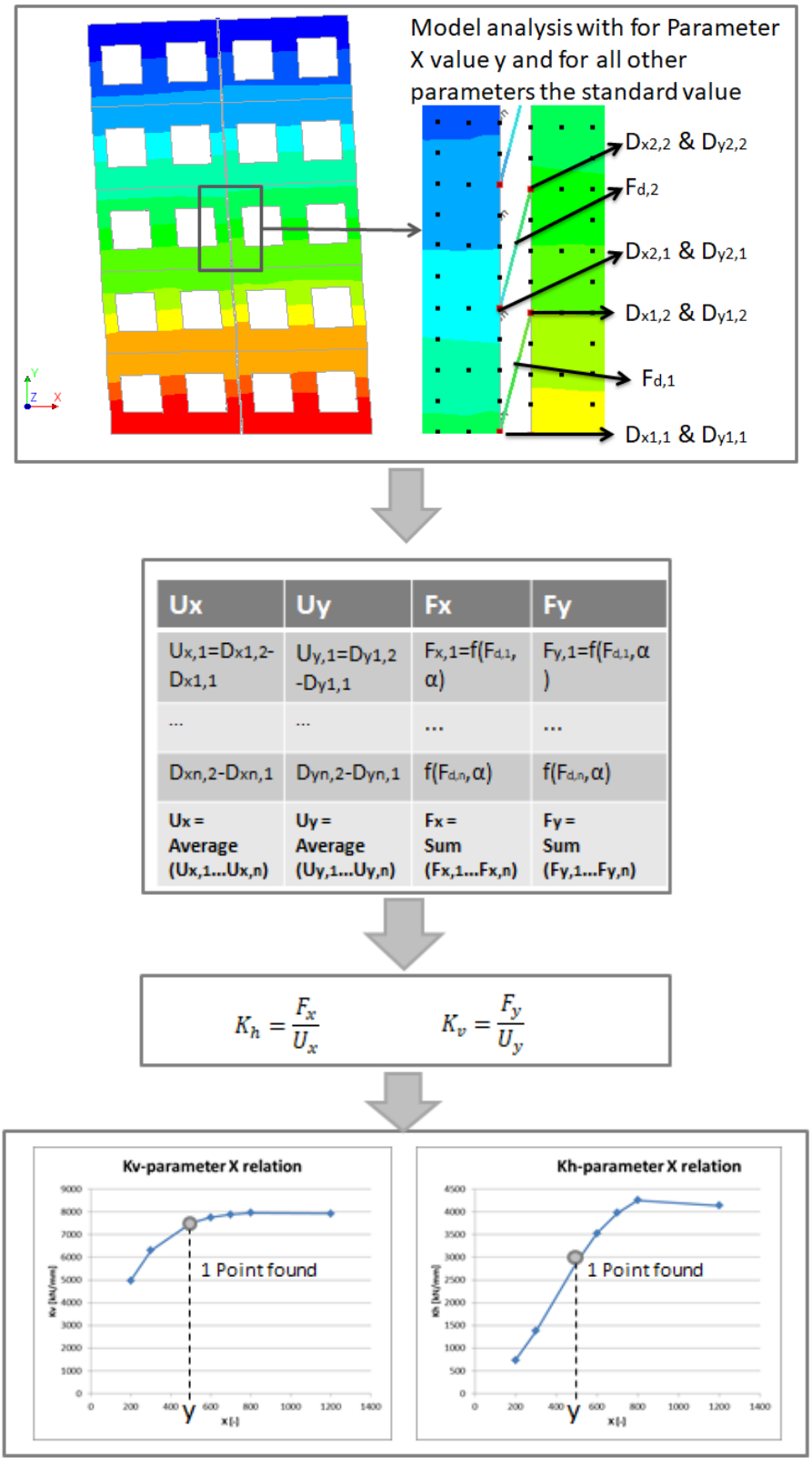

Figure 8.17 Processing of model output

8.3 Results

This paragraph contains the results of the parameter study. As illustrated in Figure 8.17, two diagrams are constructed for each parameter. One diagram indicates the influence of the parameter on the total shear stiffness, the other indicates the influence on the total lateral stiffness. Furthermore, for each parameter variation the influence on the force distribution over the diagonals is indicated. This diagram indicates whether a change of the parameter results in a change in local structural behaviour.

The diagrams that show the relation between the parameter value and the stiffness values, are normalised. Index value 1.0 is always assigned to the largest parameter value and the corresponding stiffness value. The results corresponding to the other parameter values have indices related to this reference.

Appendix E contains more results of the parameter study, including those obtained from models 2 and 3. The relations obtained for model 2 are in most cases similar to those of model 1, presented in this paragraph.

In the next paragraph it is explained, that the influence of a parameter depends on the applied standard values for the other parameters. So the presented results will change when other standard values than those of Table 8.2 are applied. It is important to keep this in mind while evaluating the parameter study results.

8.3.1 The influence of the transverse spring stiffness

The influence of the variation of the transverse spring stiffness K_s, is illustrated by the diagrams in Figure 8.18. The results obtained for K_s = 13511 kN/mm are given index 1.0.

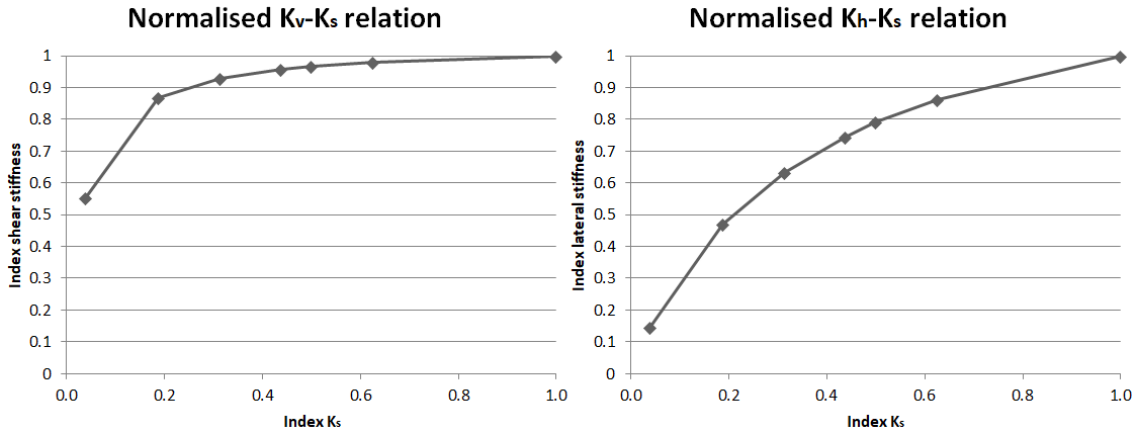

Figure 8.18 The influence of the transverse spring stiffness on K_v (left) and K_h (right)

The diagrams show that a reduction of the transverse spring stiffness leads to a reduction in both the shear and lateral stiffness. This is behaviour is expected based on the results presented in chapter 7 for a variation of the cross section of the transverse bars in the test setup model. Both relations are asymptotic, whereby the influence of increasing the value for K_s reduces when the initial value of K_s is larger.

The left diagram shows that the influence of K_s on the shear stiffness is limited. If the value of K_s is reduced to a value that is just 20 percent of the largest value, the shear stiffness is still more than 85 percent of the largest value. Only a reduction of the transverse spring stiffness to an

even smaller value results in a significant decrease of the connection's shear stiffness to a value of 55 percent. The right diagram shows that the lateral stiffness decreases gradually for decreasing values of the transverse stiffness. The influence of a variation of K_s on the lateral stiffness is larger than its influence on the shear stiffness.

The diagrams in appendix E for model 2 show that in this model the influence of the transverse spring stiffness on the shear and lateral stiffness is minimal. This is a result of the applied boundary conditions that contain horizontal supports on both sides of the joint.

Figure 8.19 shows the distribution of the diagonal forces over the height of the floor for three different values of K_s. From this graph it can be concluded that a change of K_s doesn't lead to a significant change in the shear force distribution over the connection.

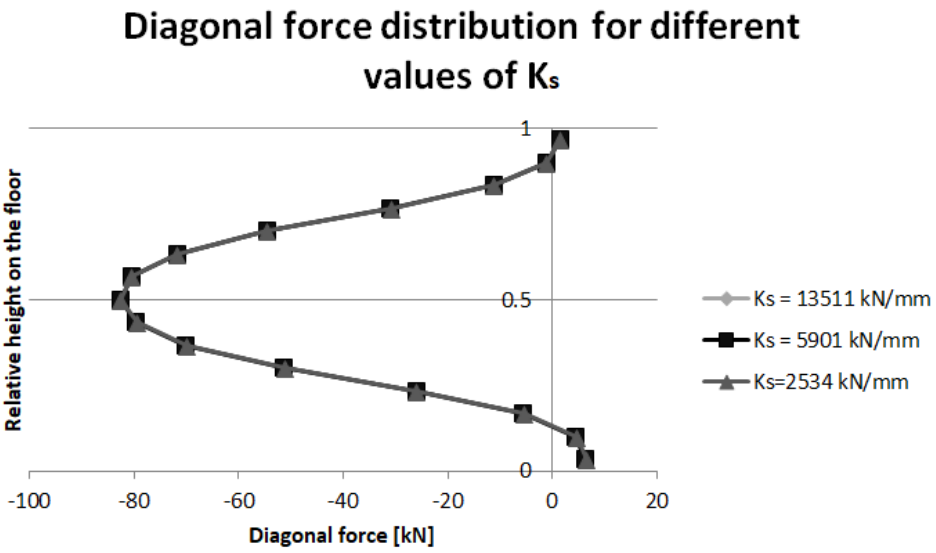

Figure 8.19 Diagonal force distribution over the floor height for different values of K_s

8.3.2 The influence of the concrete stiffness

Figure 8.20 shows the influence of the concrete stiffness E_c on the total shear and lateral stiffness of the connection. The left relation between the indices for K_v and E_c shows an asymptotic behaviour. So the increase of shear stiffness that can be obtained by increasing the concrete stiffness is limited. The right diagram shows also a relation with decreasing slope, indicating asymptotic behaviour. However, the large slope of the relation still has at point (1.0;1.0) indicates that the maximum lateral stiffness is not yet approached.

Also for this parameter's influence on the lateral stiffness is larger than its influence on the shear stiffness, as can be concluded from the slope of the diagrams.

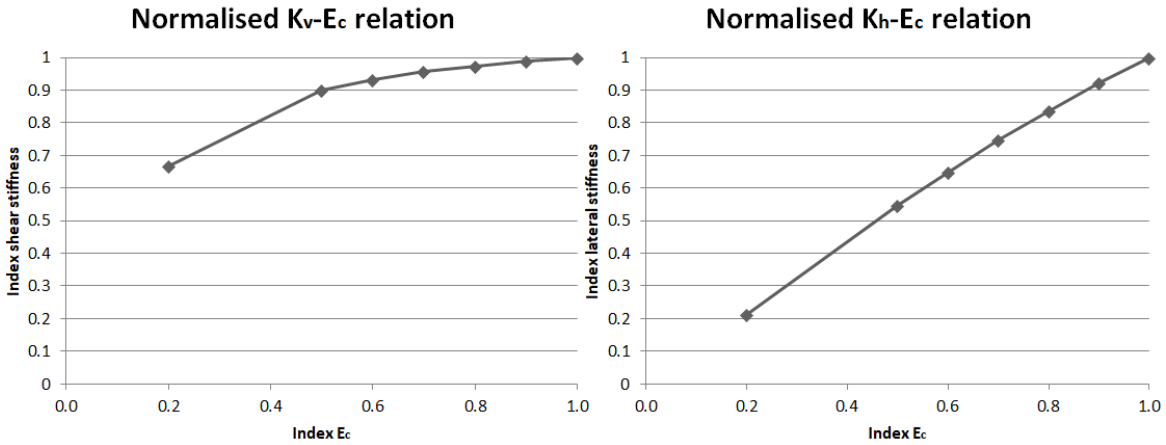

Figure 8.20 The influence of the concrete stiffness on K_v (left) and K_h (right)

Figure 8.21 shows the diagonal force distribution over the height of the considered floor. Based on the diagram it is concluded that a variation of the concrete stiffness leads to a redistribution of the shear force over the height of the connection. A smaller concrete stiffness leads to a larger difference between the smallest and largest diagonal force. In case the concrete stiffness is very large only compression forces occur in the diagonals.

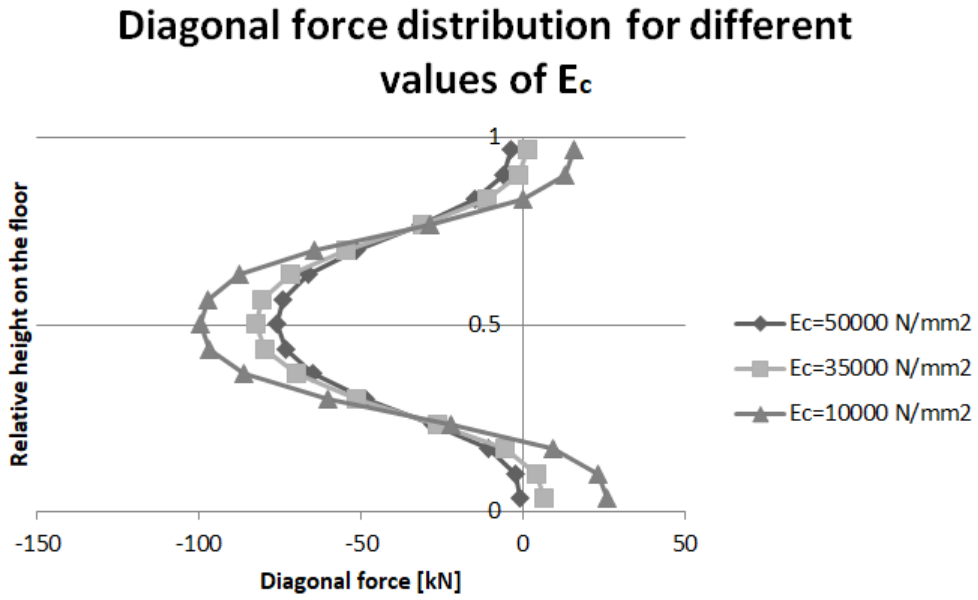

Figure 8.21 Diagonal force distribution over the floor height for different values of E_c

8.3.3 The influence of the column width

Figure 8.22 shows the diagrams that indicate the influence of the column width on the shear and lateral stiffness. The left relation is clearly asymptotic. Apparently, an increase of the column with to a value larger than 600 mm won't significantly increase the shear stiffness, for the applied combination of standard values. When the column width is reduced to 200 mm (17 percent of the maximum value), the shear stiffness is slightly larger than 60 percent.

Also for this parameter it holds that its influence on the lateral stiffness is greater. The lateral stiffness is reduced by approximately 80 percent if the column width is 200 mm.

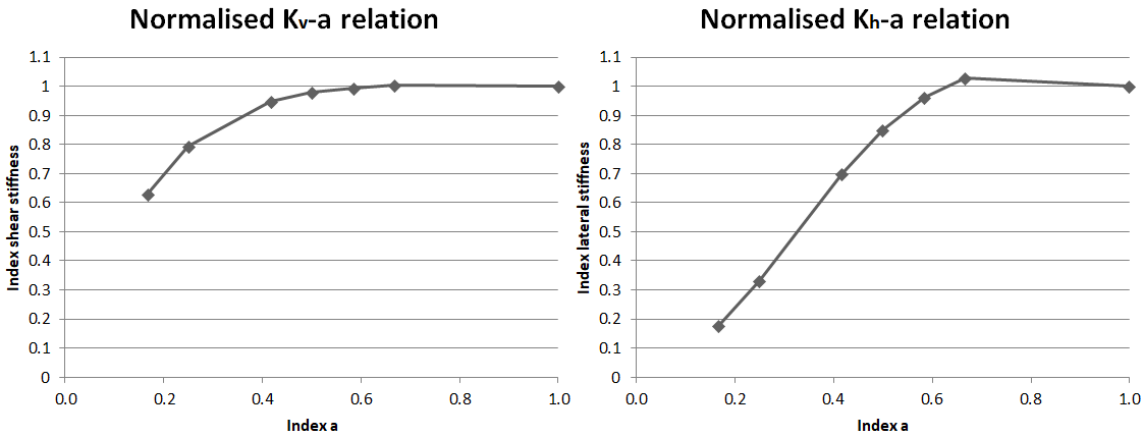

Figure 8.22 The influence of the column width on K_v (left) and K_h (right)

So the influence on the lateral stiffness is rather large. The diagram shows a strange behaviour for larger values of the column width, since the maximum shear stiffness is found for a=800 instead of 1200 mm. The cause of this behaviour isn't known. However, the global trend of a decreasing lateral stiffness by a reduction of the column width is clear and of major importance.

As can be seen in appendix E, the found influence of a variation of the column width in model 3, is completely different. This is caused by its particular behaviour that deviates from the behaviour of models 1 and 2. This behaviour is explained in appendix C. The influence of the column width in model 2 globally shows the same behaviour as indicated in Figure 8.22, the influence on both stiffness quantities is just slightly larger.

Figure 8.23 shows the diagonal force distribution over the height of the floor. A reduction of the column width leads to a concentration of the transferred shear force to the centre of the floor. Although the width of the surrounding concrete columns is reduced, the transferred shear force at centre height is increased. The effect of the compression diagonals that develop in the shear wall appears to overrule the reduced lateral stiffness halfway the floor height.

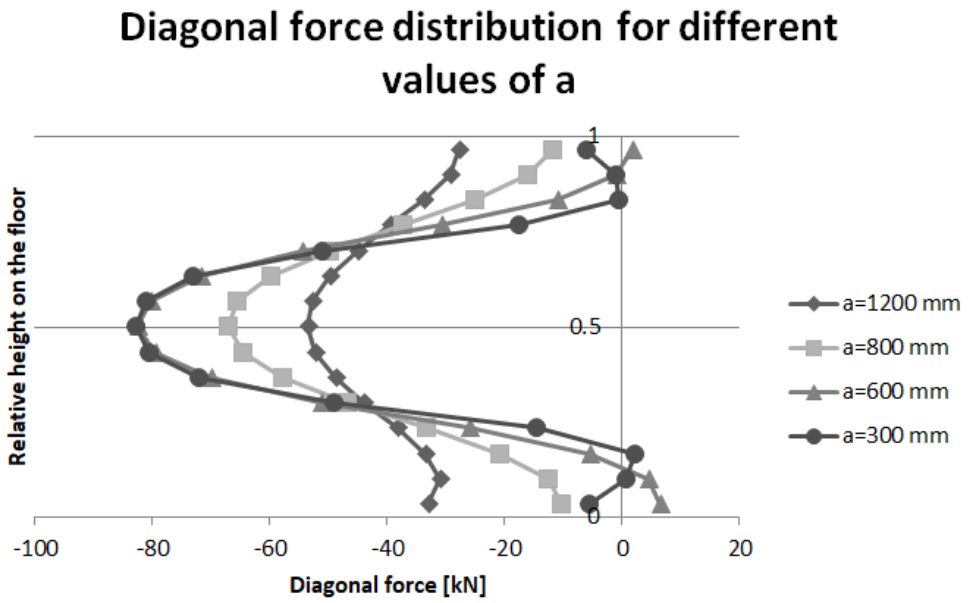

Figure 8.23 Diagonal force distribution over the floor height for different values of a

8.3.4 The influence of the window opening height

Figure 8.24 shows the normalised relations between the opening height h and the shear and lateral stiffness. The left relation shows that the shear stiffness of the connection is reduced when the opening height is larger. The relation is again asymptotic. For the applied combination of standard values, the influence on the shear stiffness is rather small, compared to the previous results. A reduction of the window height from 2500 to 700 mm (70 percent) results in a shear stiffness that is just 28 percent larger.

The influence of the opening height on the lateral stiffness is larger, just like for the previous parameters. The results in appendix E show the trend of the relation is similar in all models, but the magnitude of the influence differs a lot.

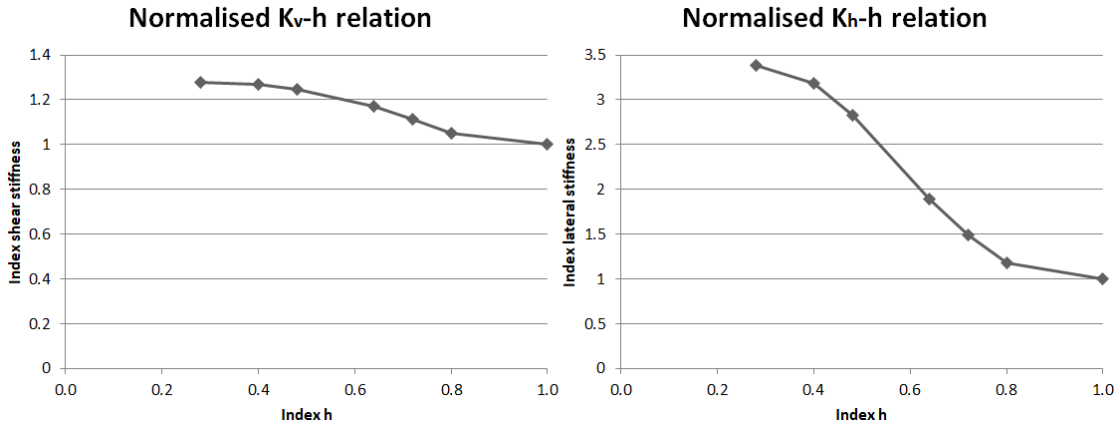

Figure 8.24 The influence of the opening height on K_v (left) and K_h (right)

Figure 8.25 shows the diagonal force distribution over the height of the floor. It can be concluded that the reduction of h results in a concentration of the shear force around the centre of the floor. So it concentrates at the part of the connection that is next to the window opening. This must again be attributed to the compression diagonals that develop in the shear wall, which effect seems to be very important, since it overrules the locally lower lateral stiffness.

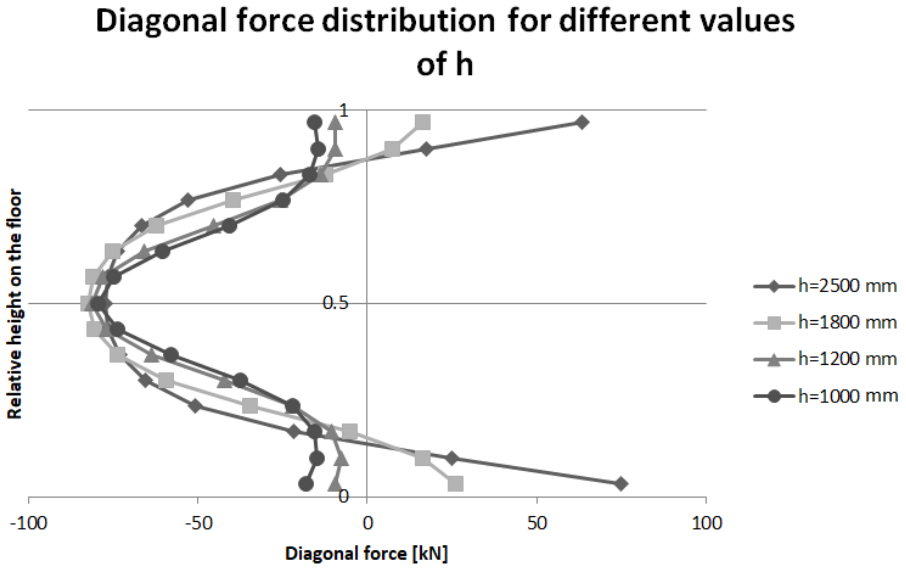

Figure 8.25 Diagonal force distribution over the floor height for different values of h

8.3.5 The influence of the diagonal stiffness

Figure 8.26 shows the influence of the diagonal stiffness on the shear and lateral stiffness of the connection. Unlike the previous parameters, the diagonal stiffness has a larger influence on the shear stiffness. Over the range of variation the minimum shear stiffness is 5 times smaller than the maximum value that is found. The minimum lateral stiffness is 3.5 times smaller than the maximum value that is found. A reduction of the diagonal stiffness leads to a decrease of the shear stiffness. This could be expected from the results of paragraph 7.4, where the shear stiffness of the test setup model was decreased by reducing the value of K_d. Since the slope of the relation decreases slightly, an asymptotic relation is expected between K_d and K_v. However, with the applied standard values the limit of this relation isn't achieved by far, as the slope at the upper end of the relation indicates.

A reduction of the diagonal stiffness appears to result in an increase of the lateral stiffness. This seems a bit contradictory and will further be discussed in chapter 10.

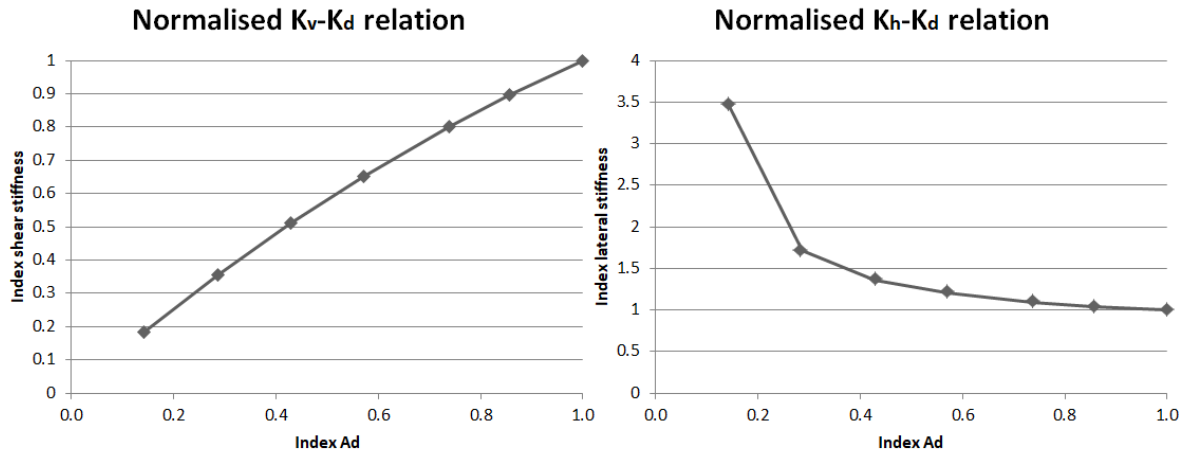

Figure 8.26 The influence of the diagonal stiffness on K_v (left) and K_h (right)

Figure 8.27 shows the diagonal force distribution over the height of the considered floor. It is seen that a reduction of K_d leads to a larger spread of the shear force, whereby the extreme values of the diagonal force are reduced. The largest shear force is always transferred halfway the floor height.

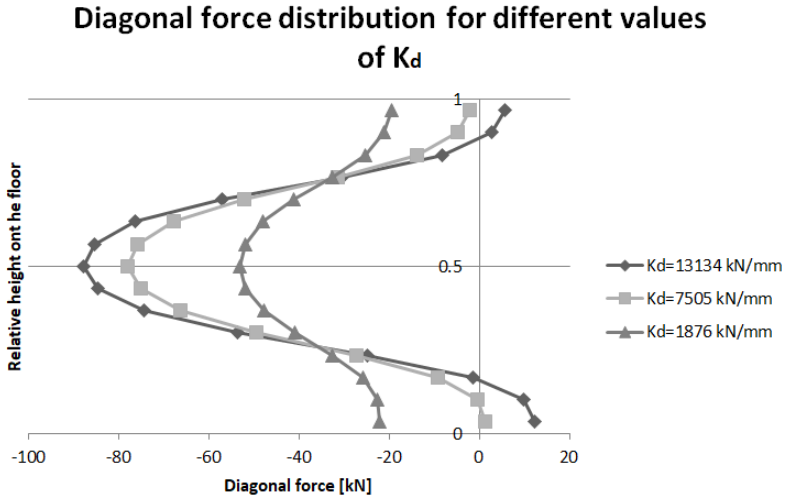

Figure 8.27 Diagonal force distribution over the floor height for different values of K_d

8.3.6 The influence of the diagonal angle

Figure 8.28 shows the influence of a variation of the diagonal angle on the shear and lateral stiffness of the connection. The influence on the shear stiffness is rather large. The relation is asymptotic, which is logical. If the diagonal bars are vertical, their axial stiffness is fully used for the transfer of the vertical shear force. This configuration of bars results in the largest possible shear stiffness. The steeper the diagonals are, the closer the stiffness gets to this limit. As the stiffness approaches the limit, the influence of a change of diagonal angle becomes lower.

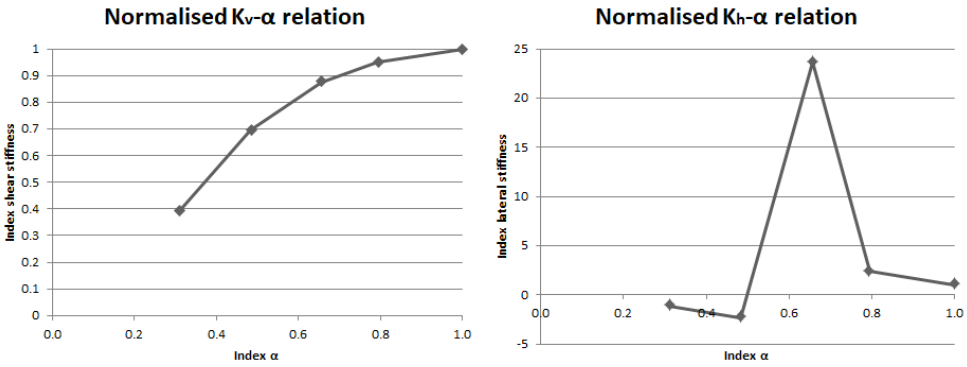

Figure 8.28 The influence of the diagonal angle on K_v (left) and K_h (right)

The relation indicating the influence of alpha on the lateral stiffness is rather odd. Unlike all previous relations, where the absolute value of the lateral stiffness was considered, this relation takes the real value into account. The negative values corresponding to the two smallest values of alpha have the same sign as the results of the previous parameters.

If steep diagonals are applied, the joint is on average not dilated, but compressed as a result of the horizontal load. This horizontal load is probably induced by the horizontal force component of the compression diagonals that develop in the shear wall. For more horizontally oriented diagonals, the joint will dilate as a result of the horizontal component of the force in the diagonal bars. For a certain value of alpha, these two effects will be in balance, whereby the horizontal displacement difference U_x approaches zero, resulting in an infinitely large lateral stiffness. The whole is illustrated in Figure 8.29, where also the complete relation between K_h and alpha is sketched.

Since the joint between the two precast concrete elements is fully filled with mortar, it is not compressible. Therefore the obtained behaviour is considered to be physically impossible. It is a consequence of the applied modelling approach. Appendix J describes this effect in more detail.

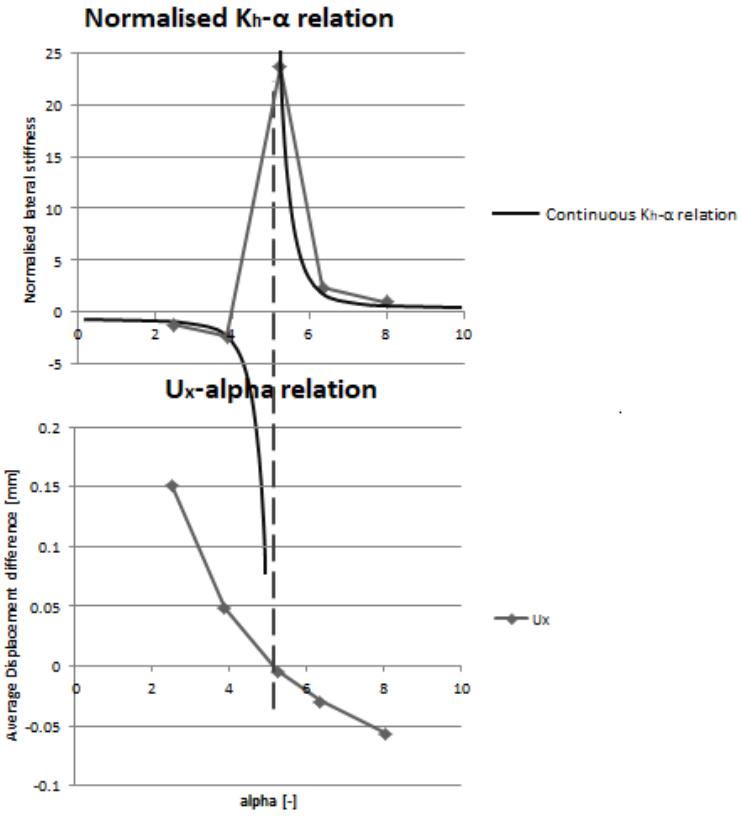

Figure 8.29 The relation between K_h and α caused by the relation between α and U_x

The results presented in appendix E show that in models 2 and 3 the lateral stiffness simply reduces for smaller values of alpha. The relations for the influence on the shear stiffness are very similar.

Figure 8.30 shows that the distribution of the diagonal forces over the height of the floor is not very much influenced by a variation of the diagonal angle.

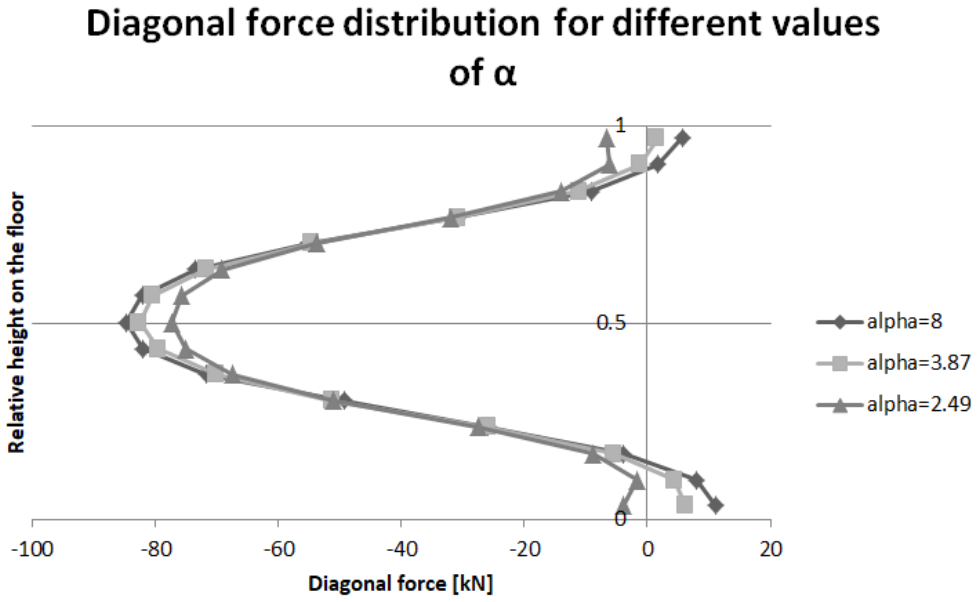

Figure 8.30 Diagonal force distribution over the floor height for different values of K_d

8.4 Overview of the results

In this paragraph the most important conclusions of the parameter study are enumerated. These conclusions are related to the goals that were formulated in the introduction of this chapter. This paragraph also discusses the validity of the presented results and conclusions.

8.4.1 The relevance of the six parameters

One of the goals of the parameter study was to indicate the relevance of each parameter based on its influence on the shear stiffness of the connection. The influence of each parameter is indicated by the ratio between the size of the range over which the parameter is varied and the corresponding range of the shear stiffness. So the following order of relevance can be made:

- The diagonal stiffness K_d is most relevant. A reduction of K_d by 86 percent leads to a reduction in shear stiffness K_v of 82 percent (Ratio: 82/86=0.95).
- The diagonal angle α. A reduction of the angle by 69 percent leads to a reduction of the shear stiffness of 61 percent (Ratio: 61/69=0.88).
- The transverse spring stiffness K_s. A reduction of K_s by 96 percent leads to a reduction of the shear stiffness of 45 percent (Ratio: 45/96=0.47).
- The column width 'a'. A reduction of a by 83 percent leads to a reduction of the shear stiffness of 37 percent (Ratio: 37/83=0.45).
- The concrete stiffness E_c. A reduction of E_c by 80 percent leads to a reduction of the shear stiffness of 34 percent (Ratio: 34/80=0.43).
- The window height 'h' is least relevant. A reduction of the window height by 72 percent leads to an increase of the shear stiffness by 28 percent (Ratio: 28/72=0.39).

So this order of relevance is obtained by dividing the relative difference in shear stiffness by the relative difference in parameter value. In this way the influence is seen as the average slope of the parameter relations presented in previous paragraph.

From the results it is concluded that the influence of the parameters K_s, E_c, a and h on the lateral stiffness is larger than their influence on the shear stiffness of the connection. In section 5.1.3 these four parameters were defined as design parameters that influence the lateral stiffness. So this result substantiates this definition. The influence of E_c, a and h on the lateral stiffness is approximately equal, the influence of K_s is slightly lower. The relevance for K_h of each parameter is therefore equal, based on these specific results.

Some important comments must be made about the determined order of relevance of the six parameters.

First of all, the range over which the parameters are varied is rather large. By considering a large range of variation, more insight is gained in the influence of each variable. The transverse spring stiffness is for example reduced by 96 percent, whereby it is possible to see that its influence is significant for a change in small values of K_s. If these values weren't included in the range of variation, the influence of K_s was thought to be insignificant. Because it is yet unknown which values are practical and realistic, for K_s and K_d in particular, it is important to use a wide range of variation to see the potential influence. However, especially for the parameter K_s, the large relevance is a direct result of the range of variation. If it appears that practical values for K_s are never lower than approximately 3000 kN/mm, the influence of this parameter is the smallest

and therefore the least relevant. So although it is possible to arrange the parameters in order of their influence, this order is dependent on the practical range over which each parameter varies.

Furthermore, all analysed parameters influence the lateral and shear stiffness. Therefore, the magnitude of the lateral and shear stiffness is determined by the combination of all the parameters. Since this is the case, the influence of the variation of a single parameter depends on the magnitude the other parameters have. So all the relations that are found in this parameter study are specifically valid for the applied standard values for each parameter. If for example the standard value of parameter K_s would be smaller, the influence of all other parameters will deviate from what is found in paragraph 8.3.

For these two reasons it is impossible to conclude from the results presented in this chapter which parameters are most relevant and which parameters the least. This conclusion can only be drawn when for each parameter the range of realistic values is defined and when more insight is gained on the influence of parameters on the other parameters. The latter is discussed in chapter 9.

8.4.2 The relevance of the lateral stiffness and the joint properties.

Another goal of the parameter study was to gain insight in the relevance of the lateral stiffness and the two joint properties, based on their influence on the connection's shear stiffness. The two parameters related to joint properties have a larger influence on the shear stiffness than the four parameters related to the lateral stiffness, as concluded in previous section. The variation of the four lateral stiffness parameters led to a variation of the lateral stiffness itself. The obtained difference between the maximum and minimum value of the lateral stiffness is approximately 90 percent. The ranges of variation of K_d and α were 86 and 69 percent respectively. So despite the lateral stiffness has been varied over a wider range, its influence of on the shear stiffness is smaller than the influence of changing K_d or α. From this it is concluded that for the chosen combination of standard values, the joint properties are more relevant than the lateral stiffness. This aspect is elaborated on in chapter 9.

8.4.3 The relation between the design parameters and the lateral stiffness

Insight into the relations between design parameters and the lateral stiffness was also aimed at. These relations indicate that in general:

- A reduction of K_s leads to a reduction of K_h.
  If the stiffness of the transverse reinforcement is reduced, the two precast concrete elements can move apart more easily, resulting in a smaller lateral stiffness.
- A reduction of E_c leads to a reduction of K_h.
  When the precast concrete elements are less stiff, they bend more easily, resulting in a larger dilatation of the joint and thus a smaller lateral stiffness.
- A reduction of 'a' leads to a reduction of K_h
  A smaller distance between the joint and the openings in the wall leads to more bending deformations of the precast concrete elements, resulting in a smaller lateral stiffness.
- A reduction of h leads to an increase of K_h
  A smaller opening height reduces the bending deformations of the precast concrete elements, resulting in a larger lateral stiffness.

The first statement is an observation and therefore really a conclusion of the parameter study. Each second statement is an explanation of a probable cause of the observed behaviour, which is not based on specific results and should be analysed in more detail.

Furthermore it is concluded that the parameters K_d and α influence the lateral stiffness as well. The lateral stiffness was thought of as the resistance to dilatation provided by the surroundings of the joint. So any influence of the diagonal properties was not really expected and needs further investigation. The relation between design parameters, diagonal properties and the lateral stiffness is further discussed in chapter 10.

8.4.4 The relation between lateral stiffness, diagonal stiffness, diagonal angle and the connection's shear stiffness

In general it could be said that an increase of the lateral stiffness by adjusting parameters K_s, E_c, a or h, an increase in the diagonal stiffness or an increase of the diagonal angle leads to an increase of the connection's shear stiffness. The relation is further analysed in chapter 9 and 10.

8.4.5 Force distribution over the joint

For each parameter variation, the effect on the diagonal force distribution was presented as well. These diagrams showed some interesting facts:

- Although the lateral stiffness must be smaller halfway the floor height, because of the location of the window openings, the shear force concentrates here.
- A reduction of the column width or the opening height concentrates the transferred shear force even more to the centre of the floor height.

These two effects must indicate that the spread of the shear force over the connection is determined by more effects than the lateral stiffness and the joint properties. The stress distribution over the model, presented in Figure 8.10, shows the development of compression diagonals in the shear wall. These compressive forces cross the joint exactly halfway the height of each floor. The force flow is apparently more determined by the configuration of the openings in the wall than the distribution of the lateral stiffness over the joint. This behaviour is analysed in more detail in chapter 10.

9 Relations between parameters

The results of the performed parameter study were discussed in chapter 8. These results are useful to gain some insight into the relevance of the six parameters that were analysed. However, it appeared hard to formulate general conclusions about the relevance of each parameter based on its influence on either the lateral stiffness or the shear stiffness of the connection. As stated in paragraph 8.4, two difficulties are faced: the uncertainty of the practical range of variation for each parameter and the interdependency between parameters. The latter means that the influence of each parameter on the connection's stiffness is dependent on the magnitude of all other parameters.

Furthermore, the parameter study results showed that the influence of the lateral stiffness on the shear stiffness of the connection was smaller than the influence of the diagonal properties. The relation between these two structural effects isn't known yet, neither the influence the two effects have on each other.

This chapter describes two analyses. The first investigates the combined contribution of the diagonal stiffness K_d and angle α and lateral stiffness K_h to the magnitude of the shear stiffness K_v. This analysis is related to the last two questions formulated in paragraph 5.3. The second is performed to describe the interdependency between the four considered parameters that define the lateral stiffness: K_s, E_c, a and h. The relevance of the parameters can be determined more precisely on the basis of this analysis, which is related to the first three questions of paragraph 5.3.

9.1 The relation between K_h, K_d, α and K_v

In order to analyse the relevance of the lateral stiffness, the diagonal stiffness and the diagonal angle, a the k_v-k_h diagram is constructed (Figure 9.1) by using all the data points that are collected during the parameter study. After all, each parameter variation led to a new shear stiffness with corresponding lateral stiffness.

9.1.1 Combined parameter study results

Figure 9.1 shows the k_v-k_h relation, the relation between the average shear and average lateral stiffness. From this diagram it can be concluded that a variation of one of the design parameters K_s, E_c, a or h always leads to a point on the same asymptotic relation (relation 1). However, when the diagonal stiffness is varied, the resulting combination of lateral and shear stiffness is not a point on the same line, but on relation 2.

So relation 1 is valid when a diagonal stiffness of 9693 kN/mm (the standard value) is applied in combination with any combination of values for the four design parameters. When the diagonal stiffness is equal to 5629 kN/mm for example and the design parameters are varied resulting in different values for k_h, then all the data points appear to lie on relation 3.

It is clear that varying all the design parameters in relation 1 leads to a greater variation of the lateral stiffness than what is obtained by varying the diagonal stiffness, since the range over the horizontal axis of relation 1 is way larger than that of relation 2. So a variation of the diagonal stiffness primarily leads to a change of the shear stiffness, whereas a variation of the design

parameters primarily leads to a change in lateral stiffness. This conclusion corresponds to the conclusion drawn in previous chapter, that states that the influence of the four design parameters on the lateral stiffness is greater than their influence on the shear stiffness.

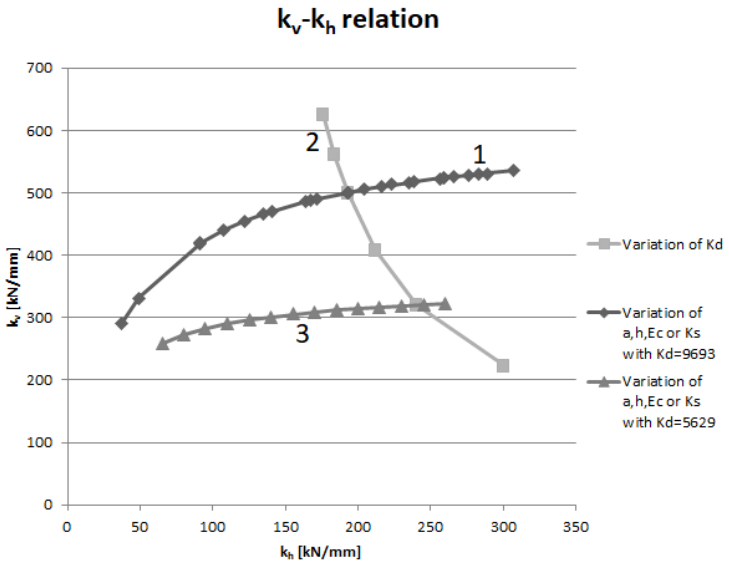

Figure 9.1 The K_v-K_h relation for the variation of the design parameters and a variation of the diagonal stiffness

Furthermore another important conclusion can be drawn based on this diagram. The slope of relation 3 is smaller than the slope of relation 1. So a variation of the lateral stiffness and thus the design parameters has a larger influence on the magnitude of the shear stiffness for a large value of K_d. Consequently, the relevance of the lateral stiffness and the design parameters is dependent on the obtained diagonal stiffness. Vice versa, the influence of a change in diagonal stiffness is greater for larger values of K_h, since the distance between relations 1 and 3 increases for larger values of K_h.

The parameter study results that were obtained for a variation of the diagonal angle alpha were a bit odd, since the lateral stiffness changed sign. This fact proves that the resulting combinations of k_h and k_v for this variation don't lie on relation 1. So its influence is similar to that of the other diagonal property, K_d, in that sense that a variation doesn't lead to a point on relation 1. Unfortunately, the applied shear wall model is not suitable for investigating the effect of a variation of alpha in the context of this diagram.

9.1.2 The relation with the test setup model and other models

In section 7.3.4 the scale effect between the small and large test setup model was analysed. It appeared that the relation between the average shear and lateral stiffness of both models was equal.

Because the applied standard values for K_d and α are equal to the uncalibrated values applied in the test setup model, the found k_v-k_h relation for the shear wall model (model 1) is easily compared with the one obtained from the test setup model. Moreover, the found relations for models 2 and 3 using the results of appendix E, can be compared as well.

Figure 9.2 contains a plot of all found k_v-k_h relations in one diagram. It is concluded that all relations are equal. All the data points with varied a, h, E_c or K_s obtained from the parameter study on the three models lie on the relation found for the two test setup models.

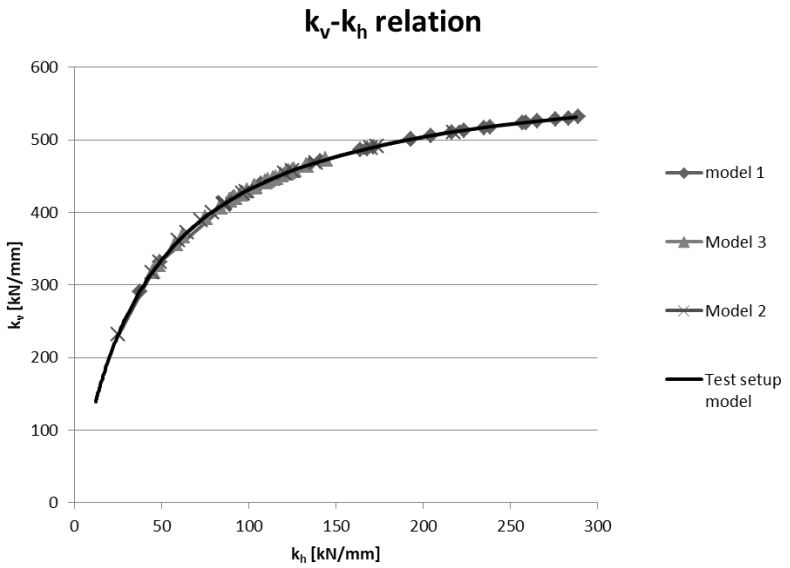

Figure 9.2 The k_v-k_h relations for all different models

This result means that the relation between the average shear and lateral stiffness is independent of the shape of the structural elements surrounding the joint. Either with the L-elements used in the test setup, with parts of wall elements in model 3 or with complete wall elements in models 1 and 2 the same relation is found.

According to this conclusion, the model shown in Figure 9.3 is constructed. The bar model in the left image contains a single diagonal bar with stiffness k_d and a support stiffness k_{sup1}. This support stiffness can be seen as the lateral stiffness that is provided by the precast concrete elements, which are not part of this model. The total diagonal, lateral and shear stiffness is equal to the average values, since there is just a single diagonal. If the connection is enlarged to a double amount of diagonals, these diagonals act as parallel springs. This is shown in the right image. The total diagonal stiffness is enlarged to $2k_d$. If it is possible to enlarge the support stiffness to a value of $2k_{sup1}$, the total lateral stiffness is doubled as well. It that case, it is easy to see that the whole model is two times stiffer, whereby the shear stiffness K_v is two times larger. The type of elements that provide the support stiffness doesn't affect this analogy, as is concluded previously.

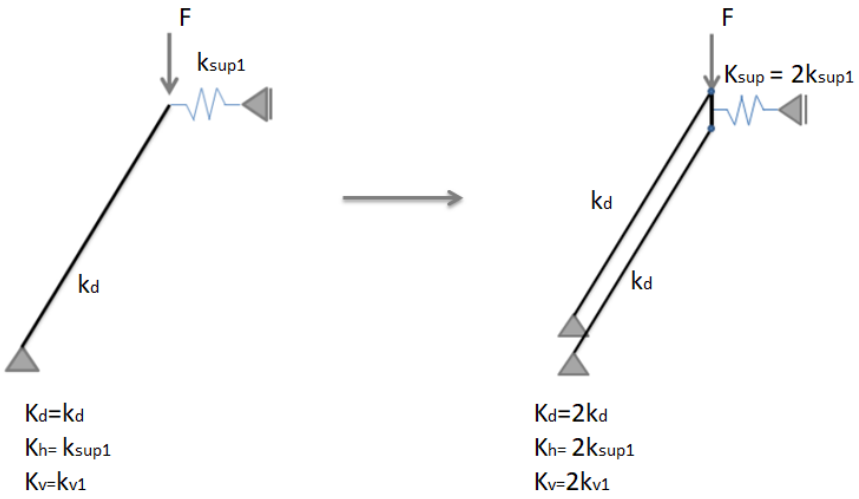

Figure 9.3 Parallel bar model

In the next chapter the relation between the joint properties, lateral stiffness and the shear stiffness is analysed in an analytical way. The outcome of this analysis will provide even more insight in the effect of a varying diagonal stiffness or angle.

9.2 Influence between the design parameters K_s, E_c, a and h

In paragraph 8.4 it was concluded that the influence of the four design parameters that determine the lateral stiffness depends on the magnitude of the other parameters. Partly because of this, it is hard to determine the relevance of each design parameter based on the parameter study results only. Therefore this paragraph contains the results of double parameter variations. These illustrate in which way the influence of a certain parameter is affected by the magnitude of another parameter.

The analysis is performed in the following way. One parameter is given another value than its standard value defined in Table 8.1. Then the other three parameters are varied one by one over the same range as indicated in Table 8.2, while two of them are given the standard value. Thereby normalised relations are obtained between the three parameter values and the shear and lateral stiffness. These can be compared with those found in chapter 8, whereby it is seen whether the influence of the parameter variation on the shear and lateral stiffness is smaller or larger due to the changed magnitude of the first parameter. This analysis is repeated four times, whereby each of the four parameters is once considered as the constant parameter with a deviated standard value. The output of the DIANA models is processed in the same manner as indicated in Figure 8.17.

9.2.1 The influence of K_s

Figure 9.4 shows the influence of the transverse spring stiffness that is affected by the magnitude of the other parameters. The blue relation is equal to the result of the parameter study that was performed with standard values of E_c, h and a. The other relations are obtained with a deviating value of E_c, a or h and the standard value assigned to the other two parameters. These relations only contain three data points, since more points are unnecessary for the goal of the analysis.

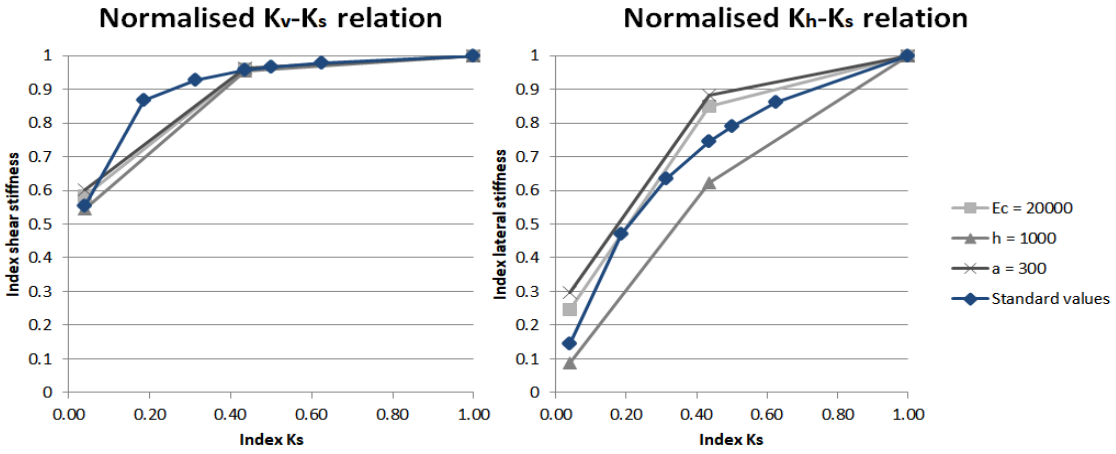

Figure 9.4 The influence of K_s affected by the magnitude of the other parameter values

The following conclusions can be drawn from these diagrams:

- Due to a reduction of the magnitude of E_c, the influence of a variation of K_s on the lateral and shear stiffness is smaller. This holds since the resulting relation corresponding to a changed E_c lies above the blue relation corresponding to the standard value.
- Based on the same observation, it can be concluded that a reduction of the column width 'a' also decreases the influence of a variation of K_s.
- A reduction of the window height leads to an increase of the influence of K_s, since the relation lies under the relation corresponding to the standard value.

In general it can be stated that the relation between K_s and K_h is more affected by the different magnitude of other parameters than that between K_s and K_v.

9.2.2 The influence of E_c

Figure 9.5 shows the different relations between the normalised value of E_c and the lateral or shear stiffness for a different value of K_s, h and a compared to their standard values.

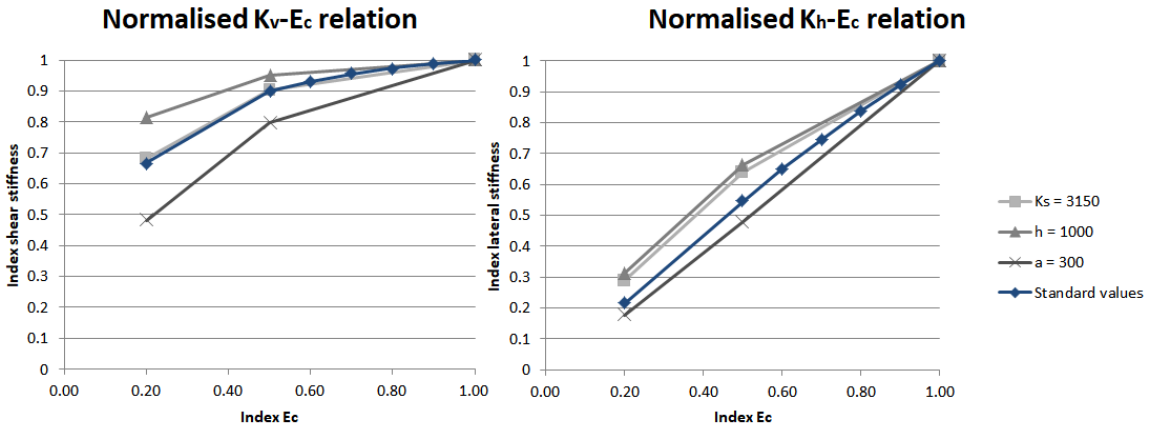

Figure 9.5 The influence of E_c affected by the magnitude of the other parameter values

The following conclusions can be drawn from these diagrams:

- A reduction of K_s reduces the influence of a variation of E_c on both the shear and lateral stiffness.
- A reduction of h reduces the influence of a variation of E_c on both the shear and lateral stiffness.
- A reduction of 'a' increases the influence of a variation of E_c on both the shear and lateral stiffness.

In this case it holds in general that the different magnitude of K_s has a larger effect on the relation between E_c and K_h, whereas the variation of h or 'a' has a larger effect on the relation between E_c and K_v.

9.2.3 The influence of 'a'

Figure 9.6 shows the different relations between the normalised value of 'a' and the lateral and shear stiffness for a different value of K_s, E_c and h compared to their standard values.

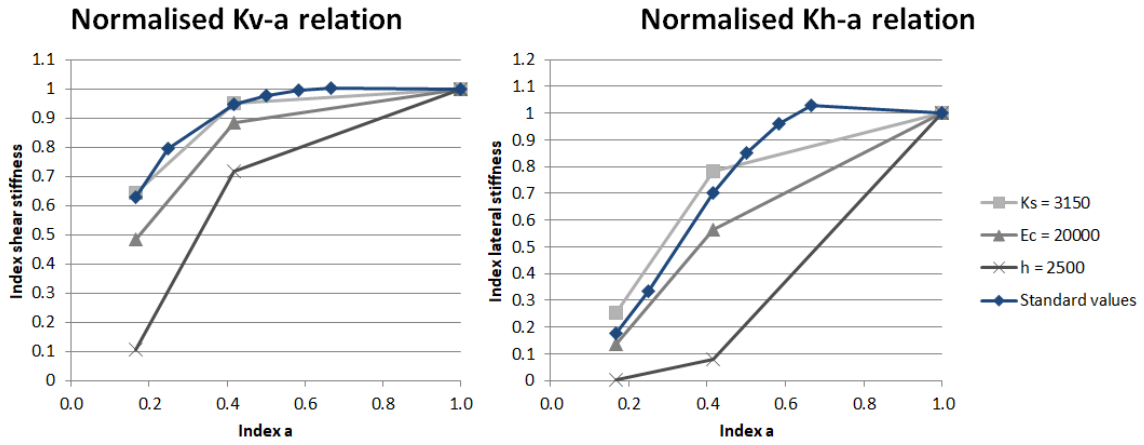

Figure 9.6 The influence of 'a' affected by the magnitude of the other parameter values

The following conclusions can be drawn from these diagrams:

- A reduction of K_s decreases the influence of a variation of 'a' on both the shear and lateral stiffness.
- A reduction of E_c increases the influence of a variation of 'a' on both the shear and lateral stiffness.
- An increase of h increases the influence of a variation of 'a' on both the shear and lateral stiffness.

A different magnitude of K_s or h has a larger effect on the relation between the parameter value and the lateral stiffness. The different magnitude of E_c has a larger consequence for the relation with the shear stiffness.

9.2.4 The influence of h

Figure 9.7 shows the different relations between the normalised value of 'h' and the lateral and shear stiffness for a different value of K_s, E_c and a compared to their standard values.

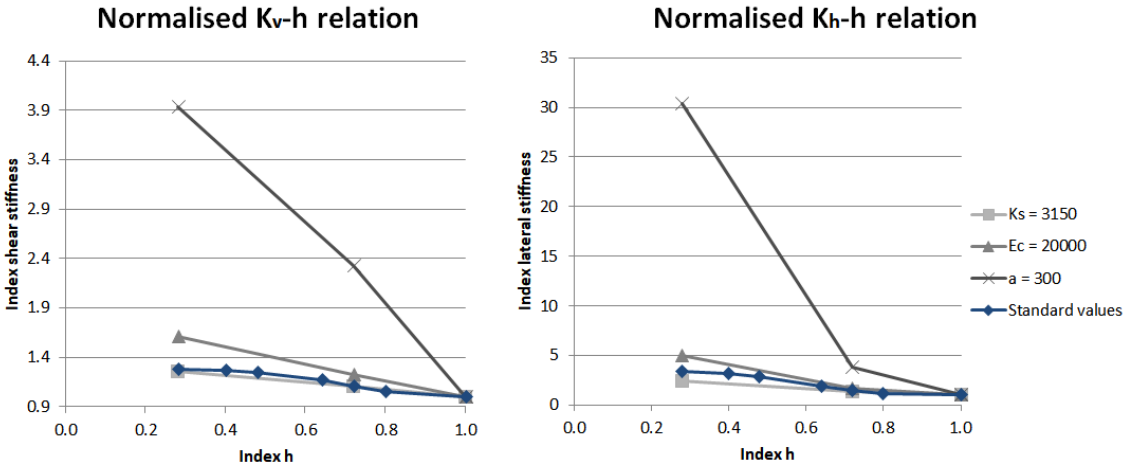

Figure 9.7 The influence of 'a' affected by the magnitude of the other parameter values

The following conclusions can be drawn from these diagrams:

- A reduction of K_s decreases the influence of a variation of 'h' on both the shear and lateral stiffness.
- A reduction of E_c increases the influence of a variation of 'h' on both the shear and lateral stiffness.
- A reduction of 'a' increases the influence of a variation of 'h' on both the shear and lateral stiffness.

The different magnitude of K_s and E_c has a small influence on the relations compared to the influence of the column width, a. Apparently, the combination of a smaller value of 'a' and a larger value of 'h' leads to a large reduction of the lateral stiffness and therefore the shear stiffness. So for a smaller value of 'a' the magnitude of the window height is far more important. Based on the results of Figure 9.6, it is also true that the magnitude of the column width is far more important if the window height is larger.

9.2.5 General behaviour

Based on the presented results it is concluded that the relation between the four parameters is well described by the spring theory. According to this theory, the equivalent stiffness of a set of springs in parallel or series is calculated by the following formulas.

$$Series: K_e = \frac{1}{\frac{1}{K_1} + \frac{1}{K_2}} \qquad Parallel: K_e = K_1 + K_2$$

Since a stiffer value of K_s leads to a larger influence of the other three parameters and vice versa, this relation is described by the formula for springs in series. In this formula the influence of K_1 is larger for larger values of K_2 and vice versa. Physically this makes sense as well, since the induced lateral forces are first transferred by the precast concrete elements, of which the stiffness is determined by E_c, a and h and then by the transverse reinforcement.

Furthermore the results show that the parameters E_c, a and h are related as parallel springs. If a stiffer value is assigned to one of them, the influence of the others is smaller.

9.2.6 Practical consequences of the result

Based on the results of chapter 8, the influence of each parameter was of the same order of magnitude, whereby the relevance of each was hard to compare. The results of this paragraph gave more insight into the influence of the four design parameters.

The influence of the transverse spring stiffness K_s on the shear stiffness K_v is hardly affected by the magnitude of the other parameters. So the influence of this parameter is more certain now and is accurately described by the relation of Figure 8.18. Moreover, the deviating value of K_s hardly affects the influence that the other parameters have on the shear stiffness, as the diagrams presented in this paragraph show. Therefore K_s is also of limited relevance for the influence of the other parameters. If a smaller value of K_s would have been applied, this effect could be slightly larger than indicated in the diagrams. Based on these two observations and the influence of K_s found in Figure 8.18, it can be concluded that K_s is only relevant for the resulting K_v when it is relatively low. A more detailed investigation of the practical range of K_s must point out whether the low values are realistic. If not, this parameter is the least relevant of them all.

The influence of K_s is the largest in the hypothetical situation where the in-plane stiffness of the precast concrete wall elements is infinitely large. In practice this means that in cases where no openings are present the transverse spring stiffness is significant for the resulting shear stiffness.

The influence of the other three design parameters is significantly affected by the magnitude of each parameter. However, the interdependency between the window height 'h' and the column width 'a' is by far the largest. So in practice this means that most attention must be paid to the design of the window openings. If a relatively high window opening is desired, it is known by now that in this case the distance of this opening to the joint is of major importance of the connection's shear stiffness. If a window is placed closed to the joint, it is best to keep its height limited, since a large opening height leads to a large reduction of the shear stiffness in this case.

The results show that a very inconvenient design combines large window openings with a small distance to the joint, whereby the stiffness of the connection is tremendously reduced. This will not be fully compensated by a realistically large Young's modulus of the precast concrete.

9.3 Overview of the results and translation to a regular shear wall

This paragraph contains a short overview of the results of the two performed analyses. It also discusses the results in the context of the behaviour of a shear wall that is part of a stability structure.

9.3.1 The relation between K_d, K_h and K_v.

The first paragraph of this chapter analysed the relation between K_h, K_d, and K_v. From this relation it is concluded that the connection's shear stiffness is generally more dependent on the magnitude of the diagonal stiffness than the magnitude of the lateral stiffness. Furthermore the influence of the diagonal and lateral stiffness are interdependent. A larger K_d increases the influence of a change in lateral stiffness. A smaller K_d reduces this influence. A larger K_h increases the influence of the diagonal stiffness on the shear stiffness and vice versa.

The parameter study was performed with a standard value for K_d of 9693 kN/mm, resulting in a certain influence of the four design parameters K_s,E_c, a and h. However, in paragraph 7.4 the diagonal stiffness was calibrated to the test results. According to the average calibrated value, the total diagonal stiffness must be 880 kN/mm for a connection with three diagonals. In the shear wall model the connection contains fifteen diagonals per floor, whereby the calibrated total diagonal stiffness should be 4400 kN/mm. This will significantly reduce the influence of the lateral stiffness and therefore the influence of the four design parameters compared to the results of chapters 8 and 9.

Shear walls used in a stability structure are generally thicker than 200 mm. However, all the presented parameter study results and the resulting calibrated values for K_d hold for a wall with a thickness of 200 mm, equal to the thickness of the test specimens. One consequence of a thicker wall is that the mortar joint will be thicker as well, resulting in a larger compression diagonal area and therefore a larger value for K_d. This will increase the influence of the lateral stiffness, whereby the influence of the four design parameters is enlarged as well. For a wall thickness of 450 mm, the value of K_d is approximately equal to that applied in the parameter study. So although the value of K_d applied in the parameter study was overestimated for t=200, it is a realistic value for shear walls of regular thickness.

It can be stated that a well-known magnitude of K_d is of major importance, since it doesn't just have a large influence on the shear stiffness, but also defines the contribution of the lateral stiffness.

The influence of the diagonal angle couldn't be analysed by the results of the applied shear wall model and will be analysed in more detail in the next chapter. However, based on the parameter study results obtained for a variation of alpha it is concluded that its influence resembles the way the diagonal stiffness influences the connection's behaviour.

9.3.2 The interdependency of the design parameters K_s, E_c, a and h.

Based on the results presented in paragraph 9.2 it can be concluded that the interdependency of the four design parameters is well described by the spring theory. The parameters 'a' and 'h' are related most strongly. Therefore the design of the openings in the wall appears to be the most relevant for the magnitude of the lateral and shear stiffness. A combination of a large window height and a small distance between the window and the joint leads to a large reduction of the connection's shear stiffness.

Again the effect of a varying thickness must be considered as well. If the thickness of the concrete elements is enlarged, the bending stiffness of the concrete elements is enlarged. This will also affect the influence of the design parameters. The thickness is a parameter related to the stiffness of the concrete elements and is therefore likely to be related to the other parameters in a way similar to E_c, a and h. Based on the results of paragraph 10.2, a greater thickness would therefore lead to a decreased influence of E_c, a and h and an increased influence of K_s.

The question is which of the two consequences of a variation of the thickness is dominant. On one hand the influence of the lateral stiffness is increased, on the other hand the influence of E_c, a and h is decreased. What is certain, is the increase of the influence of K_s as a result of a greater thickness t and corresponding K_d. Since the influence of K_s hardly varies for deviating values of E_c, a and h, it is expected that the thickness t also has a limited effect on the influence of K_s. So the increased influence of K_s is mostly a result of the larger diagonal stiffness that also increases the influence of the other design parameters. Therefore it is not expected that the influence of K_s has increased much compared to that of E_c, a and h. So also in case of a greater thickness the height and distance of the openings will be the most important design parameters for the magnitude of the shear and lateral stiffness.

10 Development of an analytical modelling approach

So far, the parameter study provided insight in the way each of the analysed parameters influences the shear stiffness of the connection. An increase of the transverse spring stiffness K_s, the concrete stiffness E_c or the column width 'a' and a reduction of the opening height 'h' results in an increase of the lateral and shear stiffness, K_h and K_v. A variation of the diagonal stiffness K_d and angle α affects the shear stiffness more than an equally large variation of the lateral stiffness, whereby an increase of K_d, α or K_h always results in an increase of the shear stiffness.

Despite the simplifications and neglected effects in this study, the amount of parameters is too much to obtain an unambiguous relation for each parameter's influence, since the influence of each parameter is dependent on the magnitude of all other parameters, as described in chapter 9. So in order to obtain complete insight in the contribution of each design parameter to the shear and lateral stiffness, a large amount of analyses must be performed.

If the whole behaviour of the connection based on the contributing design parameters can be described by analytical relations, all these analyses are unnecessary. In this chapter analytical relations are derived that describe the behaviour of the connection. The first paragraph contains the derivation of the relation between the lateral stiffness, diagonal properties and the shear stiffness and analyses the influence of K_d, α and K_h on shear stiffness K_v. The second and third paragraph zoom in on the composition of the lateral stiffness. Figure 10.1 indicates to which part of the modelling approach the content of each paragraph corresponds.

Subsequently, these derived relations are used to develop a practical modelling technique that could be applied in 3D models of complete building structures. This technique and the calculation method for K_v it comprises, are described in the fourth paragraph and may form the answer to the main question of this research. The feasibility of this modelling approach is evaluated in chapter 11

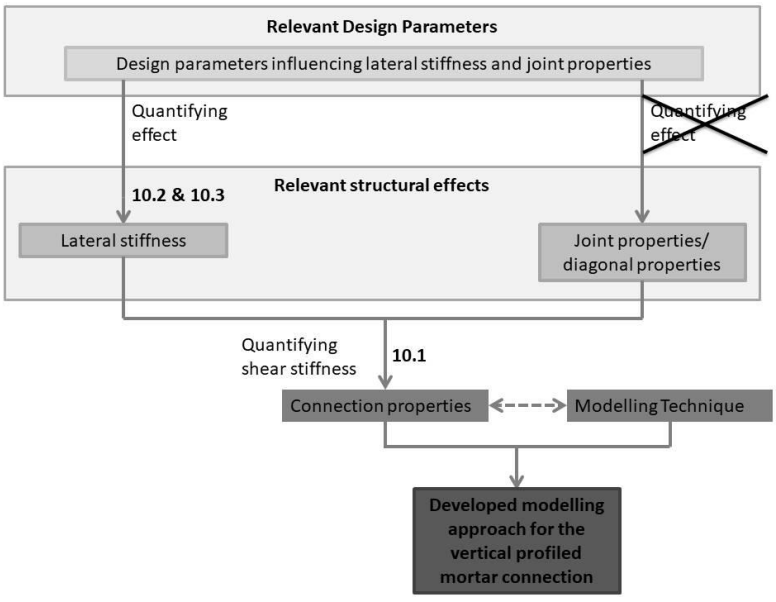

Figure 10.1 Overview of the content of chapter 10 in relation with the modelling approach

10.1 The analytical relation between K_h, K_d, α and K_v

The previous chapter already discussed the relation between the quantities K_h, K_d, α, related to the structural effects of lateral stiffness and joint properties, and the shear stiffness K_v. This relation was constructed with results. In order to develop an analytical relation between the four quantities, the model of Figure 9.3 is reviewed for a single bar. This paragraph starts with the derivation of the analytical relation and continues with an analysis of the influence of K_d, α and K_h on the shear stiffness K_v, based on the derived relation.

10.1.1 Derivation of the relations

Figure 10.2 shows this bar which has a certain diagonal stiffness K_d under angle α, indicated by the ratio between distances h_y and h_x,. The bar is supported by a hinge on one endpoint and by a hinge with finite horizontal support stiffness K_{sup} at the other endpoint. When the bar is loaded by vertical force F_v, it will deform according to the dashed line. The bar rotates around the lowest endpoint, whereby the upper endpoint translates in vertical direction by distance U_y and in horizontal direction by distance U_x.

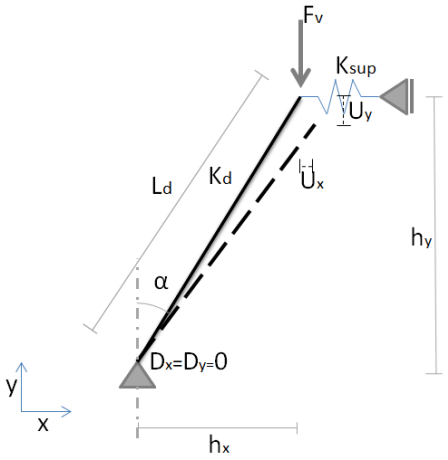

Figure 10.2 Model of a single bar

The horizontal translation is a consequence of the finite support stiffness that enables rigid rotation of the bar element. The vertical translation consists of two parts, as Figure 10.3 illustrates. Part 1 is a consequence of the axial shortening of the diagonal U_d under load F_v. If the support stiffness was infinitely large, this shortening would result in a small diagonal ration by angle theta, whereby the horizontal endpoint translation with respect to the initial orientation remains equal to zero. However, the support stiffness is finite, whereby an extra rotation of the bar by angle phi occurs. This rotation results in an endpoint displacement perpendicular to the bars initial orientation, which can be decomposed in a horizontal displacement U_x and a vertical displacement $U_{y,part2.}$ So the second part of the vertical translation is a consequence of the finite support stiffness.

The illustration of Figure 10.3 is only valid for small deformations, since it is assumed that a rigid rotation of the bar results in an endpoint translation perpendicular to the initial orientation. The described deformation behaviour corresponds to the behaviour that was observed for the test setup model, as explained in section 7.2.6.

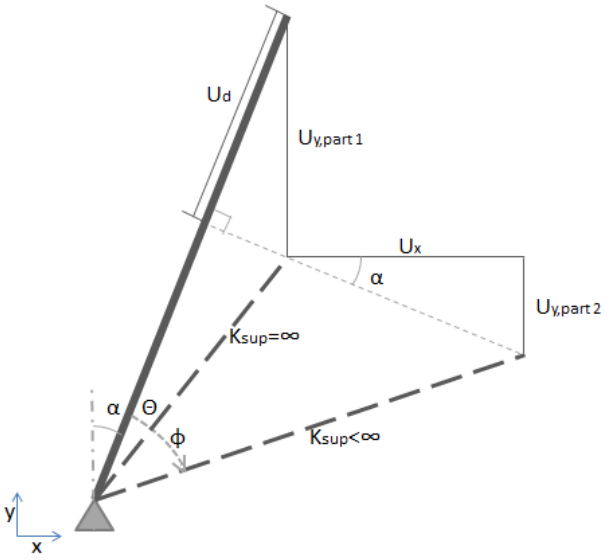

Figure 10.3 Composition of the bar deformation

The following definitions hold for the diagonal, support and shear stiffness:

$$K_d = \frac{E_d A_d}{L_d} = \frac{F_d}{U_d} \quad L_d = \sqrt{h_x^2 + h_y^2}$$

$$K_{sup} = \frac{F_h}{U_x} \quad F_h = F_d * \frac{h_x}{L_d}$$

$$K_v = \frac{F_v}{U_y} \quad F_v = F_d * \frac{h_y}{L_d}$$

These definitions are equal to those of paragraph 6.2. The equilibrium of forces is given by the diagram of Figure 6.4. The definitions for the three stiffness values already contain the contribution of the diagonal angle, since this angle determines the ratio between the vertical and horizontal force component.

It is important to note that the support stiffness in this model is by definition equal to the lateral stiffness K_h, since in this model the horizontal displacement at the lowest endpoint is zero. Thereby the horizontal displacement difference is equal to the displacement of the top endpoint, which is equal to the displacement of the support spring.

$$K_h = \frac{F_h}{U_x} = \frac{F_h}{D_{x,2} - D_{x,1}} = \frac{F_h}{D_{x,2} - 0} = \frac{F_h}{D_{sup}} = \frac{F_h}{\frac{F_h}{K_{sup}}} = K_{sup}$$

10.1.1.1 Relations in terms of stiffness

With the provided definitions, the equation that relates α, K_{sup} and K_d with the shear stiffness K_v can be derived.

According to the definition of the shear stiffness, the following holds.

$$K_v = \frac{F_v}{U_y} = \frac{F_v}{U_{ypart1} + U_{ypart2}}$$

The first part of the vertical translation is a consequence of the shortening of the diagonal. This translation is given by the diagonal shortening multiplied by a factor taking into account the angle alpha.

$$U_{y,part1} = U_d * \frac{L_d}{h_y} = \frac{F_d}{K_d} * \frac{L_d}{h_y}$$

Using the equilibrium of forces, the diagonal force can be eliminated from this equation. The definition of the diagonal length is also used to eliminate this factor from the equation.

$$U_{y,part1} = \frac{F_v}{K_d} * \frac{L_d^2}{h_y^2} = \frac{F_v\left(h_x^2 + h_y^2\right)}{K_d * h_y^2}$$

The second part of the vertical displacement is the result of the rigid rotation that can take place due to the limited support stiffness. The translation is given by the horizontal displacement multiplied by a factor taking into account the diagonal angle. The minus sign is a result of the defined positive directions, indicated by the coordinate system in Figure 10.3. The bar rotation results in a negative displacement in y-direction and a positive displacement in x-direction.

$$U_{y,part2} = -U_x * \frac{h_x}{h_y} = \frac{F_h}{K_{sup}} * \frac{h_x}{h_y}$$

Again, the equation can be simplified by using the force equilibrium.

$$U_{y,part2} = -\frac{F_v * h_x^2}{K_{sup} * h_y^2}$$

When the equations for the two parts of Uy are substituted into equation for K_v, a relation is obtained that can be used to calculate the shear stiffness when K_d, K_{sup} and α are known.

$$K_v = \frac{F_v}{\frac{F_v\left(h_x^2 + h_y^2\right)}{K_d * h_y^2} - \frac{F_v}{K_h} * \frac{h_x^2}{h_y^2}} = \frac{1}{\frac{h_x^2 + h_y^2}{K_d * h_y^2} - \frac{h_x^2}{K_{sup} * h_y^2}}$$

The equation can be generalised for cases where the support stiffness is not equal to the lateral stiffness.

$$K_v = \frac{1}{\frac{h_x^2 + h_y^2}{K_d * h_y^2} - \frac{h_x^2}{K_h * h_y^2}} \quad [10.1]$$

10.1.1.2 Relations in terms of displacement

With the provided definitions, also relations in terms of displacement can be derived. These relations can be used to define a stiffness matrix with cross-terms that link the shear and lateral displacements over the joint.

For this purpose the diagonal force is quantified first. This force is given by the axial deformation of the diagonal bar.

$$F_d = E_d A_d * \epsilon = E_d A_d * \frac{\Delta L_d}{L_d} = E_d A_d \frac{U_y * \frac{h_y}{L_d} + U_x * \frac{h_x}{L_d}}{L_d} = E_d A_d \, (U_y * \frac{h_y}{L_d^2} + U_x * \frac{h_x}{L_d^2})$$

This definition can be substituted in the relation for the lateral stiffness.

$$K_h = \frac{F_h}{U_x} = \frac{F_d * \frac{h_x}{L}}{U_x} = \frac{E_d A_d * (U_y * \frac{h_y h_x}{L_d^3} + U_x * \frac{h_x^2}{L_d^3})}{U_x}$$

This relation can be simplified

$$K_h = E_d A_d * \frac{h_y h_x}{L_d^3} * \frac{U_y}{U_x} + E_d A_d * \frac{h_x^2}{L_d^3}$$

$$F_h = K_h * U_x = E_d A_d * \frac{h_y h_x}{L_d^3} * U_y + E_d A_d * \frac{h_x^2}{L_d^3} * U_x$$

In the same way a relation for the shear stiffness is derived

$$K_v = E_d A_d * \frac{h_y h_x}{L_d^3} * \frac{U_x}{U_y} + E_d A_d * \frac{h_y^2}{L_d^3}$$

$$F_v = K_v * U_y = E_d A_d * \frac{h_y h_x}{L_d^3} * U_x + E_d A_d * \frac{h_y^2}{L_d^3} * U_y$$

Both relations can be combined to formulate a stiffness matrix

$$\begin{bmatrix} F_h \\ F_v \end{bmatrix} = \frac{E_d A_d}{L_d^3} * \begin{bmatrix} h_x^2 & h_y h_x \\ h_y h_x & h_y^2 \end{bmatrix} \begin{bmatrix} U_x \\ U_y \end{bmatrix} \quad [10.2]$$

10.1.2 The analytical diagram of structural effects

Figure 10.4 shows equation 10.1, using average stiffness values k_v, k_h and k_d, plotted with the results of the model study in one graph. From this graph it can be concluded that the derived relation corresponds exactly to the relation that was found by the data points for all the analysed models according to Figure 9.2.

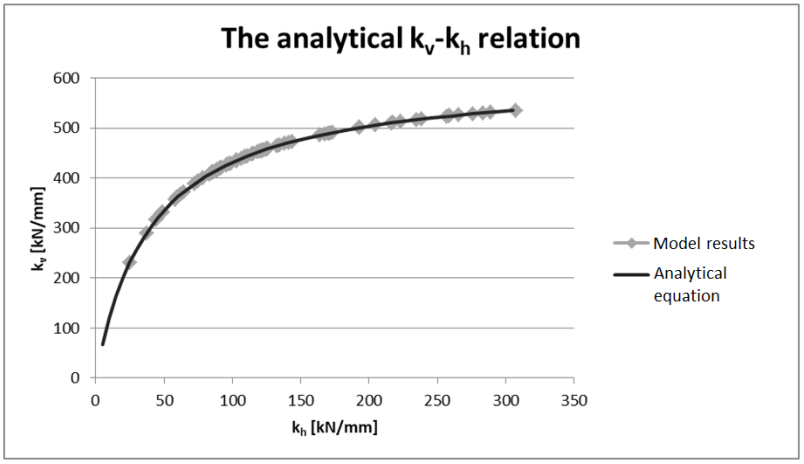

Figure 10.4 Correspondence of the analytical equation and the parameter results

The derived relation is the mathematic function that fits to the data points and therefore describes the way the shear stiffness is determined by the combination of quantities related to the structural effects. Using this function, the influence of K_h and the two diagonal properties, K_d and α, can be indicated without the need to perform many model analyses. It must be noted that the absolute value of k_h is plotted. The lateral stiffness is in fact negative since it is defined by a the horizontal component of a negative compressive force, divided by a positive displacement in x-direction. In the parameter study results the absolute value of k_h was presented as well.

10.1.2.1 The influence of K_d

Figure 10.5 shows the plot of equation 10.1 for different values of k_d. One relation shows the results obtained with the standard diagonal stiffness. This relation corresponds to the parameter study results. Three relations correspond to the calibrated values for k_d of paragraph 7.4.

The relation obtained with the average calibrated value extrapolated to a thickness of 500 mm is also included in the graph. It is important to keep in mind that the calibrated values for k_d hold for an element thickness of 200 mm. In case of a larger thickness, the cross-sectional area of the diagonal is larger and this would result in a larger value for k_d. So in case of a thickness of 500 mm instead of 200 mm, K_d is 500/200=2.5 times larger.

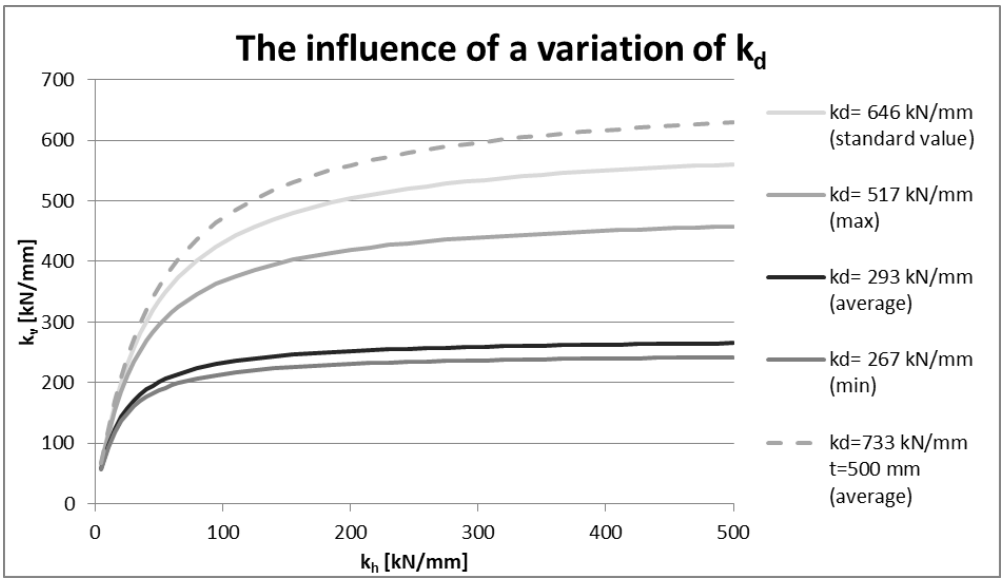

Figure 10.5 The influence of a variation of k_d on the relation between the shear- and lateral stiffness

Two important conclusions can be drawn based on this diagram:

- A smaller diagonal stiffness results in a reduced influence of the lateral stiffness.
  The relation flattens, whereby an increase of the lateral stiffness hardly increases the shear stiffness of the connection.
- A smaller diagonal stiffness results in a reduced limit value of the shear stiffness.
  The asymptote of the relation is found for a lower value of k_v. This value is never exceeded, not even with an infinitely large value of k_h.

The first conclusion is substantiated by a comparison of the relative increase of the shear stiffness for the different values of k_d. The relative increase of the shear stiffness as a

consequence of an increase of the lateral stiffness from 200 to 500 kN/mm is given in Table 10.1. The results confirm the reduced influence of the lateral stiffness for lower values of k_d.

	k_v (k_h=200) [kN/mm]	k_v (k_h=500) [kN/mm]	relative increase
k_d max	419.2	457.7	9.2%
k_d average	251.9	265.2	5.3%
k_d min	230.7	241.9	4.8%

Table 10.1 Comparison of the influence of a lateral stiffness increase with decreasing values of k_d

Secondly, the limit of the relation is dependent on the value of k_d. The analytical relation of this limit value can be derived:

$$\lim_{K_h \to \infty} K_{v,max} = \frac{1}{\frac{h_x^2 + h_y^2}{K_d * h_y^2} + \frac{h_x^2}{\infty * h_y^2}} = \frac{1}{\frac{h_x^2 + h_y^2}{K_d * h_y^2}} = \frac{K_d * h_y^2}{h_x^2 + h_y^2} = K_d * \frac{h_y^2}{L_d^2} \quad [10.3]$$

The limit value is directly proportional to the diagonal stiffness K_d. The proportionality constant is the ratio between the squared vertical distance and diagonal bar length. This ratio is dependent on the diagonal angle α. So this property will also influence the limit value.

It is clear to see that with the used standard value for k_d, the influence of the lateral stiffness and therefore the four design parameters has been overestimated compared to the calibrated situations. The same was concluded based on the analysis of paragraph 9.1. However, as also indicated in paragraph 9.3, the thickness matters as well. The analytical results confirm that for a shear wall with a larger thickness the influence of the lateral stiffness will be comparable to that found in with the parameter study results.

10.1.2.2 The influence of α

Figure 10.6 shows the plot of relation [10.1] for different values of α. The diagonal angle has been varied for the relation with k_d equal to the average calibrated value. Two conclusions on the influence of α are drawn:

- The diagonal angle affects the limit value of the shear stiffness
  The derived relation for the limit value already proved this correlation. It appears the limit value is increased for larger values of α.
- The diagonal angle affects the influence of the lateral stiffness
  The relation converges faster to its limit value if α has a larger value, whereby the influence of a change in small values of the lateral stiffness is increased, but the influence of a change in larger values is reduced.

In case α is equal to 8.0 and K_d is equal to its average value, a variation of k_h values larger than approximately 50 kN/mm hardly affects the magnitude of the shear stiffness. In next section the practically lowest value of k_h is defined as 13.2 kN/mm. So if the angle is large, the influence of the average lateral stiffness will only be significant if the lateral stiffness is almost equal to its lower limit.

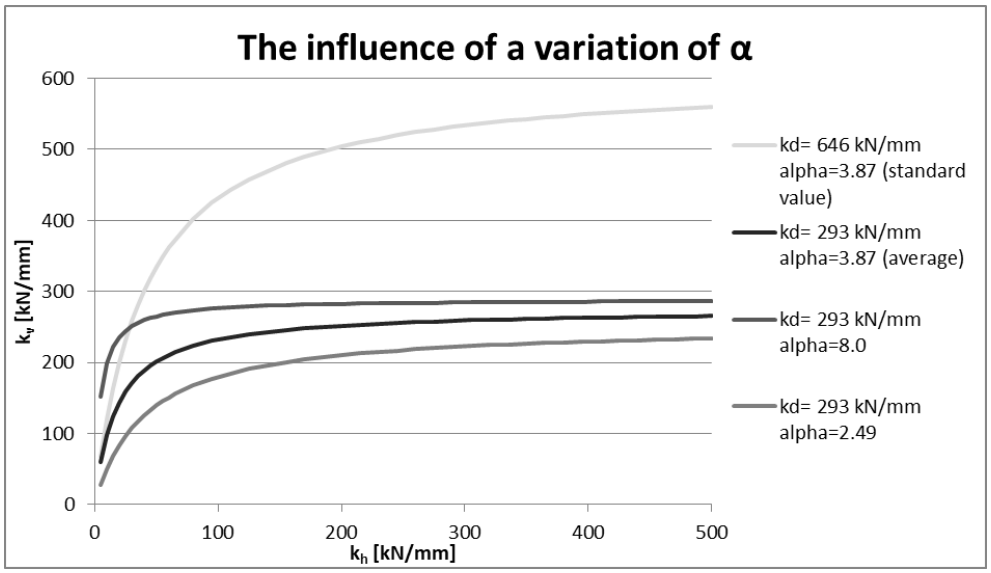

Figure 10.6 The influence of a variation of α on the relation between the shear- and lateral stiffness

10.1.3 The practically maximal influence of K_h

With the knowledge obtained in this paragraph, the maximum reduction of the shear stiffness is analysed. This occurs for the lowest practically possible value for K_h in combination with the largest practical value of K_d, which is based on the largest calibrated value of paragraph 7.4. For the diagonal angle the value of 3.87 is still applied. Since this value seems more realistic in combination with a large diagonal cross section. Table 10.2 provides an overview of the input properties that lead to the smallest practical value of K_h.

K_s	1050	kN/mm
K_d	19514	kN/mm
h	2500	mm
a	300	mm
E_c	20000	N/mm^2
t	500	mm
α	3.87	[-]

Table 10.2 Input properties corresponding to lowest K_h with largest influence on K_v

The practically lowest value for K_h is found for a combination of the smallest transverse spring stiffness, concrete Young's modulus and opening distance and largest window height. For these design parameters realistic lower limits are applied. It must be noted that this limit for the transverse spring stiffness is not yet certain and requires more research. For the concrete Young's modulus an uncracked state is considered.

Table 10.3 shows the resulting shear stiffness for two situations. The first is the maximum shear stiffness corresponding to the applied K_d and α, calculated by formula 10.3. The second is the minimum shear stiffness obtained with the parameter study model for the combination of input properties according to Table 10.2.

	K_h [kN/mm]	k_h [kN/mm]	K_v [kN/mm]	K_v [kN/mm]	Relative value
K_v max	∞	∞	18293	1220	100%
K_v min	199	13.2	2562	171	14%

Table 10.3 The maximum shear stiffness reduction caused by a limited lateral stiffness

What can be concluded from these results is in that the practically most extreme case the shear stiffness of the connection can be reduced by 86% as a result of a limited lateral stiffness. Furthermore the value of k_h of 13.2 kN/mm can be seen as practical lower limit. This value can be displayed in Figure 10.5 and Figure 10.6 to obtain the practical range of k_h over which relation 10.1 is physically meaningful.

10.2 The analytical relation for the lateral stiffness

In previous paragraph the relation that determines the shear stiffness based on known structural effects is derived. This derivation was supported by the schematisation of the bar model according to Figure 10.2. For this model the support spring stiffness is equal to the lateral stiffness, since the horizontal displacement of the supported endpoint is equal to zero. This paragraph will consider the equation for the lateral stiffness in more detail.

10.2.1 The difference between the support stiffness K_{sup} and lateral stiffness K_h

The parameter study results show the lateral stiffness depends on the magnitude of k_d and α (Figure 8.26 and Figure 8.28). The results in appendix E show this dependency is also obtained for the other parameter models. However, if the lateral stiffness is schematised by the support stiffness in the model of Figure 10.2, it cannot be influenced by the diagonal properties. So besides the support stiffness, another factor must also be involved in the definition of the lateral stiffness. Thereby the lateral stiffness that is processed from the parameter study results is generally not equal to the support stiffness.

In the applied schematisation of Figure 10.2, there is only one way to obtain a value for the lateral stiffness different from the support stiffness. This is to apply a lateral force to the horizontal spring support, as illustrated in Figure 10.7. With the definition of the lateral stiffness as defined in paragraph 6.2, the value of the lateral stiffness for the left model is equal to the support stiffness. This has been addressed in previous paragraph. For the lateral stiffness resulting in the right model, the following holds:

$$K_h = \frac{F_h}{U_x} = \frac{F_h}{D_{x,2} - D_{x,1}} = \frac{F_h}{D_{x,2} - 0} = \frac{F_h}{D_{sup}} = \frac{F_h}{\frac{F_h - F_{h,lateral}}{K_{sup}}} = \frac{F_h}{F_h - F_{h,lateral}} * K_{sup}$$

In the figure below, a lateral compressive force is added, which will increase the lateral stiffness. Thereby the translations $D_{x2,2}$ and $D_{y2,2}$ are smaller than $D_{x1,2}$ and $D_{y1,2}$. A lateral tensile force will reduce the obtained lateral stiffness.

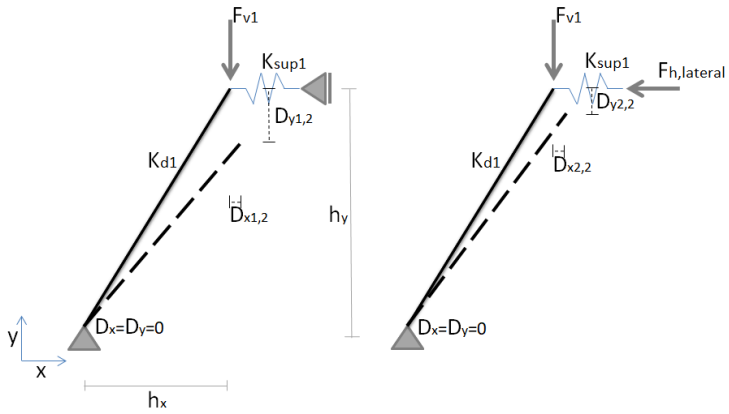

Figure 10.7 The effect of a lateral compressive force

Physically the presence of a lateral compressive force is explained by the compression diagonals that develop in a shear wall. These compression diagonals were visualised in Figure 8.10. Due to this wall behaviour, the force loading the bar elements in the joint act under an angle instead of perfectly vertical as drawn in previous figures.

Apparently, a variation of the diagonal bar properties K_d and α leads to a change of this load angle relative to the orientation of the diagonal bar, whereby the lateral stiffness changes as well. Since Figure 8.27 and Figure 8.30 show that the force distribution over the joint changes for a variation of K_d or α, it is presumable the angle of the force relative to the bar changes as well. According to Figure 8.27, an increase of K_d leads to a concentration of the shear force around the centre line of the floor. This will result in steeper compression diagonals, whereby the lateral compressive forces reduce, resulting in a smaller value for K_h. This explains the found relation of Figure 8.26 between the normalised K_d and K_h.

The variation of E_c, a and h also influence the force distribution over the height of the floor, as shown in the results of paragraph 8.3. So a variation of these parameter will also affect the amount of lateral compression.

So according to this evaluation, the model of Figure 10.2 must be expanded to include any lateral compressive force, in order to derive the equation that determines the lateral stiffness in any case.

10.2.2 Derivation of the equation for the lateral stiffness K_h

Figure 10.8 shows the expanded schematisation of the bar model. This version differs from the previous one because it includes loading forces under an angle and a finite horizontal support stiffness on the lowest endpoint as well. The load is applied under an angle β with the vertical y-axis. The load is transferred to the lower support under a different angle γ. The support stiffness at both endpoints has a different magnitude as well. In this way an equation will be derived that describes the most general case, where each load angle and support stiffness is different.

For this derivation the sign convention is important. A positive displacement is a displacement in the same direction as the defined axes. So D_{x2} is positive, D_{x1} is negative. The deformed shape drawn in the figure illustrates a dilatation of the joint, which is always positive and defined as D_{x2}-D_{x1}. A force is positive when it induces tension in the diagonal bar. All forces drawn in Figure 10.8 are therefore negative.

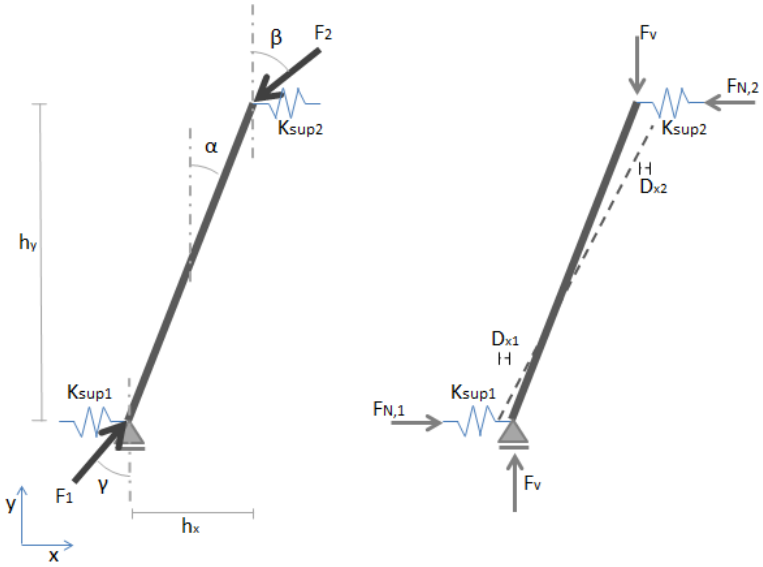

Figure 10.8 The expanded schematisation

First of all, the equations that determine the horizontal endpoint displacements D_{x1} and D_{x2} are derived. The forces F_1 and F_2 can be decomposed in order to find F_v, the vertical component of the diagonal force. This force is related to the horizontal diagonal force component by angle α.

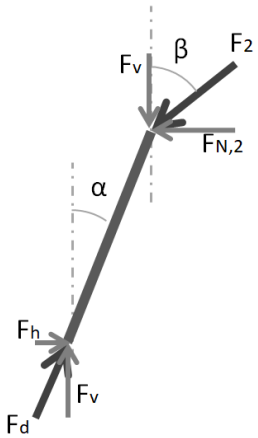

Figure 10.9 Equilibrium of forces

$$F_v = F_2 * cos\beta = F_1 * cos\gamma$$

$$F_h = F_v * tan\alpha \qquad tan\alpha = \frac{h_x}{h_y}$$

The horizontal displacements are a result of the net horizontal force and the support stiffness.

$$D_{x1} = \frac{F_h - F_{N1}}{K_{sup1}} = \frac{F_v * tan\alpha - F_1 * sin\gamma}{K_{sup1}} = \frac{F_1 * cos\gamma * tan\alpha - F_1 * sin\gamma}{K_{sup1}}$$

$$D_{x2} = \frac{F_{N2} - F_h}{K_{sup2}} = \frac{F_2 * sin\beta - F_v * tan\alpha}{K_{sup2}} = \frac{F_2 * sin\beta - F_2 * cos\beta * tan\alpha}{K_{sup2}}$$

Subsequently, these two relations are substituted into the definition of the lateral stiffness.

$$K_h = \frac{F_h}{U_x} = \frac{F_h}{D_{x2} - D_{x1}} = \frac{F_v * \frac{h_x}{h_y}}{\frac{F_2 * sin\beta - F_2 * cos\beta * \frac{h_x}{h_y}}{K_{sup2}} + \frac{F_1 * \sin\gamma - F_1 * cos\gamma * \frac{h_x}{h_y}}{K_{sup1}}}$$

This relation is simplified by dividing the numerator and denominator by the vertical component of the diagonal force F_v and the factor h_x/h_y.

$$F_v = F_2 * cos\beta = F_1 * cos\gamma$$

$$K_h = \frac{1}{\frac{\frac{h_y}{h_x} * tan\beta - 1}{K_{sup2}} + \frac{\frac{h_y}{h_x} * tan\gamma - 1}{K_{sup1}}}$$

This is further simplified by multiplying the whole equation by the factor $K_{sup1}K_{sup2}/K_{sup1}K_{sup2}$.

$$K_h = \frac{K_{sup1}K_{sup2}}{K_{sup1}\left(\frac{h_y}{h_x} * tan\beta - 1\right) + K_{sup2}\left(\frac{h_y}{h_x} * tan\gamma - 1\right)} \quad [10.4]$$

What is obtained is an equation that relates the support stiffness values and the loading angles with the lateral stiffness of the joint. Relation 10.4 is valid for the most general case, with two different horizontal supports and two different load angles. Appendix F contains simplified versions of this general formula for specific cases.

According to this equation the lateral stiffness is the resistance to the dilatation of the joint. This resistance is partly obtained by the support stiffness provided by the surroundings of the joint and partly by the lateral compressive forces along the joint caused by a difference between the load angles β and γ and the diagonal angle α.

The combination of these two factors results in a typical distribution of the lateral stiffness over the height of a floor. The support stiffness is smallest halfway the floor height, due to the present window opening and the largest distance to the tying reinforcement, but the lateral compressive force is the largest around half of the floor height since the compression diagonals that develop in the shear wall cross the joint at this location. Appendix F contains some plots of the lateral stiffness distributed over the floor height. Since the shear stiffness is related by equation 10.1 and the diagonal stiffness is equal for all diagonals, the shear stiffness is distributed over the floor height in a similar way as the lateral stiffness.

The input of the found equation consists of values for the support stiffness and the load angles. The next paragraph discusses the determination of the support stiffness. A method to determine the load angles that occur has not yet been developed. It is complicated to determine the angle of the compression diagonals, since it depends among others on the width and height of the openings in the wall, their location with respect to the joint, the amount of openings per concrete wall element and the distance between them, the floor height and the location of the considered floor in the shear wall. Furthermore the boundary conditions of the model also determine the stress distribution over the model. So the effect would be different for models 1 and 2 as well.

10.3 The approximated support stiffness

In previous paragraph the analytical relation for the lateral stiffness was derived. This relation contains the variable K_{sup}: the support stiffness. This stiffness is provided by the structural elements surrounding the mortar joint and is therefore governed by the design parameters K_s, E_c, a and h. Furthermore the thickness of the concrete elements will also be involved.

10.3.1 Composition of the support stiffness

Figure 10.10 illustrates the composition of the support stiffness. First of all the transverse reinforcement provides the spring stiffness K_{s1} and K_{s2}. These springs resist rigid translation of the wall elements on both sides of the joint. The rigid translation leads to a dilatation of the joint that is constant over its full length. Secondly, the bending stiffness of the precast concrete elements provides resistance to local extra dilatation of the joint. In Figure 10.10 the present windows induce bending deformations which are the largest halfway the height of the joint. Because of the finite bending stiffness, the support stiffness is not uniformly distributed over the height of the joint. In this case diagonal bars halfway the joint will have a smaller support stiffness than bars at the outer edges.

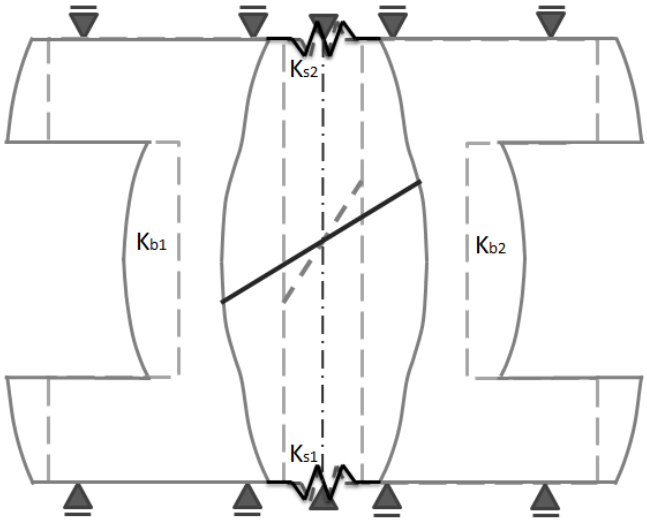

Figure 10.10 Composition of the support stiffness

Using the graphical representation of Figure 10.10, the support stiffness at the lower and upper endpoint of the diagonal can be schematised as a combination of springs. This is illustrated in Figure 10.11. The two bending springs are in series with a set of parallel transverse springs.

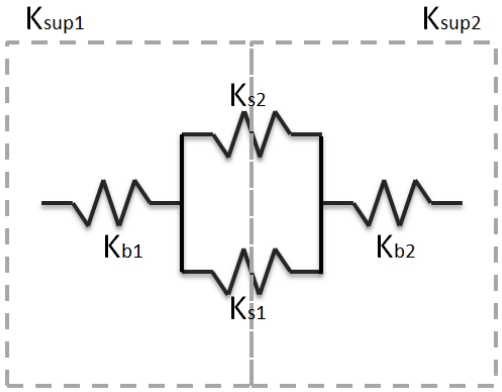

Figure 10.11 Schematisation of K_{sup} as combination of springs

For the complete system the following support stiffness can be derived.

$$K_{sup,total} = \frac{1}{\frac{1}{K_{s1}+K_{s2}} + \frac{1}{K_{b1}} + \frac{1}{K_{b2}}}$$

However, the input of equation 10.4 requires the separate values for support stiffness 1 and 2. In Figure 10.11 it is indicated what part of the spring combination determines support stiffness 1 and 2. For this division, the transverse springs are split in two parts. Since the centre of these springs is assumed to stay in the same position, half of the springs elongation is part of K_{sup1} and the other half is part of K_{sup2}. The following relations are found for the separate values of the support stiffness.

$$K_{sup1} = \frac{1}{\frac{1}{2K_{s1}+2K_{s2}} + \frac{1}{K_{b1}}}$$

$$K_{sup2} = \frac{1}{\frac{1}{2K_{s1}+2K_{s2}} + \frac{1}{K_{b2}}}$$

The value for K_s is considered as design parameter and its influence was studied in the parameter study. In this thesis its value is simply the axial stiffness of the applied transverse reinforcement. The bending stiffness is determined by the other three design parameters: E_c, a and h. Also the thickness of the concrete elements will partly determine this stiffness value.

10.3.2 Determination of the bending stiffness

In order to define the bending stiffness, the concrete elements are schematised as Timoshenko beams between to clamped supports. The Timoshenko beam theory takes into account shear deformations, as explained in chapter 3. These deformations cannot be neglected since the slenderness of the wall elements is small. Figure 10.12 illustrates the schematisation. The bending stiffness is determined by the deflection that occurs due to an applied distributed load q.

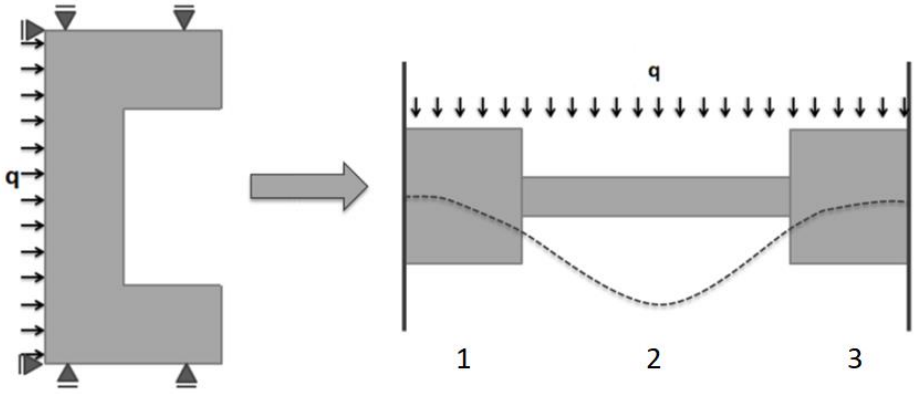

Figure 10.12 The Timoshenko beam approximation

The model contains all the defined parameters. The E-modulus of the concrete E_c is part of the differential equation. The column width 'a' is in included in the area A_2 and second moment of area I_2 for part 2 of the beam. The element thickness 't' is part of the A and I for all parts of the beam. The opening height 'h' determines the location of the two discontinuities in the beam and therefore the boundaries of the beam parts.

The differential equation for the Timoshenko beam has been solved with Maple. Appendix G contains the Maple sheet with the solution. This solution is only valid for cases with the window opening placed centrically, since the solution makes use of the symmetry of the beam. Furthermore the solution that is shown in the appendix is only valid when the discontinuities are located at 25 and 75 percent of the beam's span. But this condition can be changed in the Maple sheet by adjusting the location where the so called "matching conditions" are applied.

10.4 The developed modelling approach

With all the relations derived in this chapter, an analytical approach is developed to model the vertical profiled mortar connections in a shear wall. This paragraph describes the developed approach. Appendix H provides a more detailed description of the calculation method.

10.4.1 Overview of the analytical relations

The relations that were derived in previous paragraphs form a successive methodology to calculate the shear stiffness of the connection based on the parameters investigated in this research. With the Timoshenko approximation the support stiffness is determined and using this stiffness and the load angles the lateral stiffness can be calculated. Combining this lateral stiffness with the diagonal stiffness and angle results in a calculated shear stiffness. This successive method is illustrated in the scheme of Figure 10.13, which is used to calculate the shear stiffness K_v.

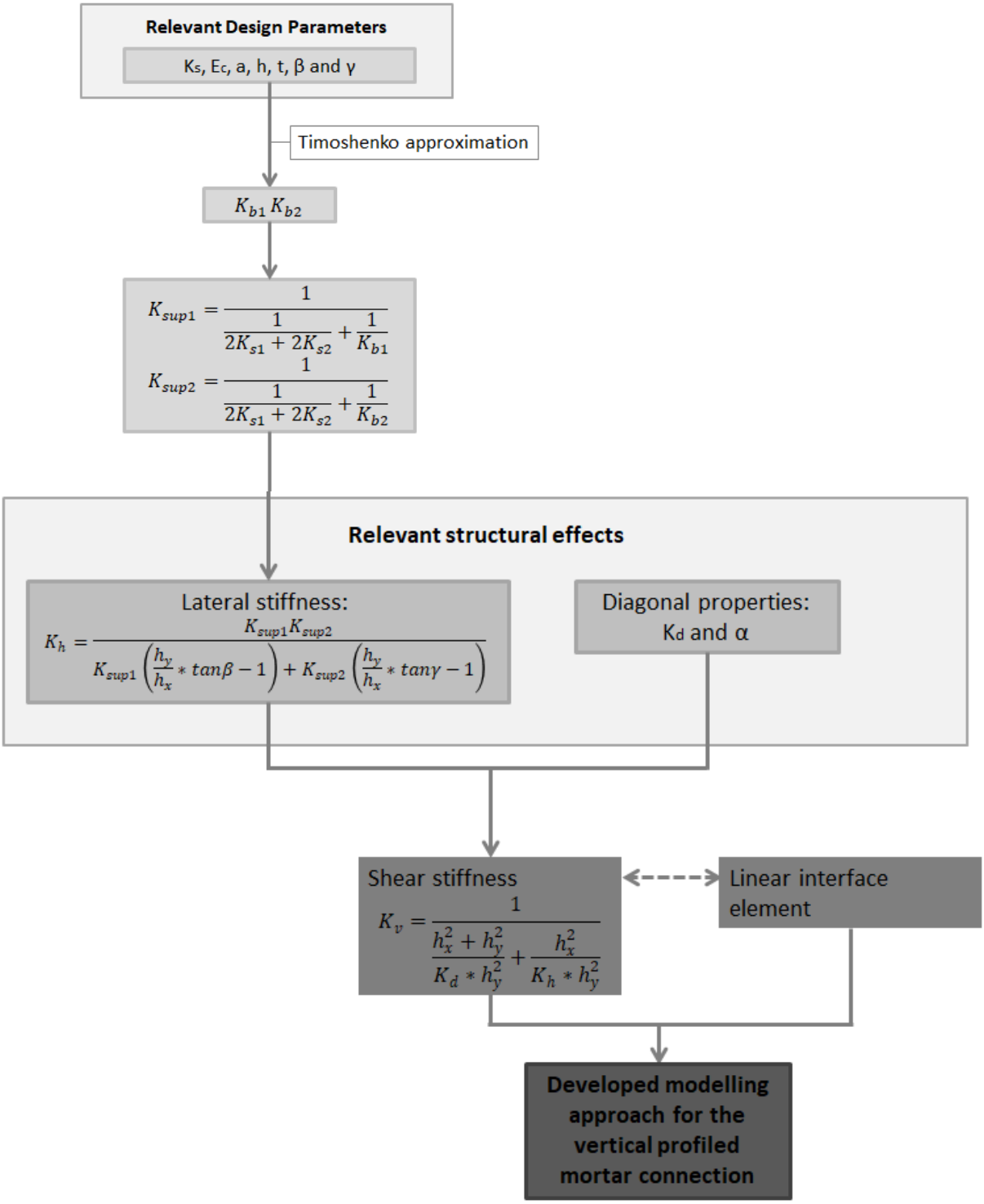

Figure 10.13 Modelling scheme including analytical relations

10.4.2 Modelling elements

The modelling approach replaces all the diagonal bars and transverse springs by one interface element per floor, to which the calculated shear stiffness is assigned. This way of modelling is only feasible for cases where the global deformation of a shear wall is of interest. The interface element doesn't contain any information about the interaction between the vertical shear force and the lateral force it induces. Therefore the model won't show any dilatation of the joint,

whereby the model isn't useful to analyse local lateral deformations and stresses that occur due to the lateral forces.

What can be done to deal with this inconvenience, is to analyse the resulting shear stress distribution over the interface. This stress distribution can be integrated over the area and subsequently multiplied by the angle α of the compression diagonals that develop in the mortar. In this way the horizontal forces that are loading the surrounding concrete elements are determined in an indirect way. Afterwards, it can be evaluated if the resistance of the concrete elements to this lateral load is sufficient. An example of this indirect approach will be provided in paragraph 11.6.

Since the relation between the lateral and shear stiffness cannot be inserted into the properties of the interface elements, it is required to include this effect in the way depicted in Figure 10.13. It would be convenient if a stiffness matrix with cross-terms, as in formula 10.2, could be assigned to the interface elements. By doing so, the interface naturally takes into account the influence of the lateral stiffness on the shear stiffness and the dilatation of the joint would occur as well. However, unfortunately this cannot be done for a linear analysis in DIANA or AxisVM, the two FE packages available for this research.

10.4.3 Determination of the lateral stiffness

As indicated in Figure 10.13, the lateral stiffness is calculated in three steps.

- Determination of the bending stiffness
- Determination of the support stiffness
- Determination of the lateral stiffness including the lateral prestress effect

As explained in paragraph 10.2 and illustrated in appendix F the lateral stiffness is not uniformly distributed over the height of the floor. Therefore the shear stiffness isn't uniform either. One way to model the shear stiffness over the complete floor height is to calculate the lateral and shear stiffness for each diagonal bar individually and to use an interface with a varying shear stiffness over the height of the floor according to the analysis of each single bar.

However, so far the lateral stiffness was always defined as the total horizontal force divided by the average horizontal dilatation over the height, resulting in an assumed uniform distribution over the floor height. Subsequently, the shear stiffness is also uniform and defined by the total shear force divided by the average shear slip. Holding on to a uniform average lateral stiffness is consistent with previous results but also more practical to model according to the developed scheme. There are three reasons for this:

Firstly, the average uniform bending stiffness can be determined by the following formula:

$$K_b = \frac{q * l}{U_{average}}$$

Where q is the fictive distributed load applied on the Timoshenko beam, l the length of the beam and $U_{average}$ the average deflection of the beam. The stiffness is independent on the value of q, since a two times larger q will also lead to a two times larger $U_{average}$. If the bending stiffness should be determined for each diagonal bar specifically, the model must be altered. In that case the beam is not subjected to a distributed load but could be loaded by a concentrated force at the location of a specific diagonal. This results in a deflection at the location of the load. The specific

bending stiffness at this location is then the force divided by the obtained deflection. This analysis must be done for each diagonal location separately. This is a more laborious method that is harder to analyse. It is only useful to apply if it appears in chapter 11 that the influence of the lateral stiffness on the behaviour of the shear wall is significant.

Secondly, the load angle and therefore the effect of a lateral compressive force varies over the height of the connection. As already explained in paragraph 10.2, the magnitude of the load angle is not easily determined. It depends on many factors and is therefore very uncertain. So defining a varying load angle over the floor height would be even more uncertain. For this reason the load angle is kept constant over the floor height and is set equal to zero. Gaining more insight in the effect of the load angle and its distribution over the floor height is only relevant if the lateral stiffness appears to have a significant contribution to the behaviour of a shear wall. If a load angle varying over the floor height would be included in the calculation method, it is best to combine this with a varying bending stiffness as well.

Finally, only a single constant value for the shear stiffness can be assigned to a single interface. So if it was desired to model an interface with a non-uniform shear stiffness, the edge between two wall elements must be manually subdivided into multiple parts with each a different shear stiffness. This is not a very practical way of modelling and it may lead to an irregular mesh around the interfaces.

The consequences of the chosen approach to consider global quantities only, are that all the equations are applied to relate the global stiffness quantities K_h, K_d and K_v instead of the specific quantities $k_{h,i}$ $k_{d,i}$ and $k_{v,i}$ and results can be visualised in the global quantities or the average values k_h,k_d and k_v. Moreover the uniform stiffness distribution over the interface will lead to a shear stress distribution that differs from the one that would occur in the mortar joint. In reality the shear stiffness of the joint is greater halfway the floor height, as seen in appendix F. So in reality the transferred shear force at this location is even greater than that resulting from the model with an interface element.

10.4.4 Error of the calculation method for K_v

As explained in previous section, the applied methodology to calculate the shear stiffness of the connection is rough and global. This unavoidably leads to an error between the shear stiffness calculated and the one resulting from the bar model.

Appendix H contains an evaluation of the error of the calculation method, which searches for the largest error within the possible and practical limits of the input properties. The largest error is found for the properties of Table 10.4, where for K_s, E_c and a the practical lower limit and for K_d and t the practical upper limit was used. In this case the transverse spring stiffness is based on at least 1000 mm^2 of reinforcement.

As can be seen, the input properties are the same as in Table 10.2, except for the opening height ‘h’. This property is set to 1600 mm since the differential equation is solved for this opening height only. In appendix H it is observed that the error of the calculation increases for smaller values of K_h. So if the opening height would be increased to its maximum practical value of Table 10.2, the error of the calculation method is also larger than indicated in Table 10.5. This is taken into account for the evaluation of chapter 11.

K_s	1050	kN/mm
K_d	19514	kN/mm
h	1600	mm
a	300	mm
E_c	20000	N/mm^2
t	500	mm
α	3.87	[-]

Table 10.4 Input properties for leading to the largest found error

Using the properties of Table 10.4, the lateral and shear stiffness are calculated according to the developed methodology of Figure 10.13, where the value zero is assigned to load angles β and γ. The outcome is compared to the stiffness resulting from the middle floor of a shear wall with equal dimensions as model 1 of the parameter study. This shear wall either has one or two windows per precast concrete element, as indicated in Figure 10.14. The resulting values for the shear and lateral stiffness are provided in Table 10.5.

	K_v [kN/mm]		K_h [kN/mm]	
Calculation method	8951	100%	1170	100%
Shear wall 1	6547	73%	680	58%
Shear wall 2	6596	74%	689	59%

Table 10.5 Largest found error of the calculation method

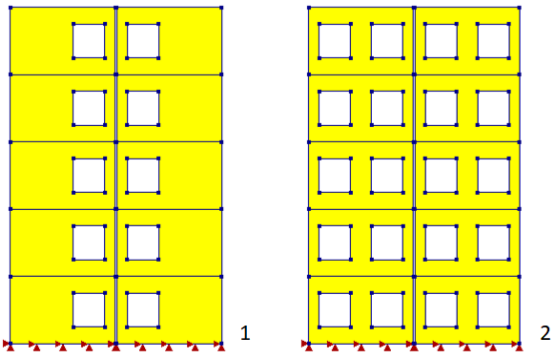

Figure 10.14 Analysed shear walls

So in this extreme case, the lateral stiffness resulting from the FE model is just 58 percent of the calculated value, whereby the shear stiffness is overestimated by almost 30 percent. It is clear that the difference of the calculated lateral stiffness and that resulting from the models is large, which indicates that the calculation method that should approximate this property is inaccurate. Since the calculated value provides an overestimation even without considering the beneficial effect of lateral compressive forces (by setting β and γ equal to zero), the determination of K_{sup} seems too positive. A less global and rough method could reduce the error. However, the determination of the lateral stiffness is very complex, since so many factors are involved. So a relatively large error is probably present for any calculation method that tries to approximate K_h.

The deviation of the shear stiffness is considerably smaller, since it is not only determined by the uncertain K_h but also partly by the certain K_d. A larger diagonal stiffness increases the influence of the lateral stiffness and therefore the error of the calculated shear stiffness. This is the reason why the largest error was found for the large calibrated value of K_d in combination with a large thickness.

The evaluation provided in appendix H shows that the error of the calculation method is smaller in more ordinary cases, where the lateral stiffness is larger due to less extreme values of K_s, E_c and a.

10.4.5 The maximum influence of the lateral stiffness on the shear stiffness

What is shown in Table 10.6, is the maximum value of the shear stiffness corresponding to the applied values for K_d and α. Since analytical formulas have been derived, this maximum value can now be calculated using formula 10.3, which assumes an infinitely large lateral stiffness. The maximum shear stiffness is 204.4 percent of the stiffness calculated by the developed method.

	K_v [kN/mm]		K_h [kN/mm]	
Maximum K_v	18293	204.4%	∞	-

Table 10.6 The maximum value of K_v

What is subsequently seen from the results is the maximum influence of the lateral stiffness on the shear stiffness for the case h=1600 mm, since to all other variables the lower limit value is assigned. So for this situation the finitely large lateral stiffness leads to a maximum shear stiffness reduction of:

$$Shear\ stiffness\ reduction\ = \frac{6547\frac{kN}{mm} - 18293\frac{kN}{mm}}{18293\frac{kN}{mm}} * 100\% = -64.2\ \%$$

According to the calculation method this maximum reduction is just:

$$Shear\ stiffness\ reduction\ calculated\ = \frac{8951\frac{kN}{mm} - 18293\frac{kN}{mm}}{18293\frac{kN}{mm}} * 100\% = -51.1\ \%$$

If the first of these results is compared to that of section 10.1.3, it can be concluded that increasing the opening height from 1600 mm to 2500 mm leads to an extra shear stiffness reduction of 86-64=22%.

Whether the error of the calculation is acceptable and the maximal stiffness reduction of the interface is significant or not, depends on their effect on the shear wall's behaviour. In the next chapter the effect on the top deflection of the shear wall is evaluated. This evaluation will indicate the need to refine the methodology.

11 Evaluation of the modelling approach in a practical situation.

Previous chapter discussed the analytical relations that describe the behaviour of the vertical profiled mortar connection as schematised by the bar model of chapter 6. With these analytical relations a modelling approach is developed that models the connections by a vertical linear interface element with a given shear stiffness K_v. This modelling approach is described in paragraph 10.4.

The next step is to evaluate the applicability of this modelling approach. This evaluation will indicate if the developed approach is useful to model the vertical profiled mortar connections in practical situations and will therefore be an answer to the main research question. For this purpose, several wall types with different layouts are developed. Each wall type is analysed as a monolithic wall, a precast wall with diagonals in the vertical joint and a precast wall with interface elements representing the joint. The comparison of the resulting horizontal deflections at the top of the wall, indicates whether the interface elements provide an acceptable approximation of the vertical profiled mortar connection's stiffness.

The first paragraph of this chapter addresses the input properties applied in the wall models and the shear stiffness of the interface elements in particular. The second contains the results of the wall analysis, which are evaluated in the third paragraph of this chapter. The fourth paragraph continues with an evaluation of the limit situation where the design parameters are such that for K_h the smallest practical value is obtained. Analysing this situation gives insight into the largest top deflection of the shear wall that can occur as a result of the influence of the lateral stiffness. Then in the fifth paragraph, the feasibility of the modelling approach with the calculation method for K_v is evaluated and a final proposal for the practical modelling approach is made. The sixth paragraph ends this chapter with a short example of a design calculation that uses the modelling approach as proposed in paragraph 11.5.

11.1 General input properties

In this paragraph an overview of the input of the wall models that are analysed in paragraph 11.2 is provided. The general input values are addressed in the first section of this paragraph. The second section discusses the applied values for K_v as input for the interface elements.

11.1.1 General input of the compact shear wall model

The dimensions of the compact shear wall are equal to those of the model that has been applied in the parameter study of chapter 8. So the wall contains five floors with a height of 3200 mm and two five metre wide precast concrete elements per floor with a 50 mm wide joint in-between. The corresponding slenderness ratio of the wall is 1.59. The wall is loaded by a distributed horizontal force on each floor, having a value of 40 N/mm. This load is equal to that of Figure 8.1 and applied in the same way.

Figure 11.1 shows the analysed compact walls. Wall 1 is closed, wall 2 contains one opening per precast element, wall 3 contains two openings per element. The three evaluated slender wall

models are illustrated in Figure 11.2. The slenderness ratio of the walls is 4.78. The geometry of the joint, the precast elements and the window openings is the same as for the compact walls.

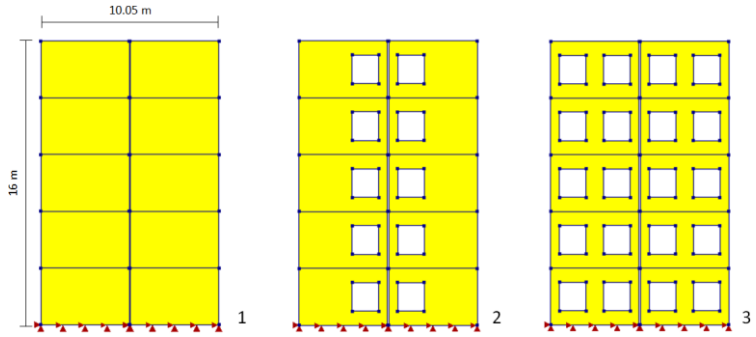

Figure 11.1 Evaluated compact walls

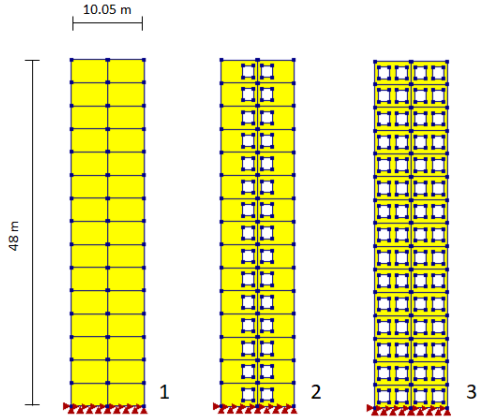

Figure 11.2 Evaluated slender walls

All wall types are analysed as a monolithic wall, a precast wall with diagonals in the vertical joint and a precast wall with interface elements representing the joint. The input properties applied in the evaluation of the wall models, are summarized in Table 11.1. Most values are equal to the standard values of the parameter study, but to some of them another value is assigned.

First of all the value for the diagonal stiffness is adapted in order to correspond with the largest calibrated value of paragraph 7.4. Using the calibrated diagonal stiffness provides results that are related to Van Keulen's tests. This leads to three important advantages.

- A comparison between the top deflection of the wall with joint and the monolithic model indicates the real stiffness reduction of the precast concrete wall and therefore the performance of the precast concrete shear wall with stacked element configuration and vertical profiled mortar connections. Thereby the performance can be related to the results of other design solutions for precast concrete shear walls that were discussed in paragraph 3.3.
- The difference between the top deflections resulting from the model with diagonals and the model with interface elements must be related to the top deflection increase compared to the monolithic wall. For this purpose a realistic deflection increase is necessary, whereby the use of the calibrated value of K_d is required.

- The influence of the lateral stiffness on the shear stiffness of the connection is not overestimated, since a realistic value of K_d is applied. It was shown in paragraph 10.1 that a larger diagonal stiffness increases the influence of the lateral stiffness.

The largest calibrated value is applied because in appendix H it was shown that a larger value of K_d leads to a larger error of K_h and K_v and the largest reduction of K_v with respect to its maximum for infinite K_h.

The second parameter, deviating from its standard value, is the transverse spring stiffness, which is given a lower value compared to the parameter study. As explained in section 8.2.1, this transverse stiffness comprises more aspects than just the axial stiffness of the reinforcement. For this reason the standard value of K_s is probably overestimated. In order to obtain more realistic results, its value has been reduced in this evaluation. However, since the exact composition of K_s was not investigated for this thesis, the value applied here is still uncertain.

Finally, the height of the openings is adjusted to a value of 1600 mm. This is exactly half of the floor height. The length of the domains over which the Timoshenko beam equation must be solved are therefore equal to 0.25, 0.5 and 0.25 times the floor height, from bottom to top (Figure 10.12). For these domain lengths, the solution of the equation is found more easily. The solution of the differential equation is found in appendix G.

About the stiffness of the interfaces, two important notifications must be made. First, the horizontal connections between the precast wall elements are not taken into account and are thus infinitely stiff. In this way the influence of the vertical connection is evaluated exclusively. Second, the magnitude of the normal stiffness of the vertical joints has no effect on the results of the analysis, because of the specific loading condition. Therefore the next section only discusses the shear stiffness of the interface elements. The applied normal stiffness is mentioned in appendix K.

Concrete Elements	
Plane stress elements CQ16M	
Thickness t	500 mm
E-modulus E_c	35000 N/mm^2
Poisson's ratio ν	0.2
Window height	1600 mm
Column width	500 mm
Diagonal bars	
Regular truss elements L2TRU	
Length	199.86 mm
Slope [h_y/h_x]	3.87
Cross-sectional area A_d	2340 mm^2
E-modulus E_d	25000 N/mm^2
Total diagonal stiffness K_d **(Minimum calibration of paragraph 7.4)**	19514 kN/mm
Poisson's ratio ν	0.2
Amount of diagonals per floor	15
Reinforcement bars	
Regular truss elements L2TRU	
Cross-sectional area A_R	3000 mm^2
E-modulus E_s	210000 N/mm^2
Length	200 mm
Transverse spring stiffness K_s	3150 kN/mm
Poisson's ratio ν	0.3

Table 11.1 General input properties

11.1.2 Applied values for the shear stiffness K_v

As explained in paragraph 10.4 the way the lateral stiffness is calculated isn't very precise. It is averaged over the complete floor height and doesn't take into account the lateral compressive forces that can occur. The error made in determining the lateral stiffness, K_h, has been analysed and was rather large. Therefore the error of the determined K_v was also significant (Table 10.5). In order to indicate the influence of this error on the shear wall behaviour, different values of K_v, based on the variation of K_h, are assigned to the interface of the wall models. Four cases are distinguished:

- The calculated value of K_v, based on the lateral stiffness calculated with the developed method of paragraph 10.4.
- The maximum value for K_v, based on an infinitely large lateral stiffness. This value is calculated using formula 10.3.
- The upper limit value of K_v, based on the maximum underestimation of K_h in appendix H: 1.28 times the lateral stiffness corresponding to the calculated value.
- The lower limit value of K_v, based on the maximum overestimation of K_h in section 10.4.5 and appendix H: 0.5 times the lateral stiffness corresponding to the calculated value.

In section 10.4.5 it is concluded that for the maximum error the real K_h is 58% of the calculated value. Nevertheless, the lower limit reduces the calculated value by 50 percent to be a bit more conservative. This is required since the error analysis was only performed for an opening height of 1600 mm. The results indicated that the calculation error becomes greater for a lower lateral stiffness. Since the openings can be higher, leading to a lower lateral stiffness, the error included in this analysis is slightly larger than observed.

The maximum value for K_v is the same for all the walls, since this value simply assumes an infinitely large lateral stiffness and is therefore only dependent on the applied value of α and K_d.

The calculated and limit values for K_v differ among the three wall types. For wall type 1 a larger value of K_v is calculated than for wall types 2 and 3. The larger value applied to the closed wall is caused by a larger lateral stiffness due to the lack of window openings. For the two walls with window openings the same value for the shear stiffness is calculated, since the developed method only takes into account window openings next to the vertical joint.

However, the lateral stiffness and consequently the shear stiffness are in fact different in both cases with openings. The configuration and amount of openings directly influence the development of stress diagonals in the shear wall. These diagonals act under an angle, which causes lateral compressive forces along the joint, as described in paragraph 10.2. These forces increase the obtained lateral stiffness, which is therefore different for walls 2 and 3. The effect can be incorporated in the calculation method for K_v by adjusting the values of β and γ, but in this evaluation these angles are set equal to zero. Any value for these angles would be based on a guess. The comparison between the results obtained from walls 2 and 3 will indicate the need for deeper research on these load angles and the need to include their effect in the calculated value for K_v.

So the lateral stiffness is varied and this leads to four different values of the interface shear stiffness K_v. This is illustrated in Figure 11.3, where the found values are indicated in the K_v-K_h diagram corresponding to the applied largest K_d value (Calibrated minimum). The chosen variation of the lateral stiffness leads to a significant change of the determined shear stiffness for

both wall 1 and walls 2 and 3. Since walls 2 and 3 contain openings, the lateral stiffness in these cases is generally lower than in wall 1. Thereby a variation of the lateral stiffness leads to a larger variation of the shear stiffness, as the indicated points are located in the steeper part of the diagram. The exact numerical values for K_v are also summarised in Table 11.2. Here it is seen that for example the lateral stiffness of the lower limit is indeed half of the calculated value, corresponding to the explanation above. Appendix H contains more explanation about the way the shear stiffness corresponding to a specific situation is calculated.

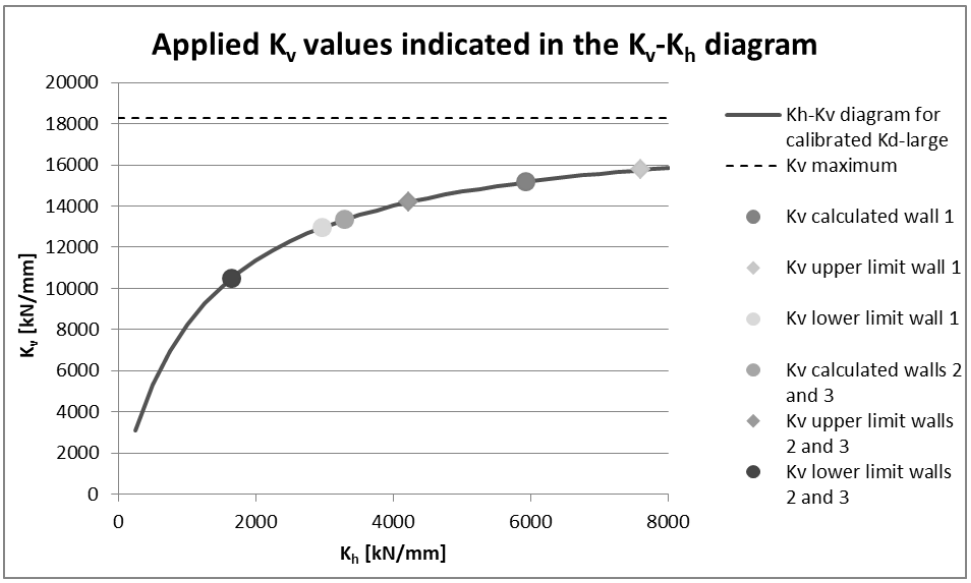

Figure 11.3 The found values for K_v and their position on the K_v-K_h curve

	Wall 1			Walls 2&3		
	K_h [kN/mm]	K_v [kN/mm]	K_v [N/mm³]	K_h [kN/mm]	K_v [kN/mm]	K_v [N/mm³]
K_v Calculated	5924	15166	9.48	3292	13342	8.34
K_v Maximum	∞	18293	11.4	∞	18293	11.4
K_v Upper limit	7603	15761	9.85	4220	14187	8.87
K_v Lower limit	2965	12956	8.10	1646	10500	6.56

Table 11.2 Applied values for the interface shear stiffness

The different values of K_v are applied to analyse two main aspects:

- The band width of the calculation: This band width is indicated by the difference in the results corresponding to the upper and lower limit of K_v.
- The maximum influence of K_h: This influence is indicated by the difference in the results corresponding to the maximum value and lower limit of K_v.

Both aspects provide information about the contribution of the inaccurately defined lateral stiffness on the wall behaviour. The next paragraph contains an overview of the resulting top deflections of all wall models. Paragraph 11.3 evaluates the two main aspects in order to assess the feasibility of the applied method of paragraph 10.4.

11.2 Results of the analysis of a compact and slender shear wall

This paragraph contains an overview of the resulting top deflection of all the different shear walls that were analysed. The first section discusses the compact shear walls, the second the slender shear walls. Appendix K contains an overview of the resulting shear stresses in the

different models. Most of the evaluation of the results is presented in paragraph 11.3. However, two aspects are elaborated on in this paragraph:

- The performance of the precast shear wall compared to the results found in the literature study
- The comparison between the result of the shear wall with diagonal bars and the wall with interface elements with "K_v Calculated".

The first comparison may give an indication of the performance of the vertical profiled mortar connection relative to other types of connections. The second comparison provides insight in the difference in behaviour of a wall where the bar model of Chapter 6 is applied and a wall where interface elements are used. Furthermore it indicates the accuracy of the modelling approach.

11.2.1 Results of the compact shear wall analysis

Table 11.3 shows the resulting horizontal top deflections of the three compact wall models for the three evaluated cases. The results are compared to those of appendix I that are obtained with a lower value of K_d (Calibrated average). According to the results of Table 11.3, the application of a vertical joint reduces the wall's stiffness by approximately 7-10 percent. This holds for all three walls. So the results show that the influence of the connection on the top deflection is independent of the stiffness of the shear wall, where wall 1 is the stiffest and wall 3 the weakest due to the openings. This was also found in results of previous research as addressed in paragraph 3.3 (Falger, 2003). The reduction of the stiffness by 7-10 percent is slightly smaller than found in appendix I, because of the larger applied value of K_d.

Because of different input properties and model dimensions, it is not easy to compare the performance of the vertical profiled mortar connection with that of other connection types that were analysed in previous studies. What can be seen from the results of the study by Van Keulen and Vamberský presented in Figure 3.16, is that even the best performing wall models (type a and e) showed a deflection increase of approximately 25 percent for a slenderness ratio of 1.6 (van Keulen & Vamberský, 2012).

However, this result was found for a closed wall with three vertical joints and horizontal joints with a finite stiffness. If the same horizontal joint stiffness is applied in wall model 1, the increase of the top deflection compared to a monolithic wall is 18.3 percent (For K_v Lower limit). If three vertical joints were applied, the performance is probably not much better than that found by Van Keulen and Vamberský.

	Wall 1			Wall 2			Wall 3		
	K_v [N/mm³]	U_{top} abs.	U_{top} rel.	K_v [N/mm³]	U_{top} abs.	U_{top} rel.	K_v [N/mm³]	U_{top} abs.	U_{top} rel.
Monolithic	-	1.20	100%	-	1.98	100%	-	3.76	100%
Diagonal bars	-	1.32	110.0%	-	2.16	109.1%	-	4.06	108.0%
K_v Calculated	9.48	1.29	107.5%	8.34	2.16	109.1%	8.34	4.09	108.8%
K_v Maximum	11.4	1.28	106.7%	11.4	2.13	107.6%	11.4	4.05	107.7%
K_v Upper limit	9.85	1.28	106.7%	8.87	2.15	108.6%	8.87	4.08	108.5%
K_v Lower limit	8.10	1.30	108.3%	6.56	2.18	110.1%	6.56	4.13	109.8%

Table 11.3 Resulting top deflection of the compact walls [mm]

The relative difference in top deflection of walls 2 and 3 between the model with diagonal bars and that with interface elements with "K_v Calculated" is equal compared to the case in appendix I

(0 and 0.8 percent point respectively). This difference is small, indicating a good accuracy of the developed calculation method for K_v. However, in wall 1 the difference between the two modelling approaches is significant. The value of K_v in this case is based though on an assumption for the bending stiffness K_b, as explained in section 11.1.2. So the difference in results for this wall mainly indicates the accuracy of this assumption than that of the calculation method in total.

11.2.2 Results of the slender shear wall analysis

Table 11.4 shows the resulting top deflection for each of the three slender wall models with different joint conditions.

The results clearly show that in a slender wall, the influence of the vertical connection on the top deflection is smaller than in a compact wall. This observation is in accordance with the results of previous research that were addressed in paragraph 3.3. Furthermore the results show that the magnitude of the increase of the top deflection caused by the connections is independent of the stiffness of the wall. This was also addressed in paragraph 3.3.

Again it is not easy to compare the resulting top deflection with results obtained in previous research. The resulting relations of Figure 3.16 show that for a slenderness ratio of 5.0 the top deflection increase is approximately 5 percent for the best performing wall models (a and e) (van Keulen & Vamberský, 2012). This includes the contribution of horizontal joints and three vertical joints in case e, where an unreinforced profiled mortar connection is applied. If for the closed wall in this analysis the same horizontal joint stiffness is applied, the deflection increase is 4.3 percent. If three vertical joints were present, the deflection increase is probably almost equal to the result found by Van Keulen and Vamberský.

Falger analysed wall models with a slenderness ratio of 6.0, three vertical joints and horizontal joints with finite stiffness. The top deflection of this wall with a reinforced profiled mortar joint was 7 percent larger than that of a monolithic wall, as seen in Table 3.1 (Falger, 2003). Comparing this result with the found 4.3 percent indicates that the developed vertical profiled mortar connection might perform better than the connection analysed by Falger. The comparison of the found results with results from previous research must be interpreted with care, since too many factors are different. Fact is that the difference between the results is small, whereby it is not yet possible to conclude that the vertical profiled mortar connection performs better than other types of connections. So far, the results indicate a small performance difference between the different connection types (e.g. reinforced profiled joints and masonry walls) and the developed vertical profiled mortar connections.

	Wall 1			Wall 2			Wall 3		
	K_v [N/mm³]	U_{top} abs.	U_{top} rel.	K_v [N/mm³]	U_{top} abs.	U_{top} rel.	K_v [N/mm³]	U_{top} abs.	U_{top} rel.
Monolithic	-	63.47	100%	-	73.59	100%	-	145.5	100%
Diagonal bars	-	64.38	101.4%	-	75.13	102.1%	-	147.7	101.5%
K_v Calculated	9.48	65.07	102.5%	8.34	76.06	103.4%	8.34	149.8	103.0%
K_v Maximum	11.4	64.96	102.3%	11.4	75.80	103.0%	11.4	149.5	102.7%
K_v Upper limit	9.85	65.05	102.5%	8.87	76.01	103.3%	8.87	149.7	102.9%
K_v Lower limit	8.10	65.18	102.7%	6.56	76.29	103.7%	6.56	150.1	103.2%

Table 11.4 Resulting top deflection for the three slender walls [mm]

The relative difference in top deflection between the models with diagonal bars and the models with interface elements "K_v Calculated" is rather large. For wall 3 the difference is 1.5 percent point. This is absolutely larger than the maximum difference obtained for a compact wall and relative to the total deflection increase tremendously larger. This result may indicate that the calculation method for K_v is inaccurate.

However, since the deflection of the model with bars is larger than the deflection of the model with K_v Maximum, the physical meaning of the diagonal bar result is questionable. The lateral stiffness cannot exceed infinity and therefore the shear stiffness cannot exceed the value of "K_v Maximum". A more detailed analysis shows that in the model with diagonal bars, part of the joint is compressed instead of dilated. This leads to a shear stiffness larger than the limit value. However, this is physically impossible, since the joint is fully filled with mortar and therefore not that easily compressible. The effect is explained in more detail in appendix J. For this reason the error of the calculation method is expressed by the size of the band width, that is analysed in the next paragraph, instead of the difference with the result of the wall with diagonal bars.

11.3 Evaluation of the results

This paragraph evaluates the results of the previous analyses in more detail. The focus is on the two main aspects that were defined in section 11.1.2:

- The band width of the calculation
- The maximum influence of K_h

11.3.1 The band width of the calculation

The band width of the calculation method is evaluated in three different manners, which are discussed in this section. In all cases the band width is analysed by considering the results of K_v upper and lower limit.

11.3.1.1 The band width in terms of top deflection difference

Based on the results of previous paragraph, the difference in top deflection between the upper and lower limit of the calculation method can be expressed in the following way:

$$Band\ width = \frac{U_{top\ Kv\ low} - U_{top\ Kv\ up}}{U_{top\ Kv\ up}} * 100\%$$

The quantity indicates the relative increase of the top deflection when the value of K_v is decreased from its upper to its lower limit. Table 11.5 summarises the resulting band width sizes for all analysed walls.

	Wall type 1	Wall type 2	Wall type 3
Compact wall	1.6%	1.4%	1.2%
Slender wall	0.2%	0.4%	0.3%

Table 11.5 Band width for the different models

It can be concluded that the band width is larger for a compact wall. In the extreme case the top deflection U_{top} obtained with "Kv Lower limit" is 1.6 percent larger than for "Kv Upper limit". This means that in the worst of all analysed cases, the top deflection might be overestimated with 1.6 percent due to the inaccuracy of the applied calculation method for K_v. Based on this small maximum band width size, the method can be classified as accurate.

11.3.1.2 The band width in terms of relative top deflection difference

Another way to express the error of the calculation is by the relative band width size. This is defined as the increase of the top deflection as a result of applying K_v lower limit instead of K_v upper limit, relative to the minimal increase of the top deflection compared to the monolithic wall. So this relative band width is calculated in the following way:

$$Relative\ band\ width = \frac{U_{top\ Kv\ low} - U_{top\ Kv\ up}}{U_{top\ Kv\ max} - U_{top\ monolithic}} * 100\%$$

The difference in top deflection between "K_v Lower limit" and "K_v Upper limit", which is the error of the calculation, is divided by the difference between "K_v Maximum" and "Monolithic", which is the minimal top deflection increase for the precast wall.

The error is expressed by the relative band width size, since the difference in total top deflection for "K_v Lower limit" and "K_v Upper limit" is small and of minor importance. What is relevant, is the difference in top deflection between the monolithic and the precast wall. So the relative band width indicates whether the error of the calculation method is significant with respect to the top deflection difference between a monolithic and a precast shear wall.

	Wall type 1	Wall type 2	Wall type 3
Compact wall	25.0%	20.0%	17.2%
Slender wall	8.7%	12.7%	10.0%

Table 11.6 Relative band with for the different wall models

For a slender wall the relative band width of the calculation method might be acceptable, but especially for a compact wall, it is probably too large. In the worst of all analysed cases the top deflection difference between the precast and monolithic wall may be over- or underestimated by 25 percent. With this uncertainty it is for example impossible to compare the performance of the vertical profiled mortar connections with that of other possible connections. For example in the study of Falger, the difference in top deflection increase between two different connection types was just a few percent points, as seen in Table 3.1 (Falger, 2003). The relative band width of Table 11.6 is larger. So if the performance of the vertical profiled mortar connection must be compared to other solutions, the band width of the applied calculation method is too large to do this properly. Based on the upper limit of K_v, the vertical profiled mortar connection could result in a stiffer shear wall than for example a masonry configuration with open joints, but based on the lower limit value the opposite could be true.

11.3.1.3 The band width in terms of difference in shear stress

In appendix K the difference in shear stress in the joint is analysed for all wall models. Based on these results the relative difference between the upper and lower limit of K_v is calculated. A lower value of K_v leads to a smaller shear stress. The results in Table 11.7 show that the largest obtained difference in shear stress is 12 percent. This difference may be rather large, but it must be noted that the absolute difference is just 0.13 N/mm^2. So the importance of this relative difference is questionable, since the shear capacity of the joint is around 5 N/mm^2 (Figure 4.7) and the applied horizontal load of 40 kN/m per floor is large.

	Wall type 1	Wall type 2	Wall type 3
Compact wall	2.3%	9.6%	12.0%
Slender wall	1.6%	8.8%	9.6%

Table 11.7 Band width of the shear stress in the joint

11.3.2 The maximum influence of K_h

The maximum influence of a limited lateral stiffness K_h on the results is analysed as well. In case the shear stiffness of the vertical connections is equal to "K_v Maximum", K_h is infinitely large. But K_h has a limited value, which is at least equal to the value corresponding to "K_v Lower limit". So a comparison of the results corresponding to these two values for K_v indicates the maximum influence of a limited K_h.

11.3.2.1 The influence of K_h in terms of top deflection difference

Similar as in previous section, the influence of K_h can be expressed in terms of the top deflection difference. Therefore the influence is calculated in the following way:

$$Influence\ K_h = \frac{U_{top\ Kv\ low} - U_{top\ Kv\ max}}{U_{top\ Kv\ max}} * 100\%$$

Table 11.8 contains an overview of these results, which shows that the influence is the largest for wall type 2 and larger for a compact than for a slender wall.

	Wall type 1	Wall type 2	Wall type 3
Compact wall	1.6%	2.3%	2.0%
Slender wall	0.3%	0.6%	0.4%

Table 11.8 Influence of K_h for the different models

The influence of K_h on the total top deflection is relatively small. In the worst of all analysed cases the top deflection is 2.3 percent larger as a result of the limited lateral stiffness. The small influence seems to be a consequence of the small importance of K_v in general. In the worst analysed case "K_v Lower limit" is just 57% of "K_v Maximum" (Calculated from Table 11.2). So the reduced K_h significantly reduces K_v, but it simply doesn't lead to a large difference in top deflection.

11.3.2.2 The influence of K_h in terms of relative top deflection difference

Also the influence of K_h can be expressed relative to the top deflection difference between a monolithic and a precast wall, which is calculated by the following formula:

$$Relative\ influence\ K_h = \frac{U_{top\ Kv\ low} - U_{top\ Kv\ max}}{U_{top\ Kv\ max} - U_{top\ monolithic}} * 100\%$$

	Wall type 1	Wall type 2	Wall type 3
Compact wall	25.0%	33.3%	27.6%
Slender wall	14.8%	22.2%	15.0%

Table 11.9 Relative influence of the lateral stiffness

According to Table 11.9, the top deflection difference with respect to a monolithic wall increases by 33.3 percent for "K_v Lower limit" compared to "K_v Maximum".

Based on this evaluation, it can be argued that the contribution of the lateral stiffness is significant when the wall's top deflection is compared with that of a monolithic wall or a wall with another type of vertical connection, whereas it is not important when the top deflection in absolute terms is of interest (2.3 percent difference). However, these two statements are based on the evaluation of wall models with the input properties of Table 11.1. The correctness of the last statement must therefore be checked for a case where the lateral stiffness is equal or close

to its practical lower limit. In that situation the influence will be the largest and therefore leads to the largest total top deflection increase.

11.3.2.3 The influence of K_h in terms of shear stress

In appendix K the difference in shear stress in the joint is analysed for all wall models. Based on these results the relative difference between the maximum and lower limit of K_v is calculated. Table 11.10 shows these results. Similar as for the band width of the method, the relative difference in shear stress is rather large, however the absolute difference is small: 0.23 N/mm^2.

	Wall type 1	Wall type 2	Wall type 3
Compact wall	4.4%	15.4%	19.5%
Slender wall	1.9%	15.0%	16.4%

Table 11.10 Influence of K_h on the shear stress in the joint

11.4 The extreme band width and influence of K_h

In section 10.1.3, the largest influence of K_h on the value of K_v was found for the practically lower limit values of the design parameters K_s, E_c, a and h. Moreover, in paragraph 10.4 and appendix H it was concluded that the error of the calculation method was also the largest for these lower limit values.

So, the band width and the contribution of K_h presented in previous paragraph is limited, since for all input parameters averagely stiff values were applied. Thereby the results of previous paragraph provide a moderate band width and lateral stiffness influence.

In order to obtain the largest band width of the calculation method and corresponding largest influence of K_h the input properties of Table 11.1 are changed into the properties for which the largest error of the calculation method was found in section 10.4.4. These input properties are again summarized in Table 11.11. It must be noted that the opening height is kept equal to 1600 mm because of the restriction of the solution for the differential equation that was derived. The results presented in this paragraph are therefore the limit when h=1600 mm.

K_s	1050	kN/mm
K_d	19514	kN/mm
h	1600	mm
a	300	mm
E_c	20000	N/mm^2
t	500	mm
α	3.87	[-]

Table 11.11 Changed input properties

Table 11.12 shows the resulting top deflections for the compact wall only, since the band width and K_h contribution appeared the largest for this wall (See paragraph 11.3). Only wall types 2 and 3 are analysed, since for the closed wall the lateral stiffness will never be equal to its lower limit value due to the lack of window openings. Table 11.13 gives an overview of the band width and K_h influence for this extreme case. The resulting shear stresses are presented in appendix K.

	Wall 2			Wall 3		
	K_v [N/mm³]	U_{top} abs.	U_{top} rel.	K_v [N/mm³]	U_{top} abs.	U_{top} rel.
Monolithic	-	4.07	100.0%	-	7.68	100.0%
Diagonal bars	-	4.42	108.6%	-	8.23	107.2%
K_v Calculated	5.59	4.39	107.9%	5.59	8.28	107.8%
K_v Maximum	11.4	4.31	105.9%	11.4	8.14	106.0%
K_v Upper limit	6.30	4.37	107.4%	6.30	8.25	107.4%
K_v Lower limit	3.70	4.45	109.3%	3.70	8.38	109.1%

Table 11.12 Top deflection of a compact wall with a smaller K_h [mm]

	Wall type 2	Wall type 3
Band width	1.8%	1.6%
Rel. Band width	33.3%	28.3%
K_h Influence	3.2%	2.9%
Rel. K_h Influence	58.3%	52.2%

Table 11.13 Band width and maximum influence of K_h in the extreme case

The band width of the calculation method and the influence of the lateral stiffness are both larger than in paragraph 11.3. Nevertheless, the maximum error of the top deflection is just 1.8% and the maximum influence of K_h is just 3.2%, illustrating both aspects are still relatively unimportant for the magnitude of the total top deflection. So when only the total top deflection is of interest, the contribution of the lateral stiffness is not very important, neither is the possible error of the calculation indicated by the difference between the upper and lower limit.

When the performance of the vertical profiled mortar connection is compared to that of other connection types or a monolithic wall, both the contribution of the lateral stiffness and the band width of the calculation method are important. This was already true for the situation of paragraph 11.4, but in this case the relative contribution is even larger, as the results of Table 11.13 show.

11.5 Assessment and the proposal for a practical modelling approach

This paragraph starts with the assessment of the modelling approach that has been developed in paragraph 10.4 and evaluated in this chapter. Based on this assessment, a final proposal for the practical modelling approach is made in the second part of this paragraph. The next paragraph ends this chapter with a practical example where this finally proposed approach is applied.

11.5.1 Assessment of the modelling approach

The modelling approach for the vertical profiled mortar connection that is developed makes use of linear interface elements to which a shear stiffness K_v is assigned that is calculated by the developed calculation method of paragraph 10.4 and appendix H. Based on the presented results and the values for the band width and the influence of K_h the following conclusions can be drawn about the developed modelling approach and its calculation method:

- The band width in terms of top displacement difference is small enough to state that the approach provides an accurate approximation.
- The relative band width is too large to be able to compare the performance of the vertical profiled mortar connection with that of other solutions for precast concrete shear walls.

- The influence of K_h on the top deflection of the shear wall is small. This is mainly a result of the unimportance of the shear stiffness of the vertical joint for this top deflection.
- The relative influence of K_h is too large to be able to compare the performance of the vertical profiled mortar connection with that of other solutions for precast concrete shear walls.
- The relative difference in results of the modelling approach and the wall with diagonal bars is small enough to state that the use of interface elements provides a good approximation of the top deflection.
- The band width of the approach in terms of shear stress in the joint is large.
- The influence of K_h on the shear stress in the joint is large (See appendix K).

These conclusions indicate the feasibility of the developed modelling approach with linear interface elements and the developed calculation method for K_h and K_v.

It can be stated that the modelling approach is useful when the magnitude of the top deflection of a shear wall is of interest, since the band width of U_{top} is small. However, it cannot be used to compare the performance of the vertical profiled mortar connections with that of other connections. For this purpose the calculation method for K_h and K_v should be refined, since the estimated value of K_h is too uncertain and too important for the top deflection difference. This refinement can include the effect of lateral prestress.

Moreover, it can be stated that the influence of the lateral stiffness on the top deflection is small enough to exclude the whole effect. This wouldn't lead to a large error of the approximated value of U_{top}. From this point of view, the suggested refinement of the calculation method for K_h is of minor importance. Again, this holds only if it is not desired to compare the performance with other solutions.

Application of the modelling approach leads to an inaccurately defined shear stress in the joint. Besides the relatively large band width of the calculation method that is analysed in appendix K, another aspect may not be forgotten. The modelling approach assumes a uniform shear stiffness distribution over the height of each floor, whereby the resulting stress distribution deviates from the real situation. In reality the shear stiffness is locally larger. Therefore the peak value of the shear stress is underestimated by the modelling approach. However, the magnitude of the shear stress is small, whereby the importance of this inaccuracy may be subject to discussion.

The goal of this thesis was to develop a practical way of modelling for the vertical profiled mortar connections. The modelling approach applied so far contains a method to estimate the lateral stiffness K_h and shear stiffness K_v that is not straight forward. It requires to derive the solution of the formulated Timoshenko Beam equation, which is different for any floor height and value of parameter h. A tool could be developed that performs this derivation and calculates K_v, based on the design parameters that are given as input by the structural engineer. Only with such a tool the method will become practical. Developing the tool won't be too complicated, since it comprises only simple algebra. However, who will develop it and make it widely available? If all structural engineers must do this for themselves, the modelling approach is in general not practical.

11.5.2 Final proposal for the practical modelling approach

The results of this chapter suggest another more practical modelling approach. The influence of the lateral stiffness on the top deflection of the shear wall appeared to be small. In the extreme case of paragraph 11.4 the top deflection was only increased by 3.2 percent due to the reduction of K_h from infinite to its minimum value for that situation. Moreover, it appears to be hard to give a good approximation of the magnitude of the lateral stiffness K_h, since many factors are involved. So refinement of the calculation method will be tough since this mainly comprises finding a better way to estimate the lateral stiffness.

Estimating the magnitude of K_h even gets more complex since the effect of lateral compressive stresses must be included as well. This effect hasn't been fully described in this research, but it is demonstrated that the magnitude of this stress also depends on many factors. However, lateral compressive stresses can never let the shear stiffness be greater than "K_v Maximum" in physically realistic situations.

So, because the top deflection deviation is small and K_h is hard to define, it will be very practical to base the shear stiffness of the interface elements on the maximum value. This is not dependent on K_h or any lateral stress, but simply calculated by formula 10.3. If just the top deflection of the wall is of interest, the overestimation of the approach leads to an error of maximal 3.2 percent (if h=1600 mm). So the input given to the interface elements is calculated by:

$$K_v = C * K_d * \frac{h_y^2}{L_d^2} \qquad [11.1]$$

In this case the factor C is a constant that can be inserted to take into account the influence of K_h including the effect of lateral stresses. The use of such a factor can reduce the error of the approximation. The largest advantage of this calculation method is the exclusion of the whole effect of K_h, whereby a refinement of the calculation method for K_h of paragraph 10.4 and more research into the effect of lateral stresses is unnecessary. What is very important, is more research into the properties of the compression diagonals in the mortar joint: K_d and α (h_y/h_x).

In the most practical case, a table is composed, that contains different values for C corresponding to a range of different cases. Most importantly, the factor C must be dependent on the magnitude of K_d and α, since these determine the influence of the lateral stiffness that is expressed by factor C. It should also depend on the thickness t and the design parameters h, a, E_c and K_s. As concluded in chapter 9, especially the thickness and parameters a and h are important. The parameters are indicated in Figure 11.4.

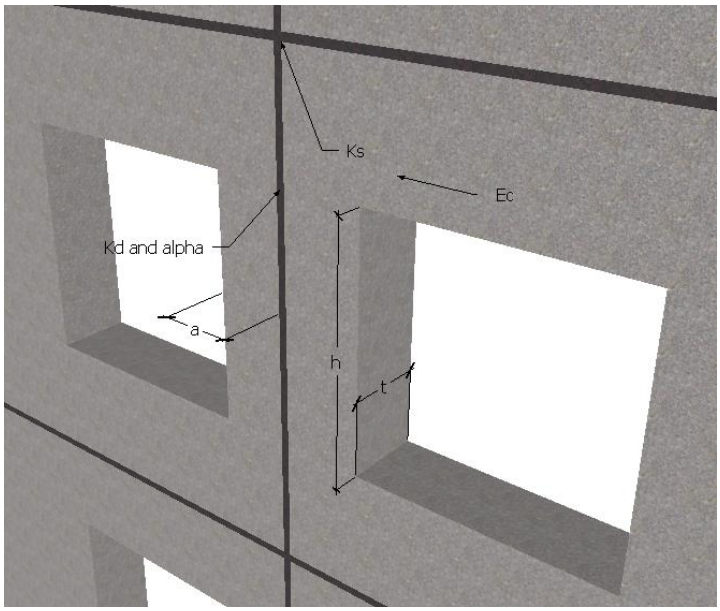

Figure 11.4 Parameters that determine the value of factor C

In further research the factor C must be determined for many combinations of the defined parameters by analysing the resulting shear stiffness K_v in the way this was done in the parameter study. By doing so, the table is composed in which the structural engineer can retrieve the value of C that must be used for the situation of interest. The value of C must be retrieved form this table in the way that is schematically visualised in Figure 11.5.

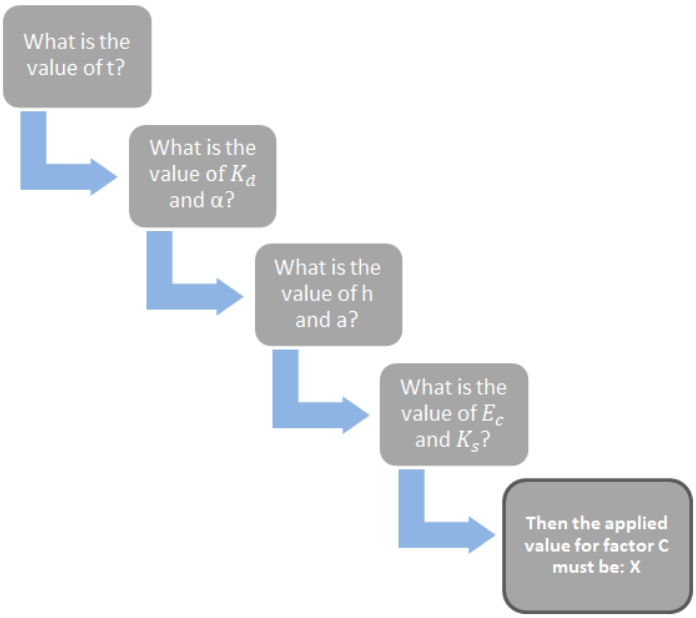

Figure 11.5 Determination of factor C from a design table

Based on the analyses that were performed in this chapter and in appendix I, for three different design situations the value of factor C is already determined. Table 11.14 contains these three values. They are based on the difference between $K_{v,max}$ and $K_{v,\ lower\ limit}$, since this difference indicates the influence of K_h that the factor C takes into account. Using "K_v Lower limit" results in conservative values.

t [mm]	K_d [kN/mm]	h [mm]	a [mm]	E_c [N/mm^2]	K_s [kN/mm]	C
500	19514	1600	500	35000	3000	6.6/11.4=0.57
500	19514	1600	300	20000	1000	3.7/11.4=0.32
200	4390	1600	500	35000	3000	5.00/6.43=0.78

Table 11.14 Values of reduction factor C corresponding to the analysed cases

Since not all cases will be very distinctive, C can be equal for different combinations of parameters. For now this is left for further research. The three cases presented here are very different, as the variation of C illustrates.

In section 10.1.3 it has been determined that in the most extreme case, the shear stiffness is reduced by 86% due to the practically lowest value of K_h. From this point of view the factor C will never be lower than 0.14. As long as the table for factor C is not complete, the structural engineer that applies this proposed practical method can estimate the factor C by the comparison of the specific design with the three results of Table 11.14 and the lower limit of 0.14.

11.6 Practical application of the proposed modelling technique

So far, this chapter focused on the feasibility of applying interface elements in precast concrete shear wall models. To finalise this chapter and the research in total, an example of a practical design calculation of a precast concrete shear wall with vertical profiled mortar connections is provided. This example deals with the following aspects:

- Development of a shear wall model
- Determination of the connection stiffness
- Evaluation of the top deflection and shear stress
- Assessment of the precast concrete elements
- Assessment of the transverse reinforcement

11.6.1 Development of the shear wall model

In this example the geometry of the shear wall model is equal to that of the previous analyses. Figure 11.6 shows a stability structure with indicated dimensions that is considered. The highlighted wall is analysed in this example.

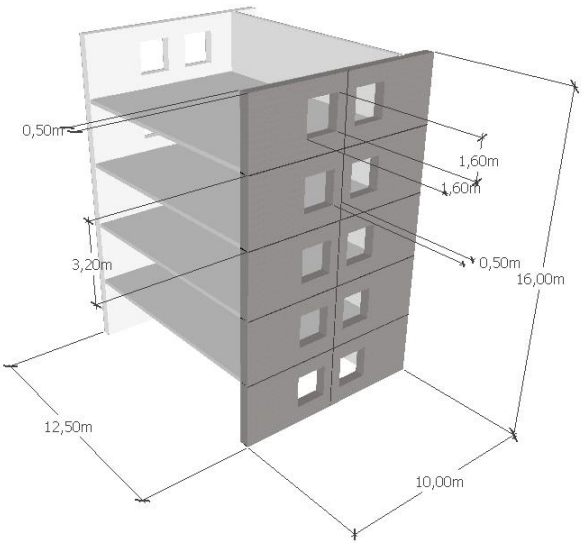

Figure 11.6 Example of a stability structure consisting of precast concrete shear walls

In DIANA 10.2 or any other FEM software the wall can be modelled using "plane stress elements". To these elements the properties of the precast concrete must be assigned. The geometry is corresponding to the stability structure design. The horizontal loads are applied as distributed forces at the location of each floor slab.

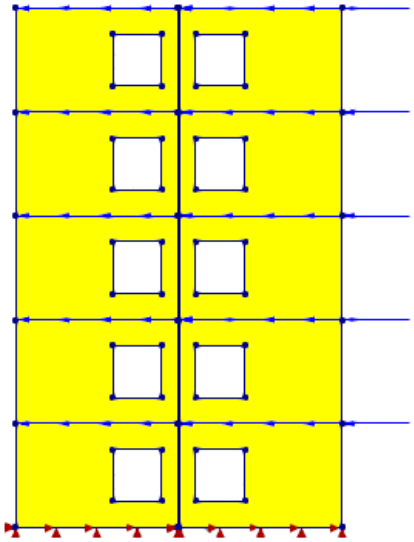

Figure 11.7 Developed wall model

For a building in the Netherlands in wind area II in a coastal environment, the extreme wind pressure at 15 metre is 1.43 kN/m^2. The C_{pe} factor is 1.3 for this building. This roughly leads to the following wind pressure per floor in the direction of the shear wall:

$$q_{wind} = \frac{(W * H_{floor} * q_p * C_{pe})}{\#walls * D} = \frac{12.5m * 3.2m * 1.43\frac{kN}{m^2} * 1.3}{2 * 10m} = 3.718\frac{kN}{m}$$

The following properties hold for the developed shear wall design:

Concrete Elements	
Plane stress elements CQ16M	
Thickness t	500 mm
E-modulus E_c	35000 N/mm^2
Poisson's ratio ν	0.2
Window height	1600 mm
Column width	500 mm
Reinforcement bars	
Cross-sectional area A_R	3000 mm^2
E-modulus E_s	210000 N/mm^2
Length	200 mm
Transverse spring stiffness K_s	3150 kN/mm
Poisson's ratio ν	0.3

Table 11.15 Properties of the designed shear wall

The shear wall model only contains the plane stress elements that model the precast concrete panels. The reinforcement is not modelled explicitly, since it is part of the vertical profiled mortar connection which is modelled by the use of interface elements.

Some specific joint properties corresponding to the vertical profiled mortar connection with staggered profile must be known to the structural engineer. These properties must be provided by literature about the connection type. For now these properties are provided in Table 11.16.

The vertical profiled mortar connection	
Staggered joint profile	
W_d (See paragraph 7.4)	20.8 mm
E-modulus E_d or E_m	25000 N/mm^2
A_d	$A_d = t * W_d$
L_d	199.9 mm
h_y	193.5 mm
h_x	50 mm
k_d	$k_d = E_d A_d / L_d$

Table 11.16 Known connection properties for a joint with a staggered profile

11.6.2 Determination of the connection stiffness

In this example only the vertical connections are modelled, just like in previous analyses. The connections are modelled by linear 2D line interface elements (CL12I- elements in DIANA 10.2). These are applied in the vertical joint between two adjacent plane stress elements. A normal and shear stiffness must be assigned to the interface elements. The normal stiffness follows from the mortar's stiffness while loaded in compression.

$$K_n = \frac{E_m A}{A W_{joint}} = \frac{E_m}{W_{joint}} = \frac{25000}{75} = 333 \frac{N}{mm^3}$$

The shear stiffness is calculated using the proposed practical calculation method of paragraph 11.5. For this method the diagonal stiffness must be calculated first, according to the connection properties that were provided to the structural engineer.

$$k_d = \frac{E_d A_d}{L_d} = \frac{25000 * 20.8 * 500}{199.9} = 1300.9\ kN/mm$$

The structural engineer knows that over a floor height of 3.2 metres 15 compression diagonals develop in the joint according to the profile dimensions. Using formula 11.1, the shear stiffness can be determined.

$$K_v = 15 * C * \frac{K_d * \frac{h_y^2}{L_d^2}}{t * H_{floor}} = 15 * 0.57 * \frac{1300.9 * 10^3 \frac{N}{mm} * \frac{193.5\ mm}{199.9\ mm}}{500\ mm * 3200\ mm} = 6.7 \frac{N}{mm^3}$$

For the reduction factor 0.57 is used, which is found in Table 11.14. This value was determined for input properties exactly equal to those of this design. As explained in paragraph 11.5, this factor is dependent on the shear wall design and the applied value of K_d and must be determined for different situations in further research.

It is clear that this method to determine the shear stiffness is very practical, since it only requires some information about the type of joint that is applied, which is provided in Table 11.16 and the reduction factor, which is read from a table.

11.6.3 Evaluation of the top deflection and shear stress

Figure 11.8 shows the resulting top deflection of the shear wall. The top deflection is within the SLS limit.

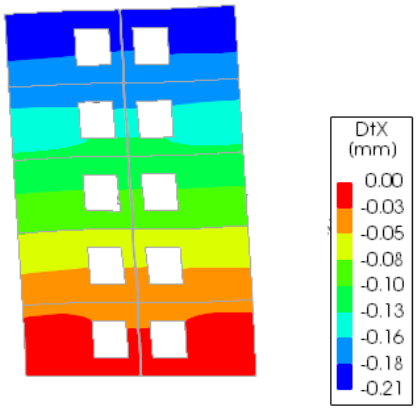

Figure 11.8 Resulting top deflection

Figure 11.9 shows the shear stresses that develop in the joint. It can be seen that the maximum shear stress occurs on the first floor. This corresponds to the theory described in paragraph 3.2.

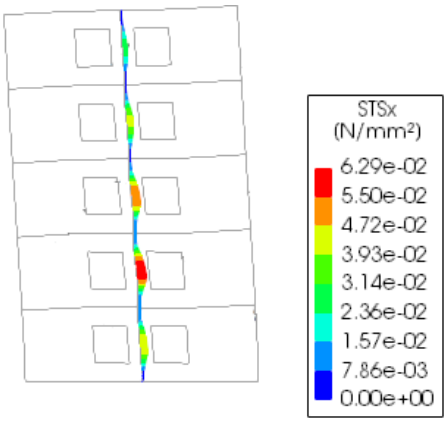

Figure 11.9 Shear stresses in the joint

The maximum shear stress is 0.0629 N/mm^2. It must be checked if this stress is smaller than the shear capacity of the joint. According to Van Keulen's test results presented in Figure 4.7, the shear capacity is at least 5 MPa, which is sufficient for the resulting shear stress.

11.6.4 Assessment of the precast concrete elements

Interface elements are applied that do not contain any information about the relation between the transferred vertical shear force and the horizontal force it induces on the surrounding concrete elements. For this reason the dilatation of the joint and local structural behaviour of the concrete elements around the joint cannot be evaluated in the developed shear wall model of Figure 11.7.

Nevertheless, the resistance of the precast concrete elements and the transverse reinforcement to the induced lateral load must be assessed. For this purpose the shear stress is integrated over the thickness of the wall and subsequently multiplied by the angle of the diagonals, whereby the induced lateral force is obtained. This procedure is executed for the floor where the maximum

shear stress develops. For simplicity a uniform shear stress distribution over the height of this floor is assumed.

$$q_h = \tau_{max} * t * \frac{h_x}{h_y} = 0.0629 \frac{N}{mm^2} * 500\ mm * \frac{5}{193.5} = 8.13 \frac{N}{mm} = 8.13 \frac{kN}{m}$$

With a simple hand calculation the bending resistance of the concrete column between the joint and the window can be assessed. This calculation assumes a column width of 500 mm over the complete floor height (indicated in Figure 11.10) , whereby the occurring bending moment is simply calculated as:

$$M_b = \frac{1}{8} * q_h * H_{floor}^2 = \frac{1}{8} * 8.13 * 3.2^2 = 10.4\ kNm$$

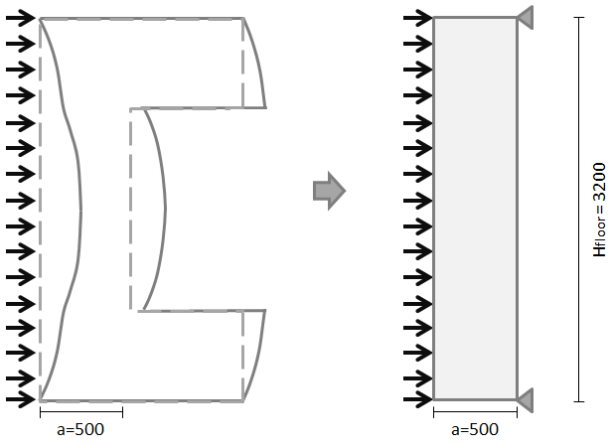

Figure 11.10 Column approximation

The maximum tensile stress in the concrete column as a consequence of the lateral force is equal to:

$$\sigma_b = M_b * \frac{z}{I} = 10.4 * 10^6 * \frac{\frac{500}{2}}{\frac{1}{12} * 500 * 500^3} = 0.50 \frac{N}{mm^2}$$

This tensile stress is smaller than the regular concrete tensile strength. It must be taken into account that the concrete column is also loaded by the weight of the structure, leading to compressive stresses that will definitely compensate this small tensile stress. So in this specific example extra bending reinforcement in the concrete elements is not necessary.

It must be noted that this calculation for the stress is not correct, since the concrete column is not slender and can therefore not be evaluated by formula's corresponding to an Euler-Bernoulli beam. However, for this simple design calculation this is ignored. Given the outcome, this methodology is acceptable, since the tensile strength isn't reached by far.

11.6.5 Assessment of the transverse reinforcement

The lateral force is transferred by the applied transverse reinforcement as tensile force. According to the shear wall design, 3000 mm² of steel reinforcement is applied at the level of each floor slab. Based on this amount of reinforcement the reduction factor C and corresponding

shear stiffness K_v have been determined. In order to complete the design calculation it must be checked whether the amount of steel reinforcement is sufficient.

The total tensile force that is transferred by the reinforcement bars at one specific floor level is equal to:

$$F_s = 8.13 \frac{kN}{m} * 3.2m = 26\ kN$$

Thereby the required cross-section for B500 steel is:

$$A_{s,required} = \frac{F_s}{f_y} = \frac{26000N}{435 \frac{N}{mm^2}} = 60\ mm^2$$

This is an insignificant amount of reinforcement, since the required tying reinforcement for robustness of the structure will be a lot more.

This paragraph contained a very simple analysis of a wall with a vertical profiled mortar connection, that is of course insufficient for more detailed design calculations. However, it addressed important steps to take into account, when the vertical profiled mortar connection is modelled by linear interface elements. These steps are the indirect assessment of the bending capacity of the precast concrete elements and the tensile strength of the transverse reinforcement.

12 Conclusions and recommendations

In chapter 1 of this report the vertical profiled mortar connections that were developed and tested by D.C. Van Keulen were introduced. This master research focussed on finding a way to model these connections in order to apply them in structural design. Therefore the main question of this research was formulated as:

"How can the vertical profiled mortar connection be modelled in practical situations?"

12.1 Conclusions

In order to answer this question, more insight was required into the main effects that determine the behaviour and properties of the vertical profiled mortar connections. Already in the introduction of this research three main effects were introduced: the lateral stiffness, the joint properties and the present normal stress perpendicular to the joint.

A bar model was developed, based on the assumptions of paragraph 5.2, that is able to describe the most important shear force transfer mechanism for the developed connection: shear locking. This model was used to analyse the influence of the lateral stiffness and joint properties on the shear stiffness of the connection. Based on all processed results of the parameter study, it can be concluded that the interaction between the shear stiffness K_v, the lateral stiffness K_h, the axial diagonal stiffness K_d and the angle of the compression diagonals that develop in the mortar α, is described by the following relations:

$$K_v = \frac{1}{\frac{h_x^2 + h_y^2}{K_d * h_y^2} - \frac{h_x^2}{K_h * h_y^2}} \quad [12.1] \qquad \lim_{K_h \to \infty} K_{v,max} = K_d * \frac{h_y^2}{L_d^2} \quad [12.2] \qquad \alpha = \frac{h_y}{h_x} \quad [12.3]$$

According to these relations, the joint properties K_d and α have the largest effect on the magnitude of K_v. Together they determine the physically possible maximum value of the connection's shear stiffness, which corresponds to the case where the lateral stiffness is infinitely large [formula 12.2]. Furthermore, these two properties define the influence of the lateral stiffness on the magnitude of the shear stiffness, as indicated in paragraph 10.1. A larger axial stiffness or a more horizontal orientation of the compression diagonal leads to a larger influence of K_h. These two conclusions lead to the statement that the properties of the mortar joint are more relevant for the resulting shear stiffness of the connection than the lateral stiffness is.

The *axial stiffness K_d and angle α* of the compression diagonal are dependent on the geometry of the joint's profile, the properties of the mortar but also on executional aspects like the filling ratio of the joint. Based on Van Keulen's test results it was investigated which stiffness can be assigned to the compression diagonals in the mortar joint. It is concluded that in a 200 mm thick joint with a staggered profile the compression diagonal's axial stiffness lies within 267 and 520 kN/mm. In case of uncracked mortar, this corresponds to a width between 10.7 and 20.8 mm that fits within the geometry of the profile.

The *lateral stiffness* K_h is determined by the combination of multiple design parameters that concern the architectural and structural design of the building. Those analysed in this research are the stiffness of the transverse tying reinforcement K_s, the Young's modulus of the precast concrete elements E_c, the height of the adjacent window openings 'h' and their distance from the joint 'a'. Based on the results of the performed parameter study, it is not possible to distinguish design parameters that have a significantly larger or lower influence on the lateral stiffness compared to the others (paragraph 8.4). The magnitude of the influence of a single design parameter is dependent on multiple factors, among which the magnitude of all other design parameters. In general, two conclusions can be drawn about this interdependency. First, if K_s is stiffer, the influence of the other parameters is greater, and vice versa. Second, if a stiffer value is assigned to the parameters h, a or E_c, the influence of the other two of these design parameters is less. The study into the interdependency also proved that the largest dependency exists between the parameters h and a, whereby it is concluded that these design parameters are most relevant for the magnitude of the lateral stiffness. The influence of parameter 'h' can be very large in combination with a low value of 'a' and vice versa (paragraph 9.2).

The presence of a *lateral compressive stress* also influences the shear stiffness of a profiled mortar connection, as mentioned in chapter 1. This effect was assumed to be of no importance for vertical joints. However, an important observation done in this research is that the presence of openings in a shear wall introduces compressive stress diagonals that cross the vertical connections under an angle. The vertical component of this compression force is transferred as shear force. The horizontal component acts as a lateral compressive force that increases the joint's resistance to dilatation and thereby the shear stiffness of the connection. The contribution of these stresses is affecting the lateral stiffness distribution over the height of the joint. So it can be concluded that the effect of lateral compressive stresses is not only relevant for horizontal connections, but for vertical connections as well.

The *influence of a limited lateral stiffness* on the shear stiffness of the connection has yet only been described qualitatively. However, it was also quantified in chapters 10 and 11. The combination of the least stiff values of K_s, E_c, a and h within their practically realistic range leads to the smallest possible lateral stiffness K_h, for which the shear stiffness K_v is most reduced compared to its maximum value defined by formula 12.2. Combined with a large value of K_d obtained for a large wall thickness (500mm is applied), the influence of the small K_h is the largest. Thereby, the maximum shear stiffness reduction is the largest. According to this performed limit analysis, the shear stiffness is at most reduced by 86 percent compared to its maximum value $K_{v,max}$ (section 10.1.3). So the influence of the lateral stiffness can be significant and can therefore not be neglected in all cases. Especially when the shear wall is thick, a large diagonal stiffness is expected and large window openings are present, the contribution of the lateral stiffness must be taken into account.

An *analytical calculation method* is developed that tries to approximate the lateral stiffness and subsequently calculates the shear stiffness by formula 12.1. This methodology simulates the surrounding concrete elements as Timoshenko beams, whereby all analysed design parameters and the thickness of the wall elements are included. In some cases this method overestimates the magnitude of the lateral stiffness by more than 40 percent, leading to an overestimation of the shear stiffness by almost 30 percent (section 10.4.4). Based on these errors, it is concluded that the calculation method is not very accurate.

A *modelling approach* is developed and tested that uses linear interface elements to which a shear stiffness is assigned, to answer the main question of this research. This modelling technique is only suitable when the global deformation of the shear wall is of interest. Due to the use of interface elements, the finite element model of the shear wall structure won't include the interaction between the transferred shear force and the induced lateral forces, whereby it cannot be used to analyse the local structural behaviour around the joint. However, integrating the resulting shear stress distribution over the joint's area and multiplying this shear force by the known angle of the compression diagonals will provide the induced lateral forces on the surrounding concrete elements (paragraph 11.6). Subsequently, the structural engineer can assess the local resistance of the concrete elements to this lateral load, be it in an indirect way. When applying interface elements a significant error in resulting shear stress should be taken into account (appendix K).

The *application of linear interface elements*, with the shear stiffness calculated by the developed calculation method as input property, was assessed in multiple shear wall models. This evaluation showed that the error of the calculation method of 30 percent leads to an error of the approximated top deflection of at most 1.8%. However, this error is 33.3% of the minimal difference in top deflection compared to a monolithic wall. Furthermore the evaluation of the wall model indicated that the practically minimal lateral stiffness in case of 1600 mm high openings increases the top deflection by 3.2% compared to the case where K_h would be infinitely large. This leads to an increase of the top deflection difference compared to a monolithic wall of 58.3% (paragraph 11.4). Based on these four results it is concluded that the performance of a wall with vertical profiled mortar connections can be approximated by the developed modelling technique combined with the calculation method for K_v. However, the calculation method cannot be applied to accurately compare the performance of the vertical profiled mortar connection with that of a monolithic wall or a wall with another type of connection. For that purpose a more refined method is required.

A *final proposal for the practical modelling approach* is made, based on the previous conclusion. It is an option to base the shear stiffness K_v applied for the interface elements on the maximum value according to formula 12.2, since this upper limit approximation leads in the analysed case to a maximum error of just 3.2% of the total top deflection. This is a more practical approach than using the developed calculation method, since it only takes into account the joint properties. Any effect of the lateral stiffness or the lateral compressive stress is ignored. In order to reduce the error of this method and to be able to apply it for a comparative analysis with a monolithic or other precast wall, a reduction factor must be used. This factor will consequently depend on the expected magnitude and influence of the lateral stiffness and the lateral compressive stress (paragraph 11.5).

So, as answer to the main question, the vertical profiled mortar connections can be modelled as linear interface elements in practical situations. Their shear stiffness mainly depends on the properties of the mortar joint itself, but is also determined by the provided lateral stiffness and present lateral compressive stress. If an indication of the shear wall's total deflection is required, the shear stiffness can be approximated by the developed calculation method in paragraph 10.4, but it is more practical to approximate it by its maximum value possibly corrected by a reduction factor, as finally suggested in paragraph 11.5. If the shear stiffness must be known with more certainty, a more refined and complete calculation method should be developed and applied.

12.2 Recommendations

This thesis gives rise to the following follow-up research.

- *Further research in the behaviour of the mortar joints*
  It is concluded that the properties of the compression diagonals that develop in the mortar are of major importance for the shear stiffness of the connection. Further research must validate the axial stiffness and the angle that can be assigned to these diagonals. It must also analyse the way these two properties are defined by parameters such as the profile geometry, enabling an early estimation of the joint properties. Thereby the magnitude of the connection's shear stiffness and the possible influence of the lateral compressive stress and stiffness are also already indicated in an early phase of design. This research is also useful to generalise the results for the staggered joint profile, presented in this report, to the other developed joint profiles for which the diagonal properties are different.
- *Refinement of the developed calculation method or accurate determination of C-factors*
  In this research it is concluded that the developed calculation method doesn't provide accurate values for K_v. This can either be solved by refining this calculation method or by defining correction factors that can be applied in the proposed method of paragraph 11.5. The latter is more practical since it doesn't require more in depth research into the contribution of the lateral stiffness and stresses to the shear stiffness of the connection.
- *Further research in the stiffness of the force transfer by transverse tying reinforcement*
  The minimum magnitude of the lateral stiffness depends on the realistic least stiff values of the design parameters. The transfer of forces by the reinforcement also includes friction between precast concrete and mortar and between mortar and steel. This research did not consider this effect explicitly. If the lower limit value of the combined stiffness of this load path is known with more certainty, the minimum value of the lateral stiffness is also more certain. Thereby the largest shear stiffness reduction can be calculated more precisely.
- *Further research in the influence of lateral compressive stress*
  This research proved the presence of lateral compressive stresses in vertical joints, which are induced by stress diagonals in the shear wall. These diagonals develop as a result of openings in the wall. Further research that analyses the relation between the orientation of the stress diagonals and the design of the shear wall will show the relevance of this effect in different cases.
- *Further research in the possible shear force transfer by adhesion*
  This research neglected adhesion in the mortar-concrete interface, since shrinkage of the mortar or executional aspects are likely to prevent shear transfer by adhesion. These executional aspects are for example the filling ratio of the joint and the cleanliness of the interface. Further research must point out whether the presence of adhesion is indeed uncertain or whether this assumption was too conservative. In the latter case, it must also analyse the contribution of adhesion to the shear force transfer. Mainly because the shear stresses in the vertical joints appear to be small, the contribution of adhesion can be very important.
- *Further research in the contribution of dowel action of the transverse reinforcement*
  Especially when significant shrinkage occurs, it is necessary to analyse the contribution of dowel action of the transferred reinforcement to the shear force transfer.

- *Further research into modelling techniques that include the relation between the transferred shear force and the induced horizontal forces*
  If a modelling technique can be applied that includes this relation, the induced lateral load on the surrounding concrete elements is immediately included in the FE results, whereby the indirect method proposed in paragraph 11.6 is unnecessary. If the relation between the shear and lateral stiffness could be included in the model input, it isn't even required anymore to manually calculate the shear stiffness based on an approximated lateral stiffness or correction factor. In this case the FE model will define the shear stiffness by itself, which would definitely be the most desirable modelling approach.

Based on this research also recommendations for the application of the vertical profiled mortar connection can be provided:

- Apply a joint in which a steep and wide compression diagonal develops.
- Estimate the axial stiffness and angle of the compression diagonal in an early design phase in order to have insight in the relevance of the lateral stiffness, but also to estimate the minimal top deflection of the shear wall.
- In case the lateral stiffness is relevant, be aware of the location and size of wall openings.
- The required amount of transverse reinforcement is most important when no or small openings are present around the joint.
- If the transverse reinforcement is not explicitly modelled, as was the case in this research, it must always be checked if the amount of reinforcement is sufficient to transfer the induced tensile force between the adjacent concrete elements and if the concrete elements have enough bending capacity for the lateral forces induced by the joint.

References

Abdul-Wahab, H. M. (1986, December). An experimental investigation of vertical castellated joints between large concrete panels. *The Structural Engineer*, 93-99.

Bachmann, H., & Steinle, A. (2011). *Precast Concrete Structures.* Berlijn: Ernst & Sohn GmbH & Co. KG. .

Chakrabarti, S. C., Nayak, G. C., & Paul, D. K. (1988, February). Shear Characteristics of Cast-in-Place Vertical Joints in Story-High Precast Wall Assembly. *ACI Structural Journal*, 30-45.

Cholewicki, A. (1971). Loadbearing capacity and deformability of vertical joints in structural walls of large panel buildings. *Build. Sci.*, 163-184.

Eriksson, A., Karrholm, G., & Petersson, H. (1978). *Ductile shear key joints in large panel structures.* Goteborg.

Falger, M. M. (2003). *Geprefabriceerde betonnen stabiliteitsconstructies met open verticale voegen in metselwerkverband.* Delft: TU Delft.

Fennis, S., & Walraven, J. (2013). *Gewapend Beton.* Delft: TUDelft.

FIB. (2008). *Structural connections for precast concrete buildings, fib bulletin 43, guide to good practice.* Lausanne: Sprint-Digital-Druck.

FIB. (2014). *FIB Bulletin 74 Planning and design handbook on precast building structures.* Lausanne: Media Cologne.

Guan, H., Loo, Y.-C., & Lee, K.-K. (2000). Simplified Analysis of shear-lag in framed-tube structures with multiple internal tubes. *Computational Mechanics*, -.

Hansen, H. (1967). *Mortar joints between concrete elements in shear walls.* Oslo: Norwegian Building Research Institute.

Hansen, K., Kavyrchine, M., Melhorn, G., Olesen, S. O., Pume, D., & Schwing, H. (1976). *SBI Rapport 97 Keyed Shear Joints.* Horsholm: Danish Building Research Institute, Statens Byggeforskningsinstitut.

Hartsuijker, C. (2001). *Toegepaste Mechanice Deel 2 Spanningen, Vervormingen, Verplaatsingen.* Den Haag: Academic Service.

Hoenderkamp, J. (2011). *High-rise structures Preliminary design for lateral load.* Eindhoven: TUEindhoven.

Hummelen, J. C. (2015). *Precast concrete in framed tube high-rise structures.* Delft: TU Delft.

Kwan, A. K. (1996). Shear Lag in shear/core walls. *Journal of Structural Engineering*, 1097-1104.

Lagendijk, P., & Hordijk, D. (2016). Details in Concrete part 2 Lecture slides CIE4281 Building Structures 2.

Lee, K.-K., Loo, Y.-C., & Guan, H. (2001). Simple analysis of framed-tube structures with multiple internal tubes. *Journal of Structural Engineering*, 450-460.

Migayrou, Y. (2016). *Design of precast concrete core structures in high-rise buildings.* Delft: TU Delft.

NEN. (2011). *NEN-EN 1992-1-1+C2 Eurocode 2: Ontwerp en berekening van betonconstructies - Deel 1-1: Algemene regels en regels voor gebouwen.* Delft: Nederlands Normalisatie-instituut.

Olesen, S. O. (1975). Effect of vertical keyed shear joints on the design of reinforced concrete shear walls. *ACI Journal Special publication 48-5*, 86-99.

Rizkalla, S. H., Foerster, H. R., & Scott Heuvel, J. (1989). Behaviour and design of shear connections for load bearing wall panels. *PCI Journal*, 102-119.

Rizkalla, S. H., Serrette, R. L., Scott Heuvel, J., & Attiogbe, E. K. (1989). Multiple shear key connections for precast shear wall panels. *PCI Journal*, 104-120.

Simone, A. (2011). *An introduction to the analysis of slender structures.* Delft: TU Delft.

Singh, Y., & Nagpal, A. K. (1994). Negative Shear Lag in Framed-Tube Buildings. *Journal of Structural Engineering*, 3105-3121.

Sorensen, J. H., Hoang, L. C., Olesen, J. F., & Fischer, G. (2017). Test and analysis of a new ductile shear connection design for RC shear walls. *Structural Concrete 18*, 189-204.

Straman, J. P. (1988). *Geprefabriceerde Stabiliteitsconstructies.* Delft: TU Delft.

ten Hagen, S. (2012). *The Zalmhaven tower, An investigation on the feasibility of prefab concrete in a high rise building, Literature Study.* Delft: TU Delft.

ten Hagen, S. (2012). *The Zalmhaven tower, An investigation on the feasibility of prefab concrete in a high rise building, Research Report.* Delft: TU Delft.

Tolsma, K. V. (2010). *Precast concrete cores in high-rise buildings.* Delft: TU Delft.

TU Delft. (2016). *Concrete Building Structures reader CIE3340/CIE4281.* Delft: TU Delft.

van Keulen, D. C. (2010, juni). Geprefabriceerde hoogbouw. *Precast*.

Van Keulen, D. C. (2013). *Prefab betonverbindingen met hoogwaardige mortelvoegen Beproeving en analyse van het afschuifgedrag.* Delft: TU Delft.

van Keulen, D. C. (2014, maart). EEM en prefab beton. *Cement*, 60-65.

van Keulen, D. C. (2015). *Prefab betonverbindingen met hoogwaardige mortelvoegen, Beproeving en analyse van het afschuifgedrag.* Delft: TU Delft.

Van Keulen, D. C. (2018). *Vertical mortar connections for shear transfer between precast concrete large panel elements.* Delft: TU Delft.

van Keulen, D. C., & Vamberský, J. (2012, juni). Vervormingen prefab wandconstructies. *Cement*, 2-6.

A Overview of definitions and symbols

The following list provides the definitions and symbols that are used for different parameters and properties that are discussed in this thesis. Often a distinction is made between total, average and specific value.

Parameter/Property	Definition	Symbol
(Total) Shear stiffness	The shear stiffness of the connection is defined by the total vertical force that is transferred by the diagonals divided by the average relative vertical displacement over the joint. This quantity is determined per floor.	K_v
Average shear stiffness	The total shear stiffness per diagonal. It is defined by the total shear stiffness divided by the number of diagonals.	k_v
Specific shear stiffness	The specific shear stiffness of a single diagonal. Defined by the vertical component of the axial force in the diagonal divided by its vertical displacement difference.	$k_{v,i}$
(Total) Lateral stiffness	The lateral stiffness of the connection is defined by the total horizontal force that is a result of the inclined force in the diagonal bars divided by the average relative horizontal displacement between the elements. The quantity is determined per floor.	K_h
Average lateral stiffness	The lateral stiffness per diagonal. It is defined by the total lateral stiffness divided by the number of diagonals.	k_h
Specific lateral stiffness	The specific lateral stiffness of a single diagonal. Defined by the horizontal component of the axial force in the diagonal divided by its horizontal displacement difference.	$k_{h,i}$
(Total) Diagonal stiffness	The summation of all specific diagonal stiffness values. It can be calculated directly by dividing the summation of all axial forces by the average diagonal displacement.	K_d
Average diagonal stiffness	The total diagonal stiffness per diagonal. It is defined by the total diagonal stiffness divided by the number of diagonals. If all diagonals have the same specific diagonal stiffness, the average diagonal stiffness is equal to the specific diagonal stiffness.	k_d
Specific diagonal stiffness	The axial stiffness of the diagonal bar that is defined by the young's modulus of the mortar times the cross-sectional area of the bar divided by the length of the bar.	$k_{d,i}$
Average vertical displacement difference	The average of the difference in vertical displacement between the two end nodes of each diagonal.	U_y
Specific vertical displacement difference	The difference in vertical displacement between two end points of a specific diagonal ($D_{yi,2}$-$D_{yi,1}$).	$U_{y,i}$
Average horizontal displacement difference	The average of the difference in horizontal displacement between the two end nodes of each diagonal.	U_x
Specific horizontal displacement difference	The difference in horizontal displacement of the two end points of a specific diagonal ($D_{xi,2}$-$D_{xi,1}$).	$U_{x,i}$
Average diagonal displacement difference	The average of the difference of the displacement in axial direction between the end nodes of each diagonal.	U_d
Specific diagonal displacement difference	The difference of the displacement between the two end points of a specific diagonal in axial direction.	$U_{d,i}$
Local vertical displacement	The vertical displacement of diagonal i at endpoint j.	$D_{yi,j}$
Local horizontal displacement	The horizontal displacement of diagonal i at endpoint j.	$D_{xi,j}$
Total diagonal force	The summation of axial forces acting in each diagonal bar.	F_d

Specific diagonal force	The axial force acting in a single diagonal.	$f_{d,i}$
Total horizontal force	The summation of the horizontal components of all diagonal forces.	F_h
Specific horizontal force	The horizontal component of the axial force of a single diagonal	$f_{h,i}$
Total vertical force	The summation of the vertical components of all diagonal forces.	F_v
Specific vertical force	The vertical component of the axial force of a single diagonal.	$f_{v,i}$
The support stiffness	The stiffness that is assigned to the spring supports in the bar model. This stiffness is provided by the surrounding concrete elements and the transverse reinforcement	K_{sup}
The bending stiffness	The bending stiffness of the Timoshenko beam that models the precast concrete elements. The bending stiffness is therefore a measure of the in-plane stiffness of the precast elements.	K_b
Total cross-section of the diagonals	The summation of all cross-sectional areas of the diagonals.	A_d
Specific cross-sectional area	The cross-sectional area of a single diagonal	$A_{d,i}$
Young's modulus of the mortar	The Young's modulus that is given to the bar that models the compression diagonal in the mortar joint.	E_d
Length of the diagonal	The length of the bar that models the compression diagonal.	L_d
Angle of the diagonal	The angle between the bar and the vertical axis.	α
Height of the diagonal	The difference in vertical y-coordinate between both end-points of the diagonal	h_y
Width of the diagonal	The difference in horizontal x-coordinate between both end-points of the diagonal	h_x
Young's modulus of steel	The Young's modulus that is assigned to the bars that model the transverse reinforcement.	E_s
Cross-section of the transverse reinforcement	The cross-sectional area that is assigned to the bars that model the transverse reinforcement.	A_R
Transverse spring stiffness	The axial stiffness of the reinforcement that is defined by the cross-sectional area times the young's modulus of steel divided by the length of the reinforcement that transfers an axial force.	K_s
Young's modulus of the precast elements	Young's modulus assigned to the concrete wall elements.	E_c
Height of the openings	Height given to the openings in the wall elements.	h
Column width	Width of the precast concrete element between the joint and the openings.	a
Wall thickness	The width of the precast concrete elements.	t
Load angle beta	The angle under which the transferred load arrives at the upper end-point of the diagonal	β
Load angle gamma	The angle of the transferred load at the lower end-point of the diagonal	γ

B Validation of the small test setup model

This appendix contains the results of the mesh size sensitivity study and the sanity checks that were performed on the small test setup model in DIANA 10.2.

The mesh is built up of rectangular elements, of which the size is varied between 10 and 400 mm. Figure B.1 shows the relation between the normalised shear stiffness and the element size for a model with M24 bars. The normalised shear stiffness is calculated by dividing the resulting shear stiffness of the model with a certain mesh size, by the resulting stiffness of the model with a mesh size of 400 mm. In this way the result corresponding to a mesh size of 400 mm is given index 1. When the analysis is performed with a size of 10 mm, the normalised shear stiffness still has index 0.96, as Figure B.1 shows. This shows the shear stiffness of the model is hardly influenced by the applied mesh size. The total shear stiffness is calculated by dividing the total vertical force that is transferred by the three diagonals by the average vertical displacement difference.

Eventually an element size of 50 mm was chosen, since for this size the stresses in the elements around the diagonal bars were close to the stress in the bars and the stress distribution over the model in total shows a smooth behaviour. Figure B.2 shows the stress distribution of Syy for a mesh size of 50 and 100 mm. The smoother results of the smaller mesh are clearly visible.

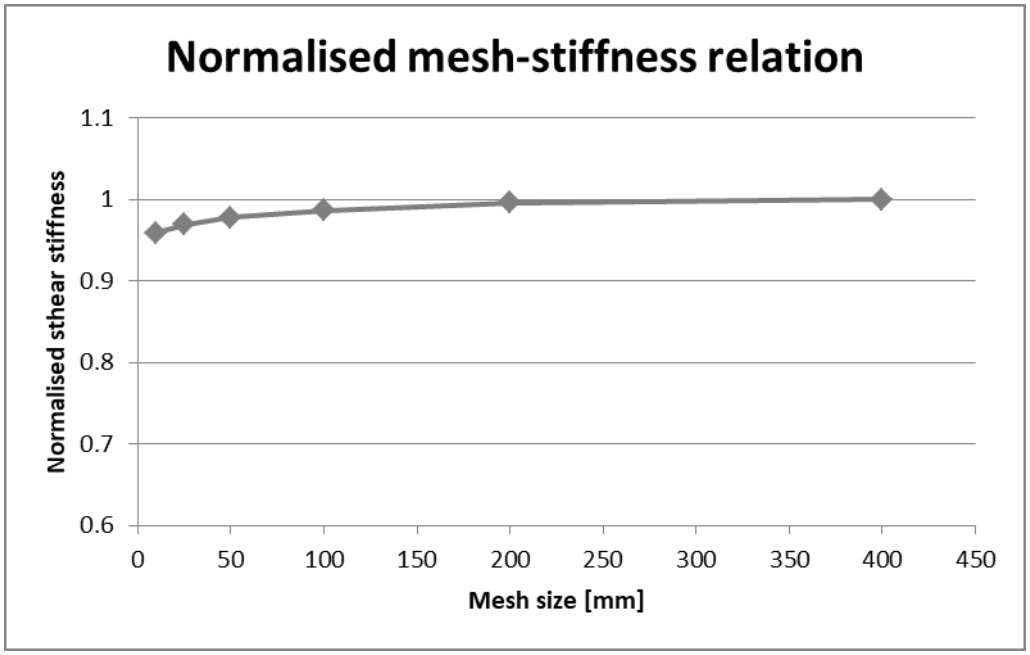

Figure B.1 Mesh size dependency for the small model (M24)

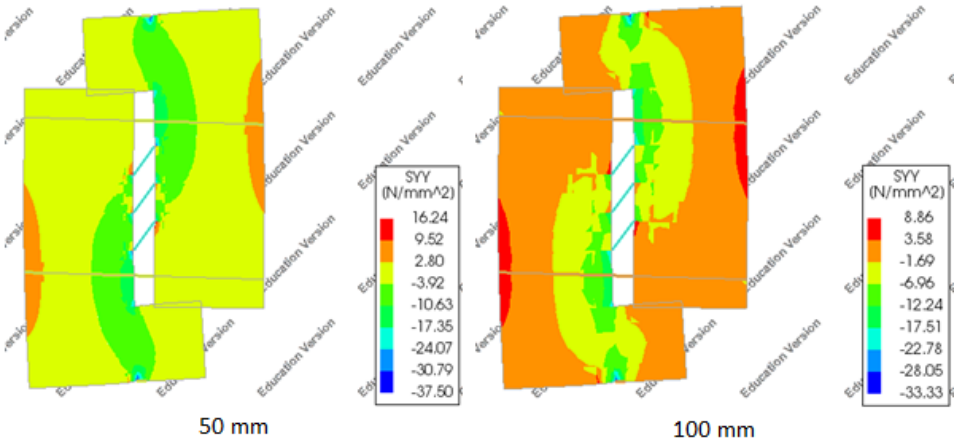

Figure B.2 Stress distribution by a mesh size of 50 and 100 mm for the small model (M24)

Table B.1 Equilibrium checks (M24) shows the state of equilibrium in the model with an element size of 50 mm. It can be concluded that the vertical reaction force is equal to the vertical component of the diagonal forces. The horizontal force in the bars almost make equilibrium with the horizontal component of the diagonal forces. The horizontal supports that must be applied to create a stable model take some of the horizontal load.

Since the model is exactly symmetric in the centre point, the results must also show this. The force in the upper and lower diagonal are equal to each other. The stress distributions in Figure B.2 are also symmetric.

	Diagonal forces [N]			**Reaction forces [N]**		**Reinforcement [N]**
	Axial	**Horizontal**	**Vertical**	**Horizontal**	**Vertical**	**Horizontal**
	-12090	-3025	-11705	1770	12479	3987
	-10821	-2707	-10477	-5101	17900	3987
	-12090	-3025	-11705	4115	3508	
SUM	**-35001**	**-8756**	**-33887**	**783**	**33888**	**7973**
Horizontal equilibrium						
diagonal+reinforcement+reaction			0			
Vertical equilbrium						
diagonal+reaction			1			
(All forces in Newton)						

Table B.1 Equilibrium checks (M24)

C Development of the wall detail model

This appendix contains the description of the wall detail model that was developed for the parameter study. However, the resulting behaviour of the model was concluded to resemble to a compression test instead of a shear test. Therefore it's resulting parameter relations deviated from the other two models.

Geometry

Figure C.3 shows the geometry of the model that is used. The model consists of two mirrored surface elements that are connected by diagonal bars in the 50 mm wide gap between the elements. Furthermore at the top and bottom edge of the model a horizontal line element is spanning the gap, this element is modelling the transverse reinforcement.

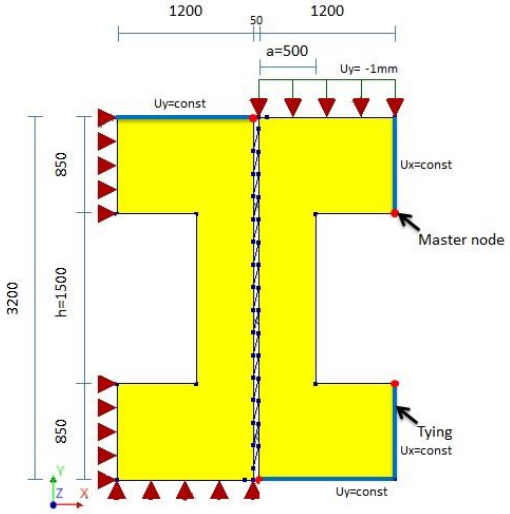

Figure C.3 Geometry of the single floor model

The concrete surface elements contain a recess that represents a window opening in the wall element. The height of this window opening, h, is one of the parameters that is investigated. Even so is the column width, a, a parameter that is investigated. The presented geometry in Figure C.3 shows the standard values.

The boundary conditions should simulate the loading state and support conditions that occur when the model is part of a complete shear wall. Figure C.4 shows a part of a shear wall with a stacked element configuration that is loaded horizontally. The dashed square marks the part of the wall that is modelled.

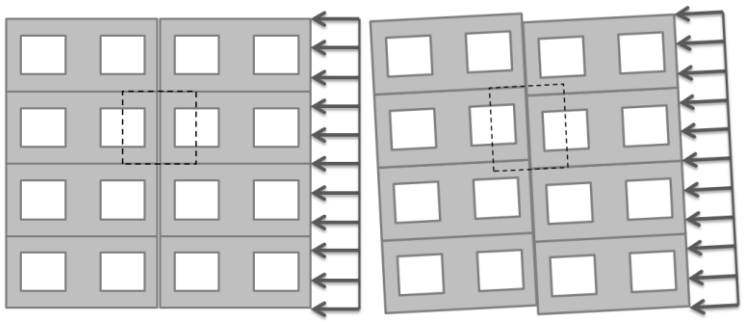

Figure C.4 The conditions in a shear wall

The image on the right hand side illustrates the state of deformation of the same part of the shear wall. Due to the bending deformations, the precast elements will slightly rotate, whereby slip translations occur in the interface. In order to simulate this loading state, specific boundary conditions are set for the model, as can be seen in Figure C.3.

First of all, the model is loaded by a prescribed downward displacement of 1 mm along the upper right horizontal edge. Application of the load at this location corresponds to the situation with a horizontal wind load coming from the right side of the wall, as indicated in Figure C.4. The vertical support is applied at the lower left horizontal edge. Thereby the translation of the left element is set to zero. This means that all slip displacements that occur in the wall are lumped into the applied load on the right element.

Secondly, horizontal supports are required to obtain a stable model. However, supporting the right concrete element horizontally will prevent the development of tying forces in the transverse bars. So in order to be able to investigate the effect of changing the cross-sectional area of the transverse reinforcement, horizontal supports may only be applied on the left concrete element.

Furthermore, some boundary conditions must be set for the unsupported edges as well. The two horizontal edges in the upper left and lower right corner of the model cannot translate in vertical direction, since this deformation will be obstructed by the adjacent concrete elements that are present in a complete shear wall. In order to keep the two edges horizontal, so called tyings are applied. These dictate the vertical displacement on each point of the edge to be equal to the vertical displacement of the "master node" that is selected. The tyings are indicated by the blue lines in Figure C.3, the corresponding master nodes are indicated by the red dot. The lower part of the right element tends to rotate downwards, which will in reality also be resisted by shear forces in the concrete below the window opening in the concrete element itself. However, since not the whole element is modelled and the right vertical edges are unsupported, this resisting shear force doesn't develop in the model. The applied tying at this location prevents the rotation.

As can be seen in Figure C.3, tyings are also applied on the two vertical edges of the right element. These are present because the other part of the concrete element that is not included in the model will prevent large horizontal displacement differences along this edge. For this reason they are kept straight as well.

Mesh sensitivity

In order to determine a proper mesh size to use, a sensitivity study is performed. This is done in the same way as for the test setup model. The mesh is going to be built up by mostly rectangular quadratic plane stress elements. Their size is varied between 15 and 400 mm.

Figure C.5 shows the shear stiffness' normalised dependency on the mesh size. The shear stiffness obtained by a mesh size of 400 mm is given index 1. As can be seen, also for this model the variation of the shear stiffness is rather limited. The range of the mesh size is quite large, but the variation of the stiffness is just slightly more than 10 percent. A model with a large mesh size dependency is very unfavourable. This can for example occur when point loads or displacements are applied, but in this case this is purposely avoided.

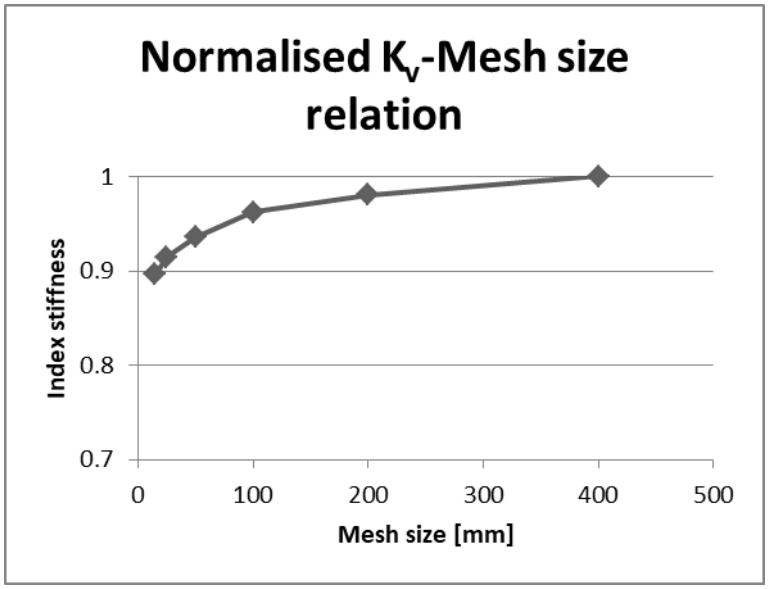

Figure C.5 K_v-Mesh size dependency

The laterals stiffness appears to be far more dependent on the mesh size, as Figure C.6 shows. With a mesh size of 15 mm the lateral stiffness is just 68 percent of the largest value. So for the lateral stiffness it is more important to choose a proper mesh size.

In order to choose a mesh size, the occurring stress peaks in the elements around the end points of the diagonals are also considered. The stress in these elements should have the same order of magnitude as the stress that occurs in the adjacent diagonal bar itself. Table C.2 shows the stress in vertical direction in the diagonal bars and the minimal and maximal stress in the adjacent surface elements. As the table shows, large stresses occur in the elements with a small mesh size. For a mesh size of 400, 200 and 100 mm the minimum stress in the elements is not far from the stress in the diagonal. However, elements with a size of 400 or 200 mm are rather coarse. Therefore a mesh size of 100 mm is going to be applied. This might lead to a slightly underestimated lateral stiffness.

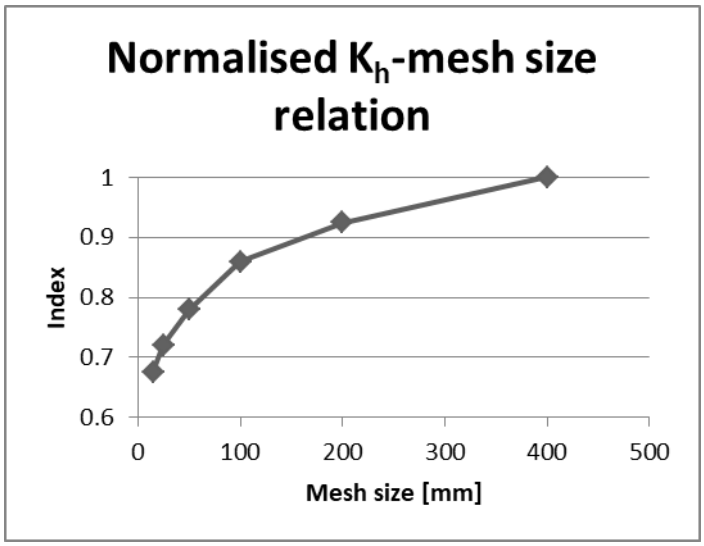

Figure C.6 K_h mesh size dependency

Mesh size	Syy dia	Syy max	Syy min
400	-30.4	13.0	-28.5
200	-30.4	9.6	-31.7
100	-29.7	13.8	-36.9
50	-28.7	24.8	-46.6
25	-27.6	47.0	-74.9
15	-26.8	75.0	-113.1

Table C.2 Peak stresses in the elements

Sanity checks

In order to validate the model, some sanity checks were performed. The checks for horizontal and vertical equilibrium are summarised in Table C.3. As can be seen, the horizontal equilibrium of forces doesn't count up to zero. The horizontal reaction force should be zero as well, since there is no horizontal load applied on the model. This is not the case.

Reinforcement	Nx [N]	Diagonal force component	F [N]	Reaction force	R [N]
Bottom	86206	Hor.	-368767	Hor.	-23
Top	282563	Vert.	-1427127	Vert.	1427127
Sum	**368769**				
		Checks			
		Fh-Nx-Rh=0	-20.83	N	
		Fv-Rv=0	0.00	N	

Table C.3 Horizontal and vertical equilibrium check

However, the summed horizontal component of the diagonal forces is approximately 370 kilo newton. So a small deviation of 20 newton seems acceptable.

The equilibrium of moments was also checked before the model was used for further analysis. Table C.4 shows the outcome of this sanity check. The load is not applied right above the vertical support. Due to this eccentricity a moment must be transferred by the connection as well. The load causes a moment of 543 kNm around the centre point of the joint. For external equilibrium,

the horizontal and vertical support reactions must create an equal moment in opposite direction. However, this appears not be the case. Furthermore, the internal equilibrium requires that the moment is transferred by the compression diagonals in the joint and the transverse reinforcement at the outer edges. This equilibrium isn't obtained either.

	Moment external [kNm]		**Moment internal [kNm]**
Load	-543	Load	-543
Vertical support	-492	Reinforcement	314
Horizontal support	644	Diagonals	12
SUM	**-391**	**SUM**	**-217**

Table C.4 Equilibrium of moments for a model with tyings

It is clear the error cannot be neglected or assigned to inaccuracies of processing the output. So what causes the huge error in this equilibrium check? The answer lies in the use of tyings. The tyings dictate a constant displacement over a whole edge of the model. In order to comply with this requirement, forces are acting on the edge. However, these forces induced by the tyings cannot be generated as output and are therefore unknown. In order to check the statement, the rotational equilibrium of a model without tyings has been analysed as well. The results can be seen in Table C.5. Adding all tyings one by one to this model lets the error in the equilibrium increase to the values found in Table C.4. So each tying partly contributes to the found error. Having the lack of equilibrium assigned to this cause, it is okay to use the model with tyings. The equilibrium of the model could be proved if it was possible to obtain the tying forces. Unfortunately DIANA 10.1 doesn't support this function.

	Moment external [kNm]		**Moment internal [kNm]**
Load	-493	Load	-493
Vertical support	-434	Reinforcement	498
Horizontal support	927	Diagonals	-5
SUM	**0**	**SUM**	**0**

Table C.5 Equilibrium of moments without tyings

Evaluation of the model

Based on the sanity checks the model is approved to use. This paragraph discusses the typical behaviour that is observed. In the first section the global behaviour is shown and explained. In the second section some specific aspects of the behaviour are addressed. In that context the applicability of the model will be discussed in more detail.

Global behaviour of the model

Figure C.7 shows the displacement field of the model loaded by a vertical displacement of 1mm along the horizontal edge in the upper right corner. The horizontal displacement field shows clearly that the left element moves a bit to the left and the right element to the right, widening the joint in-between. As can be seen as well, the horizontal displacement field is not symmetric. The horizontal supports that are only present on the left element are causing a difference in behaviour between the two elements. Figure C.8 namely shows the horizontal displacement field of the model when the horizontal supports are also applied on the right element. This displacement field is symmetric in the centre point of the model.

As the results of the real model show, the left element acts approximately as expected conform the behaviour shown in the literature study (Figure C.7). The largest horizontal displacement occurs due to bending in the column between the window opening and the joint. The right element deforms differently. Due to the lack of horizontal supports the two parts above and below the window opening can freely move in horizontal direction. It seems that the element rotates clockwise, due to the eccentricity of the load. The tyings keep most edges straight, but the horizontal displacement increases gradually from bottom to top along the edge connected to the diagonal bars.

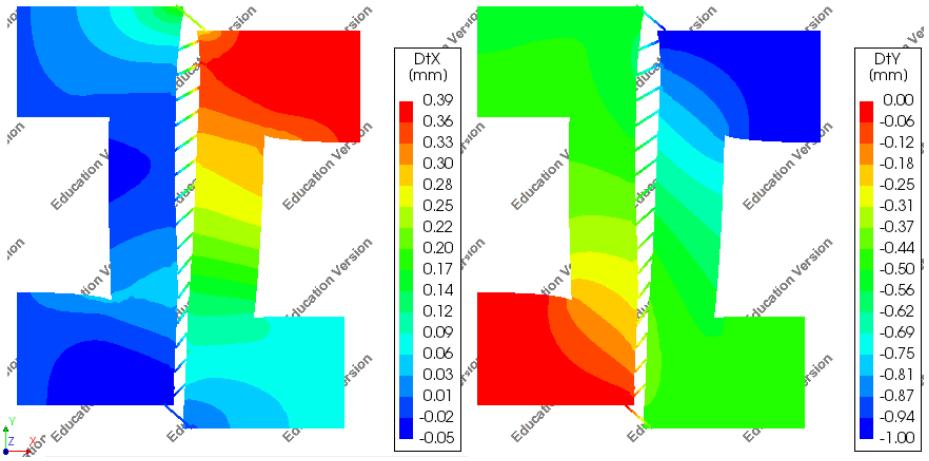

Figure C.7 The displacement field

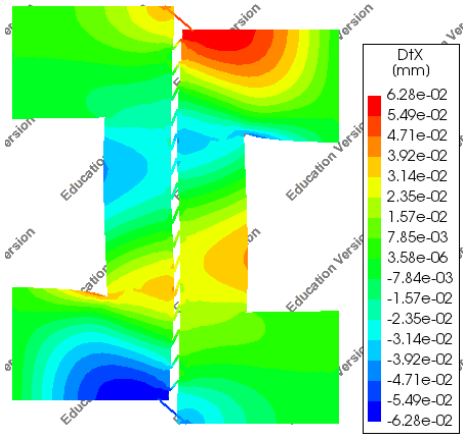

Figure C.8 Horizontal displacement field with supports on two sides

The vertical displacement field is explained more easily. Where the load is applied, the deflection is exactly 1 mm. As the induced force is gradually transferred by the diagonal bars, the vertical translation of the nodes decreases from top to bottom over the right element. The left element can be compared to a bar that is loaded by an axial line load. At the vertical support the translation is equal to zero. At the unsupported side the translation is the largest and inbetween it gradually increases from zero to the maximum value, due to the increasing load coming from the diagonals. The behaviour is almost symmetric in the centre point of the model, with a displacement of 0.50 mm as central value.

When the results for the vertical stress Syy are evaluated, a clear compression diagonal is obtained, as can be seen in Figure C.9. The load is transferred by this compression diagonal through the elements and the diagonal bars to the vertical support at opposite site.

The load is transferred by the diagonal bars, which are not all subjected to an equal axial load. The distribution of axial forces over the diagonals is provided in the graph of Figure C.10. It shows that the largest forces are transferred by the two outer diagonals, whereas the diagonals around half of the floor height transfer the smallest force. This is a result of the present window openings. The shear stress that develops in the mortar joint is distributed in the same way as the diagonal forces in Figure C.10. So producing a shear stress diagram from a model with a continuous joint should result in a similar image as is shown here.

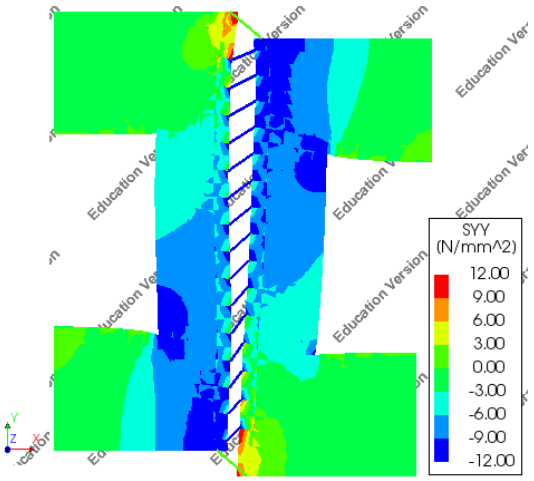

Figure C.9 Syy distribution in the concrete elements

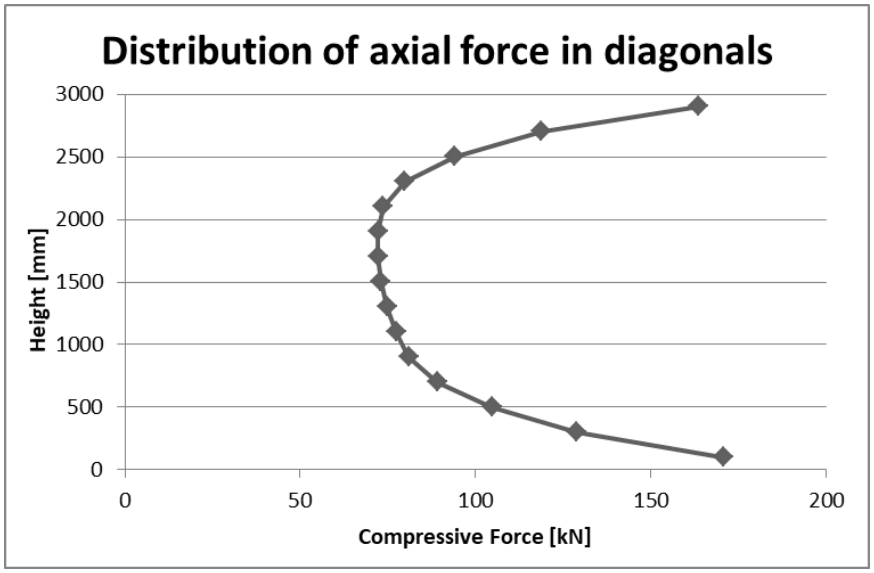

Figure C.10 Axial diagonal force distribution

Specific aspects of the behaviour

This section discusses two important specific aspects of the behaviour. The first aspect is the effect of the load eccentricity on the connection. The second aspect is the horizontal displacement of the elements that deviates from the expected pattern.

The effect of the load eccentricity

As mentioned previously, the load is applied eccentrically from the vertical support. Because the right element is loaded and the left is supported, the connecting diagonal bars need to transfer

the load, whereby the connection can be analysed. This shear force will also develop in a complete shear wall, but the accompanying moment will not.

Figure C.11 shows the two wall elements and the vertical load and support in a schematic way. The two elements will move apart by a distance Ux average, as a result of the horizontal component of the diagonal force. Due to the applied load, the right element will rotate as well. This rotation will at the bottom edge decrease the widening of the joint by Ux rotation, whereas at the top edge the joint is widened by Ux rotation. The left element will stay in place, since the supports prevent any rotation.

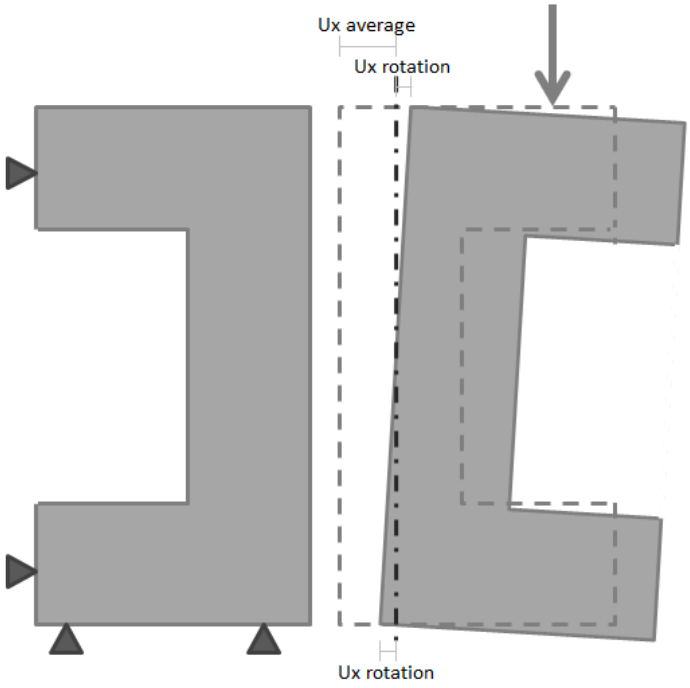

Figure C.11 Rotation of the loaded element

The difference in horizontal displacement over the height of the joint that is caused by this rotational displacement, influences the force distribution in the diagonal bars. A pure widening of the joint will lead to a tensile force in the diagonal bars. However, the vertical displacements are relatively large, whereby all the diagonals are under compression and the widening of the joint only lowers the compressive axial force. Because of the rotational displacements, the joint widens more at the top side, resulting in smaller compressive forces here compared to the lower side. The axial force distribution in Figure C.10 is in accordance with this behaviour. The compressive forces are smaller at the top edge and the minimum occurs above half the height of the connection. Table C.3 also shows that a larger tensile force is present in the top reinforcement bar, which also corresponds with the behaviour that is described here.

When the horizontal displacement of the end-points of the diagonal bars that are located on the edge of the loaded element are plotted against the y-coordinate of the end-points' locations, the approximate linear displacement distribution is clearly seen. The deviating result of the upper node is caused by the tensile force in the reinforcement that is located nearby.

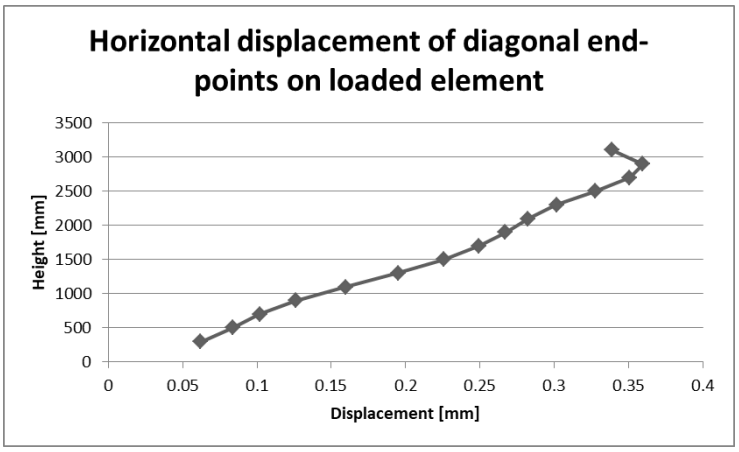

Figure C.12 Horizontal displacement distribution for the loaded element

The rotation also influences the slope of the diagonal bars. The lower diagonals become steeper than the initial slope, the upper diagonals will become flatter. This also influences the force distribution over the diagonal bars, since a steeper diagonal acts stiffer, as described in chapter 4. However, this effect is only taken into account when a geometric nonlinear analysis is performed. The linear analysis applied in this parameter will always calculate the structural response based on the initial slope of the diagonal bars.

Does the whole effect have a significant influence on the resulting lateral and shear stiffness? This may be, but the two stiffness values are determined based on average displacement differences. If the rotational displacement is exactly linearly distributed, the average displacement difference is equal to the displacement caused by the horizontal respectively vertical component of the diagonal force only. So the rotation of the element may only have a significant contribution if it directly influences the stiffness of the whole model, resulting in a different force that develops by a displacement load of 1 mm. However, since the whole parameter study is performed on a single model and only the relative results are discussed, any rotational effect is not very important for this study. In earlier chapters it was already concluded that the resulting values for the lateral and shear stiffness cannot directly be assigned as “the connection stiffness”.

Horizontal displacement along the connection edge

It may have come to notice by studying Figure C.7, that the nodal horizontal displacement along the joint edge of the left element is not completely as the theoretical model, that has been described in the literature study, suggests. Figure C.13 shows the horizontal displacements of the left element in detail, with an illustration of the theoretical deformation next to it. Theoretically the whole left element should move in negative x-direction, whereby the column next to the window opening should displace more, as a result of a lower lateral stiffness. However, the results show two parts of the element that are moving in opposite direction.

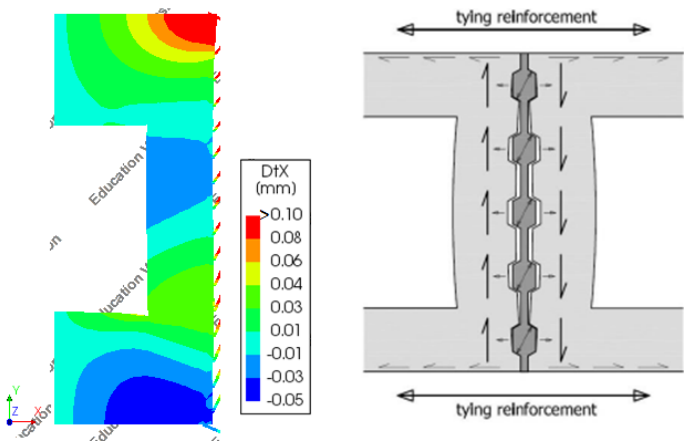

Figure C.13 Left: Horizontal displacement field in the left element Right: Theoretical behaviour

The nodes at the top move in opposite direction as a result of the locally applied tensile force in the transverse bars. This is a result of the chosen way to model this reinforcement. At the lower side of the window opening there is also a region that moves in positive x-direction. This is in conflict with the expected behaviour.

When the diagonal forces are decomposed in a horizontal and vertical component, the concrete element is basically loaded by two line loads. A vertical load acts along the edge and a horizontal line load acts perpendicular to the edge. It is obvious that the horizontal line load will lead to horizontal displacements in negative x-direction, partly because the transverse reinforcement elongates, resulting in a widening of the joint and partly because the concrete element bends, especially along the small column part. The latter behaviour can be compared with a simply supported beam subject to a line load. The vertical line load will also have an effect on the horizontal displacement field that develops in the element. This influence appears to be the cause of the horizontal displacements in positive x-direction.

Three tests were performed in order to confirm this statement. Figure C.14 shows the test setups that were used. In the first case, a simply supported beam loaded by a line load along its outer fibre is analysed. The second test comprises an element similar to the wall elements of the parameter study model subjected to a vertical line load along its edge. The third test simulates the loading state that occurs with the attached diagonal bars, whereby a vertical and horizontal line load are present along the edge.

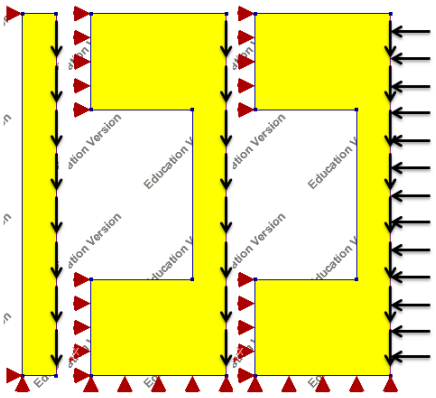

Figure C.14 Test models

The resulting deformations are found in Figure C.15. It is clearly visible from the first two tests that a vertical line load results in horizontal displacements in the positive x-direction. The behaviour of the third model is comparable to that of the element in the parameter study model.

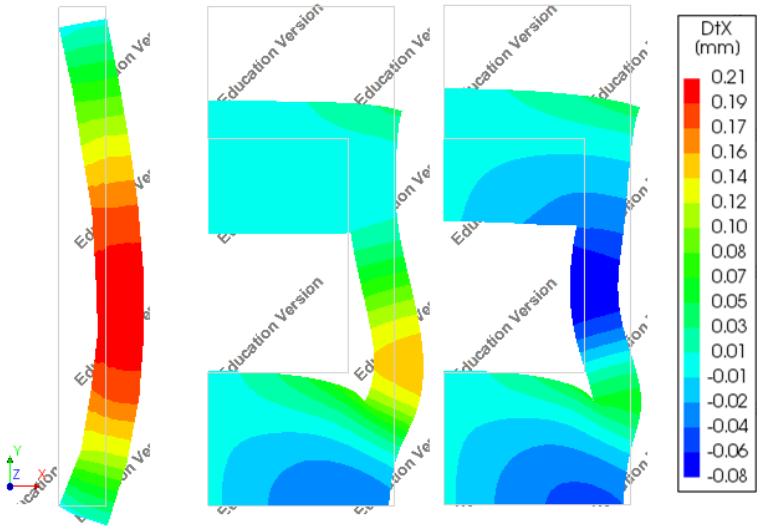

Figure C.15 Test results horizontal nodal displacements

When the bending stiffness of the column is enlarged by making it wider, the horizontal displacements decrease in both directions. When the column width is smaller, the deformations in both directions increase. This leads to a particular relation between the parameter a and the lateral and shear stiffness of model 3. This relation is shown in next appendix. This results shows that for smaller values of parameter a the stiffness increases. This is a result of the increased deflection in positive x-direction, that reduces the average dilatation over the joint U_x.

This particular behaviour doesn't correspond to that found in literature. It resembles the behaviour of a compression test. It is one of the reasons why this model is considered to be infeasible for the performed research.

D Stress distribution along model boundaries

This appendix contains an overview of the shear stress distributions along different sections. The distributions are shown for model 1 and model 2. Since the sections are made along the outer contours of model 3, plotting the shear stresses for model 3 results in distributions where the stress is almost equal to zero along the free edges, but along the supported edges as well.

Model 1

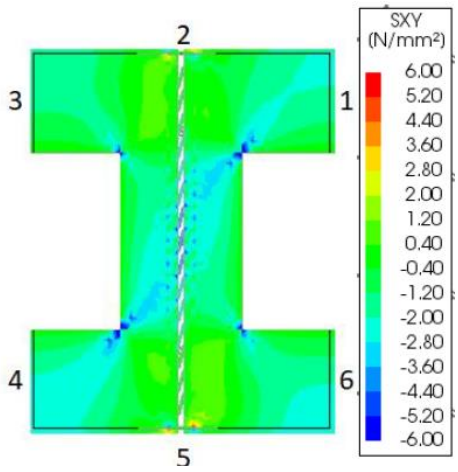

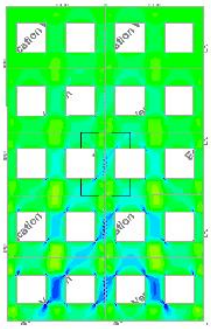

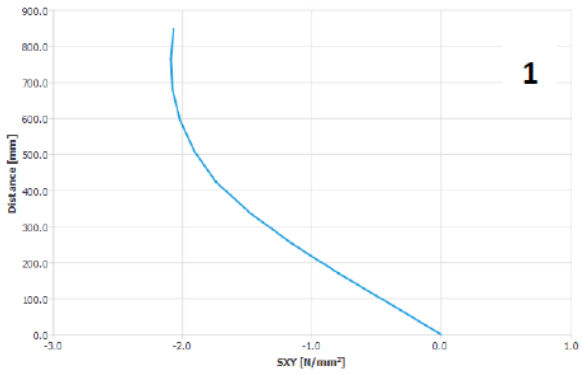

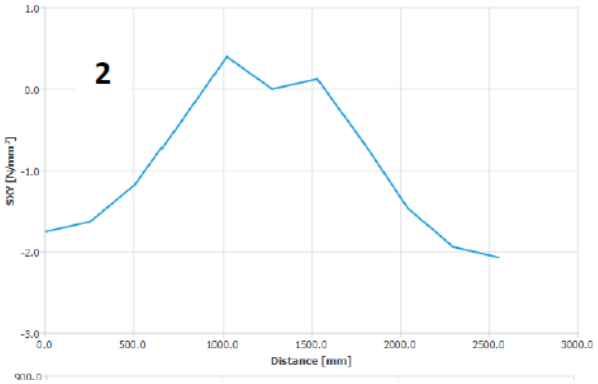

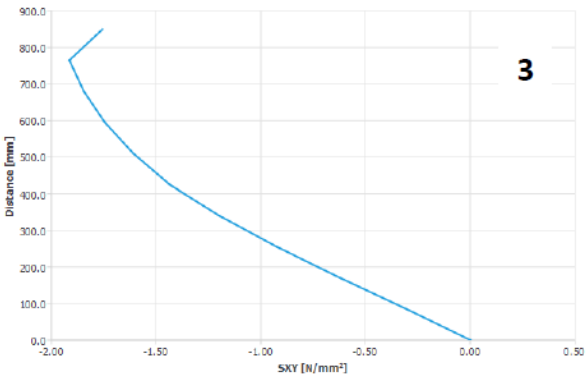

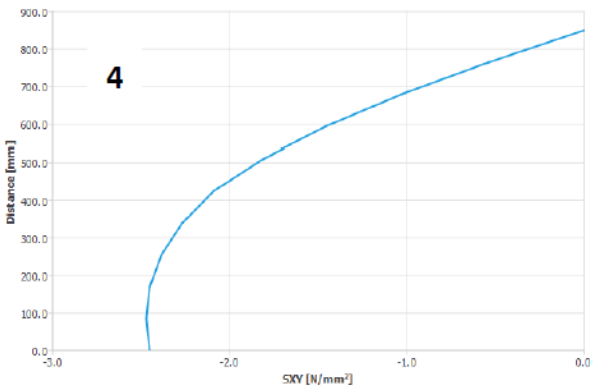

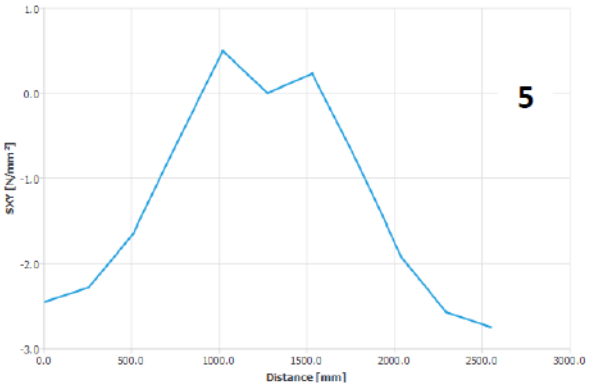
5
SXY [N/mm²]
Distance [mm]

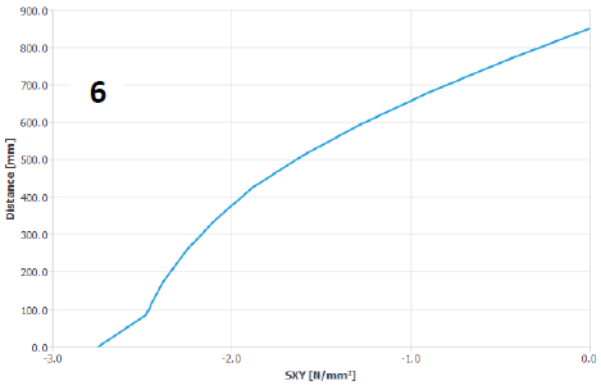
6
Distance [mm]
SXY [N/mm²]

Model 2

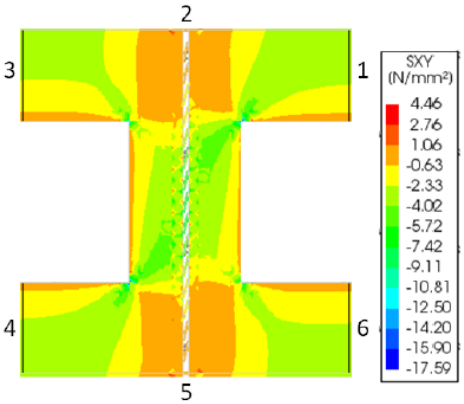
2
3
1
4
6
5
SXY (N/mm²)
4.46
2.76
1.06
-0.63
-2.33
-4.02
-5.72
-7.42
-9.11
-10.81
-12.50
-14.20
-15.90
-17.59

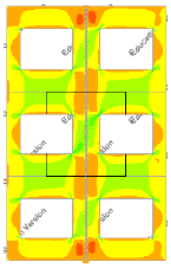

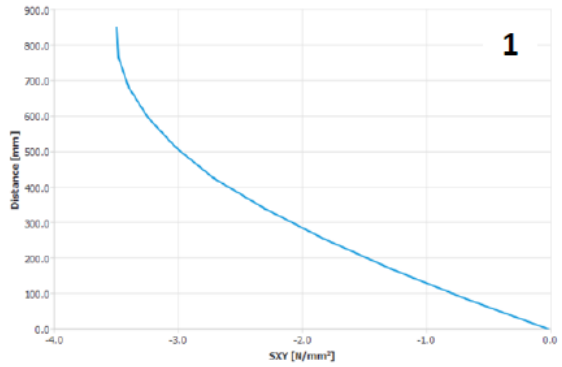
1
Distance [mm]
SXY [N/mm²]

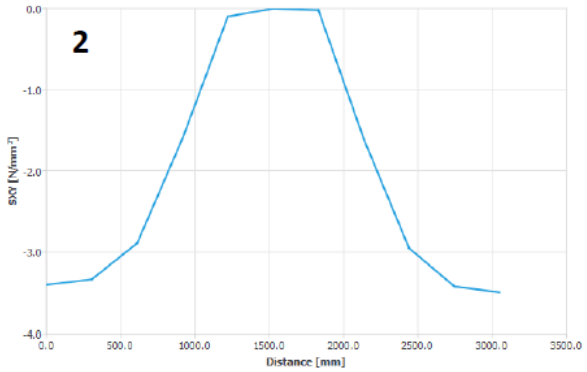
2
SXY [N/mm²]
Distance [mm]

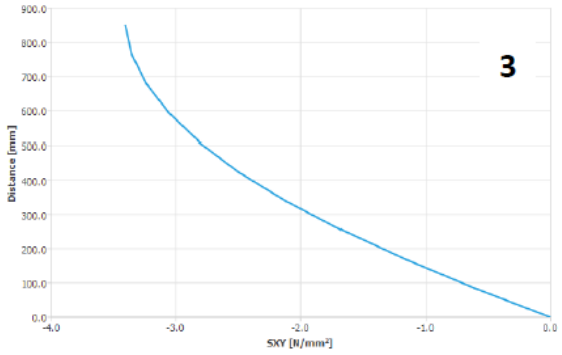
3
Distance [mm]
SXY [N/mm²]

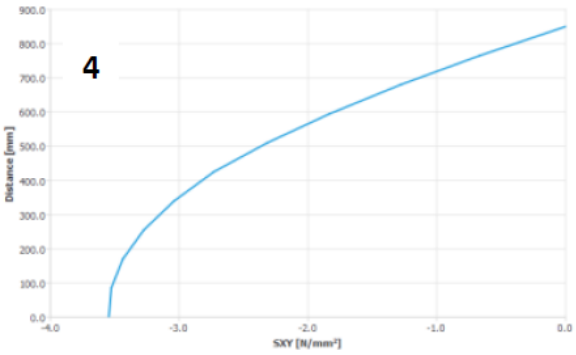
4
Distance [mm]
SXY [N/mm²]

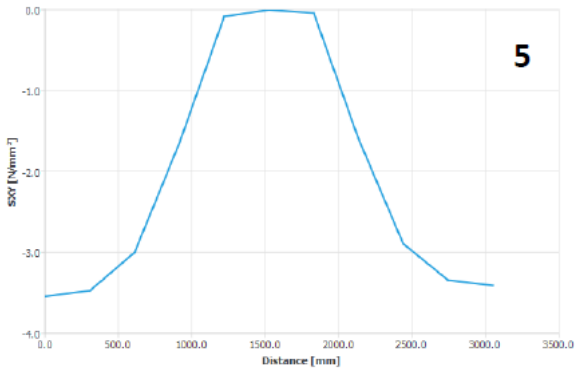
5
SXY [N/mm²]
Distance [mm]

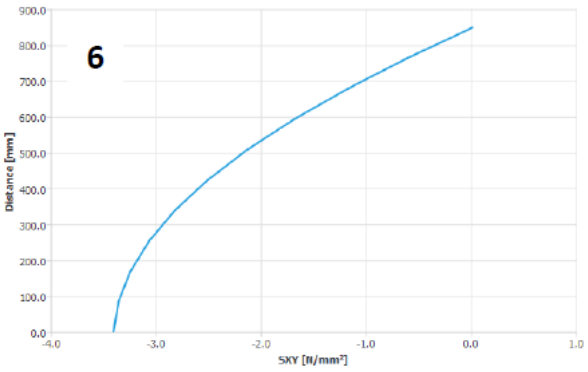
6
Distance [mm]
SXY [N/mm²]

Model 3

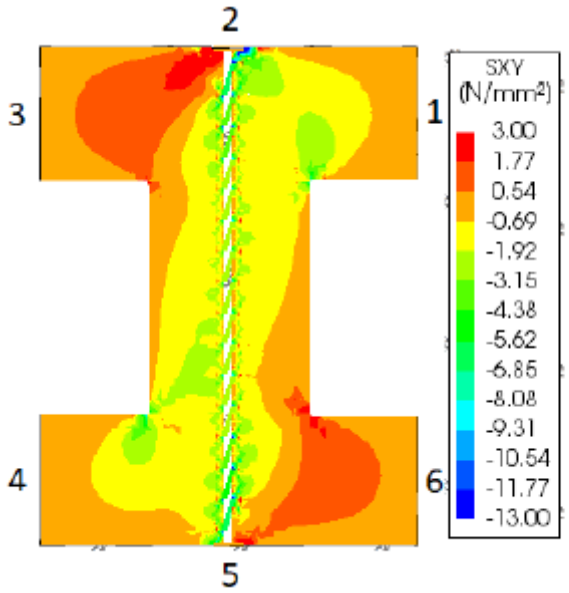
2
3
1
4
6
5
SXY
(N/mm²)
3.00
1.77
0.54
-0.69
-1.92
-3.15
-4.38
-5.62
-6.85
-8.08
-9.31
-10.54
-11.77
-13.00

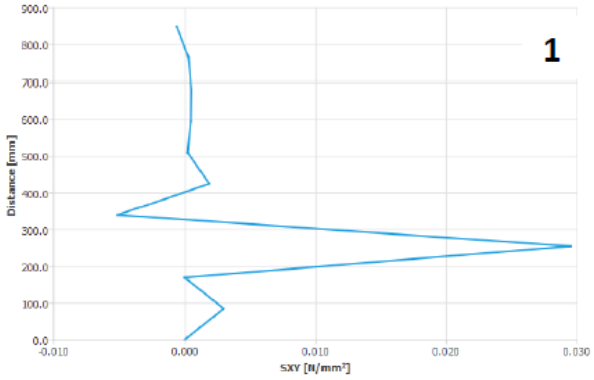
1
Distance [mm]
SXY [N/mm²]

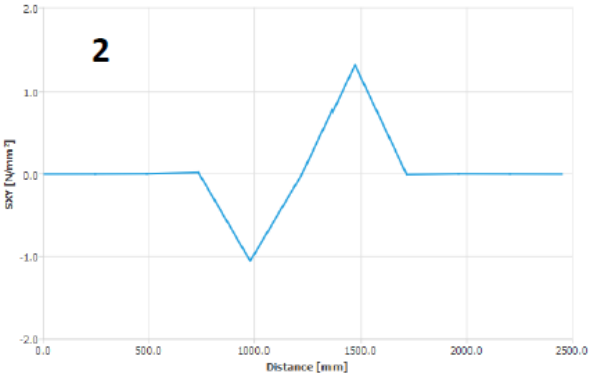
2
SXY [N/mm²]
Distance [mm]

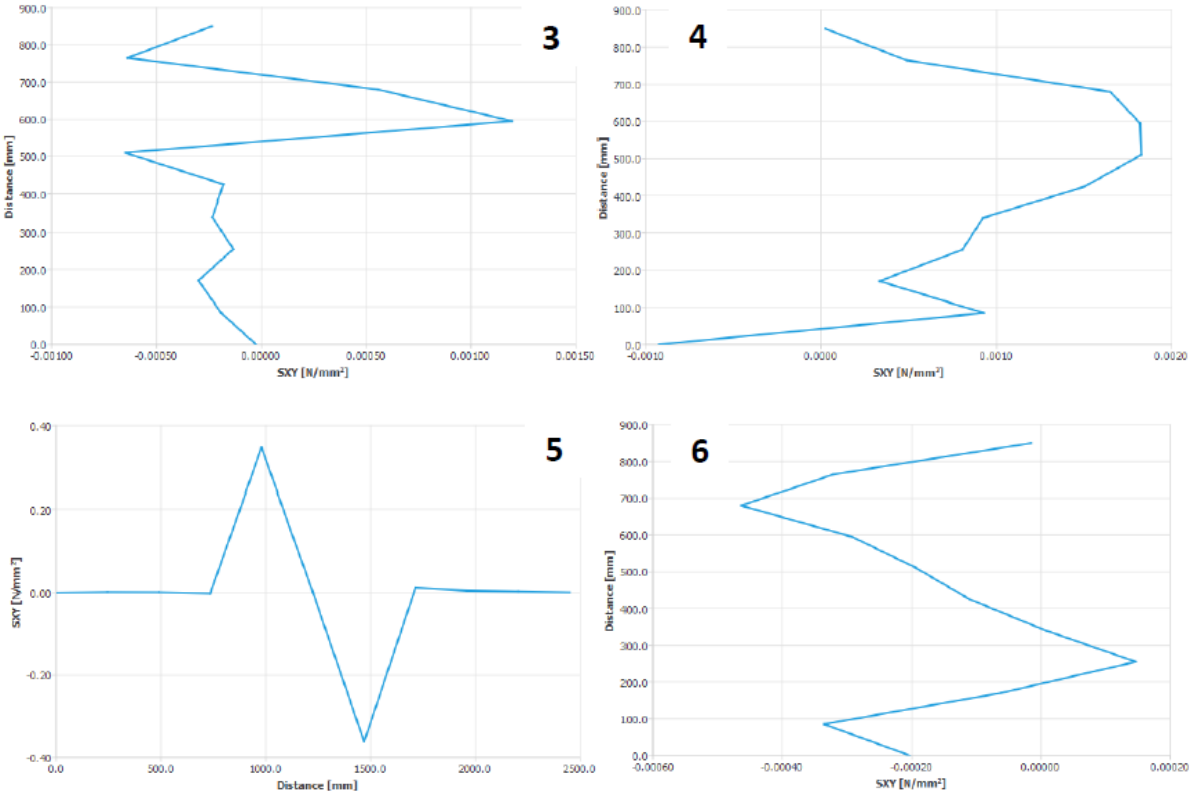
3
Distance [mm]
SXY [N/mm²]
4
Distance [mm]
SXY [N/mm²]
5
SXY [N/mm²]
Distance [mm]
6
Distance [mm]
SXY [N/mm²]

E Parameter influence in different models

This appendix contains the parameter study results for all three models that were developed.

Results parameter study Model 1

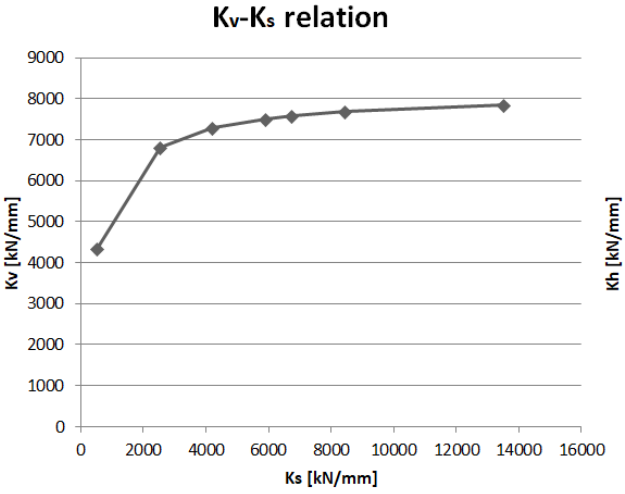

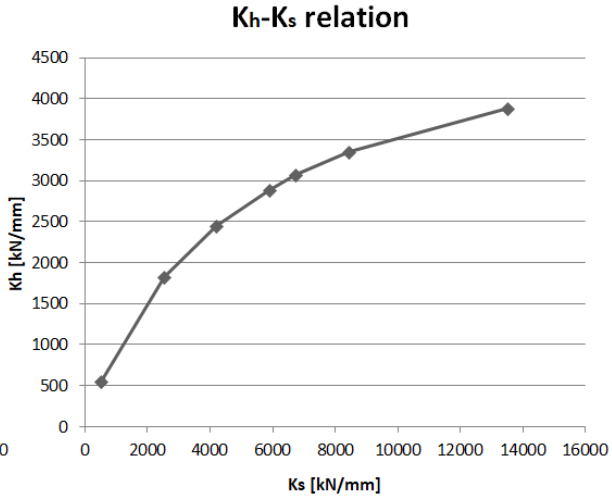

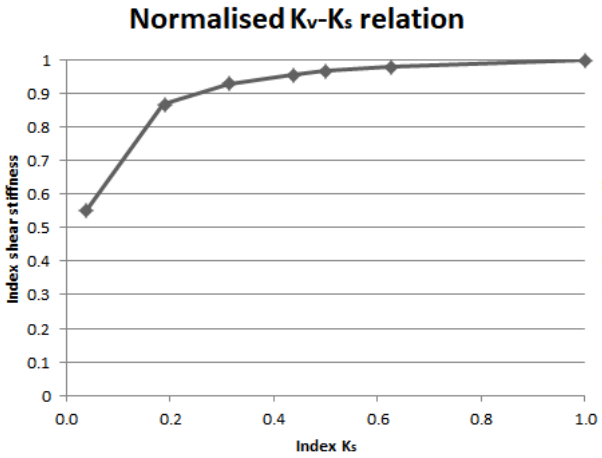

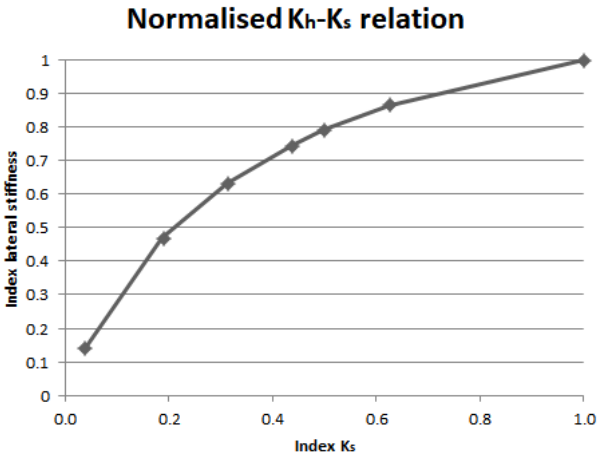

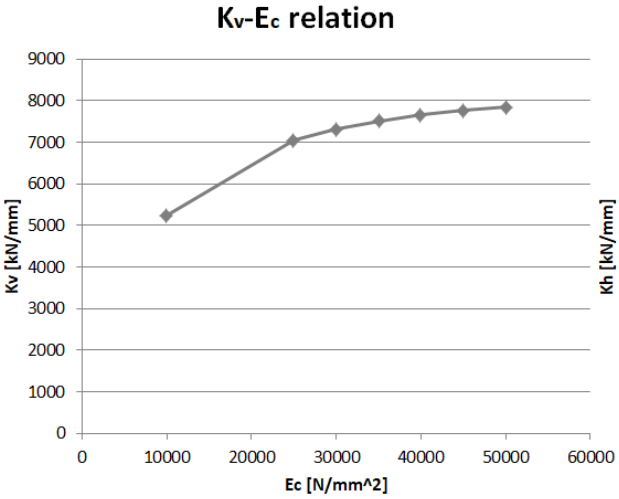

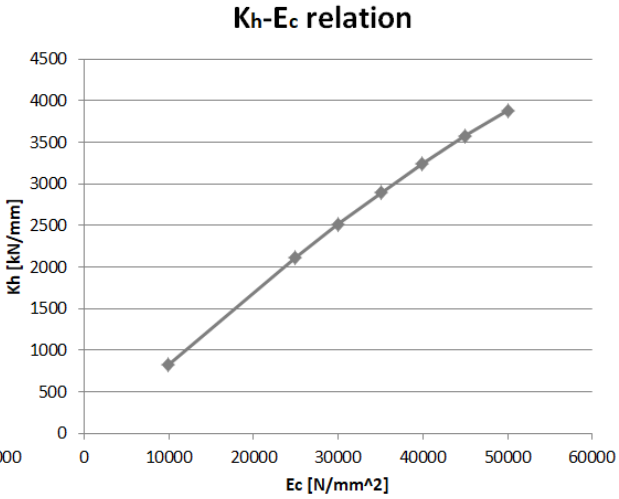

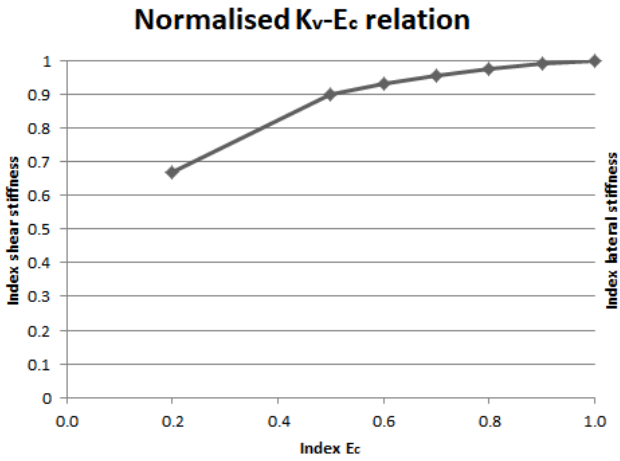
Normalised Kv-Ec relation
Index shear stiffness
Index Ec
0
0.1
0.2
0.3
0.4
0.5
0.6
0.7
0.8
0.9
1
0.0
0.2
0.4
0.6
0.8
1.0

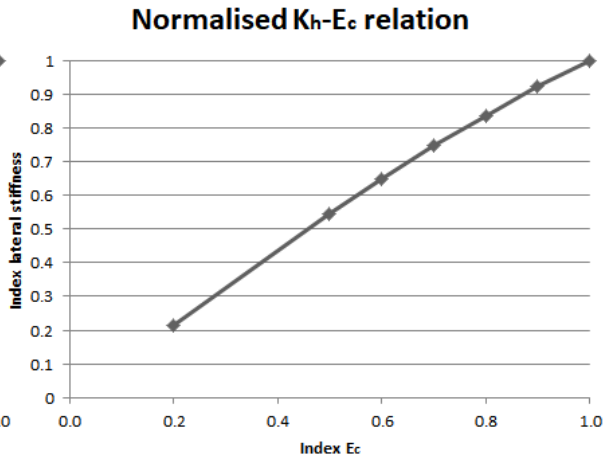
Normalised Kh-Ec relation
Index lateral stiffness
Index Ec
0
0.1
0.2
0.3
0.4
0.5
0.6
0.7
0.8
0.9
1
0.0
0.2
0.4
0.6
0.8
1.0

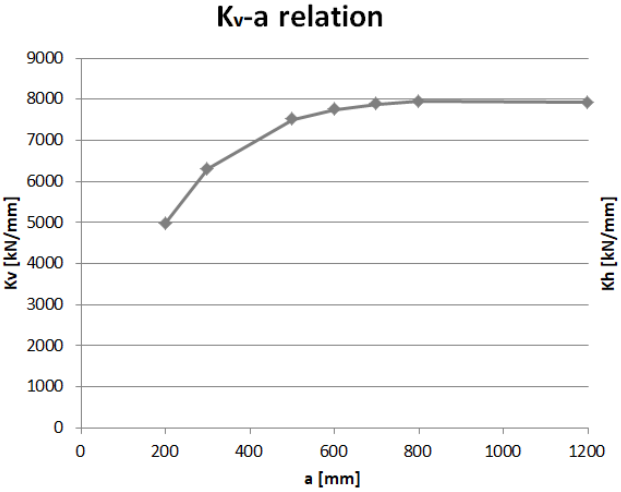
Kv-a relation
Kv [kN/mm]
a [mm]
0
1000
2000
3000
4000
5000
6000
7000
8000
9000
0
200
400
600
800
1000
1200

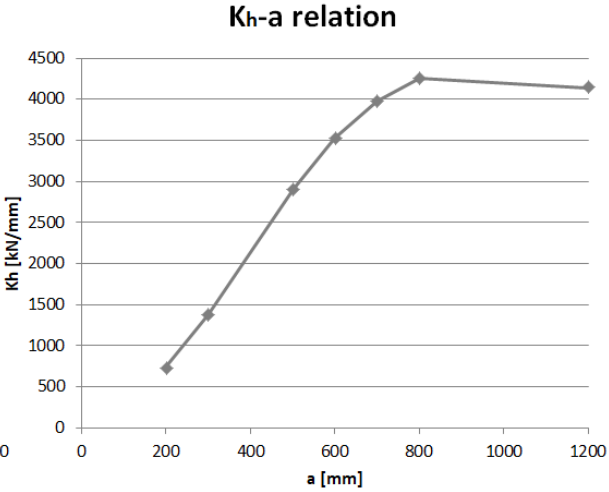
Kh-a relation
Kh [kN/mm]
a [mm]
0
500
1000
1500
2000
2500
3000
3500
4000
4500
0
200
400
600
800
1000
1200

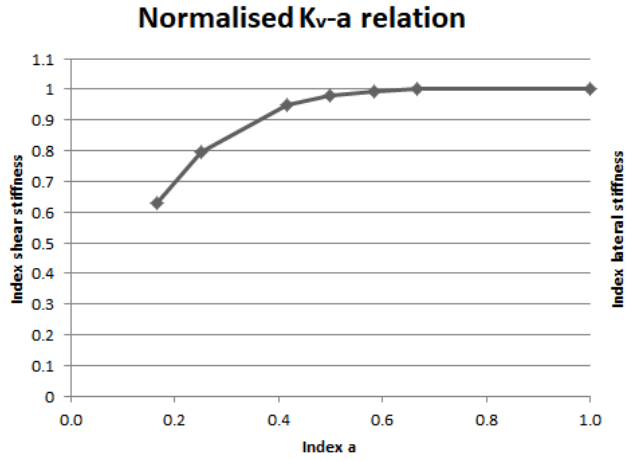
Normalised Kv-a relation
Index shear stiffness
Index a
0
0.1
0.2
0.3
0.4
0.5
0.6
0.7
0.8
0.9
1
1.1
0.0
0.2
0.4
0.6
0.8
1.0

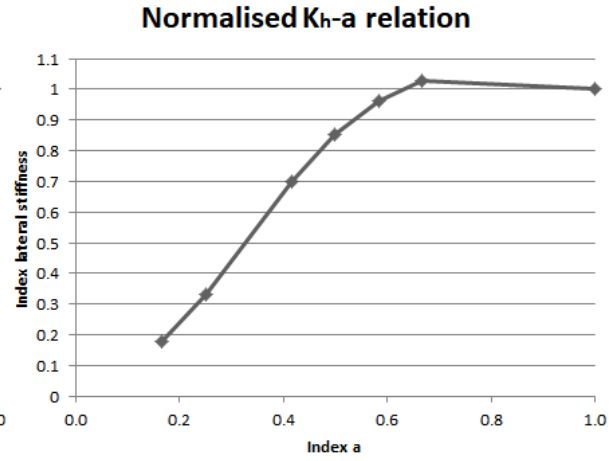
Normalised Kh-a relation
Index lateral stiffness
Index a
0
0.1
0.2
0.3
0.4
0.5
0.6
0.7
0.8
0.9
1
1.1
0.0
0.2
0.4
0.6
0.8
1.0

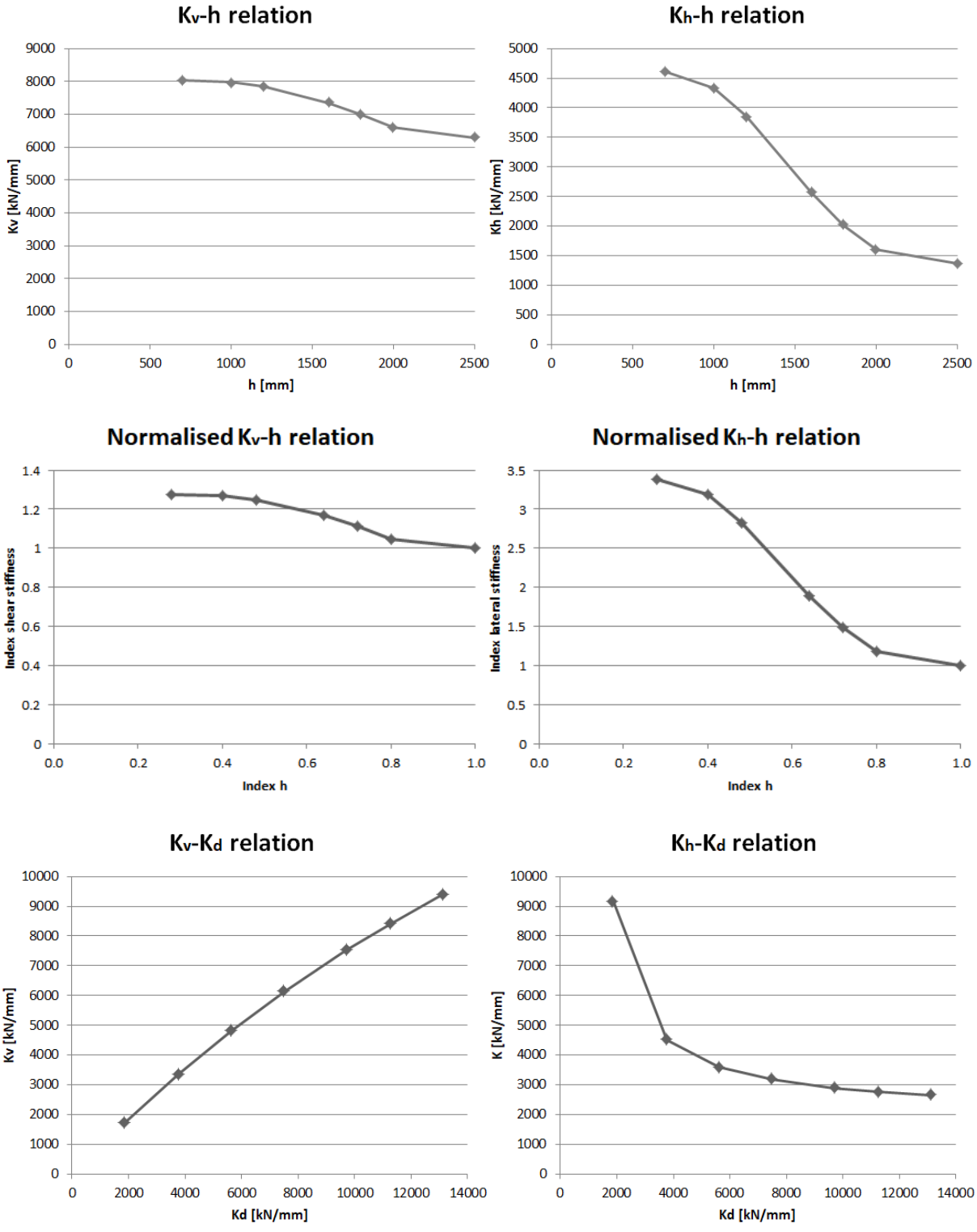
Kv-h relation
Kv [kN/mm]
h [mm]
Kh-h relation
Kh [kN/mm]
h [mm]
Normalised Kv-h relation
Index shear stiffness
Index h
Normalised Kh-h relation
Index lateral stiffness
Index h
Kv-Kd relation
Kv [kN/mm]
Kd [kN/mm]
Kh-Kd relation
K [kN/mm]
Kd [kN/mm]

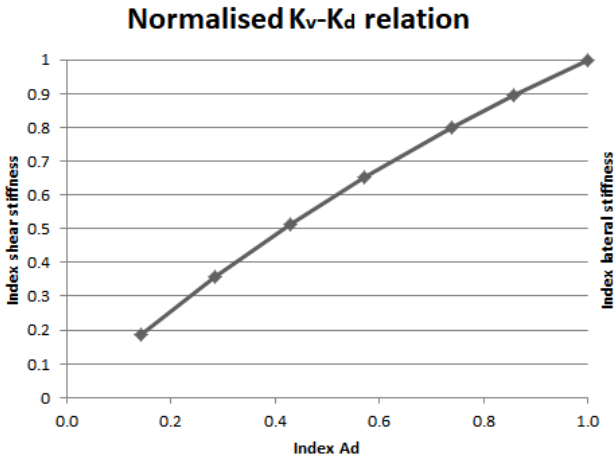
Normalised Kv-Kd relation
Index shear stiffness
Index Ad
0
0.1
0.2
0.3
0.4
0.5
0.6
0.7
0.8
0.9
1
0.0
0.2
0.4
0.6
0.8
1.0

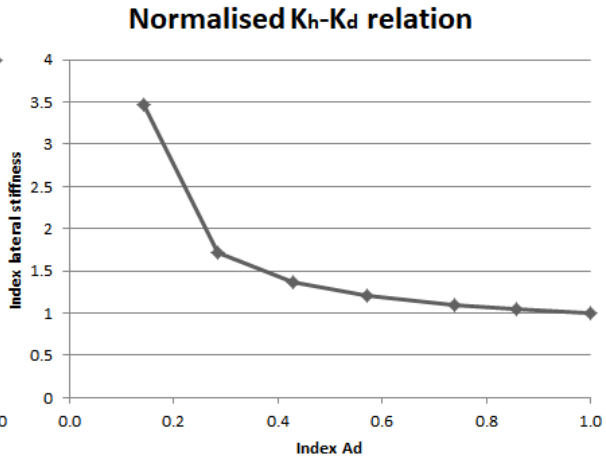
Normalised Kh-Kd relation
Index lateral stiffness
Index Ad
0
0.5
1
1.5
2
2.5
3
3.5
4
0.0
0.2
0.4
0.6
0.8
1.0

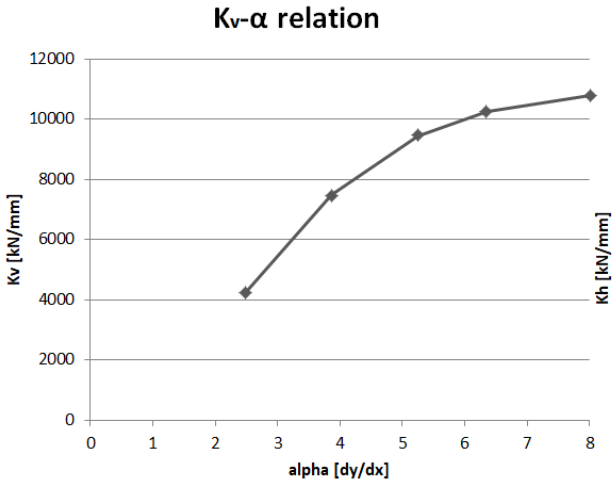
Kv-α relation
Kv [kN/mm]
alpha [dy/dx]
0
2000
4000
6000
8000
10000
12000
0
1
2
3
4
5
6
7
8

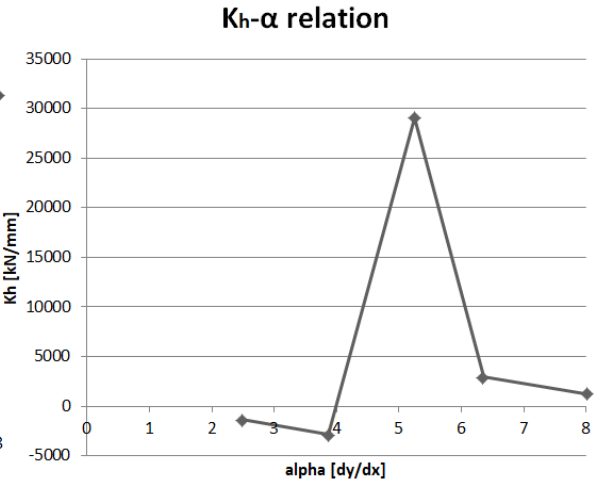
Kh-α relation
Kh [kN/mm]
alpha [dy/dx]
-5000
0
5000
10000
15000
20000
25000
30000
35000
0
1
2
3
4
5
6
7
8

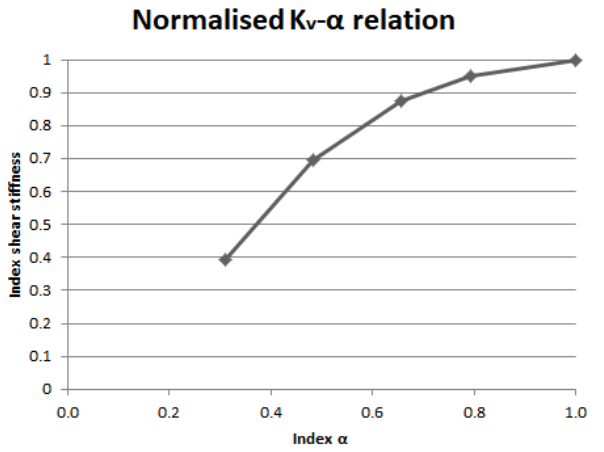
Normalised Kv-α relation
Index shear stiffness
Index α
0
0.1
0.2
0.3
0.4
0.5
0.6
0.7
0.8
0.9
1
0.0
0.2
0.4
0.6
0.8
1.0

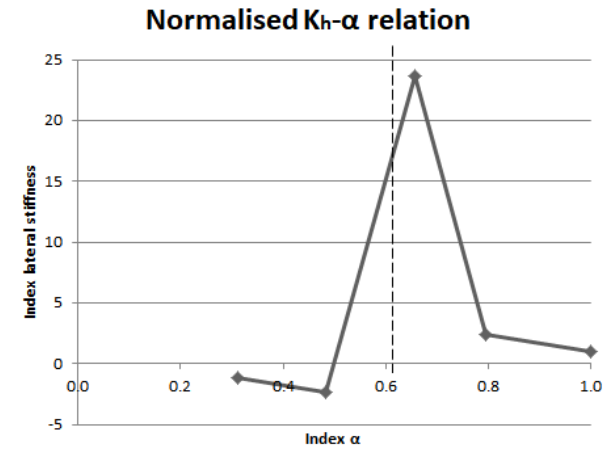
Normalised Kh-α relation
Index lateral stiffness
Index α
-5
0
5
10
15
20
25
0.0
0.2
0.4
0.6
0.8
1.0

Results parameter study Model 2

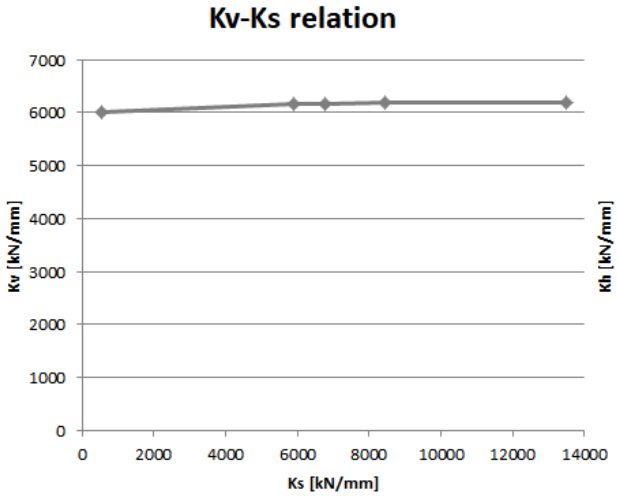

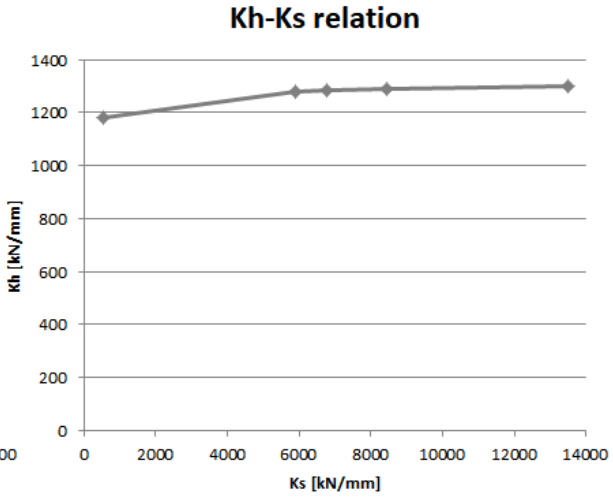

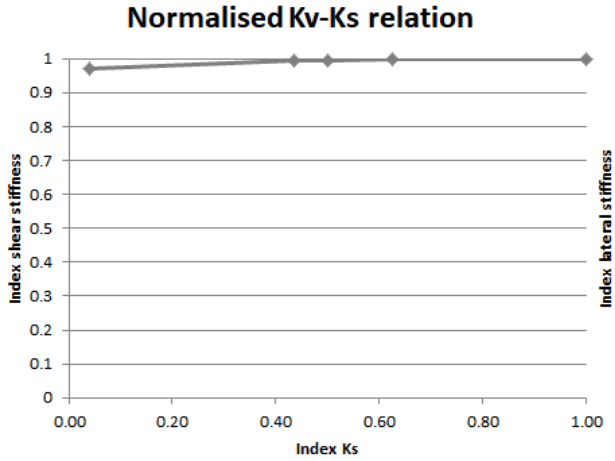

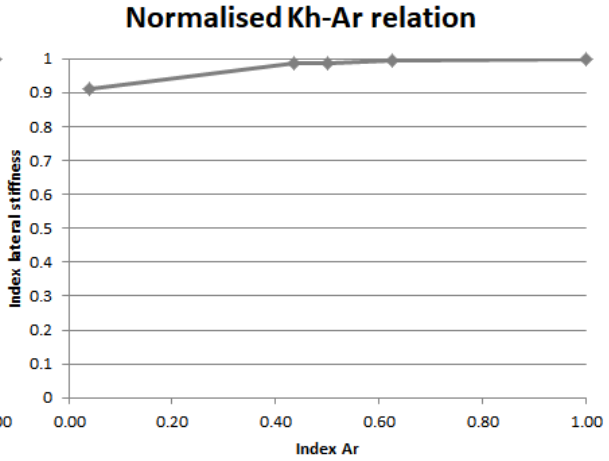

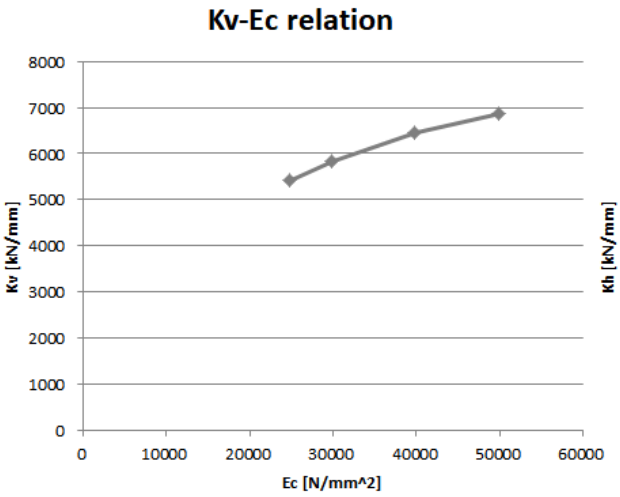

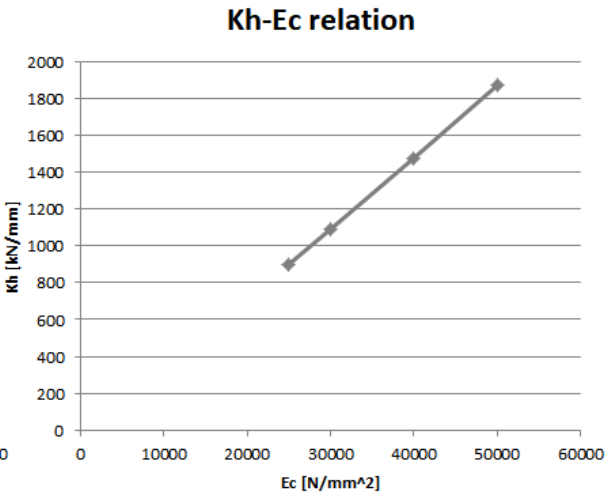

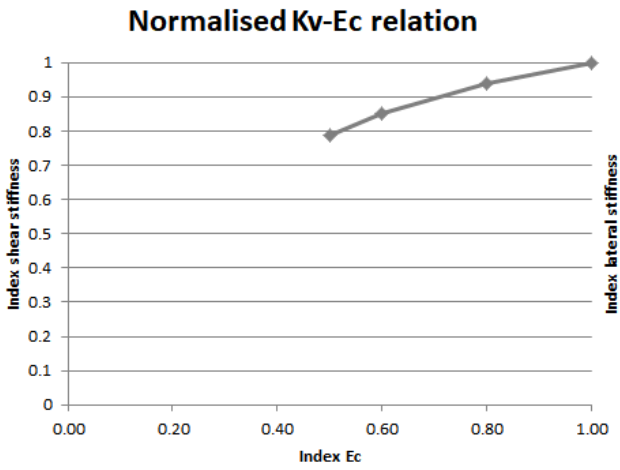
Normalised Kv-Ec relation
Index shear stiffness
Index Ec
0
0.1
0.2
0.3
0.4
0.5
0.6
0.7
0.8
0.9
1
0.00
0.20
0.40
0.60
0.80
1.00

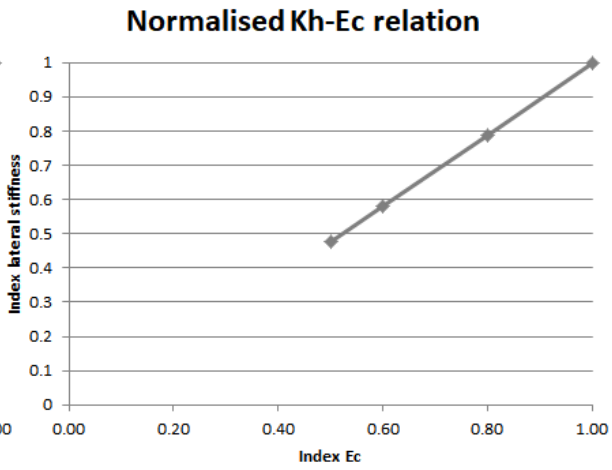
Normalised Kh-Ec relation
Index lateral stiffness
Index Ec
0
0.1
0.2
0.3
0.4
0.5
0.6
0.7
0.8
0.9
1
0.00
0.20
0.40
0.60
0.80
1.00

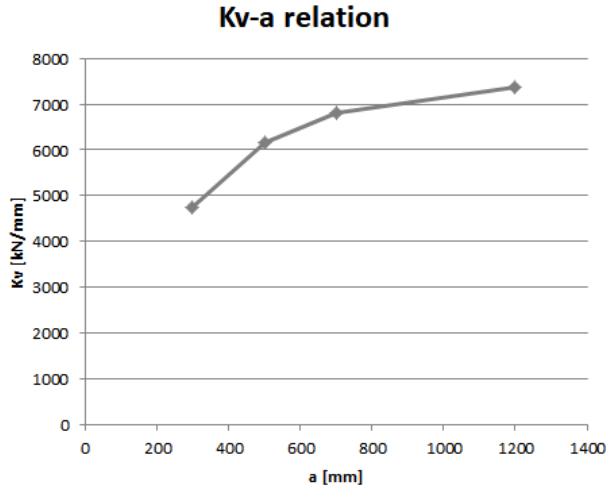
Kv-a relation
Kv [kN/mm]
a [mm]
0
1000
2000
3000
4000
5000
6000
7000
8000
0
200
400
600
800
1000
1200
1400

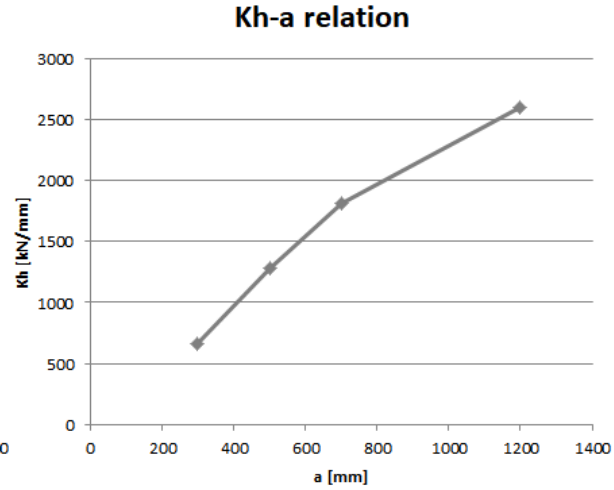
Kh-a relation
Kh [kN/mm]
a [mm]
0
500
1000
1500
2000
2500
3000
0
200
400
600
800
1000
1200
1400

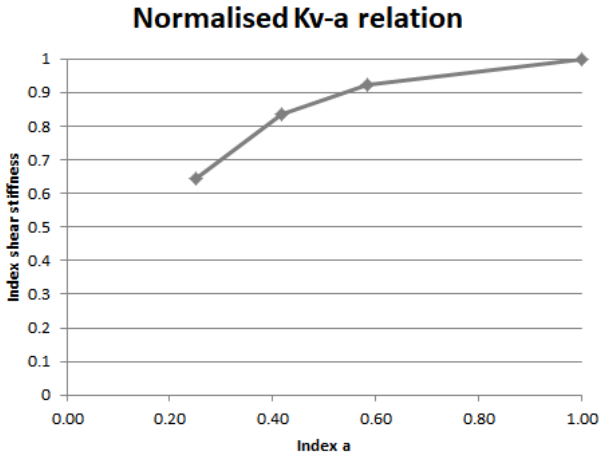
Normalised Kv-a relation
Index shear stiffness
Index a
0
0.1
0.2
0.3
0.4
0.5
0.6
0.7
0.8
0.9
1
0.00
0.20
0.40
0.60
0.80
1.00

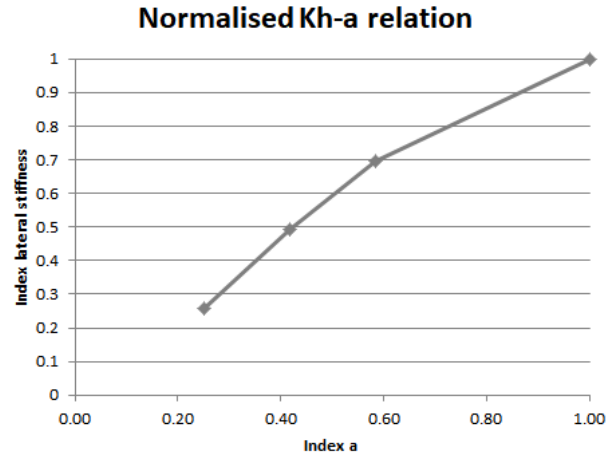
Normalised Kh-a relation
Index lateral stiffness
Index a
0
0.1
0.2
0.3
0.4
0.5
0.6
0.7
0.8
0.9
1
0.00
0.20
0.40
0.60
0.80
1.00

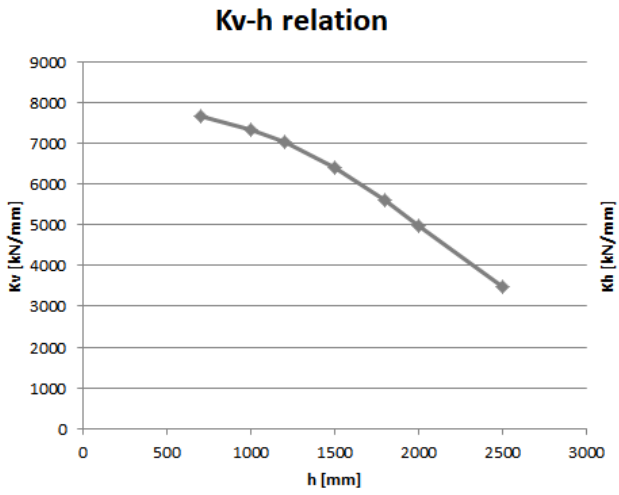
Kv-h relation
Kv [kN/mm]
h [mm]
0
1000
2000
3000
4000
5000
6000
7000
8000
9000
0
500
1000
1500
2000
2500
3000

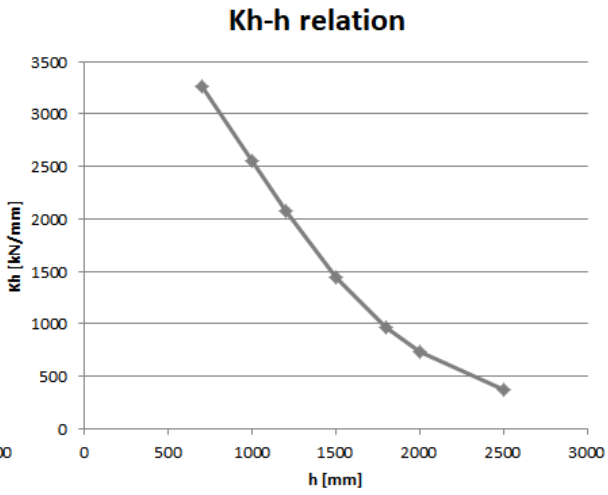
Kh-h relation
Kh [kN/mm]
h [mm]
0
500
1000
1500
2000
2500
3000
3500
0
500
1000
1500
2000
2500
3000

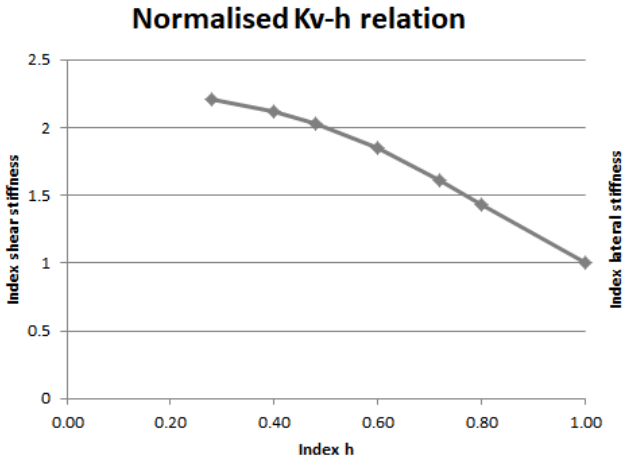
Normalised Kv-h relation
Index shear stiffness
Index h
0
0.5
1
1.5
2
2.5
0.00
0.20
0.40
0.60
0.80
1.00

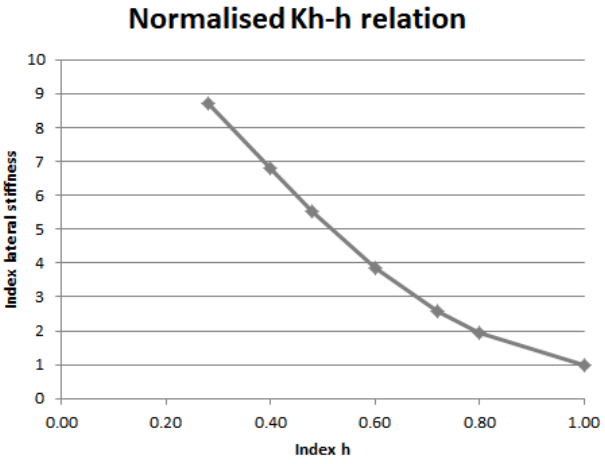
Normalised Kh-h relation
Index lateral stiffness
Index h
0
1
2
3
4
5
6
7
8
9
10
0.00
0.20
0.40
0.60
0.80
1.00

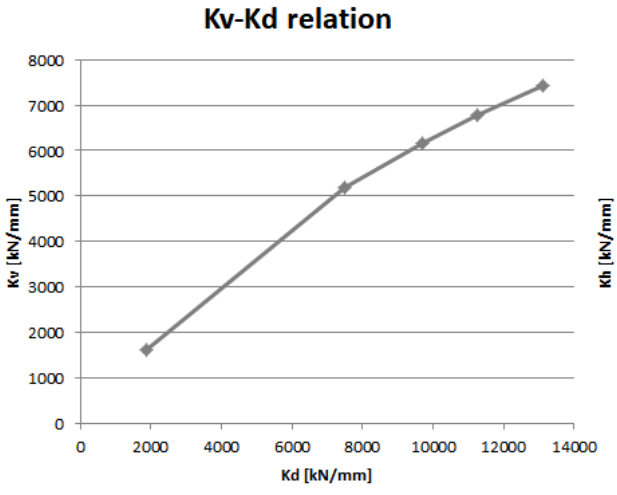
Kv-Kd relation
Kv [kN/mm]
Kd [kN/mm]
0
1000
2000
3000
4000
5000
6000
7000
8000
0
2000
4000
6000
8000
10000
12000
14000

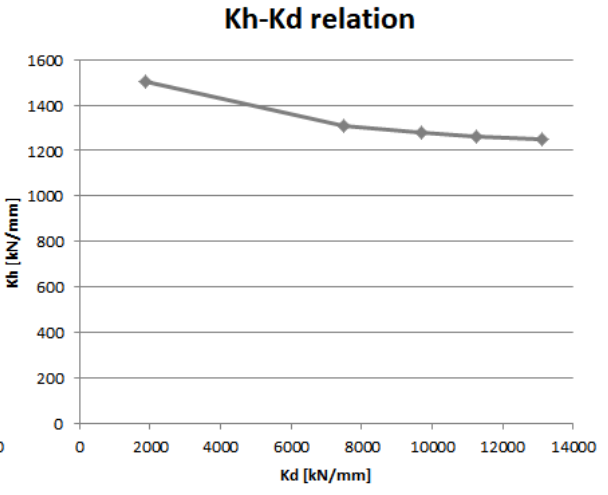
Kh-Kd relation
Kh [kN/mm]
Kd [kN/mm]
0
200
400
600
800
1000
1200
1400
1600
0
2000
4000
6000
8000
10000
12000
14000

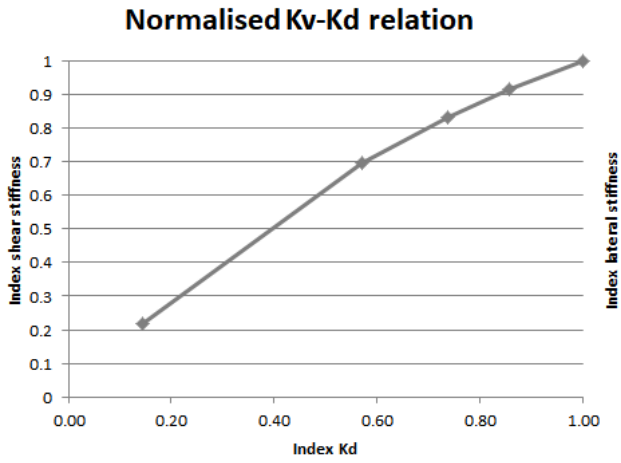
Normalised Kv-Kd relation
Index shear stiffness
Index Kd
0
0.1
0.2
0.3
0.4
0.5
0.6
0.7
0.8
0.9
1
0.00
0.20
0.40
0.60
0.80
1.00

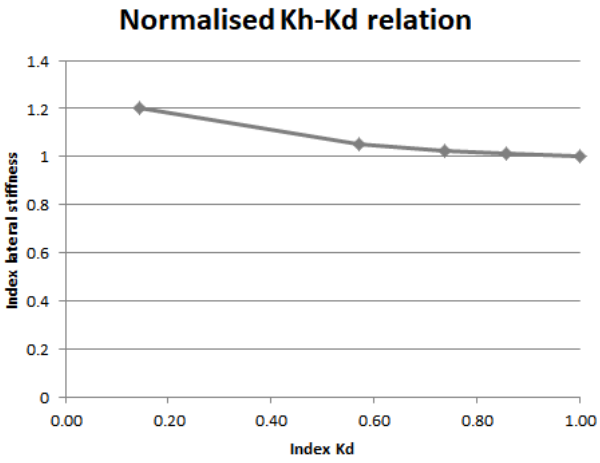
Normalised Kh-Kd relation
Index lateral stiffness
Index Kd
0
0.2
0.4
0.6
0.8
1
1.2
1.4
0.00
0.20
0.40
0.60
0.80
1.00

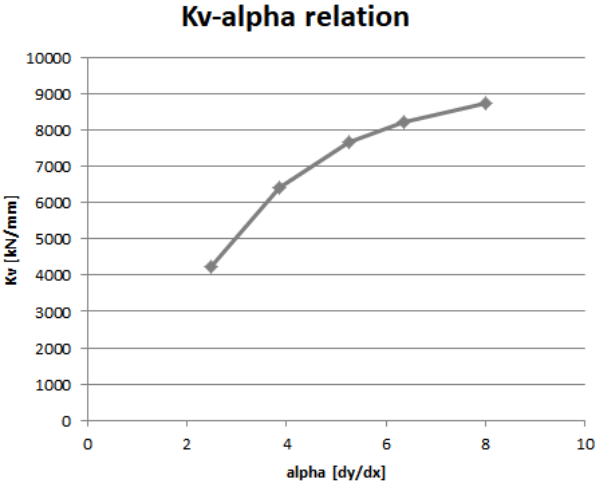
Kv-alpha relation
Kv [kN/mm]
alpha [dy/dx]
0
1000
2000
3000
4000
5000
6000
7000
8000
9000
10000
0
2
4
6
8
10

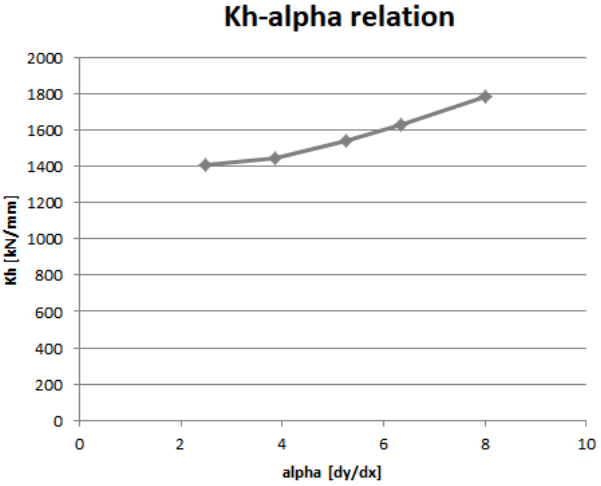
Kh-alpha relation
Kh [kN/mm]
alpha [dy/dx]
0
200
400
600
800
1000
1200
1400
1600
1800
2000
0
2
4
6
8
10

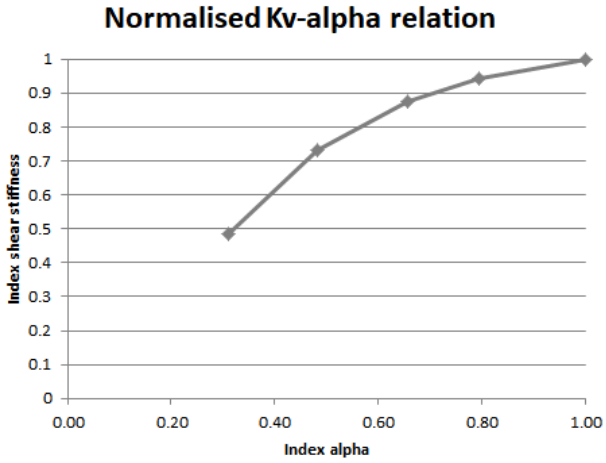
Normalised Kv-alpha relation
Index shear stiffness
Index alpha
0
0.1
0.2
0.3
0.4
0.5
0.6
0.7
0.8
0.9
1
0.00
0.20
0.40
0.60
0.80
1.00

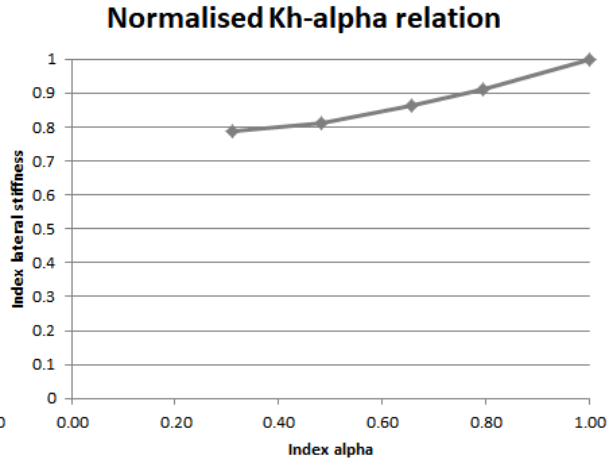
Normalised Kh-alpha relation
Index lateral stiffness
Index alpha
0
0.1
0.2
0.3
0.4
0.5
0.6
0.7
0.8
0.9
1
0.00
0.20
0.40
0.60
0.80
1.00

Results parameter study Model 3

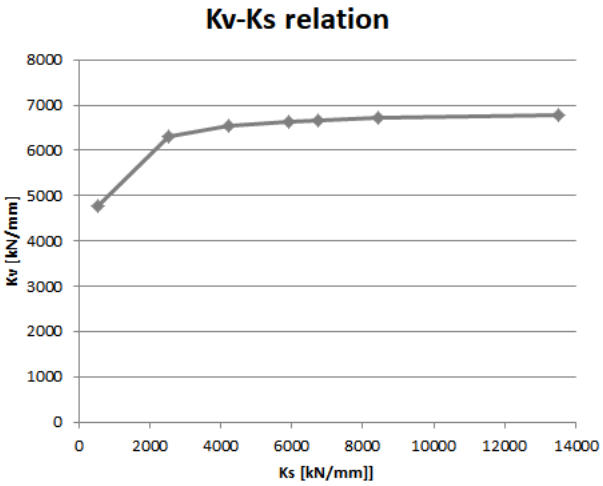

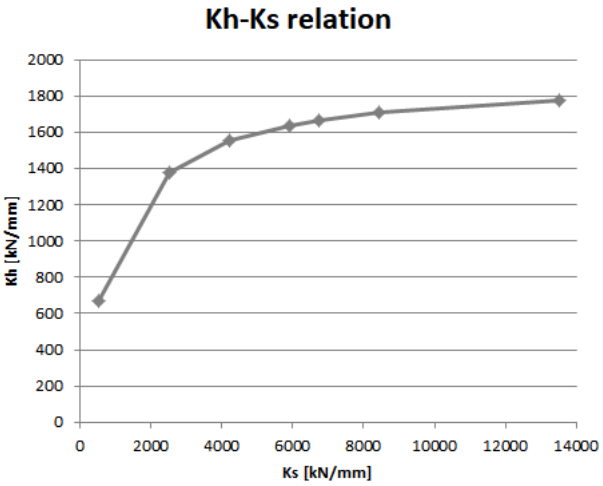

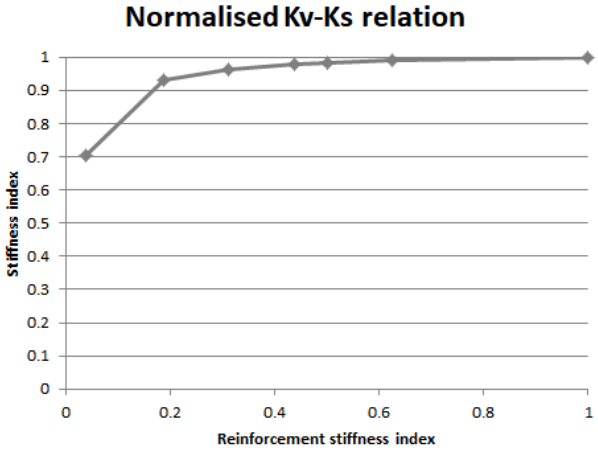

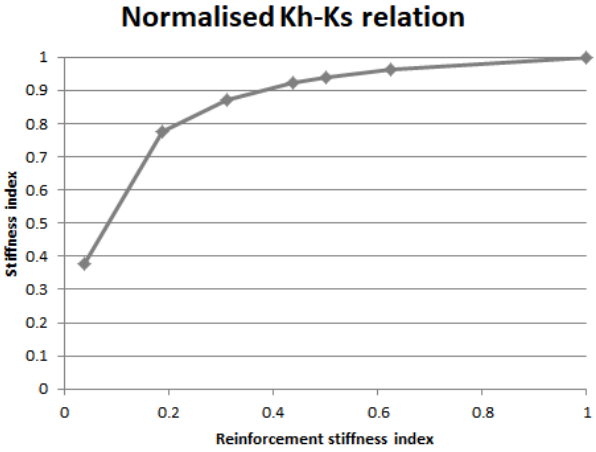

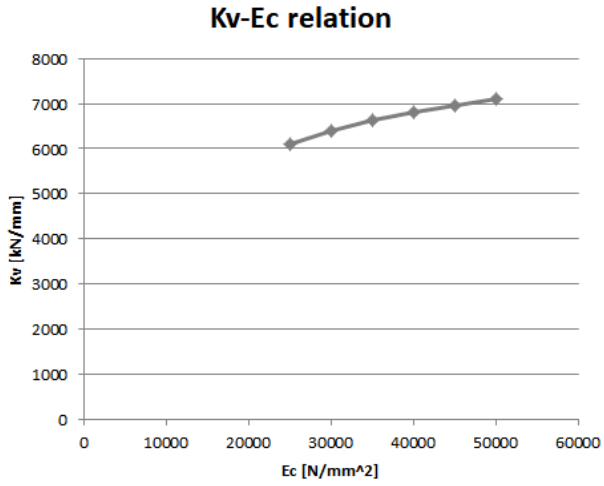

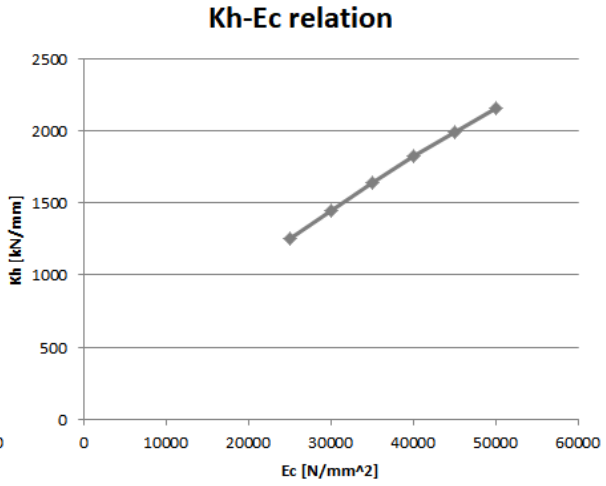

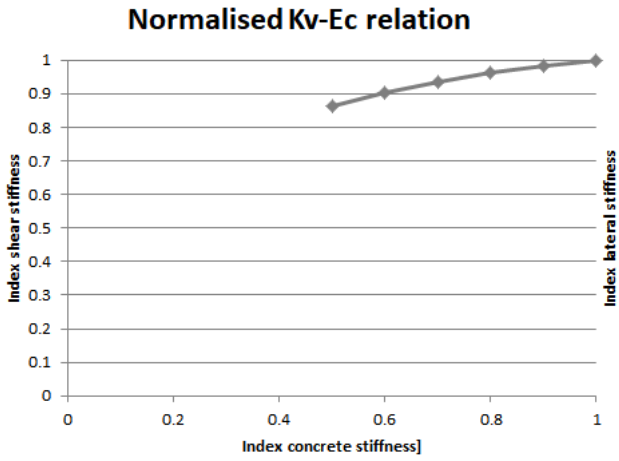
Normalised Kv-Ec relation
Index shear stiffness
Index concrete stiffness]

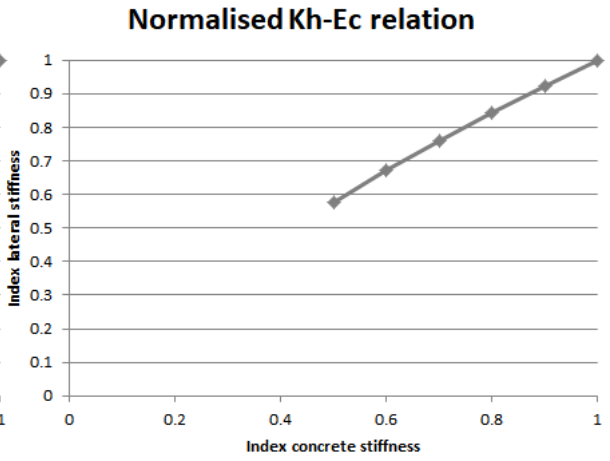
Normalised Kh-Ec relation
Index lateral stiffness
Index concrete stiffness

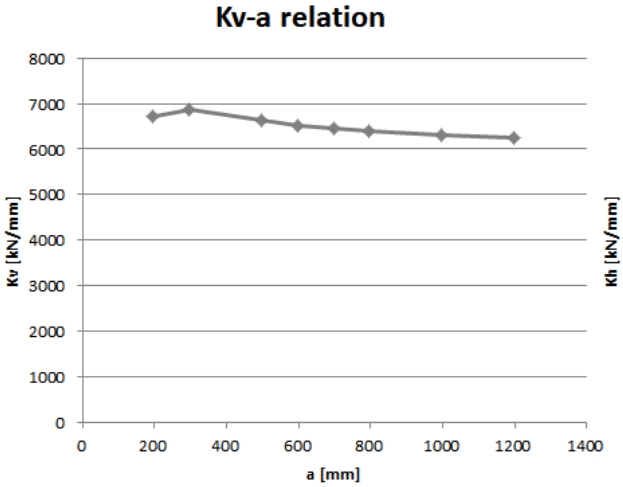
Kv-a relation
Kv [kN/mm]
a [mm]

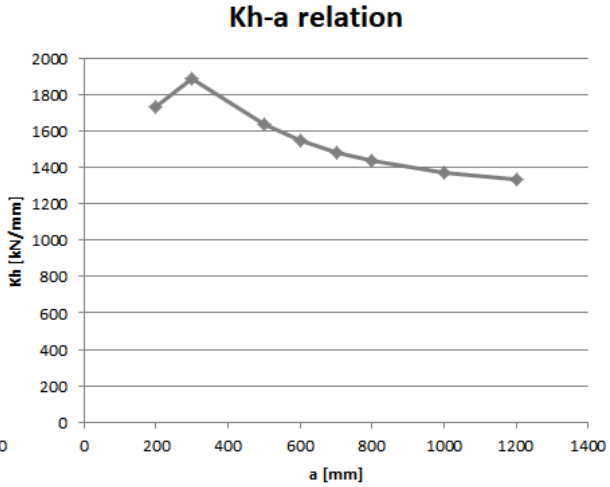
Kh-a relation
Kh [kN/mm]
a [mm]

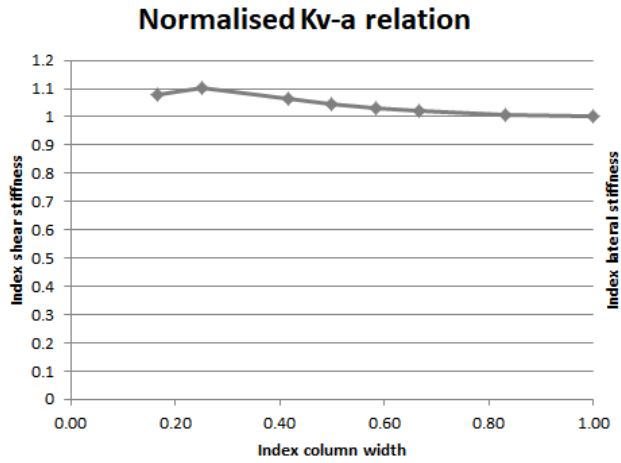
Normalised Kv-a relation
Index shear stiffness
Index column width

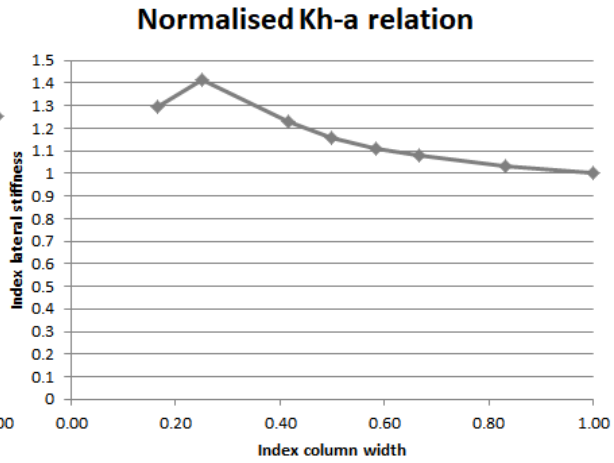
Normalised Kh-a relation
Index lateral stiffness
Index column width

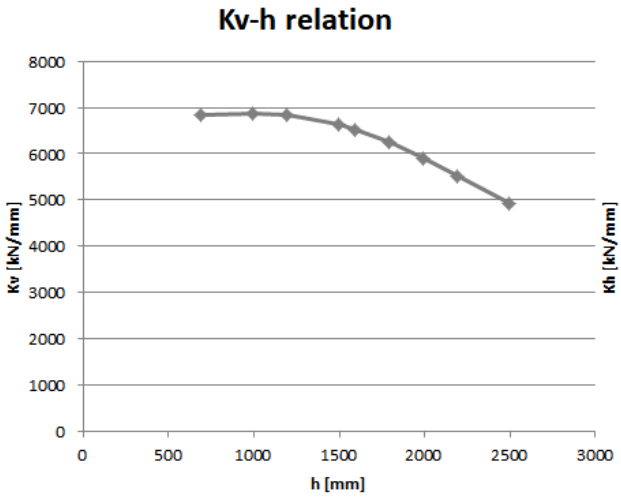
Kv-h relation
Kv [kN/mm]
h [mm]
0
1000
2000
3000
4000
5000
6000
7000
8000
0
500
1000
1500
2000
2500
3000

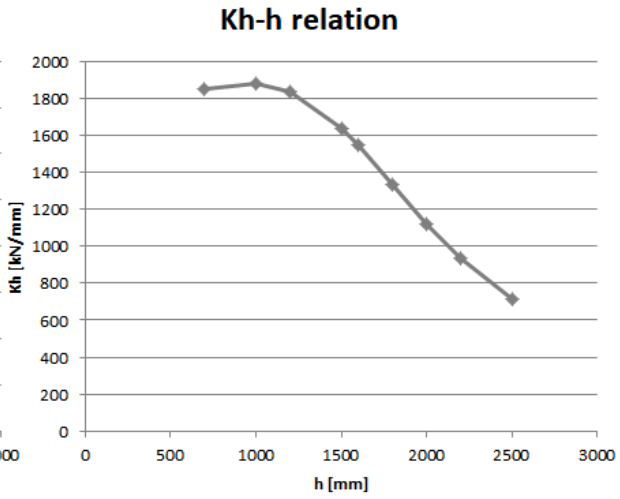
Kh-h relation
Kh [kN/mm]
h [mm]
0
200
400
600
800
1000
1200
1400
1600
1800
2000
0
500
1000
1500
2000
2500
3000

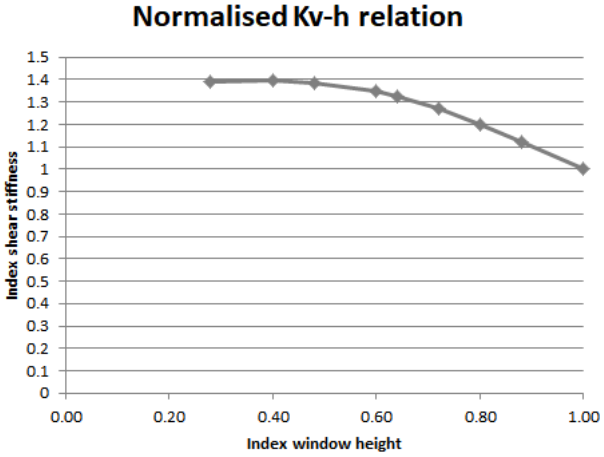
Normalised Kv-h relation
Index shear stiffness
Index window height
0
0.1
0.2
0.3
0.4
0.5
0.6
0.7
0.8
0.9
1
1.1
1.2
1.3
1.4
1.5
0.00
0.20
0.40
0.60
0.80
1.00

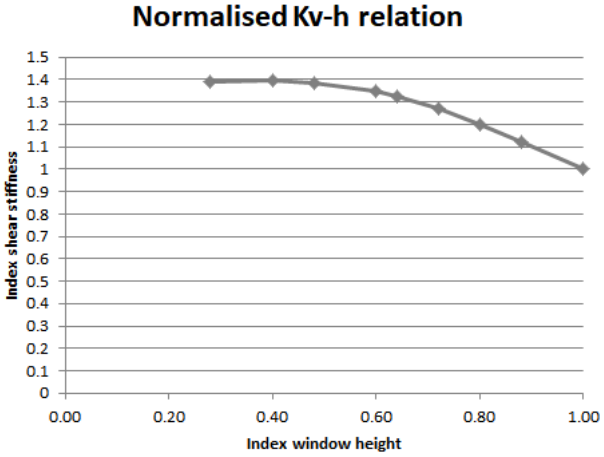
Normalised Kv-h relation
Index shear stiffness
Index window height
0
0.1
0.2
0.3
0.4
0.5
0.6
0.7
0.8
0.9
1
1.1
1.2
1.3
1.4
1.5
0.00
0.20
0.40
0.60
0.80
1.00

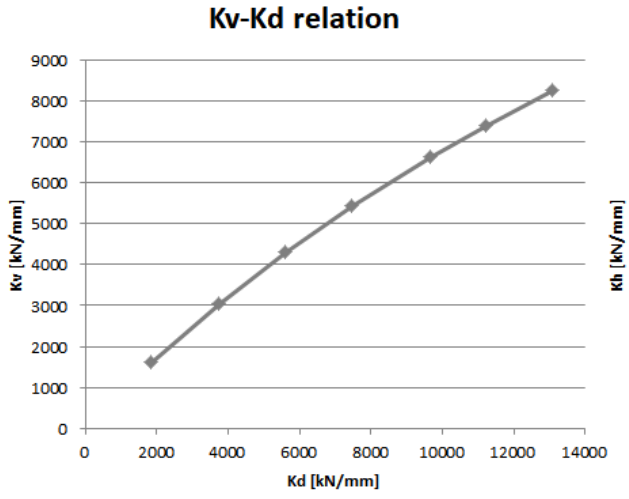
Kv-Kd relation
Kv [kN/mm]
Kd [kN/mm]
0
1000
2000
3000
4000
5000
6000
7000
8000
9000
0
2000
4000
6000
8000
10000
12000
14000

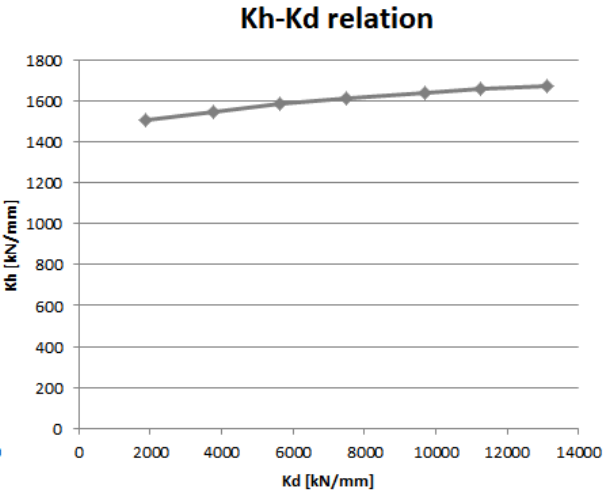
Kh-Kd relation
Kh [kN/mm]
Kd [kN/mm]
0
200
400
600
800
1000
1200
1400
1600
1800
0
2000
4000
6000
8000
10000
12000
14000

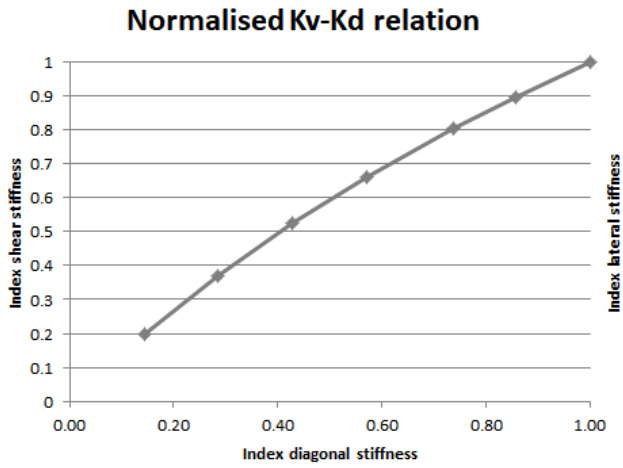
Normalised Kv-Kd relation
Index shear stiffness
Index diagonal stiffness
0
0.1
0.2
0.3
0.4
0.5
0.6
0.7
0.8
0.9
1
0.00
0.20
0.40
0.60
0.80
1.00

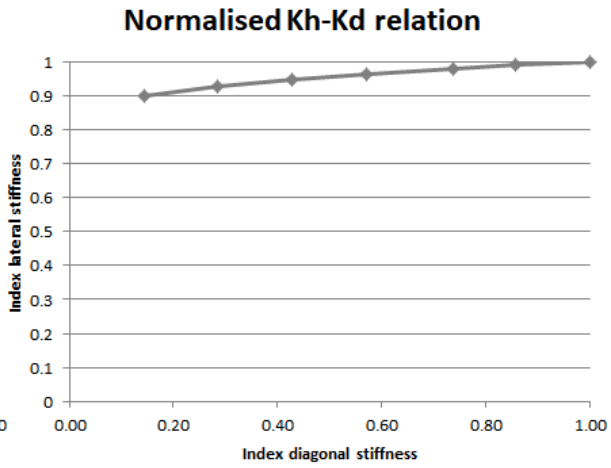
Normalised Kh-Kd relation
Index lateral stiffness
Index diagonal stiffness
0
0.1
0.2
0.3
0.4
0.5
0.6
0.7
0.8
0.9
1
0.00
0.20
0.40
0.60
0.80
1.00

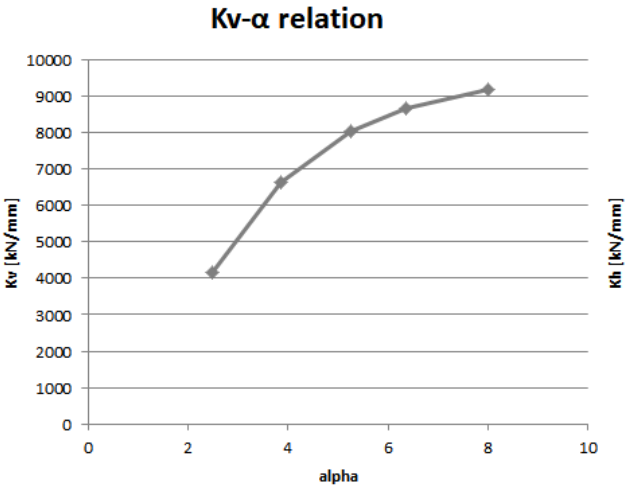
Kv-α relation
Kv [kN/mm]
alpha
0
1000
2000
3000
4000
5000
6000
7000
8000
9000
10000
0
2
4
6
8
10

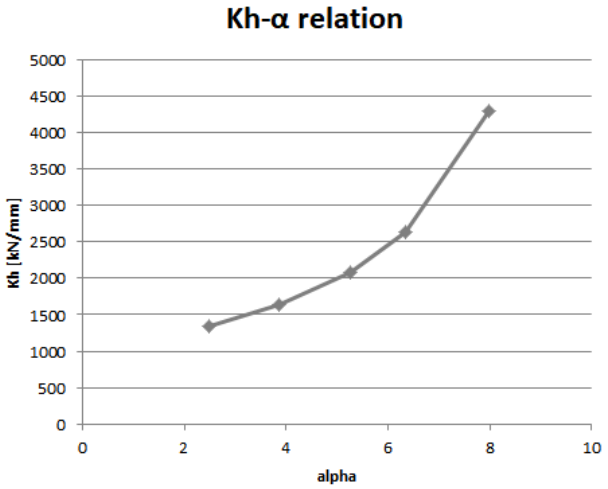
Kh-α relation
Kh [kN/mm]
alpha
0
500
1000
1500
2000
2500
3000
3500
4000
4500
5000
0
2
4
6
8
10

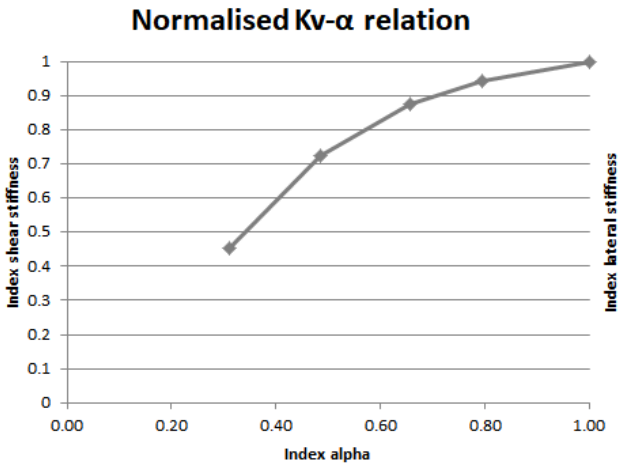
Normalised Kv-α relation
Index shear stiffness
Index alpha
0
0.1
0.2
0.3
0.4
0.5
0.6
0.7
0.8
0.9
1
0.00
0.20
0.40
0.60
0.80
1.00

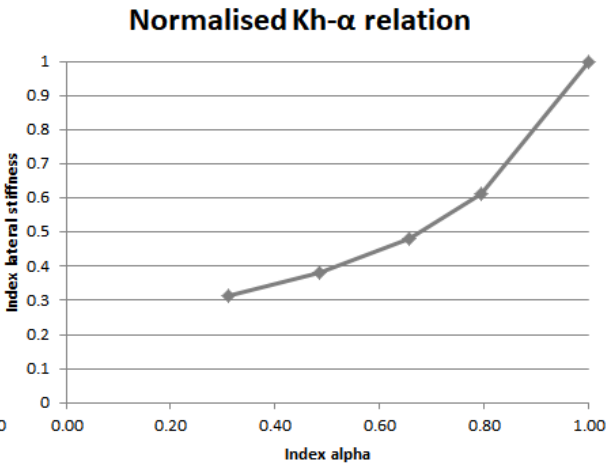
Normalised Kh-α relation
Index lateral stiffness
Index alpha
0
0.1
0.2
0.3
0.4
0.5
0.6
0.7
0.8
0.9
1
0.00
0.20
0.40
0.60
0.80
1.00

F The complete relation for the lateral stiffness

This appendix contains simplified versions of the general formula for the lateral stiffness that was derived in paragraph 10.2. Furthermore it contains plots of the distribution of K_h over the height of the floor obtained for model 2. These distributions clearly show the combined effect of the support stiffness and the lateral compressive forces.

Simplifications of K_h for specific cases

The general formula is given by:

$$K_h = \frac{K_{sup1}K_{sup2}}{K_{sup1}\left(\frac{h_y}{h_x} * tan\beta - 1\right) + K_{sup2}\left(\frac{h_y}{h_x} * tan\gamma - 1\right)}$$

Specific cases can be distinguished for which the formula can be simplified.

1. $K_{sup2}=K_{sup2}$ $K_{sup1}=\infty$ $\beta=\gamma=0$ (This case corresponds to Figure 10.2)

$$K_h = \frac{\infty * K_{sup2}}{\infty * K_{sup2}} = K_{sup2}$$

2. $K_{sup1}=K_{sup2}$ $\beta=\gamma=0$

$$K_h = \frac{K_{sup}^2}{-2K_{sup}}$$

3. $K_{sup2}=K_{sup2}$ $K_{sup1}= K_{sup1}$ $\beta=\gamma=0$

$$K_h = \frac{K_{sup1}K_{sup2}}{-K_{sup1} - K_{sup2}}$$

4. $K_{sup2}=K_{sup2}$ $K_{sup1}=\infty$ $\gamma=0$

$$K_h = \frac{K_{sup2} * \infty}{\infty\left(-1 + \frac{h_y}{h_x} * tan\beta\right) + K_{sup2}} = K_{sup2} * \frac{1}{1 - \frac{h_y}{h_x} * tan\beta}$$

5. $K_{sup2}=K_{sup1}$ $\gamma=0$

$$K_h = \frac{K_{sup}^2}{K_{sup}\left(\frac{h_y}{h_x} * tan\beta - 2\right)} = K_{sup} * \frac{1}{\frac{h_y}{h_x} * tan\beta - 2}$$

6. $K_{sup2}=K_{sup1}$

$$K_h = \frac{K_{sup}^2}{K_{sup}\left(\frac{h_y}{h_x} * tan\beta + \frac{h_y}{h_x} * tan\gamma - 2\right)} = K_{sup} * \frac{1}{\frac{h_y}{h_x} * tan\beta + \frac{h_y}{h_x} * tan\gamma - 2}$$

7. $K_{sup1}=K_{sup2}$ $\beta=\gamma$

$$K_h = \frac{K_{sup}^2}{K_{sup}\left(\frac{h_y}{h_x} * tan\beta + \frac{h_y}{h_x} * tan\beta - 2\right)} = K_{sup} * \frac{1}{2 * \frac{h_y}{h_x} * tan\beta - 2}$$

With the relation for the equivalent spring stiffness of a series spring some of the following relations can also be derived from the other. For example the last: With two equal lateral springs, the equivalent spring stiffness is halved with respect to the case with Kh2= infinite. The formula is indeed divided by two.

The lateral stiffness distributed over the floor height

According to the derived relation 10.4, the lateral stiffness that is processed from the model results is partly determined by the lateral compressive force. This force induces a prestress of the joint that increases the lateral stiffness. As the resulting behaviour of the parameter study models shows, the compression diagonals that develop in the model cross the joint halfway each floor. For this reason the lateral compressive stress must be the largest at this location.

The lateral stiffness halfway the floor height is governed by the prestress, but also by the support stiffness. This support stiffness should have the lowest value halfway the floor height, according to the schematisation of paragraph 10.3.

The figures below contain plots of the lateral stiffness distributed over the height of one floor. The plots are generated using model 2, instead of 3. As mentioned in chapter 8, the second model is more suitable for detailed evaluation of local structural behaviour. The results of model 3 are more difficult to analyse since they appear to be influenced by more effects than those considered in this research.

Figure F.16 shows the distribution of the lateral stiffness over the floor height for different values of h. This time not the absolute, but the real value of the lateral stiffness is displayed. So the negative values correspond to the regular case where the compressive diagonal force leads to a dilatation of the joint. A more negative value indicates a greater lateral stiffness. At the outer edges of the floor tensile forces occur in the diagonals, as was seen in paragraph 8.1 as well. Thereby at these locations a positive stiffness is found.

The most important aspect to see is the distribution around half of the floor height. The stiffness in this region is significantly larger than closer to the floor edges, as a result of the effect of the lateral compressive force. However, the lateral stiffness exactly halfway is slightly lower, as a result of the smaller support stiffness at this location, compared to the location at the edges of the window opening.

Figure F.17 shows the distribution for different values of a. As can be observed, the magnitude of a influences the effect of the support stiffness on the distribution. For a smaller value of a, the local minimum value halfway the floor height is smaller compared to the maximum value. For larger values of a, the effect disappears. The column width is too lead to a significant stiffness reduction.

Both figures show distributions that correspond to the theoretical behaviour described by the derived formula. So these observations substantiate the validity of the analytical relations of paragraphs 10.1 10.2 and 10.3 for the modelled vertical profiled joint connection in a shear wall.

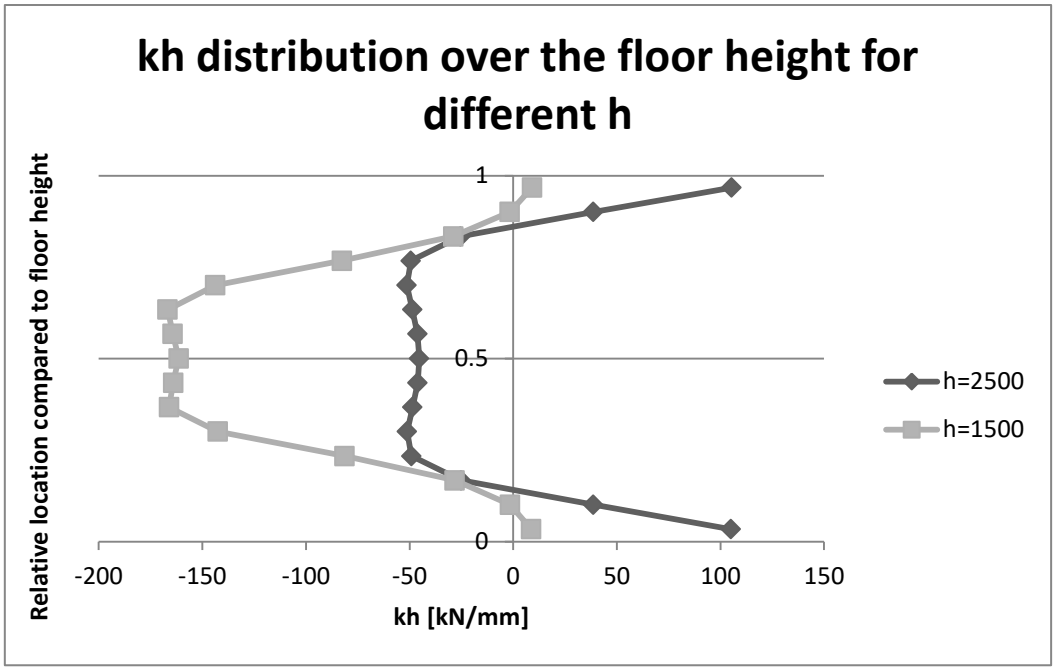

Figure F.16 distribution of the lateral stiffness over the floor height for different values of h

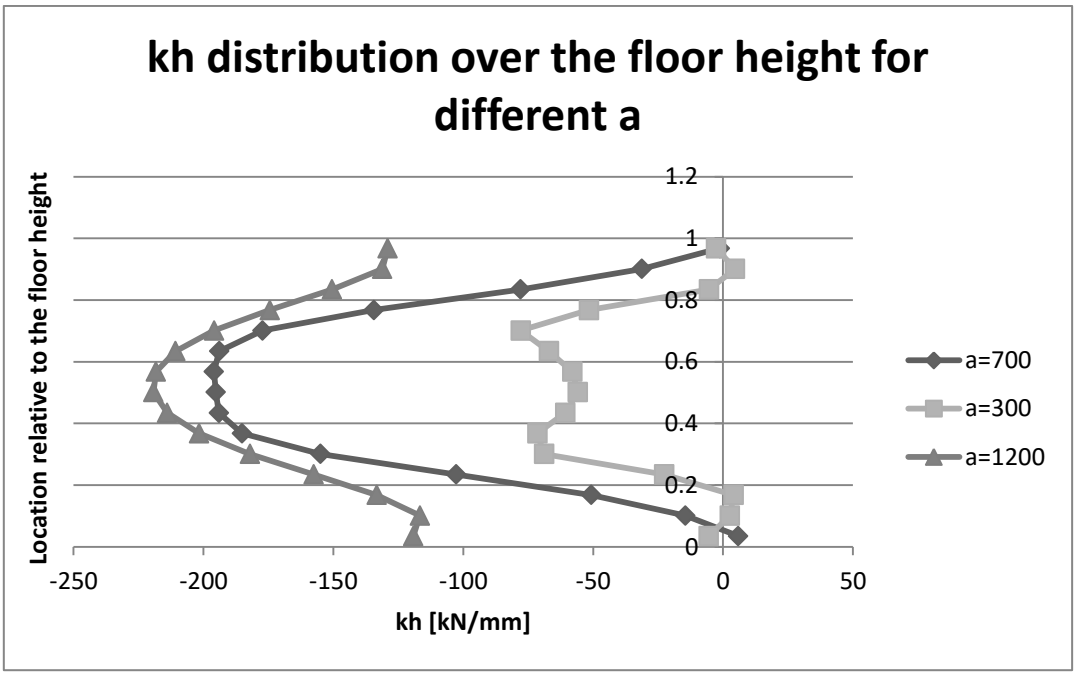

Figure F.17 Distribution of the lateral stiffness over the floor height for different values of a

G The Timoshenko beam approximation

This appendix contains the maple sheet that is produced to solve the Timoshenko beam equation for the case depicted in the figure below. The beam theory considers bending and shear deformations. The deflection caused by bending is indicated by "W", deflection caused by shear by "v" and the combination of both by "u". The solution makes use of symmetry in the axis y=0 and therefore only holds for cases with window openings centred halfway the floor height. Furthermore the ratio between the lengths of domain 1 and 2 is equal to 1.

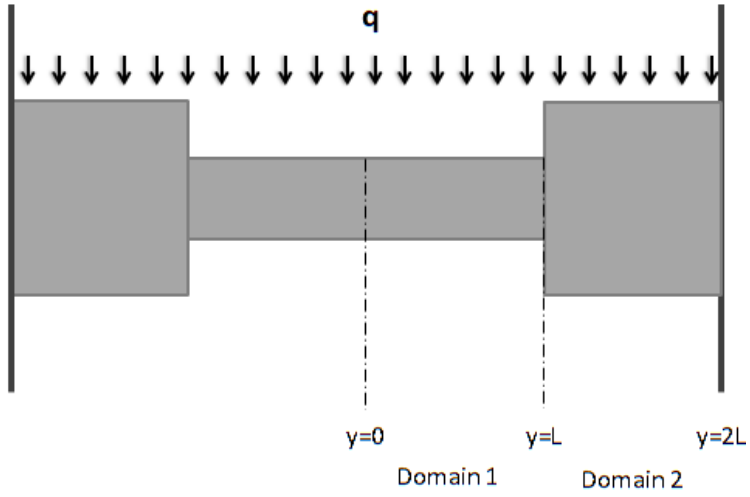

Figure G.18 The analysed beam

First of all, the applying differential equations for the bending deformations are defined for domains 1 and 2. Also the boundary and matching conditions are formulated.

$$restart;$$

$$W1 := \frac{1}{EI1}\cdot\left(\frac{1}{24}\cdot q\cdot x^4+\frac{1}{6}\cdot C1\cdot x^3+\frac{1}{2}\cdot C2\cdot x^2+C3\cdot x+C4\right):$$

$$Phi1 := \frac{1}{EI1}\cdot\left(\frac{1}{6}\cdot q\cdot x^3+\frac{1}{2}\cdot C1\cdot x^2+C2\cdot x+C3\right):$$

$$M1 := \left(\frac{1}{2}\cdot q\cdot x^2+C1\cdot x+C2\right):$$

$$V1 := q\cdot x+C1:$$

$$W2 := \frac{1}{EI2}\cdot\left(\frac{1}{24}\cdot q\cdot x^4+\frac{1}{6}\cdot D1\cdot x^3+\frac{1}{2}\cdot D2\cdot x^2+D3\cdot x+D4\right):$$

$$Phi2 := \frac{1}{EI2}\cdot\left(\frac{1}{6}\cdot q\cdot x^3+\frac{1}{2}\cdot D1\cdot x^2+D2\cdot x+D3\right):$$

$$M2 := \left(\frac{1}{2}\cdot q\cdot x^2+D1\cdot x+D2\right):$$

$$V2 := (q\cdot x+D1):$$

$$x := 0 : Eq1 := V1 = 0 : Eq2 := Phi1 = 0 :$$
$$x := L : Eq3 := W1 = W2 : Eq4 := Phi1 = Phi2 : Eq5 := V1 = V2 : Eq6 := M1 = M2 :$$
$$x := 2\,L : Eq7 := W2 = 0 : Eq8 := Phi2 = 0 :$$

$$SOL := solve(\{Eq1, Eq2, Eq3, Eq4, Eq5, Eq6, Eq7, Eq8\}, \{C1, C2, C3, C4, D1, D2, D3, D4\});$$
$$assign(SOL);$$

The solution of these differential equations is determined for domains 1 and 2. The integration constants have been solved with the boundary and matching conditions that were defined above.

$$SOL := \left\{ C1 = 0,\ C2 = -\frac{q\,L^2\,(7\,EI1 + EI2)}{6\,(EI1 + EI2)},\ C3 = 0,\ C4 = \frac{q\,L^4\,(3\,EI1^2 + 28\,EI1\,EI2 + EI2^2)}{24\,EI2\,(EI1 + EI2)},\ D1 = 0,\ D2 = -\frac{q\,L^2\,(7\,EI1 + EI2)}{6\,(EI1 + EI2)},\ D3 = \frac{q\,L^3\,(EI1 - EI2)}{EI1 + EI2},\ D4 = -\frac{q\,L^4\,(EI1 - 5\,EI2)}{3\,(EI1 + EI2)} \right\} \quad (1)$$

$x := y:$
$W1;$

$$\frac{\frac{q\,y^4}{24} - \frac{q\,L^2\,(7\,EI1 + EI2)\,y^2}{12\,(EI1 + EI2)} + \frac{q\,L^4\,(3\,EI1^2 + 28\,EI1\,EI2 + EI2^2)}{24\,EI2\,(EI1 + EI2)}}{EI1} \quad (2)$$

$W2;$

$$\frac{\frac{q\,y^4}{24} - \frac{q\,L^2\,(7\,EI1 + EI2)\,y^2}{12\,(EI1 + EI2)} + \frac{q\,L^3\,(EI1 - EI2)\,y}{EI1 + EI2} - \frac{q\,L^4\,(EI1 - 5\,EI2)}{3\,(EI1 + EI2)}}{EI2} \quad (3)$$

Then the shear deformations are considered. The differential equations and corresponding boundary and matching conditions are defined. The solution for the shear deflection v is found subsequently. This solution is added to that found for the bending deflection W, resulting in the combined total deflection u.

$$v1 := -\frac{1}{GA1}\cdot\left(\frac{1}{2}\cdot q\cdot z^2 + K1\cdot z + K2\right):$$
$$v2 := -\frac{1}{GA2}\cdot\left(\frac{1}{2}\cdot q\cdot z^2 + B1\cdot z + B2\right):$$
$$F1 := (q\cdot z + K1):$$
$$F2 := (q\cdot z + B1):$$

$$z := 0 : Eq9 := F1 = 0:$$
$$z := L : Eq10 := v1 = v2 : Eq11 := F1 = F2:$$
$$z := 2\,L : Eq12 := v2 = 0:$$
$$SOL2 := solve(\{Eq9, Eq10, Eq11, Eq12\}, \{K1, K2, B1, B2\}); assign(SOL2);$$

$$SOL2 := \left\{ B1 = 0,\ B2 = -2\,q\,L^2,\ K1 = 0,\ K2 = -\frac{q\,L^2\,(3\,GA1 + GA2)}{2\,GA2} \right\} \quad (4)$$

$z := y:$
$u1 := W1 + v1;$

$$u1 := \frac{\frac{q\,y^4}{24} - \frac{q\,L^2\,(7\,EI1 + EI2)\,y^2}{12\,(EI1 + EI2)} + \frac{q\,L^4\,(3\,EI1^2 + 28\,EI1\,EI2 + EI2^2)}{24\,EI2\,(EI1 + EI2)}}{EI1} - \frac{\frac{q\,y^2}{2} - \frac{q\,L^2\,(3\,GA1 + GA2)}{2\,GA2}}{GA1} \quad (5)$$

$u2 := W2 + v2;$

$$u2 := \frac{\frac{q\,y^4}{24} - \frac{q\,L^2\,(7\,EI1 + EI2)\,y^2}{12\,(EI1 + EI2)} + \frac{q\,L^3\,(EI1 - EI2)\,y}{EI1 + EI2} - \frac{q\,L^4\,(EI1 - 5\,EI2)}{3\,(EI1 + EI2)}}{EI2} - \frac{\frac{1}{2}\,q\,y^2 - 2\,q\,L^2}{GA2} \tag{6}$$

 # *Defining the input variables*

$h1 := 500 : h2 := 900 : E := 30000 : B := 200 : q := 200 : L := 800 : Poisson := 0.2 :$

$$EI1 := \frac{E \cdot 1}{12} \cdot B \cdot h1^3 : GA1 := \frac{E}{2(1 + Poisson)} \cdot \frac{B \cdot h1}{1.2} : EI2 := \frac{E \cdot 1}{12} \cdot B \cdot h2^3 : GA2 := \frac{E}{2(1 + Poisson)} \cdot \frac{B \cdot h2}{1.2} :$$

#Plotting the solution

$with(plots) :$

$P1 := plot(u1, x = 0..L) : P2 := plot(u2, x = L..2\,L) :$

$display(\{P1, P2\});$

#Calculation of numerical values

$y := 0 :$

#Mid span deflection

$simplify(u1);$

#subdivision of deflection in bending and shear part

$convert(simplify(W1), float);$

$simplify(v1);$

For the input properties that are defined above, the following deflection is plotted over half the beam length. Location y=0 corresponds to the centre of the beam, where symmetry conditions hold. Since the slope of the curve is horizontal, the result is in line with condition. The found result is checked with a 1D beam analysis in AxisVM for the same properties.

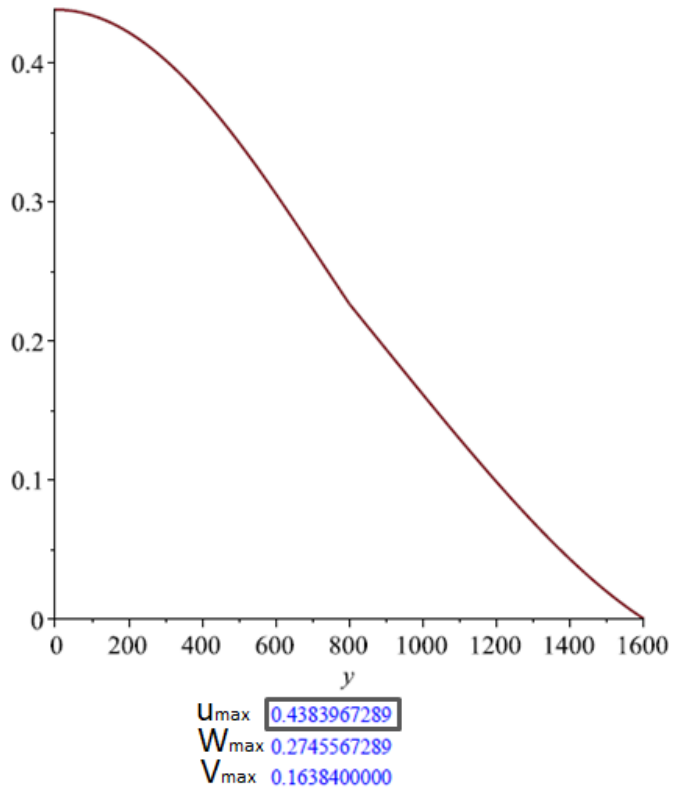

(7)

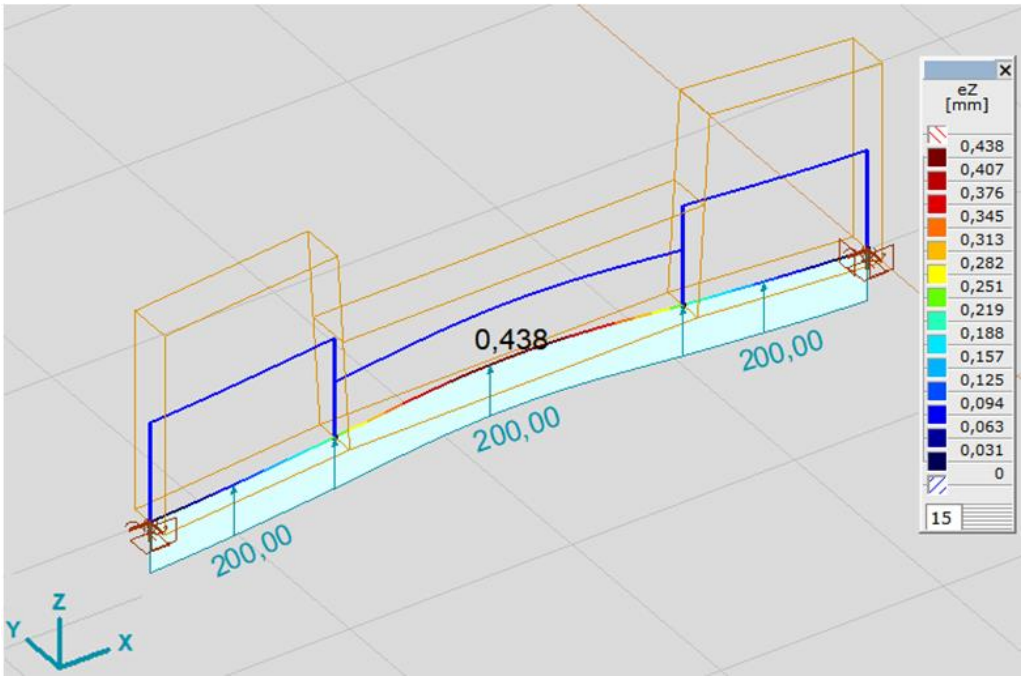
eZ
[mm]
0,438
0,407
0,376
0,345
0,313
0,282
0,251
0,219
0,188
0,157
0,125
0,094
0,063
0,031
0
15
0,438
200,00
200,00
200,00
Z
Y
X

H The calculation method for K_v

This appendix provides extra insight in the calculation method that is developed in paragraph 10.4. The first part gives a short explanation of the method, the second part contains an evaluation of the error of the calculation.

The calculation method

The table below gives an overview of the input data that is required. With this data the global lateral and shear stiffness K_h and K_v are calculated over the height of one floor. The values in the table correspond to the example that is worked out in this appendix, which corresponds to the case of appendix I.

Input data		
β	deg	0
γ	deg	0
E_c	N/mm^2	35000
ν		0.2
L_{floor}	mm	3200
q	N/mm	200
Lintel width	mm	1250
h	mm	1600
a	mm	500
t	mm	200
A_R	mm^2	3000
L_{spring}	mm	200
E_{steel}	N/mm^2	210000
E_d	N/mm^2	25000
W_d	mm	11.7
h_x	mm	50
h_y	mm	193.5
Diagonals per floor		15

Table H.6 Input of the calculation method

The load angles β and γ are set equal to zero. Their value is uncertain, since it has not been investigated in this research. The height of the floor is set equal to that used in all the phases of this research. The magnitude of distributed load q is unimportant, as explained in paragraph 10.4. The lintel width denotes the width of the precast concrete elements that is included above and below the window opening. This width influences the value of K_b. In this case the chosen value is equal to the distance between the joint and the centre line of the window opening. This is depicted in the figure below. The spring length is the length over which the transverse reinforcement is modelled. This length is according to that illustrated in Figure 8.15 and determines together with A_R and E_c the transverse spring stiffness. With the input quantity W_d the diagonal stiffness is regulated in order to let it correspond to the specific calibrated value of K_d according to paragraph 7.4. The value of the other properties must be corresponding to the design of the shear wall that is analysed, with the restriction that h must be equal to 1600mm since only the solution for this case is incorporated so far.

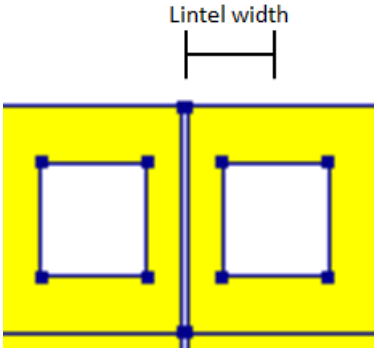

Figure H.19 Lintel width

With the input properties the following quantities are calculated. Some of these quantities are required as input for the Timoshenko beam equation that determines the bending stiffness. The bending and transverse spring stiffness are required to calculate the support stiffness subsequently. The indices 1 and 2 refer to the domains of the Timoshenko beam as depicted in appendix G.

Calculated input		
K_s	N/mm	3150000
L(beam theory)	mm	800
G	N/mm^2	14583.33333
A_1 (shear)	mm^2	83333.33333
A_2 (Shear)	mm^2	208333.3333
I_2	mm^4	3.26E+10
I_1	mm^4	2.08E+09
L_d	mm	199.8555729
A_d	mm^2	2340

Table H.7 Calculated input for further calculation

Then the bending stiffness is determined. The deflection of a single concrete element under load q is calculated at each 100mm of the floor height. The deflection is symmetric in the centre line of the floor at 1600mm. The stiffness K_b is defined as $K_b = q * \frac{L_{floor}}{U_{x,average}}$.

$U_{bending\ analytic}$			
y	**Ux [mm]**	**y**	**Ux [mm]**
0	0.0000	**900**	0.1288
100	0.0112	**1000**	0.1528
200	0.0234	**1100**	0.1760
300	0.0364	**1200**	0.1971
400	0.0500	**1300**	0.2148
500	0.0639	**1400**	0.2282
600	0.0780	**1500**	0.2364
700	0.0921	**1600**	0.2392
800	0.1060	**Average**	**0.1160462**

Table H.8 Deflection of the concrete wall elements

Subsequently the support stiffness at either side of the joint is calculated with known K_s and K_b. Since the amount of transverse reinforcement at each floor level is the same and only symmetric cases with the same openings and concrete properties at both sides of the joint are analysed, the indicated simplifications may be made.

Calculation of $K_{sup\ 1}$ and K_{sup2}	[N/mm]
K_s	3150000
K_{b1}	5515046
K_{b2}	5515046
K_{sup1}	3836015
K_{sup2}	3836015
Simplifications of this case	
Ks1=Ks2	
Kb1=Kb2	

Table H.9 Calculation of K_{sup}

The last step is to calculate the diagonal, lateral and shear stiffness. The first is determined by the known diagonal area, length and mortar young's modulus. The lateral stiffness is calculated using formula 10.4:

$$K_h = \frac{K_{sup1}K_{sup2}}{K_{sup1}\left(\frac{h_y}{h_x} * tan\beta - 1\right) + K_{sup2}\left(\frac{h_y}{h_x} * tan\gamma - 1\right)} \quad [10.4]$$

The shear stiffness is calculated using formula 10.1.

$$K_v = \frac{1}{\frac{h_x^2 + h_y^2}{K_d * h_y^2} - \frac{h_x^2}{K_h * h_y^2}} \quad [10.1]$$

For the specific input of Table H.6, the following stiffness values result, where the smeared stiffness (The stiffness divided by $t*L_{floor}$) is used as input for the interface element:

Calculated output	N/mm	N/mm^3
K_d	4390671	
K_h calculated	-1918007	
K_v calculated	3600040	5.62
K_v limit value	4115857	6.43

Table H.10 Calculated stiffness values

The limit value is the shear stiffness that corresponds to the specific diagonal stiffness combined with an infinitely large lateral stiffness, according to equation 10.3. The difference between this limit and the calculated shear stiffness indicates the contribution of the lateral stiffness.

The error of the calculation

The applied methodology to calculate the shear stiffness of the connection is rough and global. This unavoidably leads to an error between the shear stiffness calculated and the one resulting from the bar model. In order to define the error of the calculation method, the outcome is compared to that of a model of a compact shear wall similar to model 1 of the parameter study. This model contains diagonal bars in its joint. Two variants of this shear wall are considered, one with a single opening per precast concrete element and one with two openings. The latter model is equal to model 1 of the parameter study. Figure J.23 shows these shear walls.

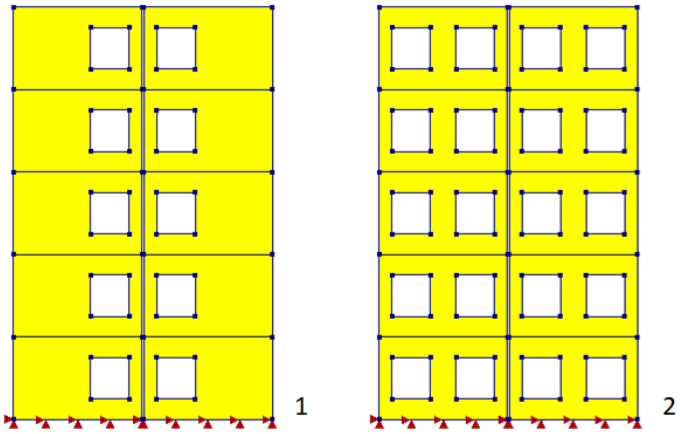

Figure H.20 Analysed shear walls

First of all, the error of the calculation method is determined for the input properties of Table H.6. In this case the average calibrated value for K_d is applied and this value is also assigned to the diagonal bars in the wall models. The transverse spring stiffness is based on at least 3000 mm² of reinforcement (4 bars Ø32), but due to the frictional force transfer this amount should be more in order to obtain the same transverse spring stiffness in reality. The lateral and shear stiffness are calculated according to the developed methodology, where the value zero is assigned to load angles β and γ. The outcome is compared to the stiffness resulting from the middle floor of the two shear wall models. Table H.11 provides the resulting values for the shear and lateral stiffness.

	K_v [kN/mm]		K_h [kN/mm]	
Calculation method	3600	100%	1918	100%
Shear wall 1	3470	96%	1476	77%
Shear wall 2	3702	103%	2456	128%
K_v Maximum	4116	114.3%	∞	-

Table H.11 Error of the calculation method for K_d average

It is clear that the approximated lateral stiffness has a large variation, whereas the variation of the shear stiffness is much smaller. This difference is caused by the relatively small value of K_d, which reduces the influence of the lateral stiffness on the shear stiffness. So for a larger value of K_d the variation of the shear stiffness will be greater.

The different results for the two walls are caused by many factors. At least, the configuration of the windows influences the orientation of the compression diagonals in the shear wall, which partly determines the lateral stiffness, as explained in paragraph 10.2. The calculation method

does not consider this effect by setting the load angles equal to zero. Apparently this leads to an overestimation of stiffness in case 1 and an underestimation of the stiffness in case 2.

Setting the load angles to zero and subsequently neglecting the positive influence of a lateral compressive force, can be seen as calculating a lower limit value for the shear and lateral stiffness. Only the support stiffness K_{sup} determines the magnitude of the lateral stiffness in this situation. However, despite the contribution of some lateral compression, the stiffness in case 1 is lower than the calculated value. This indicates that the calculated support stiffness is overestimated.

Comparison of the resulting values for K_v with the maximum value indicates the influence of the lateral stiffness on the shear stiffness of the connection. In this case the finite lateral stiffness leads to a shear stiffness reduction of -15.7 percent.

The calculation method provides a stiffness that lies between the two model results. In this case the deviation of the shear stiffness is acceptable, but this may not hold for larger values of K_d, for which the lateral stiffness has a larger influence. Therefore the error of the calculation method is also analysed for the largest calibrated value of K_d in combination with a larger thickness of 500 mm. In this case the inaccuracy of the calculated K_h leads to a larger deviation between the values of K_v, as can be seen in Table H.12.

	K_v [kN/mm]		K_h [kN/mm]	
Calculation method	13342	100%	3292	100%
Shear wall 1	11863	89%	2254	68%
Shear wall 2	12546	94%	2666	81%
K_v Maximum	18293	137.1%	∞	-

Table H.12 Error of the calculation method for K_d large and t=500mm

The resulting lateral stiffness is in all cases larger than before, because of the increased thickness. The parameter study results of Figure 8.26 show that an enlarged diagonal stiffness leads to a reduction of the lateral stiffness, since a variation of K_d alters the force distribution over the mortar joint and therefore the contribution of the lateral compressive forces. This effect is not taken into account by the calculation method, whereby the increase of the calculated K_h with respect to the results of Table H.11 is the largest. This leads to an overestimation of the lateral stiffness compared to both model results. Including the named effect in the calculation method can be done by taking into account the load angles and making them dependent on the diagonal stiffness. The overestimation of the lateral stiffness is rather big, indicating that the applied method to determine a magnitude for the support stiffness K_{sup} is inaccurate.

In this case the maximum influence of the lateral stiffness on the shear stiffness is increased. The reduction caused is equal to -35.2 percent.

Because of the larger influence of K_h, the deviation of the shear stiffness is larger than before. However, since the largest deviation is just over 10 percent, one could argue that it is still acceptable. The influence of K_h can be increased even more by reducing its value. In that way the corresponding point on the K_vK_h-diagram shifts towards the steeper part, where the influence of K_h on K_v is greater. In order to do this, the amount of transverse reinforcement is reduced to 1000 mm^2 (4 bars Ø18mm) and the concrete Young's modulus is reduced to 20000 N/mm^2. The resulting values for K_v and K_h are found in the table below.

	K_v [kN/mm]		K_h [kN/mm]	
Calculation method	9670	100%	1370	100%
Shear wall 1	7837	81%	916	67%
Shear wall 2	7954	82%	938	68%
K_v Maximum	18293	189.2%	∞	-

Table H.13 Error of the calculation method for Kd large, t=500 and reduced K_s and E_c

The results show that the error of the calculation method is indeed greater than for the case of Table H.12. The lateral stiffness has been reduced a lot compared to the previous case. The applied values for the variables E_c and K_s should almost reach their practical lower limit. For the value of K_s this limit is a bit uncertain, but for E_c it is more clear. In case the precast concrete next to the joint is cracked, the magnitude of E_c can get lower than the value applied here. Up to a value of approximately 10000 N/mm^2 at minimum.

The 20 percent error of the shear stiffness seems unacceptable. However, this depends on its effect on the behaviour of the shear wall. If for instance only the top deflection of the shear wall is of interest and the deviation of 20 percent hardly affects this deflection, the error could be acceptable. The contribution of the lateral stiffness is again larger, since its value has been reduced compared to previous case. Therefore the maximum shear stiffness is reduced by -57.2 percent.

With the restriction that h must remain 1600 mm and assuming uncracked concrete elements, only the distance between the joint and the opening can still be reduced. It is reasonable to state that the distance between the joint and the opening is at least 300 mm. So taking this as a minimum, the following calculation error is found, which is discussed in paragraph 10.4:

	K_v [kN/mm]		K_h [kN/mm]	
Calculation method	8951	100%	1170	100%
Shear wall 1	6547	73%	680	58%
Shear wall 2	6596	74%	689	59%
K_v Maximum	18293	204.4%	∞	-

Table H.14 Maximum error found for a large K_d and a small K_h

I Shear wall analysis for the average value of K_d

This appendix contains extra results of the evaluation of different compact wall models for which the average calibrated value of K_d is applied. These results can be compared with those of paragraph 11.2 and 11.4.

General input of the compact shear wall model

The input properties applied in the evaluation are summarized in Table I.15. For the diagonal stiffness, the average calibrated value is applied.

Concrete Elements	
Plane stress elements CQ16M	
Thickness t	200 mm
E-modulus E_c	35000 N/mm^2
Poisson's ratio ν	0.2
Window height	1600 mm
Column width	500 mm
Diagonal bars	
Regular truss elements L2TRU	
Length	199.86 mm
Slope [h_y/h_x]	3.87
Cross-sectional area A_d	2340 mm^2
E-modulus E_d	25000 N/mm^2
Total diagonal stiffness K_d **(Average calibration of paragraph 7.4)**	4390 kN/mm
Poisson's ratio ν	0.2
Amount of diagonals per floor	15
Reinforcement bars	
Regular truss elements L2TRU	
Cross-sectional area A_R	3000 mm^2
E-modulus E_s	210000 N/mm^2
Length	200 mm
Transverse spring stiffness K_s	3150 kN/mm
Poisson's ratio ν	0.3

Table I.15 General input properties

The dimensions of the compact shear wall are equal to those of the model that has been applied in the parameter study of chapter 8. So the wall contains five floors with a height of 3200 mm and two five metre wide precast concrete elements per floor with a 50 mm wide joint in-between. The corresponding slenderness ratio of the wall is 1.59. The wall is loaded by a distributed horizontal force on each floor, having a value of 40 N/mm. Figure I.21 shows the walls that are analysed.

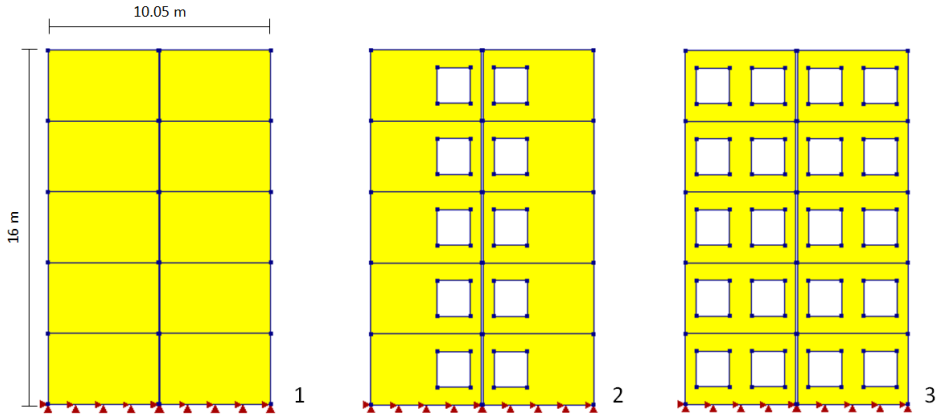

Figure I.21 Evaluated compact walls

Table I.16 shows the resulting horizontal top deflections of the three wall models for the three evaluated cases. According to these results the application of a vertical joint reduces the wall's stiffness by approximately 10-12 percent. This holds for all three walls.

	Wall 1		Wall 2		Wall 3	
	U_{top} abs.	U_{top} rel.	U_{top} abs.	U_{top} rel.	U_{top} abs.	U_{top} rel.
Monolithic	2.99	100%	4.95	100%	9.40	100%
Diagonal bars	3.36	112.4%	5.49	111%	10.30	109.6%
Interface with calculated K_v	3.31	110.7%	5.49	111%	10.38	110.4%

Table I.16 Resulting top deflection of the compact walls [mm] (Wall 1: K_v= 6.12 N/mm³ Wall 2&3: 5.62 N/mm³)

The difference between the approximated deflection of the model with interface elements and the deflection of the model with bar elements is rather small compared to the difference with the monolithic wall. This means that based on these results the diagonal bars may be replaced by the interfaces with calculated K_v, keeping an accurate approximation of the wall deflection. The difference in top deflection is even equal to zero for wall 2. For wall 3 the difference is still small, despite the fact that the load angle is not taken into account for the calculated value of K_v. This may indicate a limited need to consider this effect while calculating the magnitude of K_h.

It is interesting to see that the interfaces underestimate the top deflection of the model with diagonal bars for the closed wall, whereas they give an overestimation in case of the wall with double openings. The underestimation may be due to an overestimation of the lateral stiffness in the closed wall, where K_b was assumed to be more than fifteen times larger than in the other two walls. Since the calculation method has yet only been developed for the case where a window opening is present, it is not very suitable to apply for a closed wall. Furthermore, another effect influences the resulting deflection of the wall with a joint with diagonal bars. The occurrence of this effect is explained using the results of next section of this appendix.

The influence of the error of K_h

Similar as in chapter 11, the lateral stiffness is varied according to the error obtained in appendix H. This leads to four different values of the interface shear stiffness K_v. This is illustrated in Figure I.22, where the found values are indicated in the K_v-K_h diagram corresponding to the applied K_d value (Calibrated average). The chosen variation of the lateral stiffness leads to a significant change of the determined shear stiffness for both wall 1 and walls 2 and 3.

Since walls 2 and 3 contain openings, the lateral stiffness in these cases is generally lower than in wall 1. Thereby a variation of the lateral stiffness leads to a larger variation of the shear stiffness, as the indicated points are located in the steeper part of the diagram.

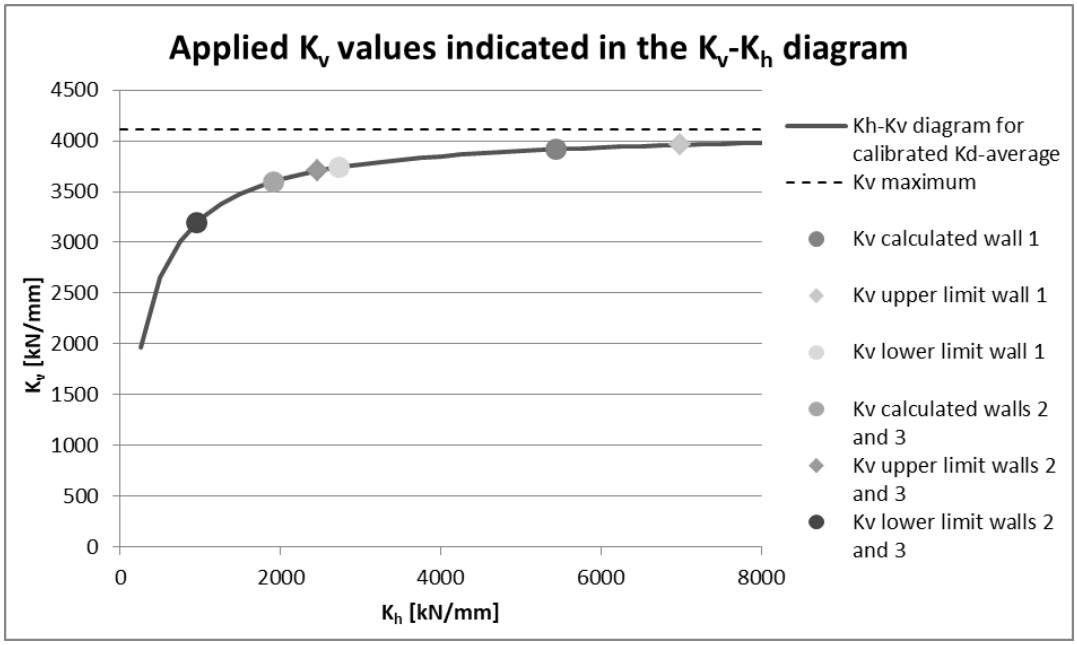

Figure I.22 The found values for K_v and their position on the K_v-K_h curve

Table I.17 provides the resulting top deflection of each wall for the different values of K_v and their relative value compared to the monolithic wall.

	Wall 1			Wall 2			Wall 3		
	K_v [N/mm³]	U_{top} abs.	U_{top} rel.	K_v [N/mm³]	U_{top} abs.	U_{top} rel.	K_v [N/mm³]	U_{top} abs.	U_{top} rel.
K_v Calculated	6.12	3.31	110.7%	5.62	5.49	110.9%	5.62	10.38	110.4%
K_v Maximum	6.43	3.30	110.4%	6.43	5.45	110.1%	6.43	10.33	109.9%
K_v Upper limit	6.19	3.31	110.7%	5.78	5.48	110.7%	5.78	10.37	110.3%
K_v Lower limit	5.84	3.32	111.0%	5.00	5.53	111.7%	5.00	10.44	111.1%

Table I.17 Resulting top deflections for different values of K_v, based on a variation of K_h [mm]

The difference between the top deflection corresponding to the calculated shear stiffness and the maximum value in case of infinite lateral stiffness is relatively low. This indicates that the influence of the lateral stiffness on the top deflection is limited for the applied input properties. For wall 2, the difference between the maximum and the lower limit is with a value of 1.6 percent point the largest. This is 1.6/10.1= 15.8 percent of the minimal top deflection increase. So the influence of the lateral stiffness on the top deflection increase is at most 15.8 percent. This holds only for the applied input properties of Table 11.1. For larger values of K_d and smaller values of α and K_h, the influence of K_h is greater, as explained in paragraph 10.1 and shown in chapter 11.

The error of the calculation method is indicated by its band width (the difference between the lower and upper limit result). This is at most 1.0 percent point for wall 2. This is 1.0/10.1=9.9% of the minimal top deflection increase. The results of chapter 11 show that the band width increases for a larger value of K_d and a smaller value of K_h.

A final comment must be made about the results of Table 11.3 and Table I.17. It is observed that the top deflection of wall 3 with diagonal bars is smaller than the top deflection with the upper limit value of K_v. This shouldn't be possible, since the lateral stiffness cannot exceed infinity and therefore the shear stiffness can't exceed the limit value. A more detailed analysis shows that in the model of wall 3 with diagonal bars, part of the joint is compressed instead of dilated. This leads to a shear stiffness larger than the limit value. However, this is physically impossible, since the joint is fully filled with mortar and therefore incompressible. So a more realistic top deflection of the model with diagonal bars will be equal to the deflection obtained with the K_v upper limit. Appendix J provides a more detailed analysis of this theoretical effect.

J Theoretical evaluation of the derived K_vK_h-relation

Figure J.23 shows the complete diagram that relates the shear and lateral stiffness for a certain value of K_d and α. In the main report only part 1 has been shown with the lateral stiffness displayed as absolute value. The analytical relation of the diagram is given by equation 10.1. The domain of this relation is [-∞,∞] and in this domain three characteristic parts are distinguished.

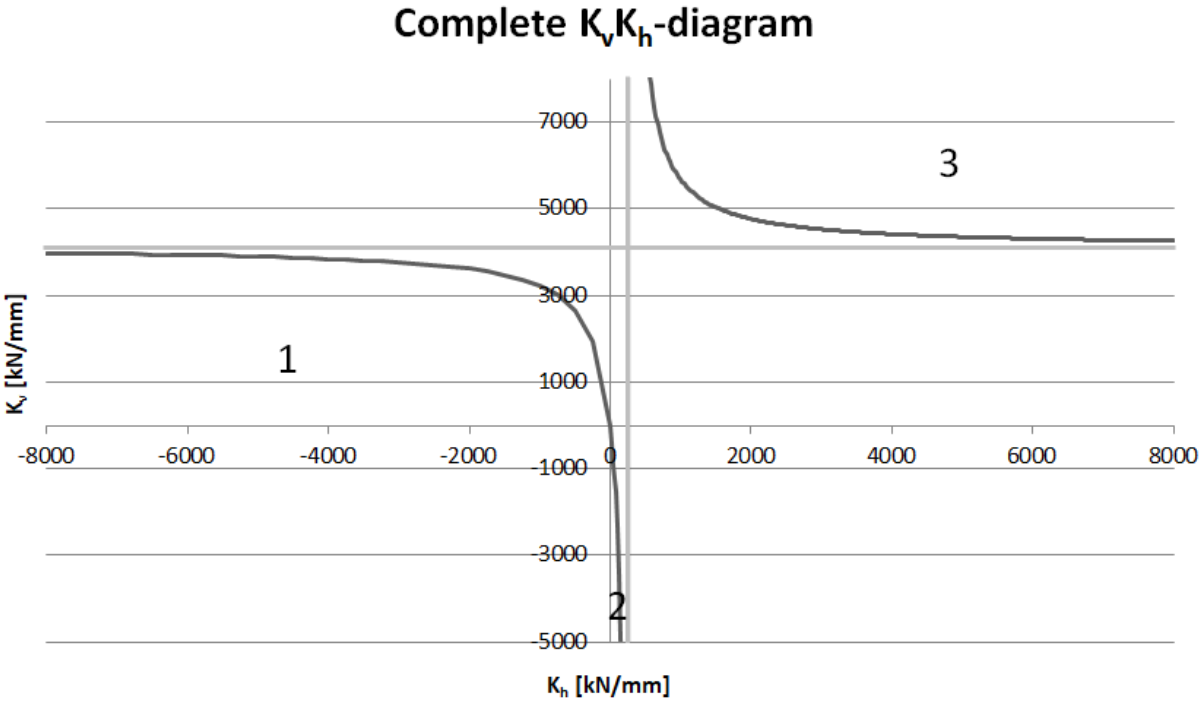

Figure J.23 Complete K_vK_h-diagram

The behaviour of a single diagonal bar that corresponds to part 1 is shown in the left image of Figure J.24. The angle of the load is such that the lateral stiffness is negative, which means that a dilatation occurs. This coincides with a negative shear displacement, where the top of the diagonal deflects more than its lower end.

In part 2, the lateral stiffness is positive, which means that the joint narrows down. The positive lateral stiffness is caused by the angle of the load, which is larger than in part 1. The shear stiffness is negative, which means that the top end translates upwards relative to the lower end of the diagonal bar. This happens as a result of the negative horizontal displacement and the bar rotation it induces.

In part 3, the lateral stiffness is positive, but the shear stiffness is negative. The upward rotation of the upper end of the bar due to the negative horizontal displacement results in a displacement in positive y-direction. However, the shortening of the diagonal bar causes a translation of the upper end of the bar in negative y-direction which is greater. This results in a net translation in negative y-direction.

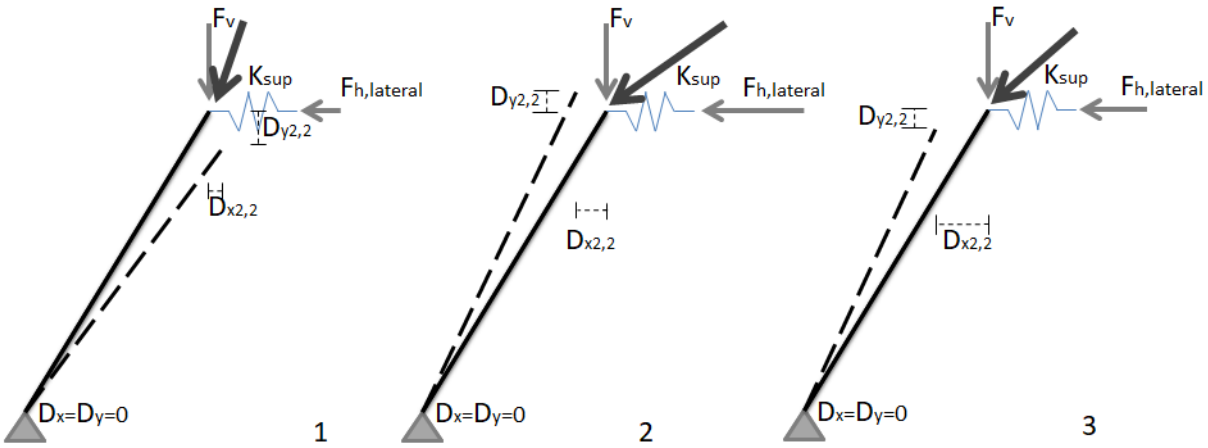

Figure J.24 Physical behaviour corresponding to the different parts of the K_vK_h-diagram

The results presented in chapter 11 show that the wall with diagonals in its joint is sometimes stiffer than the wall with interface elements to which the maximum shear stiffness is assigned. This maximum is equal to that corresponding to the horizontal asymptote in Figure J.23. In the wall with diagonals the situation corresponding to part 3 occurs in some cases for part of the diagonals in the joint. As the complete diagram shows, in this part the shear stiffness is greater than the asymptotic value, which explains the obtained results.

The joint with diagonal bars is compressible in x-direction, since the bars are connected to the precast elements by hinges. However, in reality the joint is completely filled with mortar and therefore not easily compressible. So the behaviour corresponding to parts 2 and 3 of the diagram is not realistic.

The boundaries between the three different parts are dependent on the values for K_d and α. The value of the lateral stiffness corresponding to the vertical asymptote is given by:

$$K_h^* = h_x^2 * \frac{K_d}{L_d^2}$$

This is obtained by setting relation 10.1 equal to infinity.

K Evaluation of stresses in the shear wall models

In paragraph 10.4 the developed method to calculate the shear stiffness that must be assigned to linear interface elements that model the vertical profiled mortar connections was described. Subsequently, this method was evaluated in chapter 11 on multiple shear wall models. However, in this chapter only the resulting top deflections were compared. This appendix contains the comparison of the resulting shear stresses in the joint and in the precast wall elements.

For this analysis two stiffness properties are assigned to the interface elements that model the vertical connection: a normal and a shear stiffness. The shear stiffness is determined according to section 11.1.2. The normal stiffness is found in the following way:

$$K_n = \frac{E_m A}{A W_{joint}} = \frac{E_m}{W_{joint}} = \frac{25000}{75} = 333 \frac{N}{mm^3}$$

Shear stresses in the compact wall of paragraph 11.2

First of all the compact walls are analysed. Figure K.25 shows the results that are exported for one of the different walls. The shear stress in the joint, τ, and the shear stress in the wall S_{xy} are reviewed. The left image shows that the shear stress distribution in the joint corresponds to the theoretical distribution that was described in paragraph 3.2, since the maximum stress occurs a couple of metres above the base of the wall.

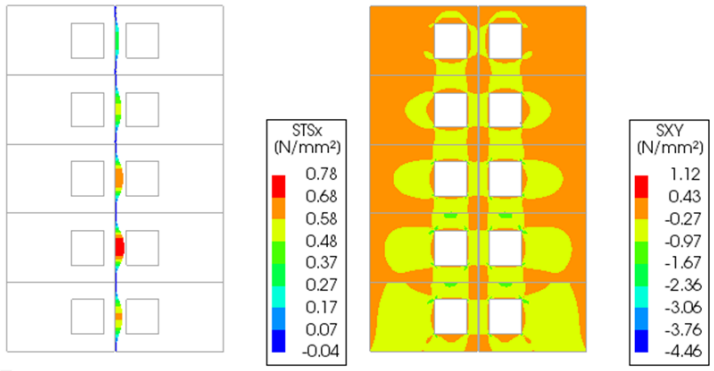

Figure K.25 Shear stresses in the vertical joint and the precast concrete wall elements in compact wall 2

The maximum occurring stresses are stored in Table K.18 and Table K.19 and subsequently compared among the different walls with varying joint stiffness. The numbering of the walls is equal to that applied in chapter 11, as indicated in Figure 11.1.

The purpose of this analysis is first of all to analyse the error of the calculation method for K_v of paragraph 10.4 in terms of resulting shear stress. To this purpose the results of "K_v Upper limit" and "K_v Lower limit" are compared, since these values of the shear stiffness correspond to the obtained band width of the calculation method for K_v.

The second purpose is to indicate the maximum influence of the lateral stiffness, K_h, on the occurring stress distribution. For this purpose the resulting stress for "K_v maximum" is compared to that of "K_v Lower limit", since the former is the shear stiffness corresponding to an

infinitely large lateral stiffness and the latter is corresponding to the smallest possible lateral stiffness for this specific wall. The following tables contain the resulting stresses, based on which the following is observed:

	Wall 1			Wall 2			Wall 3		
	K_v [N/mm³]	τ_{max}	τ_{max} rel.	K_v [N/mm³]	τ_{max}	τ_{max} rel.	K_v [N/mm³]	τ_{max}	τ_{max} rel.
K_v Maximum	11.4	0.45	100.0%	11.4	0.78	100%	11.4	1.18	100.0%
K_v Upper limit	9.85	0.44	97.8%	8.87	0.73	93.6%	8.87	1.08	91.5%
K_v Lower limit	8.10	0.43	95.6%	6.56	0.66	84.6%	6.56	0.95	80.5%

Table K.18 Maximum shear stresses in the joint (τ_{max}) [N/mm²] for different values of K_v for a compact wall

	Wall 1			Wall 2			Wall 3		
	K_v [N/mm³]	S_{xy} max	S_{xy} rel.	K_v [N/mm³]	S_{xy} max	S_{xy} rel.	K_v [N/mm³]	S_{xy} max	S_{xy} rel.
K_v Maximum	11.4	0.19	100.0%	11.4	1.12	100.0%	11.4	2.43	100.0%
K_v Upper limit	9.85	0.20	105.3%	8.87	1.13	100.9%	8.87	2.45	100.8%
K_v Lower limit	8.10	0.20	105.3%	6.56	1.14	101.8%	6.56	2.47	101.6%

Table K.19 Maximum shear stresses in the structure (S_{xy}) [N/mm²] for different values of K_v for a compact wall

First of all, the results of Table K.19 show that the shear stress in the shear wall itself is hardly affected by the magnitude of K_v. A less stiff joint leads to a slight increase of this stress, but this is negligible. This conclusion holds for all three wall designs.

Secondly, the maximum shear stress that occurs in the joint decreases for lower values of K_v. This is true for all three wall designs.

Furthermore, the band width of the calculation method is the largest in wall type 3. For the upper limit a shear stress of 1.08 N/mm² is observed, for the lower limit a shear stress of 0.95 N/mm². This is a difference of 13.7%.

Moreover, the influence of the lateral stiffness, K_h, is also the largest for wall type 3. In this case the maximum shear stress is just 80.5% of the value that would occur in case the lateral stiffness was infinitely large, a stress reduction of almost 20 percent.

Shear stresses in the slender wall of paragraph 11.2

Then a slender wall is evaluated using the same procedure as before. Figure K.26 shows the stresses that develop in type 2 of this slender wall for "K_v maximum".

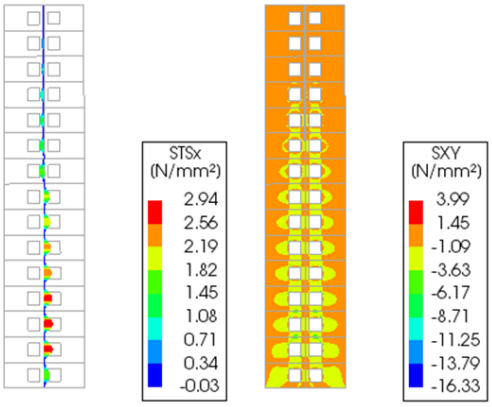

Figure K.26 Shear stresses in the vertical joint and the precast concrete wall elements in slender wall 2

Table K.20 and Table K.21 contain the resulting maximum values for the shear stress in the vertical joint and the shear wall itself.

	Wall 1			Wall 2			Wall 3		
	K_v [N/mm³]	τ_{max}	τ_{max} rel.	K_v [N/mm³]	τ_{max}	τ_{max} rel.	K_v [N/mm³]	τ_{max}	τ_{max} rel.
K_v Maximum	11.4	1.60	100.0%	11.4	2.94	100.0%	11.4	3.73	100.0%
K_v Upper limit	9.85	1.59	99.4%	8.87	2.74	93.2%	8.87	3.45	92.5%
K_v Lower limit	8.10	1.57	98.1%	6.56	2.50	85.0%	6.56	3.12	83.6%

Table K.20 Maximum shear stresses in the joint (τ_{max}) [N/mm²] for different values of K_v for a slender wall

	Wall 1			Wall 2			Wall 3		
	K_v [N/mm³]	S_{xy} max	S_{xy} rel.	K_v [N/mm³]	S_{xy} max	S_{xy} rel.	K_v [N/mm³]	S_{xy} max	S_{xy} rel.
K_v Maximum	11.4	1.24	100.0%	11.4	3.99	100.0%	11.4	9.59	100.0%
K_v Upper limit	9.85	1.24	100.0%	8.87	4.00	100.2%	8.87	9.62	100.3%
K_v Lower limit	8.10	1.24	100.0%	6.56	4.00	100.2%	6.56	9.66	100.7%

Table K.21 Maximum shear stresses in the structure (S_{xy}) [N/mm²] for different values of K_v for a slender wall

First of all, the results of Table K.21 show that the shear stress in the shear wall itself is hardly affected by the magnitude of K_v. A less stiff joint leads to a slight increase of this stress, but this is negligible. This conclusion holds for all three wall designs.

Secondly, the maximum shear stress that occurs in the joint decreases for lower values of K_v. This is true for all three wall designs.

Furthermore, the band width of the calculation method is the largest in wall type 3. For the upper limit a shear stress of 3.45 N/mm² is observed, for the lower limit a shear stress of 3.12 N/mm². This is a difference of 10.6%.

Moreover, the influence of the lateral stiffness, K_h, is also the largest for wall type 3. In this case the maximum shear stress is just 83.6% of the value that would occur in case the lateral stiffness was infinitely large, a stress reduction of almost 20 percent.

Finally, it can be observed that in a slender wall, the relative deviation of the shear stress in both the structure and the joint is smaller than in a compact wall.

Shear stresses in the compact wall of paragraph 11.4

In paragraph 11.4 the largest error in terms of top deflection was found for the case of a compact wall where the lateral stiffness was maximally reduced. Table K.22 and Table K.23 show the resulting maximum shear stresses corresponding this wall.

	Wall 2			Wall 3		
	K_v [N/mm³]	τ_{max}	τ_{max} rel.	K_v [N/mm³]	τ_{max}	τ_{max} rel.
K_v Maximum	11.4	0.85	100.0%	11.4	1.22	100.0%
K_v Upper limit	8.87	0.74	87.1%	8.87	1.04	85.2%
K_v Lower limit	6.56	0.62	72.9%	6.56	0.87	71.3%

Table K.22 Maximum shear stresses in the joint (τ_{max}) [N/mm²] for different values of K_v for a compact wall with least stiff design parameters

	Wall 2			Wall 3		
	K_v [N/mm³]	S_{xy} max	S_{xy} rel.	K_v [N/mm³]	S_{xy} max	S_{xy} rel.
K_v Maximum	11.4	1.32	100.0%	11.4	2.67	100.0%
K_v Upper limit	8.87	1.33	100.8%	8.87	2.68	100.4%
K_v Lower limit	6.56	1.34	101.5%	6.56	2.70	101.1%

Table K.23 Maximum shear stresses in the structure (S_{xy}) [N/mm²] for different values of K_v for a compact wall with least stiff design parameters

Again the deviation of the shear stress in the wall elements is not significant. Also the same relation between the magnitude of K_v and the maximum shear stress is observed as before.

The band width of the calculation method is the largest in wall type 3. For the upper limit a shear stress of 1.04 N/mm² is observed, for the lower limit a shear stress of 0.87 N/mm². This is a difference of 19.5%.

Moreover, the influence of the lateral stiffness, K_h, is also the largest for wall type 3. In this case the maximum shear stress is just 71.3% of the value that would occur in case the lateral stiffness was infinitely large, a stress reduction of almost 30 percent.

Concluding remarks

The relative error of the calculation and the relative influence of a limited lateral stiffness are larger in terms of shear stress than in terms of top deflection. However, since their absolute difference of the shear stress is rather small, the importance of this difference may be questionable. If a more refined calculation method for the magnitude of K_v is developed, the band width is reduced and therefore the difference in resulting shear stress.